



Bayerische Julius-Maximilians-
Universität Würzburg
Fakultät für Biologie

**Lamin A and Lamin C are Differentially
Dysfunctional in Autosomal Dominant
Emery-Dreifuss Muscular Dystrophy**

Dissertation zur Erlangung des naturwissenschaftlichen Doktorgrades
der Bayerischen Julius-Maximilians-Universität Würzburg

Vorgelegt von
Isabell Motsch
aus Bad Kissingen

Würzburg 2005

Eingereicht am:.....

Mitglieder der Promotionskommission

Vorsitzender: Prof. Dr. U. Scheer

Erstgutachter: Prof. Dr. M.-C. Dabauvalle

Zweitgutachter: Prof. Dr. C.R. Müller-Reible

Tag des Promotionskolloquiums:.....

Doktorurkunde ausgehändigt am:.....

Table of contents

1 Introduction 1

1.1 Emery-Dreifuss muscular dystrophy 2

1.1.1 First description and inheritance.....2

1.1.2 Clinical symptoms.....2

1.2 The nuclear envelope 4

1.2.1 Structure and functions of the nuclear envelope.....4

1.2.2 Proteins of the nuclear envelope and their interaction partners.....5

1.2.2.1 Integral proteins of the inner nuclear membrane.....7

1.2.2.1.1 Lamin B receptor.....7

1.2.2.1.2 Lamina-associated proteins 1 and 2.....7

1.2.2.1.3 Nesprins 1 and 2.....8

1.2.2.1.4 MAN1.....9

1.2.2.1.5 Emerin.....10

1.2.2.2 Main components of the nuclear lamina – nuclear lamins.....15

1.3 Nuclear envelope proteins in disease – the laminopathies 23

1.3.1 Human diseases due to mutations in lamins or lamin-associated proteins.....23

1.3.2 How do mutations in lamins A and C cause disease ?.....26

1.3.2.1 The structural weakness hypothesis.....26

1.3.2.2 The gene expression hypothesis.....27

1.3.2.3 Other models to explain laminopathies.....28

1.3.3 Mutations of the *LMNA* gene used in this study.....28

1.4 Aim of this study 31

2 Materials 33

2.1 Cell biology materials 33

2.1.1 Cell lines.....33

2.1.2 Antibodies.....33

2.1.3 Secondary antibodies.....33

2.2 Molecular biology materials 34

2.2.1 Bacteria, vectors, constructs.....34

2.2.2 Enzymes, kits.....37

2.3 Chemicals 38

2.4 Equipment 38

2.5	Photographic materials.....	38
3	Methods	39
3.1	Microbiology.....	39
3.1.1	Bacterial growth.....	39
3.1.2	Competent cell formation.....	39
3.1.3	Transformation.....	40
3.2	Molecular biology.....	40
3.2.1	Preparation of plasmid DNA.....	40
3.2.2	Determination of DNA concentration.....	40
3.2.3	Hydrolysis of DNA with restriction endonucleases (restriction digest).....	41
3.2.4	DNA separation by agarose gel electrophoresis.....	41
3.2.5	Isolation of DNA fragments from agarose gels.....	43
3.2.6	Ligation.....	43
3.2.7	Creation of lamin A cDNA constructs by site-directed mutagenesis.....	43
3.2.8	Creation of lamin C cDNA constructs by site-directed mutagenesis.....	44
3.2.9	Emerin cDNA construct.....	45
3.2.10	<i>In vitro</i> transcription/translation of lamins A/C and emerin.....	45
3.3	Protein biochemistry.....	46
3.3.1	Cell culture.....	46
3.3.2	Transfection of adherent cells.....	46
3.3.3	Cell harvest for SDS-PAGE.....	47
3.3.4	SDS polyacrylamide gel electrophoresis.....	48
3.3.5	Immunoblot.....	51
3.3.6	Immunoprecipitation of <i>in vitro</i> synthesised proteins.....	53
3.4	Light and electron microscopy.....	54
3.4.1	Immunofluorescence microscopy.....	54
3.4.2	FRAP analysis of living cells.....	55
3.4.3	Electron microscopy.....	56
4	Results	58
4.1	Exogenous expression of lamin A and C constructs in COS7 cells analysed by immunofluorescence microscopy.....	58

4.1.1	Do mutations in the lamins A and C affect their intracellular localisation ?.....	58
4.1.2	The lamin A and C constructs expressed by COS7 cells are of the expected sizes.....	59
4.1.3	Exogenously expressed lamin A with the mutation T150P does not disrupt the distribution of endogenous A-type lamins.....	60
4.1.4	Exogenously expressed lamin A proteins do not form heterodimers with endogenous lamin B2.....	61
4.1.5	Exogenous expression of lamin A constructs reveals 3 categories of localisation phenotypes.....	63
4.1.5.1	Category 1: wild type phenotype of exogenous lamin A mutations.....	63
4.1.5.2	Category 2: a range of phenotypes of exogenous lamin A mutations.....	66
4.1.5.3	Category 3: mis-localisation of exogenous lamin A mutations	69
4.1.5.4	Endogenous lamin C is affected by some of the lamin A mutations.....	71
4.1.6	Exogenously expressed lamin C constructs form aggregates in the nucleus.....	73
4.1.7	Lamin C requires co-expression with lamin A to be targeted to the nuclear lamina.....	74
4.1.8	Exogenous wild type lamin A can correct the localisation of all lamin C mutants, but not vice versa.....	76
4.1.9	Most lamin A mutants form heterodimers with wild type lamin C.....	76
4.1.10	Altered nuclear localisation of mutated lamins A/C may cause EDMD.....	79
4.2	Exogenous expression of lamin A constructs in COS7 cells analysed by electron microscopy.....	82
4.2.1	Are there ultrastructural changes of the nuclear envelope in cells expressing lamin A mutations ?.....	82
4.2.2	Exogenous expression of wild type lamin A thickens the nuclear lamina.....	83
4.2.3	Lamin A mutations of category 1 show a wild type phenotype.....	85
4.2.4	Lamin A mutations of category 2 present a variety of phenotypes.....	87
4.2.5	Lamin A mutations of category 3 are strongly mis-localised.....	90
4.2.6	Ultrastructural changes in nuclear lamina architecture caused by lamin A mutations may contribute to EDMD.....	92
4.3	Altered mobility of exogenously expressed lamin A mutants analysed by fluorescence recovery after photobleaching (FRAP).....	95
4.3.1	Do mutations in lamin A alter its mobility within the nuclear lamina ?.....	95

4.3.2	The E361K mutation in the rod domain of lamin A increases its mobility.....	96
4.3.3	Mutations in the lamin A globular domain have no effect on protein mobility.....	100
4.3.4	Altered protein mobility may explain some lamin A mutants causing EDMD.....	103
4.4	Lamin A/C-emerin interactions <i>in vitro</i>.....	106
4.4.1	Do mutations in lamin A and C impair their binding to emerin ?.....	106
4.4.2	<i>In vitro</i> synthesis of lamin A/C mutants and emerin.....	106
4.4.3	Mutant lamin A proteins show different emerin-binding capabilities.....	108
4.4.4	Lamin C mutants T150P, R527P and L530P maintain a wild type-like emerin interaction.....	111
4.4.5	Weakened emerin interaction of some lamin A mutations may lead to EDMD.....	112
4.4.6	Summary of results.....	113
5	Discussion	115
5.1	How to study disease-causing mutations in human genes.....	115
5.2	Possible molecular mechanisms of lamin A mutations leading to Emery-Dreifuss muscular dystrophy.....	116
5.2.1	Mutations in the rod domain of lamin A mainly impair lamin filament assembly.....	116
5.2.1.1	R50S.....	116
5.2.1.2	R133P.....	117
5.2.1.3	T150P.....	118
5.2.1.4	DelQ355.....	119
5.2.1.5	E358K.....	120
5.2.1.6	E361K.....	121
5.2.2	Mutations in the globular tail domain of lamin A are likely to disturb protein-protein interactions.....	122
5.2.2.1	R527P.....	122
5.2.2.2	L530P.....	123
5.2.2.3	R541S.....	124
5.2.2.4	G602S.....	125
5.2.2.5	C<T1698 and E358K+C<T1698.....	126
5.2.3	Classification of <i>LMNA</i> mutations.....	127

5.3	Lamin A and lamin C are differentially dysfunctional in Emery-Dreifuss muscular dystrophy.....	129
6	Summary	133
7	Zusammenfassung	134
8	Abbreviations	135
9	References	137
10	Curriculum vitae	158

Table of figures and tables

Fig. 1.1.	Distribution of muscle wasting (red) in different forms of muscular dystrophies.....	1
Fig. 1.2.	A 17-year-old male with EDMD.....	3
Fig. 1.3.	Schematic diagram of a human cell showing the nucleus and other selected structures.....	4
Fig. 1.4.	Schematic diagram of the NE showing the association between the nuclear membranes, nuclear pore complexes (Npcs), ER and lamina (pink filaments).....	5
Table 1.1.	Known nuclear envelope proteins (without nuclear pore complex proteins).....	6
Fig. 1.5.	Schematic diagram of emerin structure and of regions to which partners bind.....	11
Fig. 1.6.	Schematic diagram of lamin A/C structure and of regions to which partners bind...	18
Fig. 1.7.	A summary of interactions between the proteins of the nuclear lamina.....	22
Table 1.2.	Diseases related to mutations of lamins or lamin-associated proteins.....	24
Table 1.3.	Overview of <i>LMNA</i> mutations used in this thesis.....	29
Fig. 1.8.	Schematic diagram of lamin A with the distribution of the <i>LMNA</i> mutations used in this thesis.....	30
Fig. 2.1.	Restriction map and multiple cloning site (MCS) of pEGFP-C1.....	34
Fig. 2.2.	Restriction map and multiple cloning site (MCS) of pEGFP-C3.....	35

Fig. 2.3. Restriction map and multiple cloning site (MCS) of pDsRed2-C1.....	36
Fig. 2.4. Restriction map and multiple cloning site (MCS) of pcDNA3.1(+/-).....	36
Fig. 2.5. Restriction map and multiple cloning site (MCS) of pCMV-Tag2A.....	37
Table 3.1. Restriction endonucleases and their target sequences.....	41
Fig. 3.1. Size standard for agarose gel electrophoresis.....	43
Fig. 3.2. Neubauer counting chamber.....	47
Fig. 3.3. Marker proteins for SDS-PAGE (18% acrylamide concentration).....	50
Fig. 3.4. Stacking scheme for an immunoblot (Western blot).....	52
Table 3.2. Dilution of primary antibodies for immunoblot.....	52
Table 3.3. Dilution of primary antibodies for immunofluorescence microscopy.....	55
Fig. 4.1. Immunoblot showing the expression levels of EGFP-lamin A and pDsRed2- lamin C transfected into COS7 cells alongside endogenous lamin A/C levels.....	59
Fig. 4.2. Immunofluorescence analysis of the influence of exogenous EGFP-lamin A expressed by transiently transfected COS7 cells on the endogenous lamin A/C.....	60
Fig. 4.3. Immunofluorescence analysis of the influence of exogenous EGFP-lamin A expressed by transiently transfected COS7 cells on the endogenous lamin B2.....	62
Table 4.1. Transfection efficiencies and percentage of cells exhibiting abnormalities when exogenously expressing EGFP-lamin A in COS7 cells.....	64
Fig. 4.4. Intracellular localisation of wild type and lamin A mutants as EGFP fusion proteins transiently expressed by COS7 cells: category 1 (wild type-like appearance).....	65
Fig. 4.5.1-2. Intracellular localisation of lamin A mutants as EGFP fusion proteins transiently expressed by COS7 cells: category 2 (range of phenotypes).....	67-68
Fig. 4.6. Intracellular localisation of lamin A mutants as EGFP fusion proteins transiently expressed by COS7 cells: category 3 (severe mis-localisation).....	70
Fig. 4.7. Immunofluorescence analysis of the influence of exogenous EGFP-lamin A expressed by transiently transfected COS7 cells on the endogenous lamin C.....	72
Fig. 4.8. Intracellular localisation of transiently expressed lamin C DsRed2 or EGFP fusion proteins and DsRed2 alone in COS7 cells.....	74
Fig. 4.9. Intracellular localisation of EGFP-lamin A and DsRed2-lamin C fusion proteins transiently expressed together in COS7 cells: expression of lamin A mutants with the equivalent lamin C mutants.....	75
Fig. 4.10. Intracellular localisation of EGFP-lamin A and DsRed2-lamin C fusion proteins transiently expressed together in COS7 cells: expression of one wild type A-type lamin with the opposing mutant A-type lamin.....	77

Fig. 4.11. Intracellular localisation of EGFP-lamin A and DsRed2-lamin C fusion proteins transiently expressed together in COS7 cells: expression of wild type lamin C with different lamin A mutants.....	78
Fig. 4.12. Schematic diagram of the lamin A sequence indicating the positions of EDMD causing mutations of category 1 (black), 2 (blue) and 3 (red).....	80
Fig. 4.13. Electron micrographs from ultra-thin sections of COS7 fibroblasts exogenously expressing wild type EGFP-lamin A and untransfected control cells....	84
Fig. 4.14. Electron micrographs from ultra-thin sections of COS7 fibroblasts exogenously expressing EGFP-lamin A mutations of category 1.....	86
Fig. 4.15.1-2. Electron micrographs from ultra-thin sections of COS7 fibroblasts exogenously expressing EGFP-lamin A mutations of category 2.....	88-89
Fig. 4.16. Electron micrographs from ultra-thin sections of COS7 fibroblasts exogenously expressing EGFP-lamin A mutations of category 3.....	91
Fig. 4.17. Schematic diagram of the lamin A sequence indicating the positions of EDMD causing mutations of localisation category 1 (black), 2 (blue) and 3 (red)....	93
Fig. 4.18.1-3. FRAP analysis of wild-type EGFP-lamin A and its mutations in the rod domain.....	97-99
Fig. 4.19.1-2. FRAP analysis of EGFP-lamin A mutations in the globular domain.....	101-102
Fig. 4.20. Overview of results obtained by FRAP analysis from exogenously expressed EGFP-lamin A mutants.....	104
Fig. 4.21. Autoradiographs of <i>in vitro</i> transcription/translation reactions of lamin A/C constructs.....	107
Fig. 4.22. Co-immunoprecipitation of wild type and mutant lamin A constructs with emerin.....	109
Table 4.2. Quantitative analysis of mutant lamin A-emerin co-immunoprecipitation assays.....	110
Fig. 4.23. Co-immunoprecipitation of wild type and mutant lamin C constructs with emerin.....	111
Fig. 4.24. Schematic diagram of the lamin A sequence indicating the positions of EDMD causing mutations with normal (black) or strongly reduced (red) emerin binding....	113
Table 4.3. Summary of results obtained by analysis of <i>LMNA</i> mutations.....	114
Fig. 5.1. Proposed functional defects of lamin A mutations causing Emery-Dreifuss muscular dystrophy.....	128

1 Introduction

Imagine yourself to be the proud parent of a newborn baby son. As he grows up, you suddenly notice that he seems to differ from other children: maybe he waddles rather than walks or he has difficulties in rising from a lying or sitting position. If he is already five or six years old, he may start to walk on his toes and carry his arms flexed like a cowboy. Worried as you are, you consult your paediatrician who, after a series of examinations and tests involving other specialists, confronts you with the shattering truth: your child suffers from an inherited disorder, a muscular dystrophy.

But he is lucky to only be affected by one of the milder forms where he can expect to live until at least a middle age. Nevertheless, the disease cannot be healed and therapies can only delay its progressive nature. Since you want to know more about this particular form of muscular dystrophy, known as the type Emery-Dreifuss, which affects your son, you do a little library research and you unearth the puzzling feature of this distinctive disorder. Unlike other muscular dystrophies which are caused by defects in muscle-specific proteins such as dystrophin in the Duchenne and Becker types, this one (and a form of limb girdle muscular dystrophy, see also Fig. 1.1) is due to the lack, or to mutations of proteins existing in nearly every cell of the human body: proteins of the cell nucleus.

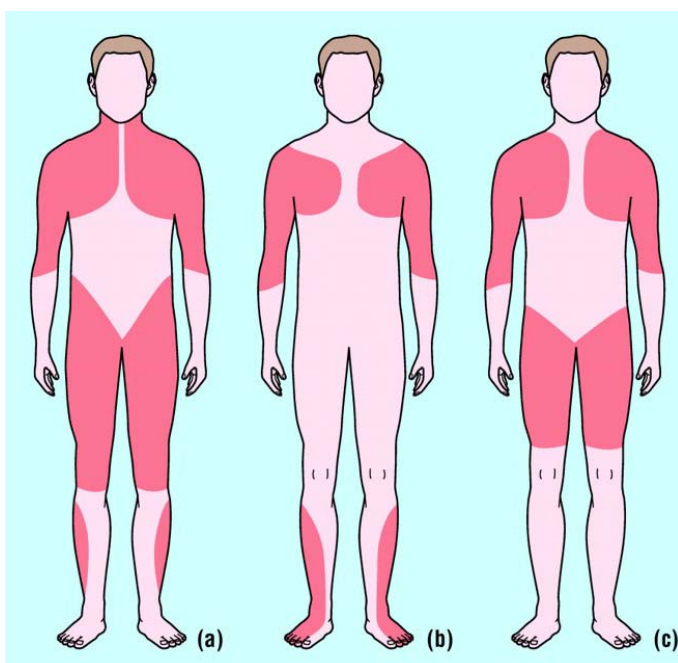


Fig. 1.1. Distribution of muscle wasting (red) in different forms of muscular dystrophies. (a) Type Duchenne and Becker, (b) type Emery-Dreifuss, and (c) type limb girdle. Picture from www.neuro24.de/muscle.htm.

1.1 Emery-Dreifuss muscular dystrophy

1.1.1 First description and inheritance

In 1966, the physicians Emery and Dreifuss described in detail for the first time a new, relatively benign form of a X-linked muscular dystrophy [Emery and Dreifuss, 1966]. At the time, they considered it to be possibly a distinct entity, restricted to one family from Virginia, USA, with eight affected male members from three generations. The distinguishing features of this same disorder, however, may have been noted earlier in two french brothers in 1902 by Cestan and Lejonne of the Salpêtrière [Cestan and Lejonne, 1902] and, in another case, by Schenk and Mathias of Breslau in 1920 [Schenk and Mathias, 1920].

A rarer autosomal form of this muscular dystrophy has been found in 1941 in a family of Franco-Canadian descent [Hauptmann and Tannhäuser, 1941], though neither this report nor any of the early reports of the X-linked form mentions the distinctive cardiac features of the disease. The eponymous association (Emery-Dreifuss muscular dystrophy or EDMD) was first suggested in 1979 by Rowland [Rowland *et al.* 1979] and is now commonly used.

1.1.2 Clinical symptoms

The clinical features of Emery-Dreifuss muscular dystrophy, which appears first in early childhood and thereafter has a relatively slow progression, are now clearly defined. The disorder is characterized by the triad of (i) early contractures of the Achilles tendons, elbows and postcervical muscles, (ii) slowly progressive muscle wasting and weakness with a humeroperoneal distribution early in the course of the disease and (iii) cardiac conduction defects and cardiomyopathy [for reviews see Emery 1989 and Emery 2000].

Muscle and tendon contractures develop in the first decade of life of the patients, often before there is any significant weakness. These involve the elbows, leading to the arms being carried in a semi-flexed position, the Achilles tendons, so that the patients walk on their toes, and the postcervical muscles with restriction of the neck flexion. Later, forward flexion of the entire spine becomes limited. Also in childhood, muscle wasting and weakness occur in the patients, predominantly affecting the biceps, triceps, anterior tibial and peroneal muscles. Thus, the weakness is more proximal in the upper limbs and distal in the lower limbs.

Subsequently, weakness of the pectoral girdle musculature and the knee and hip extensor muscles develop. The distribution of muscle weakness may therefore be described as humeroperoneal in the beginning and as scapulohumeropelvoperoneal in later stages (Fig. 1.1b). Since muscle wasting progresses only slowly, most patients are able to walk up into their fourth decade of life. However, there is a big variability concerning the severity of symptoms, with the most affected persons being confined to a wheelchair even in young years.

Cardiac involvement is the most serious and important aspect of the disease. It usually becomes evident as muscle weakness progresses (before 30 years of age), but can exceptionally occur before there is any significant weakness. Cardiac conduction defects range from sinus bradycardia, prolongation of the PR interval on electrocardiography to complete heart block, frequently resulting in a sudden death of the patients because of heart failure. Therefore, an early diagnosis in the patients and monitoring of at-risk family members is essential, since the timely insertion of a cardiac pacemaker can be life-saving (Fig. 1.2).

Life expectancy of EDMD patients is slightly reduced, but they can expect to survive into at least middle age provided that a cardiomyopathy does not intervene. Mental retardation seems not to occur. The serum level of creatine kinase as a marker of muscle necrosis is usually moderately elevated, but can be normal. In general, women are only affected by the autosomal dominant form of EDMD; female carriers of the X-linked form rarely have any weakness, but a proportion of otherwise healthy carriers may exhibit varying degrees of heart block and may require a pacemaker [Review of clinical symptoms and diagnosis: Emery 2000, Yates 1997, Emery 1989, Voit *et al.* 1988].

Mutations in two genes have been identified to cause Emery-Dreifuss muscular dystrophy. The proteins encoded by these two genes, emerin and the lamins A and C, both localise in the nucleus of the cell at the nuclear envelope whose structure and functions will be highlighted in the following chapter.

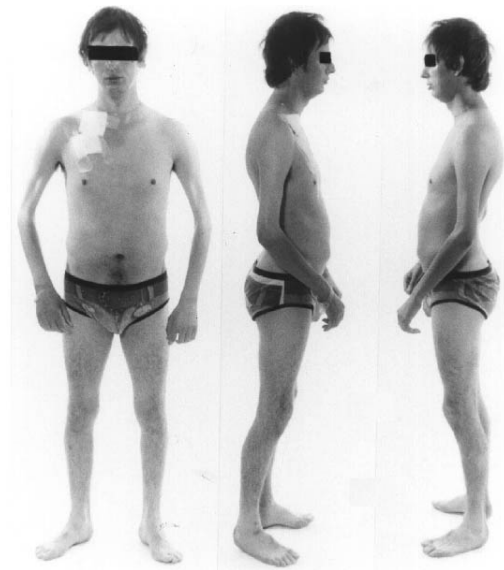


Fig. 1.2. A 17-year-old male with EDMD. Note the flexion contractures of the elbows and wasting of the lower legs. A cardiac pacemaker has been inserted [from Emery 1989].

1.2 The nuclear envelope

1.2.1 Structure and functions of the nuclear envelope

Compared to the relatively simple nucleoid of prokaryotes, the nucleus of eucaryotic cells represents a highly complex organelle, not only in its structure, but also in its unique biological activities. Taking up approximately 10% of the total cell volume and therefore being visible by light microscopy, it is the cellular compartment where such important processes like DNA replication, DNA transcription and the processing of mRNA as well as the synthesis of ribosomes take place. Fig. 1.3 gives a simplified schematic diagram of a nucleus, its main features and its connections to the cytoskeleton in a human cell.

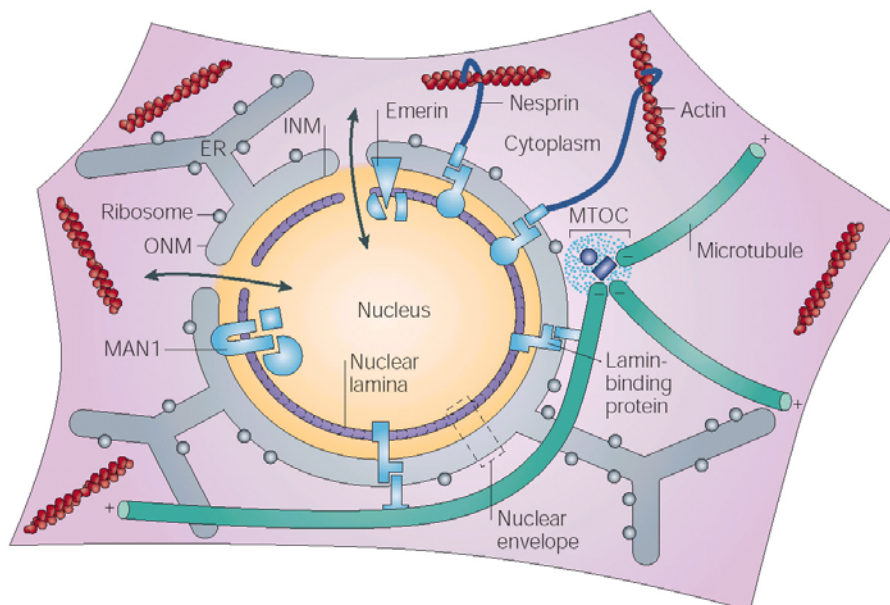


Fig. 1.3. Schematic diagram of a human cell showing the nucleus and other selected structures (not to scale). Inner and outer nuclear membranes (INM and ONM, respectively) of the nuclear envelope (NE) are joined to form pores that are occupied by nuclear pore complexes (NPCs, not depicted). NPCs mediate traffic in and out of the nucleus, as indicated by double-headed arrows. The NE is continuous with the endoplasmic reticulum (ER) network. It contains a wide range of proteins (light blue) some of which connect the nucleus to the microtubule network (originating from the microtubule organizing centre, MTOC) or to actin filaments, thereby regulating its position within the cell. The lamin-filament network of the nuclear lamina (purple) underlines the INM. Picture from Gruenbaum *et al.* 2005.

The nuclear envelope (NE) acts as the interface between the nucleus and the rest of the cell. The NE consists of two concentric membranes (inner and outer nuclear membrane), the nuclear pore complexes and the nuclear lamina network [for review, see Stuurmann *et al.*

1998 or Gerace and Burke, 1988]. The inner and outer nuclear membranes (INM and ONM, respectively) enclose the perinuclear space which is functionally equivalent to the lumen of the rough endoplasmic reticulum (ER). In fact, ONM and ER represent continuous lipid bilayers covered with ribosomes. In contrast, the INM lacks ribosomes, but contains a unique set of both integral and peripheral proteins by which it is closely associated with the underlying chromatin. Although functionally distinct, the INM and ONM are contiguous and join at the nuclear pores – sites that are occupied by nuclear pore complexes (NPCs). These huge macromolecular channels ($M_w \approx 120\text{MDa}$) span the nuclear membranes and mediate bi-directional transport of proteins, nuclear acids and other molecules between the cytoplasm and the nucleus [for review, see Macara, 2001, or Görlich and Mattaj, 1996].

Underlying the INM is the nuclear lamina, a thin (20nm) filamentous meshwork which represents an essential structural element of the NE. The main components of the nuclear lamina are type V intermediate filament proteins – the nuclear lamins – with molecular weights from 60-80 kDa [McKeon *et al.* 1986, Fisher *et al.* 1986]. In interphase, lamin filaments confer mechanical stability and shape to the nucleus and play a central role in chromatin organisation, DNA replication and mRNA synthesis [for reviews, see Goldman *et al.* 2002 or Hutchison, 2002]. Since the lamins are so important for nuclear function, they will be described in more detail in a following chapter (see 1.2.2.2).

1.2.2 Proteins of the nuclear envelope and their interaction partners

To date, a multitude of proteins have been identified that locate to the two nuclear membranes and/or the nuclear lamina. An overview of all proteins is given by Table 1.1, while Fig. 1.4 shows a selection which will be discussed below.

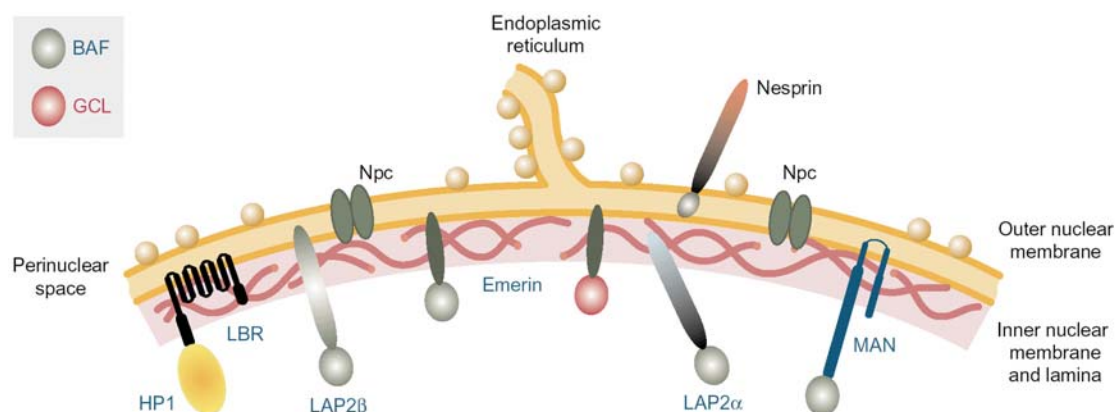


Fig. 1.4. Schematic diagram of the NE showing the association between the nuclear membranes, nuclear pore complexes (NPCs), ER and lamina (pink filaments). Selected proteins are also shown (note that nesprins can also project into the nucleoplasm). Picture from Mounkes *et al.* 2003.

Table 1.1. Known nuclear envelope proteins (without nuclear pore complex proteins).

	Protein type	Known other associated proteins	Occurrence	Special domains	References (first description)
LAP1A-C	Structural in INM	Lamins A, B1, C	Vertebrates	TM	Senior and Gerace 1988, Foisner and Gerace 1993
LAP2 α - ζ	Structural in INM (β - ϵ), nucleoplasmic (α , ζ)	Lamins A, B1, C, BAF, GCL, HA95, pRb, chromatin	Vertebrates	LEM, TM (β - ϵ)	Harris <i>et al.</i> 1994
Emerin	Structural in INM	Lamins A, B, C, BAF, GCL, MAN1, actin, etc.	Vertebrates, <i>Drosophila</i> , <i>C. elegans</i>	LEM, TM	Bione <i>et al.</i> 1994
MAN1	Structural in INM	BAF, CGL, Btf, emerin, lamins A, B1	Vertebrates, <i>Drosophila</i> , <i>C. elegans</i>	LEM, TM	Lin <i>et al.</i> 2000
p18	Structural in INM and ONM	Lamin B, LBR	Vertebrates		Simos <i>et al.</i> 1996
LBR	Structural in INM	Lamin B, HP1, p18, HA95, DNA, histone H3/H4 tetramer	Vertebrates, sea urchins, <i>Drosophila</i>	8 TM	Worman <i>et al.</i> 1990
Nurim	Structural in INM	ND	Vertebrates, <i>Drosophila</i>	5 TM	Rolls <i>et al.</i> 1999
Nesprin-1 (Enaptin)/1 α , β	Structural in NE (INM and ONM)	Lamin A, emerin, Unc-84, actin	Vertebrates, <i>Drosophila</i> , <i>C. elegans</i>	TM, spectrin repeats	Zhang <i>et al.</i> 2001
Nesprin-2 (NUANCE)/2 α - γ	Structural in NE (INM and ONM)	Lamin A, emerin, Unc-84, actin	Vertebrates, <i>Drosophila</i> , <i>C. elegans</i>	TM, spectrin repeats	Zhang <i>et al.</i> 2005
RFBP	Structural in INM	RUSH	mammals	9 TM, ATP binding	Mansharamani <i>et al.</i> 2001
AKAP149	Structural in INM	PP1, RNA, PKARII	Vertebrates	TM	Steen <i>et al.</i> 2000
Unc-83	Structural in ONM	Unc-84	<i>C. elegans</i>	TM	Starr <i>et al.</i> 2001
Unc-84	Structural in NE	Unc-83, ANC-1	<i>C. elegans</i>	SUN, TM (Klarsicht)	Malone <i>et al.</i> 1999
Matefin/SUN-1	Structural in INM	Lamins, ZYG-12	<i>C. elegans</i>	2 TM, SUN	Fridkin <i>et al.</i> 2004
ZYG-12	Structural in ONM	Matefin/SUN-1, centrosomes	<i>C. elegans</i>	TM	Malone <i>et al.</i> 2003
LUMA	Structural in INM	ND	Vertebrates, <i>Drosophila</i>	4 TM	Dreger <i>et al.</i> 2001
Otefin	Structural in INM	Lamin Dm ₀ , chromatin	<i>Drosophila</i>	LEM	Padan <i>et al.</i> 1990
Bocksbeutel	Structural in INM (α), nucleoplasmic (β)	Lamin Dm ₀	<i>Drosophila</i>	LEM	Wagner <i>et al.</i> 2004
UNCL (Unc-50)	Structural in NE	RNA	<i>C. elegans</i> , mammals, yeast, plants	RNA binding	Lewis <i>et al.</i> 1987
GCL	Nucleoplasmic near INM	Emerin, LAP2 α , DP3 α , chromatin, MAN1	Vertebrates, <i>Drosophila</i> , <i>C. elegans</i>	BTB/POZ	Jongens <i>et al.</i> 1992
YA	Nucleoplasmic near INM	Lamin Dm ₀ , chromatin, histone H2B	<i>Drosophila</i>	Zinc fingers, SPKK	Liu <i>et al.</i> 1995
Lamin A/C	Structural in nuclear lamina	LAP2 α , chromatin, lamins, emerin, etc.	Vertebrates, <i>Drosophila</i>	α -helical rod, globular tail	Fisher <i>et al.</i> 1986
Lamin B	Structural in nuclear lamina	LAP2, chromatin, lamins, LBR, etc.	Vertebrates, <i>Drosophila</i> , <i>C. elegans</i>	α -helical rod, globular tail	McKeon <i>et al.</i> 1986 Gerace <i>et al.</i> 1978

TM transmembrane domain, ND not determined

1.2.2.1 Integral proteins of the inner nuclear membrane

1.2.2.1.1 Lamin B receptor

The lamin B receptor (LBR, also termed p58) locates to the inner nuclear membrane where it is anchored by its eight putative transmembrane domains [Worman *et al.* 1990]. As its name suggests, LBR binds B-type lamins, but *in vitro*, it also seems to interact directly with double stranded (ds) DNA [Duband-Goulet and Courvalin, 2000], histone H3/H4 tetramer [Olioudaki *et al.* 2001], chromatin-associated protein HA95 [Martins *et al.* 2000] and heterochromatin protein-1 (HP1) [Ye and Worman, 1996]. HP1 contains both a chromodomain and a chromoshadow domain and mediates gene silencing by binding to ‘silenced’ forms of histone H3 that are methylated at Lys9 (Me-K9H3) [Lachner *et al.* 2001], suggesting a role for LBR in anchoring transcriptionally inactive heterochromatin at the nuclear periphery. The membrane-embedded domain of LBR exhibits sterol C14-reductase activity when expressed in yeast [Silve *et al.* 1998], but whether this nuclear enzyme activity and the chromatin-binding functions of LBR are related, is still not known.

1.2.2.1.2 Lamina-associated proteins 1 and 2

In mammals, the lamina-associated polypeptide 1 (LAP1) has been found [Senior and Gerace 1988], a membrane protein of the INM. It contains a single transmembrane segment [Martin *et al.* 1995] and encodes at least three splicing isoforms, termed LAP1A, LAP1B and LAP1C [Foisner and Gerace 1993]. LAP1A and LAP1B bind to both lamins A/C and B1, whereas LAP1C forms complexes with only lamin B1 [Foisner and Gerace 1993], but also with a protein kinase [Maison *et al.* 1997].

The family of LAP2 proteins comprises several alternatively spliced isoforms derived from a single gene and was previously termed thymopoietin [Harris *et al.* 1994]. Four of the six mammalian LAP2 isoforms (β - ϵ) are type II integral membrane proteins with a N-terminal nucleoplasmic domain, a single transmembrane region and a short C-terminal domain located in the perinuclear space, whereas the other two (α , ζ) are entirely nucleoplasmic [Berger *et al.* 1996]. All isoforms share a ~40 amino acids, homologue domain near their N-terminus with emerin, MAN1 and several other inner nuclear membrane proteins, the so called LEM-domain (LAP2, emerin, MAN1) [Berger *et al.* 1996]. The LEM domain mediates binding to BAF (barrier-to-autointegration factor) [Furukawa, 1999, Shumaker *et al.* 2001], an 89-

residues long, DNA-bridging protein that is involved in establishing higher order chromatin structure [Lee and Craigie, 1998, Cai *et al.* 1998]. The LAP2 α isoform localizes to both the nuclear interior and the nuclear periphery and binds A-type lamins, retinoblastoma protein (Rb) and chromatin [Dechat *et al.* 2000, Vlcek *et al.* 2001].

LAP2 β has many interaction partners, including B-type lamins [Foisner and Gerace, 1993], DNA, BAF [Shumaker *et al.* 2001], germ cell-less (GCL) [Nili *et al.* 2001] and HA95 [Martins *et al.* 2000]. LAP2 β together with GCL, a ubiquitous transcriptional regulator [Jongens *et al.* 1992], inhibits the DP3 subunit of the E2F-DP3 transcription factor, thereby silencing E2F-DP3 dependent reporter genes [Nili *et al.* 2001]. However, LAP2 β alone seems able to repress E2F-DP3 dependent reporter genes, providing first evidence for gene regulation by a LEM-domain protein and indicating that LAP2 β might recruit other endogenous regulators [Nili *et al.* 2001]. Interestingly, LAP2 β also contributes to the initiation of DNA replication by its interaction with chromatin protein HA95; this complex stabilizes cell-division-cycle protein-6 (CDC6), a key component of the pre-replication complex [Martins *et al.* 2003].

1.2.2.1.3 Nesprins 1 and 2

The human nesprin-1 and -2 genes give rise to many splicing isoforms of strongly differing sizes which have acquired many names including cpg-2 [Nedivi *et al.* 1996], syne-1 and syne-2 [Apel *et al.* 2000], myne-1 and myne-2 [Mislow *et al.* 2002a], enaptin [Padmakumar *et al.* 2004] and NUANCE [Zhen *et al.* 2002]. *Drosophila* and *C. elegans* each encode one nesprin homologue, known as MSP-300 [Rosenberg-Hasson *et al.* 1996] and ANC-1 [Starr and Han, 2002], respectively. Small isoforms of nesprins, nesprin-1 α and nesprin-2 α and β , localise at the inner nuclear membrane and bind to lamin A and emerin [Mislow *et al.* 2002b, Zhang *et al.* 2005]. The longest isoforms, nesprin-1 and -2 (also termed enaptin and NUANCE, respectively) contain an actin-binding domain at their N-terminus which co-localises with actin *in vivo* [Starr and Han, 2002, Zhen *et al.* 2002, Padmakumar *et al.* 2004] and a Klarsicht domain at their C-terminus [Zhang *et al.* 2002]. This Klarsicht domain spans the membrane and anchors the proteins in the outer nuclear membrane of the nuclear envelope [Starr and Han, 2002]. Nesprin-2 also binds emerin and lamin A/C [Libotte *et al.* 2005].

Nesprins contain several spectrin repeat (SR) domains, each of which consists of ~106 residues that form a triple-helical bundle. SR domains mediate protein-protein interactions, crosslink actin and microtubules and function as molecular scaffolds or stabilizers. Specific nesprin isoforms seem to anchor cell organelles to the cytoskeleton, since over-expression of the Golgi-binding domain of nesprin-1 causes the Golgi apparatus to collapse [Gough *et al.* 2003], and *C. elegans* ANC-1 mutants are defective in the positioning not only of the nucleus, but also of mitochondria [Malone *et al.* 1999, Hedgecock and Thomson, 1982]. Additionally, the giant *C. elegans* ANC-1 interacts with cytoplasmic F-actin via its N-terminus, while the Klarsicht domain of its C-terminus is anchored in the outer nuclear membrane by binding to Unc-84, an inner nuclear membrane protein [Starr and Han, 2002]. Since the smaller, nucleoplasmic nesprin isoforms bind to lamins, the nesprin family may function as a nuclear envelope-bridging complex, mechanically connecting the nucleoskeleton with the actin cytoskeleton via small isoforms, lamins, unc-84 and the giant nesprin isoforms [Gruenbaum *et al.* 2005].

1.2.2.1.4 MAN1

MAN1, an inner nuclear membrane protein with two putative transmembrane domains (thus exposing both the N- and C-termini to the nucleoplasm) and a LEM domain near its N-terminus, was initially identified by an autoantibody from a patient with a collagen vascular disease [Lin *et al.* 2000]. In *Xenopus*, MAN1 binds directly to receptor-regulated SMAD (R-SMAD) proteins [Osada *et al.* 2003], which mediate signalling downstream of bone morphogenetic proteins (BMPs) and other members of the TGF β -superfamily [ten Dijke and Hill, 2004]. MAN1 inhibits this signal transduction pathway and can therefore regulate gene expression notably that of SMAD-dependent genes such as Msx1, a transcription factor involved in repressing muscle differentiation [Nakayama *et al.* 2000, Lee *et al.* 2004].

MAN1 also interacts with BAF via its LEM domain and a second binding site and reveals an extensive functional overlap with emerin, another inner nuclear membrane protein [Mansharamani and Wilson, 2005]. Apart from binding to emerin directly, MAN1 binds *in vitro* to many of its interaction partners like the lamins A and B1 and the transcription regulators GCL and Btf [Mansharamani and Wilson, 2005], suggesting that MAN1 and emerin form functional complexes at the inner nuclear membrane.

1.2.2.1.5 Emerin

Structure and distribution

Human emerin is a serine-rich protein of 254 amino acids with a molecular mass of 34 kDa and is encoded by the *STA* gene which locates to the X chromosome (Xq28) and consists of six exons of 2100 base pairs [Bione *et al.* 1994]. Emerin is evolutionary conserved, it was found in a range of vertebrates like primates, rodents, amphibians and marsupials [Dabauvalle *et al.* 1999] and in *C. elegans* [Lee *et al.* 2000]. In humans, mRNA and protein studies show an ubiquitous tissue distribution, with the highest expression in skeletal and cardiac muscle [Bione *et al.* 1994, Manilal *et al.* 1996, Nagano *et al.* 1996]. Immunological staining with antisera raised against regions of emerin demonstrated that the majority of the protein is localised to the nuclear envelope [Manilal *et al.* 1996, Nagano *et al.* 1996], with small percentages of emerin residing in the endoplasmic reticulum (ER) [Östlund *et al.* 1999] and in the nucleoplasm [Manilal *et al.* 1998, Squarzoni *et al.* 1998]. Structural analysis predicts emerin to be a type II membrane protein, with a transmembrane region 11 residues from the C-terminus and a large hydrophilic N-terminal domain oriented towards the nucleoplasm. This N-terminal domain contains 22 potential phosphorylation sites for a wide range of kinases, including those associated with cell cycle-mediated events [Manilal *et al.* 1996, Nagano *et al.* 1996, Cartegni *et al.* 1997, Ellis *et al.* 1998].

Apart from the transmembrane domain, emerin possesses another region of high sequence identity, the LEM module, with the inner nuclear membrane proteins LAP2 and MAN1 [Lin *et al.* 2000] and several *Drosophila* proteins like Otefin and Bocksbeutel [Padan *et al.* 1990, Wagner *et al.* 2004]. This LEM domain with its ~40 residues appears to be the only region in the protein with stable globular structure [Wolff *et al.* 2001], leading to the speculation that, outside of the LEM domain, emerin may be flexible and may adapt specific structural configurations only when bound to its partners [Bengtsson and Wilson, 2004]. Figure 1.5 gives a schematic overview of emerin structure and interaction partners.

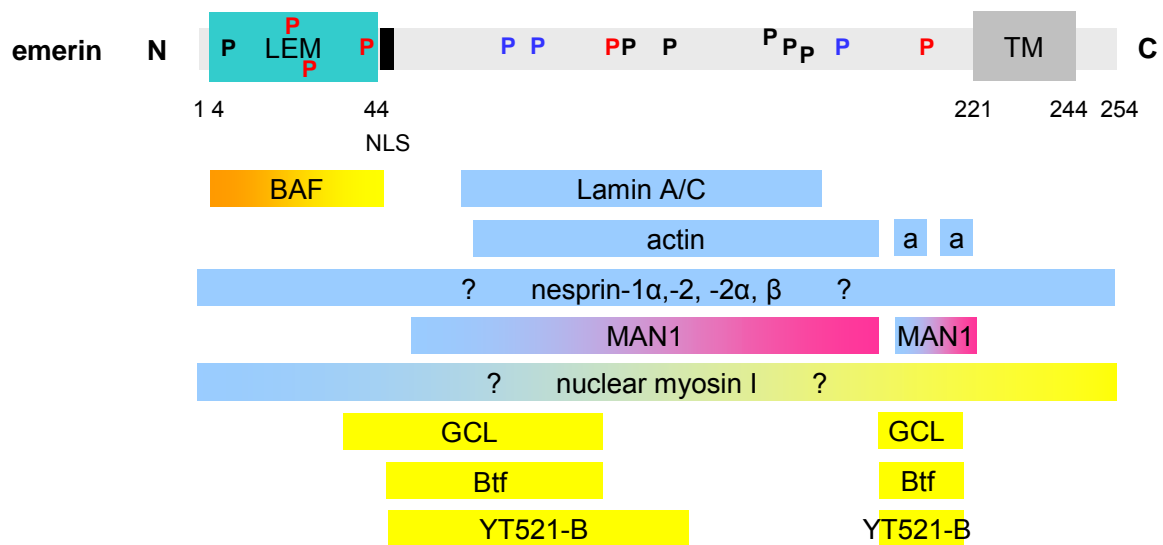


Fig. 1.5. Schematic diagram of emerlin structure and of regions to which partners bind (not to scale). Numbers indicate amino acid positions, P potential phosphorylation sites: casein II-kinase (black), protein kinase C (red), cAMP-dependent kinase (green) and tyrosine kinase (blue). The LEM domain is shown in turquoise, the nuclear localisation signal (NLS) in black and the transmembrane domain (TM) in dark grey. Coloured bars indicate the region(s) in emerlin required for each named partner to bind; for partners with question marks, the binding region in emerlin is unmapped. Based on current incomplete knowledge, interactions were loosely colour-coded as blue (architectural), orange (chromatin), yellow (gene regulation) and pink (signal transduction). N amino-, C carboxyl-terminus.

The nuclear envelope localisation of emerlin is only valid for cells in interphase of the cell cycle; in mitosis with its profound rearrangements and molecular alterations, emerlin distribution also changes dramatically [Haraguchi *et al.* 2000, Dabauvalle *et al.* 1999, Manilal *et al.* 1998]. At prometaphase, when nuclear envelope disassembly has been completed, emerlin is released into the cytoplasm [Dabauvalle *et al.* 1999, Manilal *et al.* 1998], where it is restricted to vesicles or ER tubules [Collas and Courvalin, 2000]. During anaphase, emerlin is observed around the condensed chromosomes, with a focal concentration in the area of the spindle poles [Haraguchi *et al.* 2000, Dabauvalle *et al.* 1999]. At the initial stage of nuclear reassembly in early telophase, emerlin shows a focal accumulation on either side of the chromosomes and a clear labelling of the mid-body [Dabauvalle *et al.* 1999]. By late telophase, emerlin is redistributed over the nuclear periphery, and this occurs before nuclear import activity is regained [Haraguchi *et al.* 2000, Dabauvalle *et al.* 1999, Manilal *et al.* 1998].

Interestingly, emerlin co-localises with A-type lamins but not with either LAP2, LBR or B-type lamins during telophase [Haraguchi *et al.* 2000, Dabauvalle *et al.* 1999], suggesting a

specific role for emerin and lamins A/C in the early steps of nuclear envelope reassembly at the end of mitosis [Dabauvalle *et al.* 1999]. This theory is supported by the existence of four differently phosphorylated forms of emerin, three of which are associated with cell cycle-dependent events [Ellis *et al.* 1998], and the fact that over-expression of mutated forms of emerin can perturb cell cycle timing in cultured cells [Fairley *et al.* 2002]. Also, emerin depletion by microinjection of anti-emerin antibodies into culture cells inhibits cell division in telophase [personal observation].

Interaction partners and functions

The number of proteins that have been identified as emerin binding partners is constantly rising, thus emphasising its involvement in many nuclear functions. Although the absence of emerin does not impair cell viability neither in human (HeLa) cells nor in *Xenopus* oocytes or in *C. elegans* embryos [Harborth *et al.* 2001, Gareiss *et al.* 2005, Gruenbaum *et al.* 2002], experiments with emerin-deficient *C. elegans* embryos showed that LEM-domain proteins, collectively, are essential [Liu *et al.* 2003]. Emerin interaction partners can be roughly divided into two groups: architectural proteins, important for maintaining nuclear structure and its position within the cell, and proteins associated with the chromatin and gene regulation (see also Fig. 1.5) [Bengtsson and Wilson, 2004].

First evidence for an emerin binding to A-type lamins was provided by co-immunoprecipitation and protein overlay assays which demonstrated an interaction of emerin with lamin A/C and, to a lesser extent, with B-type lamins and nuclear actin [Fairley *et al.* 1999]. Direct interaction of emerin to lamin A has been confirmed on the molecular level [Clements *et al.* 2000], and the lamin A binding region in emerin was mapped to residues 70-178 [Lee *et al.* 2001, Sakaki *et al.* 2001]. This central domain includes residues 117-170, which function as a nuclear membrane retention signal for emerin [Östlund *et al.* 1999, Tsuchiya *et al.* 1999]; indeed, lamin A is required for both emerin and lamin C nuclear envelope localisation [Vaughan *et al.* 2001]. Emerin is proposed to anchor the filament network formed by A-type lamins to the inner nuclear membrane and therefore acts as a part of a nuclear stabilising system [Manilal *et al.* 1999]. However, since both emerin and the A-type lamins interact with a large range of other proteins, the emerin-lamin A/C complex is more likely to provide a nuclear scaffolding of multiple interactions sites for these proteins and their specific functions (see below and 1.2.2.2).

Other architectural partners for emerin are proteins of the nesprin family: emerin binds tightly to the nesprin isoforms 1 α , 2, 2 α and 2 β , which in turn interact with lamin A [Mislow *et al.* 2002b, Zhang *et al.* 2005, Libotte *et al.* 2005]. Since the nesprins are thought to mechanically bridge the nuclear envelope and connect the nucleo- with the cytoskeleton [Gruenbaum *et al.* 2005], emerin may play a role in cross-linking the smaller isoforms with lamin A, thereby stabilising these protein complexes at the inner nuclear membrane [Zhang *et al.* 2005].

MAN1, a LEM-domain protein of the INM, is another recently identified binding partner of emerin with which it shares interactions to several gene regulatory proteins like BAF, GCL and Btf as well as to the lamins [Mansharamani and Wilson, 2005]. The two proteins have at least partially overlapping functions, being essential for cell division and chromosome segregation in *C. elegans* embryos [Liu *et al.* 2003]. Since MAN1 inhibits the SMAD-signal transduction pathway [Osada *et al.* 2003], emerin may also be involved in this form of gene regulation, either by binding to a yet unknown protein or via its MAN1 interaction.

Emerin binds filamentous (F)-actin *in vitro* [Fairley *et al.* 1999] and it co-immunoprecipitates with lamins, α -actin, β -actin and protein kinase A (PKA) from mature muscle and differentiating myotubes [Lattanzi *et al.* 2003], indicating that the composition or function of nuclear emerin-lamin-actin complexes might be regulated via phosphorylation by PKA. Nuclear actin is involved in many activities including chromatin remodelling, the formation of heterogeneous nuclear RNA particles, stress responses, nuclear export and transcription [for review, see Pederson and Aebi, 2002]. Emerin also co-purifies with nuclear-specific isoforms of α II-spectrin, a filamentous protein that binds F-actin [Holaska *et al.* 2004], and with a nuclear-specific isoform of myosin I [Bengtsson and Wilson, 2004], an actin-dependent motor which is required for transcription by RNA polymerase II [Pestic-Dragovich *et al.* 2000]. Thus, emerin may contribute to the formation of an actin-based cortical network at the inner nuclear membrane, conceptually analogous to the actin cortical network at the plasma membrane [Holaska *et al.* 2004].

The group of known emerin interaction partners that are implicated in gene expression comprise four proteins so far: barrier-to-autointegration factor (BAF) [Lee *et al.* 2001], germ-cell-less (GCL) [Holaska *et al.* 2003], BCL2-associated transcription factor (Btf) [Haraguchi *et al.* 2004] and YT521-B [Wilkinson *et al.* 2003].

Similar to all characterized LEM-domain proteins, emerin binds to BAF via its LEM-domain (residues 4-44), although the physiological BAF-binding domain might extend beyond this 40 amino acid fold [Lee *et al.* 2001]. Interaction with BAF is essential for emerin's reassembly at the nuclear envelope after mitosis [Haraguchi *et al.* 2001]. BAF binds directly to dsDNA

[Zheng *et al.* 2000] and, in retinal cells, to the homeodomain transcription activator cone-rod homeobox protein (CRX), and represses CRX-dependent genes *in vivo* [Wang *et al.* 2002]. While BAF is highly mobile in interphase cells, it has a decreased rate of diffusion near the nuclear envelope, due to frequent but transient binding to emerin and, presumably, other LEM-domain proteins [Shimi *et al.* 2004].

Emerin co-immunoprecipitates with GCL from HeLa cells and forms a stable trimeric complex with GCL and lamin A *in vitro* [Holaska *et al.* 2003]. GCL is a transcriptional regulator which represses E2F-DP3-dependent gene expression [Nili *et al.* 2001, de la Luna *et al.* 1999]. Probably due to partially overlapping binding sites for GCL, BAF and lamin A in emerin, GCL is displaced by BAF *in vitro* [Holaska *et al.* 2003, Lee *et al.* 2001]. The mutually exclusive binding of GCL and BAF to emerin indicates that emerin can form at least two distinct lamin-anchored complexes at the nuclear membrane [Gruenbaum *et al.* 2005].

As another gene regulatory interaction partner, emerin binds Btf [Haraguchi *et al.* 2004], a transcription repressor that induces cell death when overexpressed [Kasof *et al.* 1999]. Emerin is speculated to sequester Btf and, thus, suppress apoptosis [Tzur *et al.* 2002]. While emerin is not cleaved during apoptosis in either *C. elegans* [Tzur *et al.* 2002] or mammalian Jurkat T cells [Gotzmann *et al.* 2000], apoptotic cleavage occurs in proliferating mouse myoblasts and differentiating myotubes in a caspase-6-dependent manner [Columbaro *et al.* 2001].

The last protein of this gene regulation group binding to emerin is YT521-B which recognizes the GCL-binding region in emerin [Wilkinson *et al.* 2003], similar to Btf. YT521-B is involved in choosing sites for alternative mRNA splicing, and emerin influences splice site selection by YT521-B *in vivo* [Wilkinson *et al.* 2003].

The discovery that emerin interacts with several transcription regulators and an RNA splicing factor implies that it might be involved in the regulation of transcription. Indeed, DNA microarray experiments have compared the gene expression profiles of fibroblasts from X-EDMD patients and controls and identified ~60 affected genes in the patients, most of them being upregulated [Tsukahara *et al.* 2002]. By exogenously expressing wild-type emerin in the X-EDMD cells, normal expression was restored for 28 of these genes, i.e. those encoding for the lamins A and C and α II-spectrin [Tsukahara *et al.* 2002].

Emerin seems to anchor a variety of protein complexes at the inner nuclear membrane. These complexes, and emerin itself, are likely to have multiple and distinct functions, including roles (direct or indirect) in gene expression, roles in regulating a functional actin cortical network at the NE and roles in nuclear assembly after mitosis [Bengtsson and Wilson, 2004].

1.2.2.2 Main components of the nuclear lamina – nuclear lamins

Structure and distribution

Lamin proteins are the major components of the nuclear lamina [for review, see Stuurman *et al.* 1998]. They are grouped into A- and B-types based on their biochemical and structural properties and their behaviour during mitosis. B-type lamins are essential for cell viability, are expressed in all cells during development, have acidic isoelectric points when separated on the basis of their electric charge, and are post-translationally modified by isoprenylation [Georgatos *et al.* 1994, Gerace and Burke, 1988]. This modification helps B-type lamins attach to the INM during interphase and to remain attached to membranes (specifically, ER membranes) when the nuclear envelope disassembles during mitosis. A-type lamins are dispensable, are expressed in a tissue-specific manner, have neutral isoelectric points, disperse as soluble proteins during mitosis and are probably incorporated into the nuclear lamina later than B-type lamins during post-mitotic nuclear assembly [Georgatos *et al.* 1994, Gerace and Burke, 1988].

No lamin genes have been found in the genome of the plants *Arabidopsis thaliana* and rice or in the yeast species *S. cerevisiae* and *S. pombe*. During evolution, lamins probably appeared first in animal cells during the transition from a closed to an open mitosis [for review, see Cohen *et al.* 2001]. The number of lamin genes seems to increase in evolution: while the genome of *C. elegans* contains only one lamin gene, encoding a B-type protein termed Ce-lamin [Liu *et al.* 2000], the *Drosophila* genome already possesses two lamin genes, one for a B-type (lamin Dm₀) and the other for an A-type lamin (lamin C) [Gruenbaum *et al.* 1988, Bossie and Sanders, 1993]. Vertebrates have three or four different lamin genes; mammalian genomes typically contain three lamin genes, two B-type (*LMNB1* and *LMNB2*) [Höger *et al.* 1988, 1990] and one A-type lamin gene (*LMNA*) [Fisher *et al.* 1986, McKeon *et al.* 1986].

The mammalian *LMNB1* gene encodes for only one protein (lamin B1), whereas the *LMNB2* gene gives rise to at least two isoforms generated by alternative mRNA splicing, lamin B2 and the germ line-specific lamin B3 [Furukawa and Hotta, 1993]. Humans synthesise four A-type lamins from their *LMNA* gene, with the two most abundant isoforms being the lamins A and C. These two proteins are identical for their first 566 amino acids (exons 1-10 of 12) and differ only in their carboxyl-terminal tail, the lamin C carboxyl domain extending 6 amino acids beyond the point of divergence from lamin A and the lamin A carboxyl domain extending 98 amino acids further [Fisher *et al.* 1986]. Another splice variant encodes lamin

A Δ 10 which lacks the small exon 10 in the lamin A tail domain [Machiels *et al.* 1996]. Lamin C2 is a germ line-specific lamin [Furukawa *et al.* 1994] possessing a unique hexapeptide in its amino-terminus while lacking the head and part of the lamin C rod domain [Alzheimer *et al.* 2000].

As type V intermediate filament proteins, lamins consist of an N-terminal head domain, a central α -helical coiled-coil (rod) domain responsible for dimerisation, and a large globular C-terminal domain [for review, see Krohne 1998]. The head domain of most lamins contains a conserved p34^{cdc2} site which undergoes phosphorylation during mitosis [Heald and McKeon, 1990, Peter *et al.* 1990, 1991]. The α -helical rod domain is similar to all intermediate filaments and consists of four helices termed 1A, 1B, 2A and 2B, which are separated by highly conserved linkers (L1, L12 and L2) [Stuurman *et al.* 1998]. The most conserved sequences between all lamins are the beginning of coil 1A and the end of coil 2B plus the first 10 residues in the tail domain, which are responsible for their head-to-tail filament assembly [Strelkov *et al.* 2002]. The tail includes an immunoglobulin (Ig)-fold domain, the backbone organisation of which is unique to lamins (in A-type lamins formed by residues 430-545) [Dhe-Paganon *et al.* 2002, Krimm *et al.* 2002], and a nuclear localisation signal (NLS) which targets the lamins to the nucleus [Loewinger and McKeon, 1988].

All lamins except C and C2 also contain a CAAX (Cys-aliphatic-aliphatic-any residue) box at the C-terminus which is essential for their NE targeting [Nigg, 1992]. The CAAX motif is farnesylated on the cysteine *in vivo* prior to proteolytic removal of the AAX sequence and subsequent methyl esterification of the cysteine residue [Hennekes and Nigg, 1994, Kitten and Nigg, 1991]. This modified cysteine plus 14 additional residues (647-661) are then cleaved from pre-lamin A to yield mature lamin A [Krohne 1998]. A site-specific protease termed ZMPSTE24 is proposed to perform both cleavage events [Pendas *et al.* 2002]; to date, lamin A is the only known substrate for this protease in mammals.

The assembly of lamin proteins into the nuclear lamina is not fully understood yet [Krohne 1998]. The α -helical segments of the lamin rod domain are composed of heptad repeats with hydrophobic amino acids at the first and fourth positions [Krohne 1998]; as expected for this characteristic for coiled-coil-forming proteins, lamins produce parallel aligned homodimers during or immediately after translation [Krohne *et al.* 1987]. After transport into the nucleus, the farnesylated cysteine mediates the attachment at the inner nuclear membrane [Kitten and Nigg, 1991], although this domain in itself is not sufficient for the retention of lamins at the NE [Schmidt-Zachmann *et al.* 1993]. Since lamin C lacks the CAAX box, it relies on the formation of heterodimers with lamin A for correct nuclear lamina incorporation [Vaughan *et*

al. 2001]. Finally, lamin dimers assemble into the pre-existing lamina by forming longitudinal polymers in a head-to-tail manner [Heitlinger *et al.* 1991, Aebi *et al.* 1986]. How these polymers are woven into the meshwork of the existing lamina is not clear yet; *in vitro*, head-to-tail polymers aggregate laterally and form paracrystals with alternating light-and dark-stained bands and an axial repeat of 22-25nm [Heitlinger *et al.* 1991, Klapper *et al.* 1997]. However, only in manually isolated *Xenopus* oocyte nuclear envelopes a similar periodicity was found in the lamina filaments [Aebi *et al.* 1986], whereas such a paracrystalline morphology is not apparent even in the thick nuclear lamina of mammalian cells [Höger *et al.* 1991].

The mitotic disassembly of the nuclear lamina is achieved by the phosphorylation of SP/TP motives (S serine, T threonine, P proline) flanking the central rod domains of the lamins [Nigg 1992]. A-type lamins are released into the cytoplasm as soluble proteins, whereas B-type lamins remain attached to vesicles of the nuclear membranes. Lamins are likely to play a role in the reassembly of the nuclear envelope after mitosis, although there are some contradictory results [for review, see Gruenbaum *et al.* 2003]. Figure 1.6 gives a schematic overview of the structure of the lamins A and C and their interaction partners.

Interaction partners of A-type lamins and functions

The nuclear lamins bind to and interact with a confusing multitude of proteins, so for better clarity, priority is set upon the A-type lamins. Their interaction partners form four loose groups: architectural, chromatin, gene regulatory and signal transduction partners, some of them fitting more than one category [Zastrow *et al.* 2004].

By definition, architectural interaction partners form stable complexes with A-type lamins during interphase, show a tight *in vitro* binding to them or have known structural roles in other contexts, i.e. actin. They might connect lamins to the nuclear envelope, to the chromatin and other subnuclear structures or to the cytoskeleton of the cell [Gruenbaum *et al.* 2005, Cohen *et al.* 2001]. This group includes several integral membrane proteins like LAP1 [Foisner and Gerace, 1993], the nesprin isoforms 1 α , 2, 2 α and 2 β [Mislow *et al.* 2002b, Zhang *et al.* 2005, Libotte *et al.* 2005], emerin [Fairley *et al.* 1999] and MAN1 [Mansharamani and Wilson, 2005], but also non-membrane proteins like the lamins itself [Stuurman *et al.* 1998], nuclear actin [Sasseville and Langelier, 1998] and LAP2 α [Dechat *et al.* 2000].

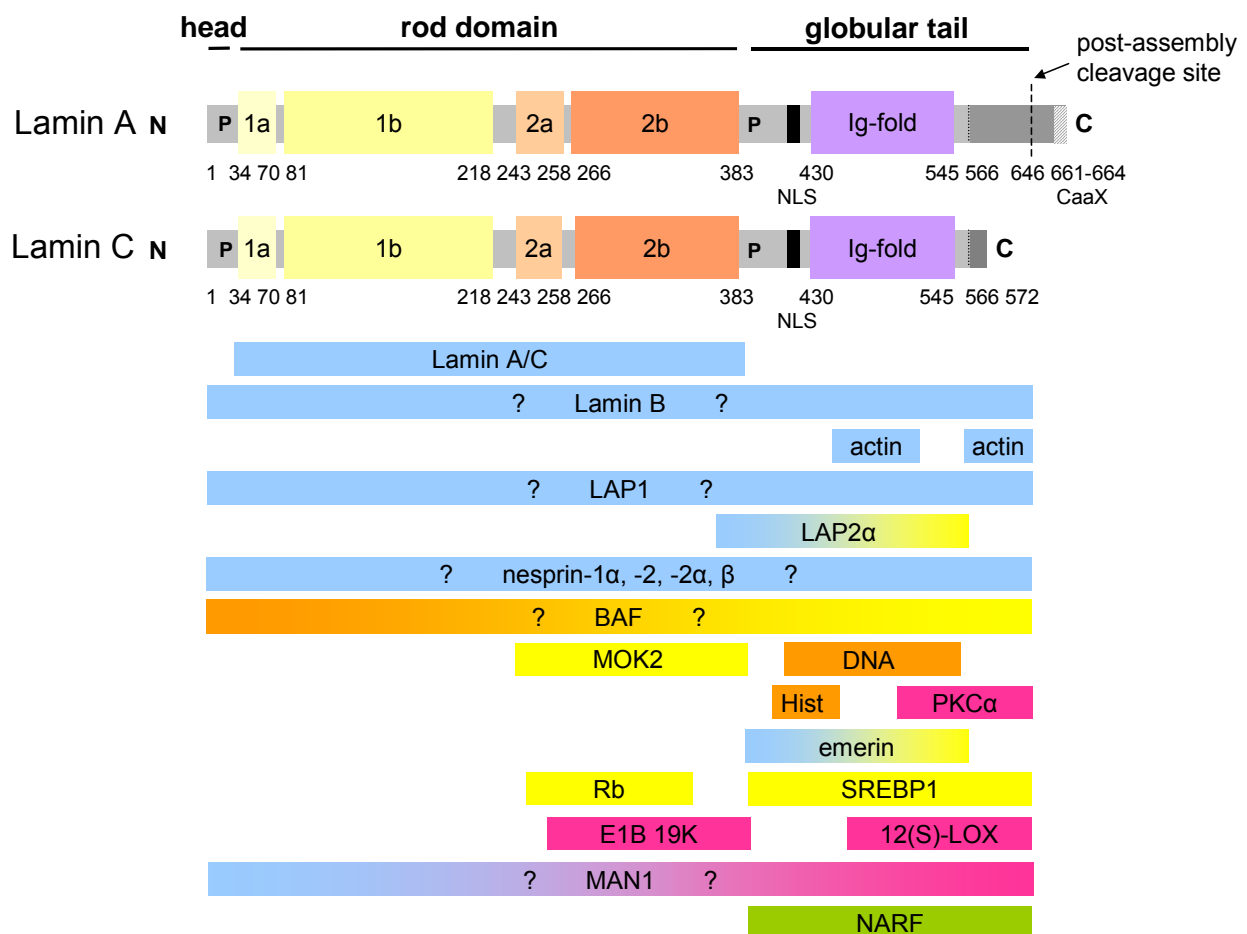


Fig. 1.6. Schematic diagram of lamin A/C structure and of regions to which partners bind (not to scale). Numbers indicate amino acid positions, P potential phosphorylation sites. The four helices of the rod domain are shown in light yellow (1A, 1B) and in light orange (2A, 2B), the nuclear localisation signal (NLS) in black and the immunoglobuline-like fold in purple. The lamins A and C differ only in their C-terminal tail, indicated by different shades of grey. The CAAX box at the C-terminus of lamin A is marked by diagonal bars. Coloured bars indicate the region(s) in lamins A/C required for each named partner to bind; for partners with question marks, the binding region is unmapped. Based on current incomplete knowledge, interactions were loosely colour-coded as blue (architectural), orange (chromatin), yellow (gene regulation), pink (signal transduction) and green (unknown). N amino-, C carboxyl-terminus.

A-type lamins dimerise with each other for correct nuclear lamina localisation [Vaughan *et al.* 2001], but it is not clear whether they bind directly to B-type lamins *in vivo*. Since A- and B-type lamins have distinct assembly pathways [Moir *et al.* 2000] they might form separate networks. Although B-type lamins are probably necessary for the formation of A-type filaments [Gruenbaum *et al.* 2003].

LAP1 has an unusually large luminal domain and is expressed as multiple isoforms, but its interaction with lamins has not been further characterised [Foisner and Gerace, 1993, Martin *et al.* 1995]. More information is available for the other LEM-domain proteins emerin and MAN1: they cross-link the architectural function of the nuclear lamina with gene regulatory aspects by binding various transcription regulators like GCL or Btf [Holaska *et al.* 2003, Haraguchi *et al.* 2004, Mansharamani and Wilson, 2005]. Via its interaction with SMAD proteins, MAN1 might also connect A-type lamins with this signal transduction pathway and a role during embryonic development [Osada *et al.* 2003]. The emerin binding domain lies within the C-terminal tail of lamin A/C (residues 384-566) [Lee *et al.* 2001, Sakaki *et al.* 2001] and its high *in vitro* affinity to emerin of 40nM suggests a very tight binding [Holaska *et al.* 2003]. Emerin is involved in the stabilisation of nuclear actin filaments; lamin-bound, it is proposed to anchor an actin-and spectrin-containing structural network at the INM [Holaska *et al.* 2004]. This model is supported by the fact that actin also binds directly to two regions in the lamin A/C tail (residues 461-536 and residues 563-646) [Zastrow *et al.* 2004, Sasseville and Langelier, 1998], thus providing this cortical network with additional strength.

The giant isoform 2 as well as the small isoforms 1 α , 2 α and 2 β of the nesprin protein family bind both A-type lamins and emerin [Libotte *et al.* 2005, Mislou *et al.* 2002b, Zhang *et al.* 2005] and are thought to link the nucleoskeleton via the nuclear lamina and a nuclear membrane bridging complex to the cytoskeleton, therefore playing a role in the positioning of the cell nucleus [Gruenbaum *et al.* 2005].

The best studied and last architectural partner for A-type lamins in the nuclear interior is LAP2 α , with separate binding sites for BAF, lamins and chromatin [Dechat *et al.* 1998, 2000, Vlcek *et al.* 1999]. LAP2 α binds tightly to residues 319-566 of lamin A/C in interphase [Dechat *et al.* 2000], but has dynamic architectural roles during nuclear envelope assembly [Vlcek *et al.* 2002]. It is proposed to tether A-type lamins to intranuclear sites and to cooperate with lamins in organizing chromatin [Foisner, 2003]. Similar to emerin and other LEM-domain proteins, it also connects the architectural function with an influence on gene regulation by interaction with transcription regulators like BAF [Vlcek *et al.* 2001].

Lamins bind DNA directly but non-specifically *in vitro* by contacting the minor groove [Luderus *et al.* 1994]. The DNA-binding region of the lamins A and C with a DNA affinity of 420 nM was mapped to residues 411-553, thus including both the Ig-fold domain and the NLS in the tail [Stierle *et al.* 2003]. DNA is wound around core histone octamers to form nucleosomes, the fundamental unit of chromatin structure. The human lamin A/C tail (residues 396-430) binds to mixtures of core histones with an affinity of 300 nM [Taniura *et al.* 1995]. In a nucleus full of histones and DNA, this proximity to chromatin allows the A-type lamins to serve as possible scaffolds for multiprotein complexes associated with chromatin [Zastrow *et al.* 2004].

BAF qualifies as a chromatin as well as a gene regulatory partner for lamin A, to which it binds with 1 μ M affinity *in vitro* [Holaska *et al.* 2003]. Apart from its function as a repressor of CRX-dependent genes [Wang *et al.* 2002], BAF binds non-specifically to dsDNA [Zheng *et al.* 2000] and co-localises with chromatin in *Drosophila* embryos, where loss of BAF also causes chromatin and nuclear envelope defects [Furukawa *et al.* 2003]. In *Xenopus* egg extracts, excess BAF present during nuclear assembly can profoundly alter chromatin structure [Segura-Totten *et al.* 2002], confirming its importance as an architectural partner for lamin A.

Other gene regulatory partners for lamin A/C include hypophosphorylated retinoblastoma protein (Rb) [Ozaki *et al.* 1994], sterol-response-element-binding proteins 1a and 1c (SREBP1a/c) [Lloyd *et al.* 2002] and Krüppel-like protein (MOK2) [Dreuillet *et al.* 2002].

Rb, a transcriptional regulator with central roles in cell-cycle control, binds the rod domain of lamin A (residues 247-355) [Ozaki *et al.* 1994]. As a repressor, Rb inhibits E2F-dependent gene expression through a variety of mechanisms, including the recruitment of histone deacetylase complexes (HDACs), and is involved in regulating apoptosis [Chau and Wang, 2003]. A scaffolding model has been proposed in which Rb activity depends on its attachment to lamins and LAP2 α [Zastrow *et al.* 2004].

Encoded by alternatively spliced mRNAs, SREBP1a and SREBP1c are basic helix-loop-helix leucine zipper transcription factors that, when activated, are released from the ER by proteolytic cleavage. Once moved into the nucleus, they activate genes required for cholesterol biosynthesis and lipogenesis and promote adipocyte differentiation [Horton, 2002]. Their binding region in the A-type lamins lies in the Ig-fold domain, at residues 389-664 [Lloyd *et al.* 2002]. However, SREBP1 seems to interact preferentially with the lamin A precursor *in vivo* [Capanni *et al.* 2005].

Three signalling proteins are known to bind A-type lamins *in vivo*; lamin filaments might therefore provide a structural basis for signal transduction pathways. Protein kinase C α (PKC α) binds to residues 500-664 in the C-terminal tail of lamin A/C and has distinct lamin- and substrate-binding regions [Martelli *et al.* 2002]. In response to elevated diacylglycerol levels, PKC α translocates to the nucleus and interacts with lamins, suggesting that signal transduction by PKC α might involve its attachment to a lamin scaffold [Ron and Kazanietz, 1999].

12(S)-lipoxygenase (12(S)-LOX) also binds the lamin A/C tail (residues 463-664) and is present in the cytoplasm as well as in the nucleus of cells [Tang *et al.* 2000]. It is part of a lipid-signalling pathway that converts arachidonic acid into an activator of PKC α [Liu *et al.* 1994]. Speculatively, PKC α moves into the nucleus and co-docks with 12(S)-LOX on lamin A/C filaments, or nuclear-localised PKC α is activated in a 12(S)-LOX-dependent manner [Zastrow *et al.* 2004]. The third signalling partner, E1B 19K, is an adenovirus early protein [Cuconati and White, 2002] which binds directly to lamin A in yeast two-hybrid assays (to residues 252-390) and co-fractionates with lamins *in vivo* [Rao *et al.* 1997]. In adenovirus-infected cells, E1B 19K localises to the ER and nuclear membranes and blocks apoptosis in a lamin-dependent manner [Rao *et al.* 1997]. It also interacts with (and potentially inactivates) the death promoting repressor Btf [Kasof *et al.* 1999] which in turn binds to emerin *in vitro* [Holaska *et al.* 2004]. Emerin-lamin complexes might thus provide assembly sites for these regulatory proteins.

Apart from the many lamin A/C interaction partners which can be classified, there are some that have no known functions. One of these proteins is the nuclear pre-lamin A recognition factor (Narf), which is expressed at its highest levels in heart, skeletal muscle and brain, localises to the nuclear envelope and intranuclear foci and binds specifically to farnesylated lamin A precursors (at residues 389-664) [Barton and Worman, 1999]. Fig. 1.7 gives a short overview of the interactions between proteins of the nuclear lamina.

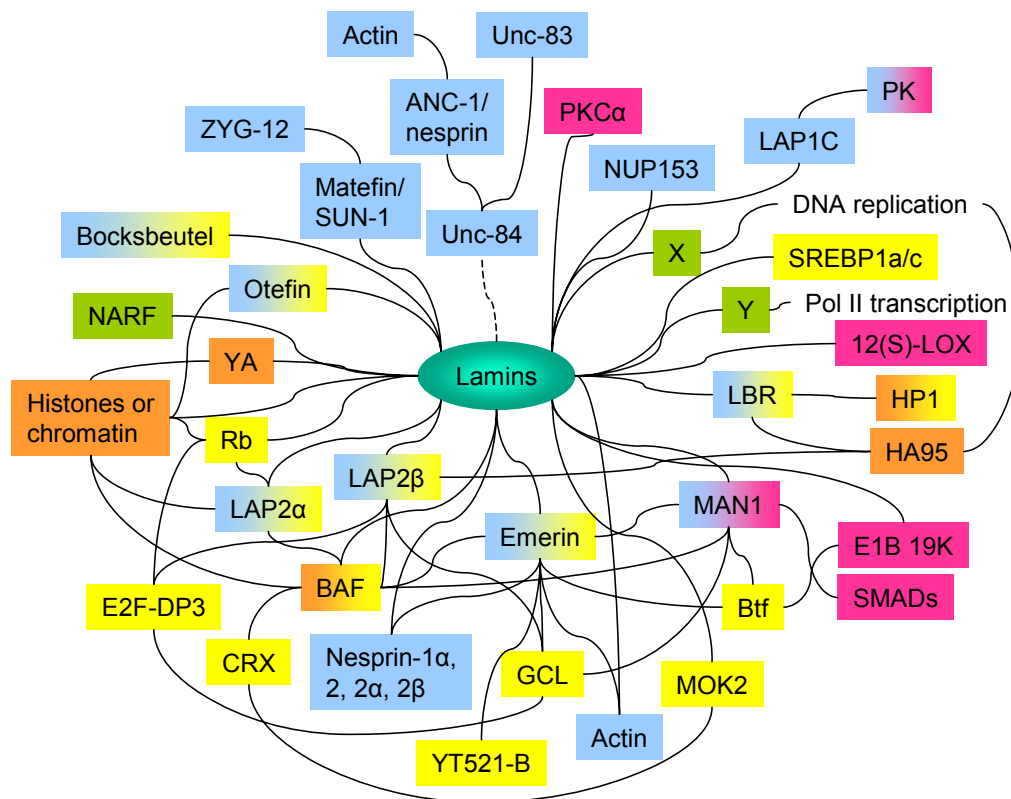


Fig. 1.7. A summary of interactions between the proteins of the nuclear lamina. Lines connect pairs of proteins that interact directly *in vitro*, or indicate activities (i.e. DNA replication) that depend on lamins. For interrupted lines, direct interaction has not been shown yet. Protein functions are loosely colour-coded again, as blue (architectural), orange (chromatin), yellow (gene regulation), pink (signal transduction) and green (unknown). X and Y represent unknown proteins. See text for abbreviations of proteins.

To summarize, A- and B-type lamins and their associated proteins are proposed to have roles in large-scale chromatin organisation [Liu *et al.* 2000, 2003, Sullivan *et al.* 1999, Guillemin *et al.* 2001], the spacing of nuclear pore complexes [Liu *et al.* 2000, Schirmer *et al.* 2001], the positioning of the nucleus in the cell [Starr *et al.* 2001, Starr and Han, 2002] and the reassembly of the nucleus after mitosis [Lopez-Soler *et al.* 2001]. Furthermore, essential nuclear functions depend on lamins, notably DNA replication [Spann *et al.* 1997], RNA polymerase II-dependent gene expression [Spann *et al.* 2002] and apoptosis [Earnshaw, 1995]. Lamins might further anchor multiprotein complexes in which integral proteins of the ONM and INM bridge the perinuclear space, thereby mechanically coupling the nucleoskeleton with the cytoskeleton [Starr *et al.* 2001, Lee *et al.* 2002, Malone *et al.* 2003, Zhen *et al.* 2002].

1.3 Nuclear envelope proteins in disease – the laminopathies

1.3.1 Human diseases due to mutations in lamins or lamin-associated proteins

Since the lamins play such a crucial role in the functioning of the cell nucleus, being at the centre of an intricately woven web of protein interactions, it is not surprising to find a multitude of human diseases caused by mutations in the *LMNA* gene (mutations in B-type lamins are presumably prenatally lethal) or in lamin-associated proteins. These diseases are collectively called ‘laminopathies’; table 1.2 gives a short overview.

Laminopathies fall into four classes: those diseases affecting striated muscle, those affecting adipose tissue, those displaying peripheral neuropathy and those involving bone malformations [Broers *et al.* 2004, Gruenbaum *et al.* 2005]. However, all of them are related via some rare premature aging syndromes that form links between the different tissues affected [Worman and Courvalin, 2004].

The striated muscle disorders include autosomal dominant, autosomal recessive and X-linked Emery-Dreifuss muscular dystrophy (AD-, AR- and X-EDMD, respectively), limb girdle muscular dystrophy type 1B (LGMD1B) and dilated cardiomyopathy with conduction system defect type 1A (DCM1A) [Bonne *et al.* 1999, Di Barletta *et al.* 2000, Bione *et al.* 1994, Muchir *et al.* 2000, Fatkin *et al.* 1999]. The common feature of these diseases is cardiac arrhythmia which can be life-threatening if left untreated without defibrillation or the insertion of a pacemaker. Except X-EDMD, all diseases are caused by mutations in the *LMNA* gene; the mutations occur throughout the coding region and lead to dominant point mutations (via amino acid substitutions) or null phenotypes due to frameshift or premature stop codons [Bonne *et al.* 1999, Di Barletta *et al.* 2000, Muchir *et al.* 2000, Fatkin *et al.* 1999]. Mutations in the *STA* gene encoding emerin cause X-linked EDMD [Bione *et al.* 1994]; the mutations are also distributed throughout the coding region and generally give rise to a null phenotype, although some lead to emerin’s aberrant targeting to the ER [Fairley *et al.* 1999, Ellis *et al.* 1998].

Dunnigan-type familial partial lipodystrophy (FPLD), mandibular acral dysplasia (MAD) and generalised lipodystrophy (LIRLLC) all involve white fat atrophy throughout the torso, thus leading to severe insulin resistance. In addition, MAD also displays phenotypes typical of premature aging syndromes, whereas LIRLLC is related to the striated muscle diseases through its cardiomyopathy feature [Cao and Hegele, 2000, Novelli *et al.* 2002, Caux *et al.* 2003]. In all diseases, the *LMNA* gene harbours mutations which occur as recurrent mis-sense

mutations in exons 8 and 11 (in the tail domain of lamin A/C) in the case of FPLD [Cao and Hegele, 2000, Shackleton *et al.* 2000] and as the single point mutation R527H in the case of MAD [Novelli *et al.* 2002]. Intriguingly, mutations in the ZMPSTE24 protease which processes pre-lamin A also cause MAD [Agarwal *et al.* 2003], thus presenting a second pair of proteins, next to emerin-lamin A/C, in which mutations can give rise to the same disease.

Table 1.2. Diseases related to mutations of lamins or lamin-associated proteins.

	Major phenotypes	Mutated protein	References (first description)
Autosomal dominant / recessive Emery-Dreifuss muscular dystrophy (EDMD)	Early contractures of tendons, progressive muscle weakness and wasting, conduction defects in heart	Lamin A/C	Bonne <i>et al.</i> 1999, Di Barletta <i>et al.</i> 2000
X-linked EDMD	As above	Emerin	Bione <i>et al.</i> 1994
Limb girdle muscular dystrophy type 1B (LGMD1B)	Progressive muscle weakness of hip girdle and proximal arm and leg muscle	Lamin A/C	Muchir <i>et al.</i> 2000
Dilated cardiomyopathy with conduction system defects (DCM1A)	Impaired systolic function and dilation of the left or both ventricles. Variable skeletal muscle involvement	Lamin A/C	Fatkin <i>et al.</i> 1999
Generalised lipodystrophy (LIRLLC, see symptoms)	Lipoatrophy with insulin-resistant diabetes, leukomelanodermic papules, liver steatosis, hypertrophic cardiomyopathy	Lamin A/C	Caux <i>et al.</i> 2003
Dunnigan-type familial partial lipodystrophy (FPLD)	Loss of subcutaneous adipocyte tissue from extremities and trunk, excessive fat deposition in neck. Insulin resistance and diabetes	Lamin A/C	Cao and Hegele, 2000
Mandibular acral dysplasia (MAD)	Hypoplastic mandibles, dental crowding, stiff joints, partial lipodystrophy, insulin resistance	Lamin A/C or ZMPSTE24	Novelli <i>et al.</i> 2002, Agarwal <i>et al.</i> 2003
Restrictive dermopathy (RD)	Intra-uterine growth retardation, tight/rigid skin with erosions, facial abnormalities, bone-mineralization defects, neonatal lethality	Lamin A/C or ZMPSTE24	Navarro <i>et al.</i> 2004
Autosomal recessive Charcot-Marie-Tooth disorder type 2 (AR-CMT2)	Motor and sensory neuropathies with muscle weakness and wasting, foot deformities and axonal degeneration	Lamin A/C	De Sandre-Giovannoli <i>et al.</i> 2002
Hutchinson-Gilford progeria syndrome (HGPS)	Short stature, alopecia, loss of subcutaneous fat, osteolysis, musculoskeletal abnormalities, diabetes type II, premature atherosclerosis	Lamin A/C	Cao and Hegele, 2003, De Sandre-Giovannoli <i>et al.</i> 2003, Eriksson <i>et al.</i> 2003
Atypical Werner's syndrome (WS)	Scleroderma-like skin changes, cataract, subcutaneous calcification, premature atherosclerosis, diabetes mellitus	Lamin A/C	Chen <i>et al.</i> 2003
Pelger-Huët anomaly (PHA)	Hyperlobulated nuclei in blood granulocytes, developmental delay, epilepsy, skeletal abnormalities	Lamin B receptor	Hoffmann <i>et al.</i> 2002
Greenberg skeletal dysplasia (HEM)	Embryonic lethal chondrodystrophy with defective sterol $\delta(14)$ -reductase	Lamin B receptor	Waterham <i>et al.</i> 2003
Osteopoikilosis, Buschke-Ollendorff syndrome and melorheostosis	Skeletal dysplasia with increased bone density, disseminated connective-tissue nevi and hyperostosis of the cortex of tubular bones	MAN1	Hellems <i>et al.</i> 2004

Interestingly, disorders affecting mainly bone tissue are caused not by mutations in A-type lamins, but by mutated inner nuclear membrane proteins. Several mutations in the lamin B receptor (the *LBR* gene) give rise to the autosomal dominant Pelger-Huët anomaly (PHA) [Hoffman *et al.* 2002], while other, homozygous mutations cause a deficiency in LBR's function as a cholesterol biosynthetic enzyme in patients affected by Greenberg skeletal dysplasia (HEM) [Waterham *et al.* 2003]. Loss-of-function mutations in *MAN1* result in osteopoikilosis, Buschke-Ollendorff syndrome and melorheostosis [Hellemans *et al.* 2004].

Although in all diseases presented so far, the affected tissues were of mesenchymal origin, this is not completely true for Charcot-Marie-Tooth disorder type 2 (CMT2), a heterogeneous group of peripheral neuropathies. Autosomal recessive CMT2 (AR-CMT2), a rare motor and sensory neuropathy with de-myelination of peripheral nerves, is caused by a specific and unique point mutation in *LMNA*, leading to the amino acid substitution R298C [De Sandre-Giovannoli *et al.* 2002] and implying an important function of this residue in axonal survival [Broers *et al.* 2004].

The link between the tissue-specific defects of the previously described laminopathies is provided by certain premature aging (progeria) syndromes and restrictive dermopathy which are also due to *LMNA* mutations and which affect skin, hair, fat, muscle, bone and the cardiovascular system [Cao and Hegele, 2003, De Sandre-Giovannoli *et al.* 2003, Eriksson *et al.* 2003, Chen *et al.* 2003, Navarro *et al.* 2004]. Therefore, the milder laminopathies can be thought of as less severe premature aging syndromes [Broers *et al.* 2004]. Hutchinson-Gilford progeria (HGPS) is caused by *de novo* dominant mutations in exon 11 (at residue 608) of *LMNA* that activate a cryptic splice donor site resulting in the generation of a truncated lamin lacking the last 50 amino acids [Cao and Hegele, 2003, De Sandre-Giovannoli *et al.* 2003, Eriksson *et al.* 2003]. In atypical Werner's syndrome (WS), mis-sense mutations alter relatively conserved residues within the rod domain of lamin A/C (A57P, R133L, L140R) [Chen *et al.* 2003]. A neonatally lethal syndrome, restrictive dermopathy (RD), is caused by tail deletions in A-type lamins or by mutations in the gene that encodes the lamin A-processing metallo-proteinase ZMPSTE24 [Navarro *et al.* 2004].

The range, diversity and tissue-specificity of laminopathy phenotypes provide valuable clues about the functions and specific roles of the lamins A and C within the cell, and researchers have developed several models to explain these diseases.

1.3.2 How do mutations in lamins A and C cause disease ?

1.3.2.1 The structural weakness hypothesis

Since a major function of the lamina is to provide structural support for the nuclear envelope, it has been proposed that like other intermediate filament diseases, laminopathies arise because the integrity of the lamina is compromised. This would lead to structural weakness of the nucleus and an early cell death [for reviews, see Maraldi *et al.* 2005, Broers *et al.* 2004].

The structural weakness theory is based on the assumption that skeletal and cardiac muscle cells are particularly subjected to mechanical stress and that the lamins (and emerin) are part of a protective nucleo-cytoplasmic skeleton. If this reinforcing scaffold is impaired by the lack of wild type protein, the loss of integrity of the nuclear envelope would finally cause tissue degeneration leading to muscular dystrophy [Manilal *et al.* 1999, Morris and Manilal, 1999, Tsuchiya *et al.* 1999]. Indeed, ultra-structural investigations of skeletal muscle from EDMD patients reveal that the nuclear envelope is often torn, with chromatin leaking into the cytoplasm [Fidzianska *et al.* 1998, Markiewicz *et al.* 2002] or that membraneous invaginations appear [Reichart *et al.* 2004].

Further support for the mechanical stress hypothesis is provided by the *Lmna*^{-/-} mouse model: *Lmna*^{-/-} cells exhibit decreased mechanical stiffness, increased nuclear deformation, defective mechanotransduction and impaired viability under mechanical strain [Broers *et al.* 2004a, Lammerding *et al.* 2004]. In addition, defects in nuclear architecture have been detected in cardiac muscle cells which appear to promote cardiomyopathy [Nikolova *et al.* 2004]. One of these defects is the disorganisation and detachment of desmin filaments from the nuclear surface with progressive disruption of the cytoskeletal desmin network, suggesting that A-type lamins are necessary to link the cytoskeleton to the nucleus via unidentified proteins [Nikolova *et al.* 2004]. The most likely candidates for this function are members of the nesprin protein family, isoforms of which have been shown to interact with actin, emerin and lamins A/C [Mislow *et al.* 2002b, Zhang *et al.* 2005, Starr and Han, 2002].

The expression of mutated A-type lamins in the cells of laminopathy patients might therefore have two important consequences: a weakening of the cell because of a nuclear lamina with little tensile strength, unable to resist compression, and an inability to produce stress response elements due to impaired force transduction pathways [Broers *et al.* 2004].

1.3.2.2 The gene expression hypothesis

While the structural weakness hypothesis seems to provide a mechanism to explain striated muscle degeneration, it is more difficult to imagine how this contributes to white fat atrophy. To explain the laminopathies in which the affected tissues do not undergo strong mechanical stress, like FPLD, MAD and the progeria syndromes, the gene expression hypothesis has been proposed [Wilson, 2000].

This hypothesis suggests that A-type lamins are important regulators of gene expression and that certain mutations alter the way in which lamins organise the chromatin and associate with transcription factors. First evidence for a change in gene regulation was provided by the finding that the layer of heterochromatin at the nuclear lamina was disorganised, thinned or absent in cells from EDMD patients or *LMNA*^{-/-} cells [Ognibene *et al.* 1999, Sabatelli *et al.* 2001, Sullivan *et al.* 1999]. In general, heterochromatin is transcriptionally repressed or silenced by the interaction with nuclear envelope associated proteins, namely lamins, LAP2 and LBR [for review, see Stuurman *et al.* 1998], so if emerin or lamin A/C-deficient nuclei have difficulties in attaching heterochromatin to the nuclear periphery or in stabilising its structure, gene expression might change.

The importance of the nuclear envelope as a silencing environment for chromatin is further emphasised by the multitude of transcription repressors which interact with A-type lamins and emerin (see 1.2.2.1.5 and 1.2.2.2). At least two of these interactions appear to be functional. SREBP1 is a silencing factor involved in adipocyte differentiation, and mutations that cause FPLD inhibit its lamin A binding *in vitro*, but maintain its interaction with pre-lamin A [Lloyd *et al.* 2002, Capanni *et al.* 2005]. Retinoblastoma protein (Rb) not only plays a role in cell proliferation, but also in the differentiation of mesenchymal cells, including skeletal muscle and adipocytes [Novitch *et al.* 1999, Hansen *et al.* 2004]. Lamin A/C regulates Rb function [Johnson *et al.* 2004], and, in complex with LAP2 α , tethers Rb to the nucleoskeleton [Markiewicz *et al.* 2002]. In fact, expression of lamin A mutants that cause AD-EDMD in C2C12 mouse myoblasts inhibits their differentiation and promotes apoptotic cell death *in vitro* [Favreau *et al.* 2004]. Moreover, this failure to differentiate is correlated with disruption of LAP2 α /Rb complexes and loss of expression of Rb isoforms [Markiewicz *et al.* 2005].

Therefore, loss of lamin A/C function results in the loss of the capacity of muscle stem cells to differentiate; if other laminopathy mutations have similar effects on either Rb or other transcription repressors in other stem cell populations, this would lead to a failure to replace

damaged cells and tissue degeneration, as is observed in FPLD, MAD and progeria syndromes.

1.3.2.3 Other models to explain laminopathies

Apart from the two main hypotheses, a number of other theories have been developed to explain the tissue-specific damage of the laminopathies. The hypothesis that any defect of the nuclear membrane could interfere with satellite cell function, and thereby impair skeletal muscle regeneration, was advanced [Fairley *et al.* 1999]. It has also been suggested that an increased apoptosis may play a pathogenic role, at least in EDMD [Morris, 2000, Cohen *et al.* 2001, Haraguchi *et al.* 2004]. *LMNA* mutations, resulting in changes in the lamina and/or nuclear membrane composition, may also have dominant effects on the structure and function of the peripheral endoplasmic reticulum (ER), implying that impaired function of the ER, such as cholesterol regulation, fatty acid synthesis and Ca²⁺ release, accounts for the tissue specificity of the laminopathies. Alternatively, accumulation of nuclear envelope proteins like emerin in the ER could affect intracellular signalling pathways with downstream effects on gene expression and cell viability [Mounkes *et al.* 2001].

Although each of the proposed hypotheses provides a plausible explanation for the tissue defects of a specific laminopathy, it would be naïve to assume that they are mutually exclusive. It is most likely to assume that two or more mechanisms are responsible for each laminopathy and that the degree to which they contribute to the disease depends on the site and kind of the mutation, thus underlining the importance of mutation analysis.

1.3.3 Mutations of the *LMNA* gene used in this study

To date, more than 70 mutations have been detected in the *LMNA* gene, leading to a variety of laminopathies [Novelli and D'Apice, 2003]. Since it is impossible to examine them all during the course of one study, we decided to concentrate on the mutations of only one disease, so a dozen mutations (or a polymorphism, respectively) from within the known protein-binding domains of lamin A/C were selected for further analysis. All mutations originate from patients diagnosed with the classical Emery-Dreifuss muscular dystrophy phenotype, with the exception of the polymorphism C<T1698. Table 1.3 presents a short overview.

Table 1.3. Overview of *LMNA* mutations used in this thesis.

Mutation	Nucleotide position	Mutation type	Protein domain affected	Diseases caused	First description
R50S	C148A	Missense	Central rod	EDMD	Brown <i>et al.</i> 2001
R133P	G398C	Missense	Central rod	EDMD	Brown <i>et al.</i> 2001
T150P	A448C	Missense	Central rod	EDMD	Felice <i>et al.</i> 2000
DelQ355	Δ1063-1065	Deletion	Central rod	EDMD, CMD1A	Higuchi <i>et al.</i> 2005
E358K	G1072A	Missense	Central rod	EDMD	Bonne <i>et al.</i> 2000
E361K	G1081A	Missense	Central rod	EDMD	UP
R527P	G1580C	Missense	C-terminal tail	EDMD, FPLD	Bonne <i>et al.</i> 1999
L530P	T1589C	Missense	C-terminal tail	EDMD	Bonne <i>et al.</i> 1999
R541S	C1621A	Missense	C-terminal tail	EDMD, DCM	UP
G602S	G1805A	Missense	C-terminal tail, lamin A specific	EDMD, type A insulin resist.	Young <i>et al.</i> 2005
C<T1698	C<T1698	Polymorphism	C-terminal tail	none	Hegele <i>et al.</i> 2000
E358K+	G1072A+	Missense +	Central rod + C-	EDMD	UP
C<T1698	C<T1698	Polymorphism	terminal tail		

UP unpublished from C.A. Brown's laboratory

The identification of *LMNA* mutations R50S, R133P, T150P and delQ355 as well as that of the polymorphism C<T1698 has been published before [Brown *et al.* 2001, Felice *et al.* 2000, Higuchi *et al.* 2005, Hegele *et al.* 2000], but no further information about localisation and protein-protein interaction ability is available. The mutants E361K, R541S and G602S were identified in C.A. Brown's laboratory (Department of Pediatrics, Carolinas Medical Centre, Charlotte, North Carolina, USA) as causing AD-EDMD, only G602S has been published as causing type A insulin resistance [Young *et al.* 2005]; none has been analysed further on the protein level.

The lamin A/C mutations E358K, R527P and L530P are well documented and have been the subject of several studies so far [Bonne *et al.* 2000, 1999]. Exogenously expressed in cultured cells, the lamin A mutants exhibit a wild type localisation pattern, with the additional formation of intranuclear loci in the case of E358K and a disturbed endogenous emerin nuclear envelope localisation in the case of L530P [Holt *et al.* 2003, Bechert *et al.* 2003, Östlund *et al.* 2001, Raharjo *et al.* 2001]. However, little research has been undertaken to evaluate the contribution of the mutated lamin C isoform towards the EDMD phenotype, thus leading to the selection of these mutations for analysis.

The single nucleotide polymorphism (SNP) C<T1698 was included in this study because of its special interest: although it does not cause EDMD, it has been associated with obesity-related traits and metabolic syndrome in three distinct North-American populations [Steinle *et al.* 2004, Hegele *et al.* 2001, 2000]. The polymorphism affects residue H566 which is the last shared by both A-type lamins before alternative splicing occurs. In addition, patients with a combination of the mutation E358K and the 1698T allele appear to suffer from a more severe phenotype than those with the 1698C allele [C.A. Brown, personal communication], and the ‘double mutant’ E358K+C<T1698 was therefore also included. Fig. 1.8 gives an overview of the distribution of the mutations throughout the *LMNA* coding sequence.

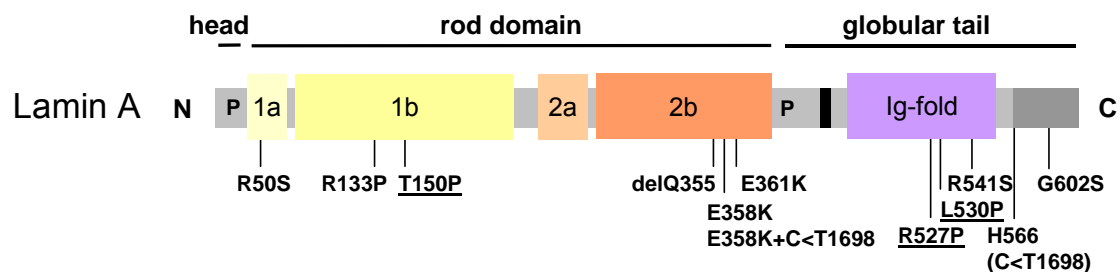


Fig. 1.8. Schematic diagram of lamin A with the distribution of the *LMNA* mutations used in this thesis. Numbers indicate the residue position, letters the amino acids in single-letter code. Underlined mutations were also analysed in the lamin C sequence. N amino-, C carboxyl-terminus, P phosphorylation sites.

The analysis of such a wide range of lamin A/C mutations may provide clues as to why seemingly small point mutations can cause muscular dystrophy and may improve our understanding of the specific role of each residue in lamin A/C function.

1.4 Aim of this study

Emery-Dreifuss muscular dystrophy (EDMD) manifests in childhood and is characterised by early contractures of the elbows, Achilles tendons and spine in addition to slowly progressive muscle wasting and weakness with a predominantly humeroperoneal distribution. Cardiac involvement is constant in nearly all patients by the third decade, starting with arrhythmias, and progressing towards complete heart block with a substantial risk of sudden death in middle age [Emery, 1989].

As cause of the autosomal dominant form of the disorder, mutations in the *LMNA* gene encoding the nuclear envelope proteins lamin A and C have been identified [Bonne *et al.* 1999]. The mutations occur throughout the coding sequence, include amino acid substitutions, frameshifts and premature stop codons and mainly affect both protein isoforms, lamin A and lamin C, although there are a few exceptions with mutations in the lamin A or C-specific tail, respectively [Broers *et al.* 2004]. However, not many studies have been published that have tried to distinguish the functions of lamin A from C either as wild type proteins or when defective in EDMD. Lamin C appears to depend on lamin A to be correctly incorporated into the nuclear lamina [Horton *et al.* 1992, Raharjo *et al.* 2001], where both isoforms interact with a multitude of other proteins, such as integral membrane proteins like emerin or nucleoplasmic ones [Zastrow *et al.* 2004].

In order to characterise the processes underlying protein localisation and interaction, nine missense (R50S, R133P, T150P, E358K, E361K, R527P, L530P, R541S, G602S) and one deletion (delQ355) *LMNA* mutant as well as a polymorphism (C<T1698) were chosen for further analysis. All mutations give rise to the AD-EDMD phenotype and were used to ascertain whether lamin A and C contribute differently or equally to the phenotype for each mutation.

To examine protein localisation and nuclear morphology, both mutant lamin A cDNAs and the corresponding mutant lamin C cDNAs, tagged with a fluorescent marker protein (EGFP and DsRed2, respectively) at the amino terminus, were exogenously expressed in different culture cells under three conditions: individually, together, or with the wild type form of the opposing A-type lamin. Localisation of the exogenous proteins as well as that of several endogenous proteins like emerin, lamin B2 and lamin C were analysed by fluorescence microscopy, and, in the case of exogenous lamin A constructs, also on the ultra-structural level by electron microscopy. Since many of the exogenous lamin A mutants exhibited a wild

type-like localisation in fixed cells, their protein mobility within the nuclear lamina was tested by the fluorescence recovery after photobleaching (FRAP) technique in living cells.

The protein interaction between the lamins A and C and emerin appears vitally important for human health, as not only mutations in *LMNA* cause EDMD, but also mutations in the emerin gene. Therefore, mutant forms of lamin A and C were synthesised *in vitro* and subjected to a protein binding assay with emerin, to determine the mutants' ability to interact with this partner.

The work undertaken in this study concentrates on the effects of different *LMNA* mutations on cell function, but also on the differences between the two A-type lamin isoforms and how they are affected by different EDMD mutations. Our findings will shed light on the underlying molecular causes of human disease, since the different contributions of lamins A and C to cell function and of their mutations to the EDMD phenotype have not been studied in such detail and in relation to such a wide range of mutants before.

2 Materials

2.1 Cell biology materials

2.1.1 Cell lines

- i) COS7, Green monkey kidney fibroblast cells
- ii) C2C12, mouse myoblast cells

2.1.2 Antibodies

- i) anti-emerin AP8, rabbit polyclonal [Ellis *et al.* 1998]
- ii) anti-lamin A/C R27, mouse monoclonal [Höger *et al.* 1991]
- iii) anti-lamin C (AB3702), rabbit polyclonal (Chemicon, USA)
- iv) anti-lamin B2 X223, mouse monoclonal [Höger *et al.* 1991]
- v) anti-GFP (1814460), mouse monoclonal (Roche Diagnostics Corp., USA)
- vi) anti-FLAG M2, mouse monoclonal (Stratagene, USA)
- vii) anti-actin 2G2, mouse monoclonal (a kind gift from Prof. B. Jokusch, University of Braunschweig)

2.1.3 Secondary antibodies

- i) anti-rabbit and anti-mouse IgG, goat polyclonal, rhodamine conjugated (Chemicon, USA)
- ii) anti-rabbit and anti-mouse IgG, goat polyclonal, Texas-Red (tetramethylrhodamine) conjugated (Dianova, Germany)
- iii) anti-rabbit and anti-mouse IgG, goat polyclonal, horseradish peroxidase conjugated (Amersham Biosciences, UK, from ECL kit)
- iv) anti-rabbit and anti-mouse IgG, goat polyclonal, horseradish peroxidase conjugated (Dianova, Germany)

2.2 Molecular biology materials

2.2.1 Bacteria, vectors, constructs

- i) *Escherichia coli* strains DH5 α and XL1-Blue MRF' for DNA amplification.
- ii) pBluescript II KS- with human pre-lamin A cDNA sequence (cloned via *Bam*H1 and *Eco*R1)[Ellis *et al.* 1998].
- iii) pBluescript II KS+ with human lamin C cDNA sequence (cloned via *Eco*R1 and *Bam*H1, a kind gift from Prof. G. Krohne, University of Würzburg).
- iv) pBluescript KS- with full-length human emerin cDNA sequence (cloned via *Bam*H1 and *Sal*I [Ellis *et al.* 1998].
- v) pEGFP-C1 (Clontech, UK) with human lamin A cDNA sequence, wild type and mutations T150P, E358K, R527P, L530P, C<T1698, E358K+C<T1698 (Fig. 2.1, a kind gift from Dr. J.A. Ellis, King's College, London, UK; for details about synthesis see 3.2.7).

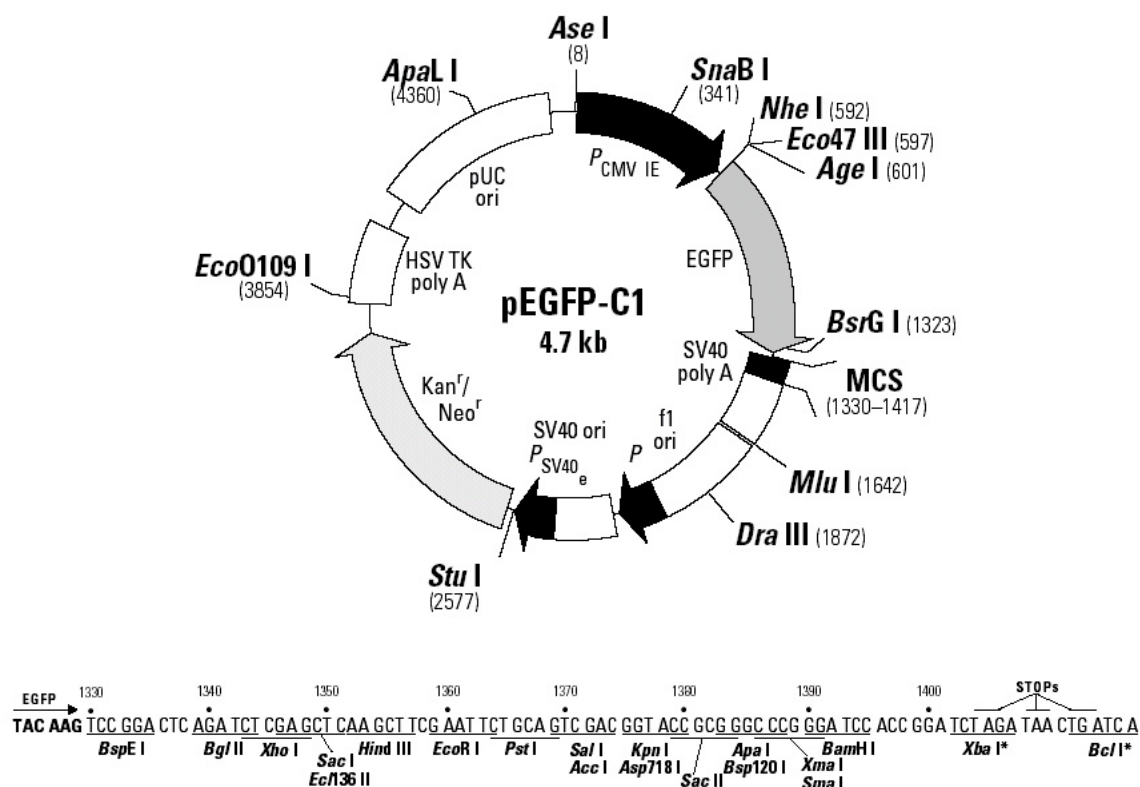


Fig. 2.1. Restriction map and multiple cloning site (MCS) of pEGFP-C1. All restriction sites shown are unique. The human lamin A sequences were cloned via the restriction sites *Bam*H1 and *Xba*I into the MCS. Human lamin C sequences were also cloned via *Bam*H1 and *Xba*I into the MCS. Picture from BD Biosciences Clontech, UK.

- vi) pEGFP-C3 (Clontech, USA) with human lamin A cDNA sequence with mutations R50S, R133P, delQ355, E361K, R541S, G602S (Fig. 2.2, a kind gift from Dr. C.A. Brown, Carolinas Medical Centre, Charlotte, USA; for details about synthesis see 3.2.7).

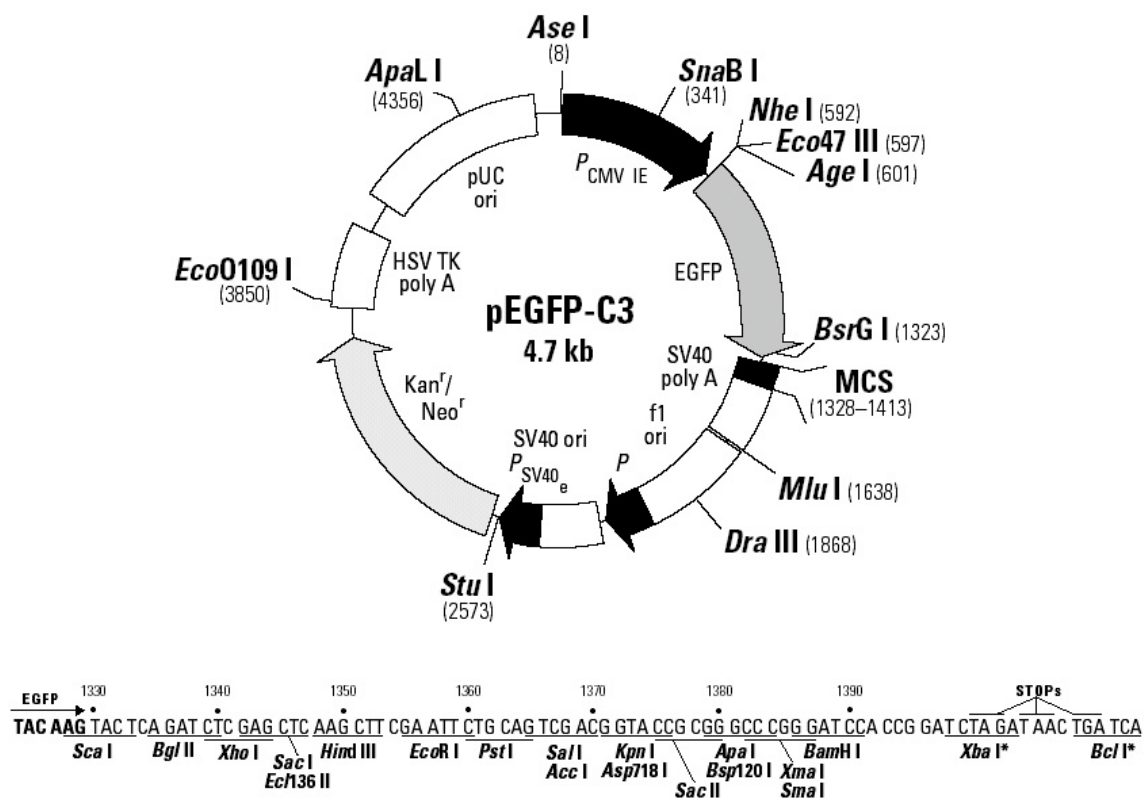


Fig. 2.2. Restriction map and multiple cloning site (MCS) of pEGFP-C3. All restriction sites shown are unique. The human lamin A sequences were cloned via the restriction sites *Sal*I and *Bam*H I into the MCS. Picture from BD Biosciences Clontech, UK.

- vii) pDsRed2-C1 and pEGFP-C1 (both vectors from Clontech, UK) with human wild type lamin C cDNA sequence and mutations T150P, R527P, L530P (Figs. 2.1 and 2.3, a kind gift from Dr. J.A. Ellis, King's College, London, UK; for details about synthesis see 3.2.8).

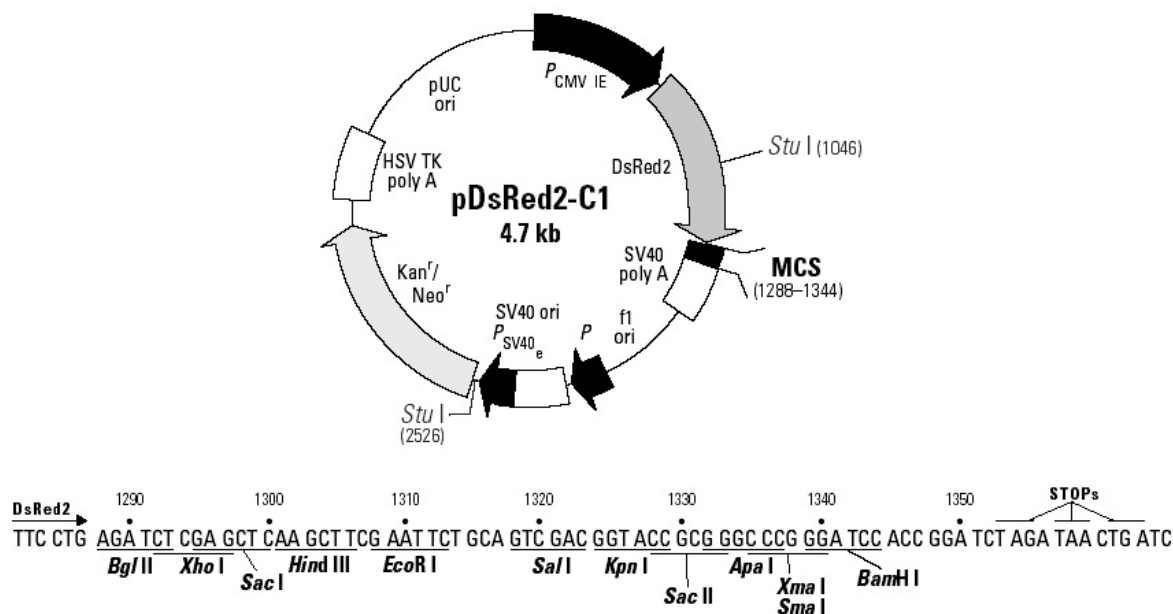


Fig. 2.3. Restriction map and multiple cloning site (MCS) of pDsRed2-C1. Unique restriction sites are in bold. The human lamin C sequences were cloned via the restriction sites *Bam*H1 and *Xba*1 (not shown, restriction site TCTAGA at first stop codon) into the MCS. Picture from BD Biosciences Clontech, UK.

viii) pcDNA3.1(+)(Invitrogen, UK) with wild type or mutated cDNA sequences of either human lamin A or lamin C or with human emerin cDNA sequence for use in the transcription/translation reactions (Fig. 2.4).

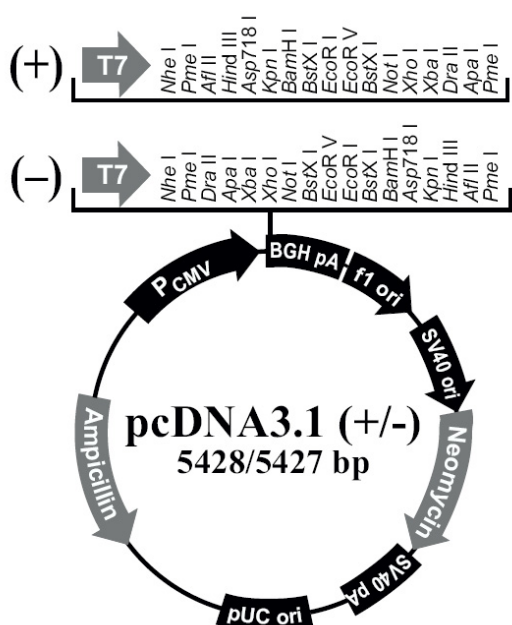


Fig. 2.4. Restriction map and multiple cloning site (MCS) of pcDNA3.1(+/-). All restriction sites shown are unique. The human wild type lamin A sequence and the mutations T150P, E358K, R527P, L530P, C<T1698 and E358K+C<T1698 were cloned via the restriction sites *Bam*H1 and *Xba*1 into the + MCS (top row). The lamin A sequences of mutations R50S, R133P, delQ355, E361K, R541S and G602S were cloned via *Eco*R1 and *Xba*1 into the MCS. The human wild type lamin C sequence and the mutations T150P, R527P and L530P were cloned via *Bam*H1 and *Eco*R1 into the MCS. The human emerin sequence was cloned via *Bam*H1 and *Xho*1 into the MCS. Picture from Invitrogen, UK.

- ix) pCMV-Tag2A (Stratagene, UK) for the creation of FLAG tagged lamin C in the transcription/translation reactions (Fig. 2.5).

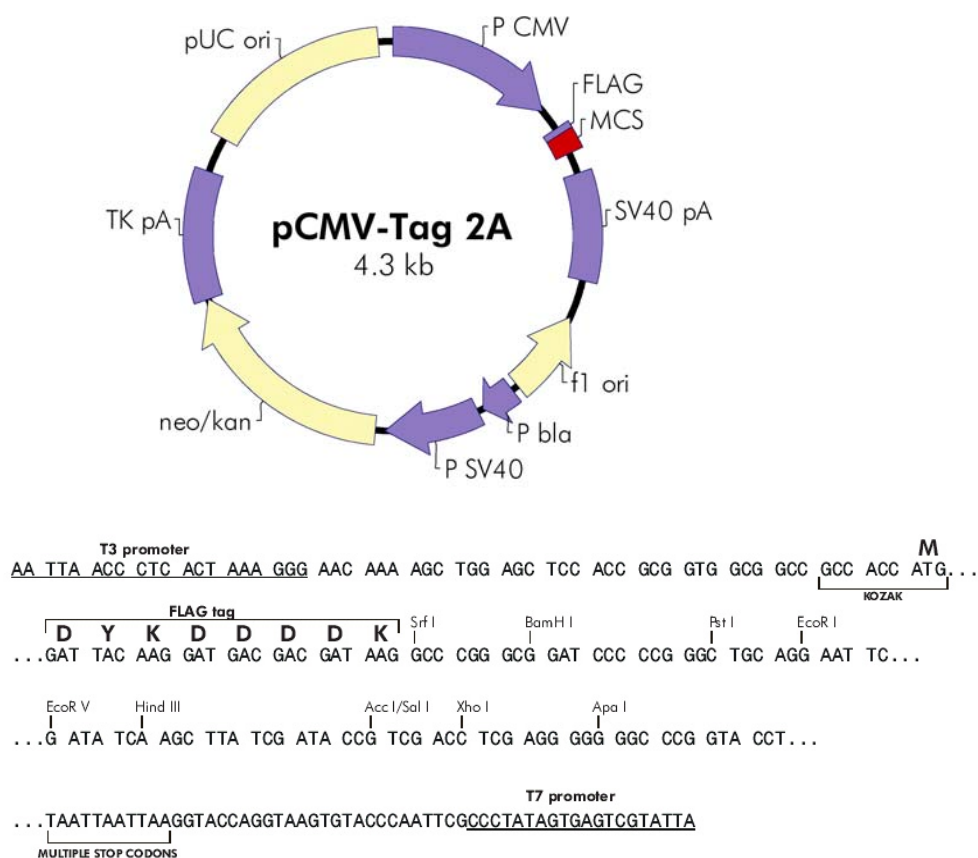


Fig. 2.5. Restriction map and multiple cloning site (MCS) of pCMV-Tag2A. All restriction sites shown are unique. The human wild type lamin C sequence and the mutations T150P, R527P and L530P were cloned via restriction sites *Bam*H1 and *Eco*R1 into the MCS. Picture from Stratagene, UK.

2.2.2 Enzymes, kits

- i) Restriction enzymes were supplied by New England Biolabs, UK and MBI Fermentas, Latvia. T4 ligase and RNA polymerases came from Promega, UK.
- ii) Kits for DNA isolation and purification as well as cell transfection reagents were supplied by Qiagen, UK or Germany, respectively. The *in vitro* transcription/translation reaction kit was from Promega, UK.

2.3 Chemicals

If not mentioned otherwise, all chemicals and solvents used were supplied by the following companies:

Sigma, UK

Roth, Germany

Merck, Germany

2.4 Equipment

The technical appliances used in this study agree with standard laboratory equipment, special pieces of equipment are listed in the appropriate methods section.

2.5 Photographic materials

All light microscopic pictures were taken digitally and further enhanced with Adobe Photoshop 6.0 (Adobe Systems Inc., Canada).

For electron microscopy, a plate camera was used with Kodak Electron image film ESTAR (SO-163). After developing, the negatives were scanned with a X-finity pro42 scanner (Quatographic AG, Germany) at high resolution and further processed digitally with Adobe Photoshop 6.0.

3 Methods

3.1 Microbiology

3.1.1 Bacterial growth

LB broth (Luria-Bertani)	10g Bacto-Trypton (Difco Laboratories, USA) 5g Yeast extract (Difco Laboratories, USA) 10g NaCl up to 1l, pH 7.2
LB agar	1.5% (w/v) Bacto-agar (Difco Laboratories, USA) in LB broth
Ampicillin stock solution	10mg/ml (stored at -20°C)
Kanamycin stock solution	25mg/ml (stored at -20°C)

For the production of agar plates, LB agar was autoclaved (120°C , 1.4bar, 30 minutes) and, after cooling down to $<50^{\circ}\text{C}$, poured into sterile plastic petri dishes (\varnothing 10cm, Nunc, UK). Appropriate antibiotics were added either before pouring or by plating after the plates were dried. To obtain single colonies, cells from a glycerol stock or from a transformation reaction were plated on an agar plate and incubated overnight at 37°C . For short term storage (3-4 weeks), the plates with bacterial cultures were kept at 4°C .

All media were autoclaved (120°C , 1.4bar, 30 minutes) and antibiotics added prior to their use. To amplify bacterial clones, single colonies were picked of an agar plate and grown in LB broth overnight at 37°C . For long term storage, an aliquot was mixed with 10-15% glycerol and placed on ice prior to being stored at -80°C .

3.1.2 Competent cell formation

The cell membrane of bacterial cells was permeabilised by a method of Chung *et al.* 1989, to enable them to take in plasmid DNA from the culture medium.

TSS (transformation and storage solution)	20-50mM MgCl_2 10% (w/v) PEG 3500, 3350 or 8000 5% (v/v) DMSO in LB broth Filter sterilise, aliquot and keep at 4°C or -20°C
--	--

The bacterial cell strain of choice was plated on a fresh agar plate and incubated overnight at 37°C. A single colony was picked and grown in appropriate culture medium, i.e. LB broth, overnight at 37°C. Thereafter, cells were diluted 1:100 in culture medium and grown at 37°C until they reached an OD_{600nm} of ~0.4-0.6. Cells were then centrifuged at 5000rpm, 5 minutes, 4°C (Sorvall centrifuge, 5534 rotor, UK), gently resuspended in ice-cold TSS (1ml per 10ml starting culture) and aliquoted on ice. After an immediate shock-freezing in liquid N₂, competent cells were stored at -80°C.

3.1.3 Transformation

For the transformation of competent cells, an aliquot was thawed on ice, mixed with 50-100ng plasmid DNA and incubated on ice for 45 minutes. After a heat shock of 90 seconds at 42°C, 1ml of culture medium, i.e. LB broth, was added and cells grown for 1hour at 37°C. Thereafter, cells were spread onto an agar plate containing the appropriate selection antibiotic prior to being incubated overnight at 37°C.

3.2 Molecular biology

3.2.1 Preparation of plasmid DNA

For the purification of plasmid DNA the Qiaprep Spin Miniprep Kit (for 5-15µg DNA from 5ml bacterial suspension) was used according to the manufacturer's instructions (Qiagen, UK).

The DNA isolation follows the modified alkaline lysis method developed by Birnboim and Doly (1979), prior to the DNA being absorbed by an anion exchange column containing silica gel. Several washes with appropriate buffers remove endonucleases and salts, after which the high purity plasmid DNA is eluted and stored at -20°C.

3.2.2 Determination of DNA concentration

To determine the concentration of DNA, the fragments or plasmids were either run on an agarose gel and compared to a known amount of reference DNA (usually *EcoR1/HindIII* digested λ phage DNA), or measured photometrically. The absorption maximum of

desoxyribonucleic acids lies at 260nm; at this wavelength, an OD value of 1.0 equals approximately the following DNA concentrations:

- 30µg/ml of oligonucleotides
- 40µg/ml of larger single stranded DNA fragments
- 50µg/ml of double stranded DNA

The aqueous DNA solution was diluted 1:20 to obtain an OD between 0.1 and 0.8 at the photometer (Biophotometer, Eppendorf, Germany) which calculated the DNA content of each sample measured. To check the purity of the DNA preparation, the ratio of absorption at 260nm and 280nm was determined and proved to be at 1.8 or above (no impurities).

3.2.3 Hydrolysis of DNA with restriction endonucleases (restriction digest)

Restriction endonucleases of class II split double stranded DNA at specific target sequences usually 4-8 bp long with a palindrome structure. Table 3.1 shows the restriction enzymes used in this thesis and their target sequences. The activity of these enzymes is measured in units (U). One unit equals the amount of enzyme sufficient for the digest of 1µg of a standard DNA (i.e. genomic DNA of the λ phage) in 1 hour under optimal conditions (pH, temperature, ionic strength).

Restriction digests were performed at 37°C with the appropriate reaction buffers and BSA as recommended by the manufacturer for at least 1 hour (up to 5 hours) in a minimal reaction volume of 8µl.

Table 3.1. Restriction endonucleases and their target sequences.

Enzyme	Target sequence (in direction 5'-3')
<i>Bam</i> H1	G↓GATCC
<i>Eco</i> R1	G↓AATTC
<i>Sal</i> 1	G↓TCGAC
<i>Xba</i> 1	T↓CTAGA
<i>Xho</i> 1	C↓TCGAG

3.2.4 DNA separation by agarose gel electrophoresis

On account of the negatively charged phosphate, DNA fragments in aqueous solution behave in an electric field like anions. Matrices in this aqueous solution (i.e. polyacrylamide or

agarose) can slow down the DNA molecules depending on their size and the polymerisation level of the matrix. Therefore, smaller DNA fragments migrate faster through the matrix than larger ones and separation of the differently sized molecules occurs. Since DNA conformation affects the migration speed of DNA (Thorne 1967), only molecules of the same conformation can be compared size wise which is the case for hydrolysed ('digested') DNA.

Agarose gels are commonly used for their easy handling, peculiar bands can be isolated very conveniently and a broad range of DNA molecule sizes can be separated by variation of the agarose concentration. More detailed information about agarose gel electrophoresis can be found at Southern (1979).

10x DNA loading buffer	10mM Tris-HCl, pH 8.0
	30% Ficoll
	1% SDS
	50mM EDTA
	0.05% bromophenole blue
	0.05% xylene cyanol
50x TAE (Tris-acetate-EDTA)	242g Tris base
	57.1ml acetic acid
	100ml 0.5M EDTA
	add ddH ₂ O to 1l, pH 8.5

A gel tray for agarose gels was sealed with either spacers or tape and a comb inserted the teeth of which would later form the wells of the gel. Agarose for a concentration of 1-1.5% was dissolved in 0.5-1x TAE by boiling, after cooling down to below 60°C mixed with ethidium bromide (stock solution 10mg/ml in dH₂O) to a final concentration of 0.5µg/ml and poured carefully into the gel tray to avoid air bubbles. After the gel had set the comb and spacers were removed and the tray inserted into the electrophoresis chamber which was filled with 0.5x TAE as running buffer. To the DNA samples was added 1/10 of their volume of 10x DNA loading buffer, prior to loading them into the wells of the gel. As a size standard, the DNA of the λ phage cut with *EcoR*1 and *Hind* III was used in one lane (see Fig. 3.1).

After loading of the samples, the gel was connected to a power supply which generated the electric field (approx. 10V/cm gel). To visualise DNA separation, the gel was subjected to UV light of 256nm on a UV transilluminator and photographed. The DNA was visualised by the fluorescent dye ethidium bromide which intercalates into the bases of the DNA and emits orange light after excitation with UV light.

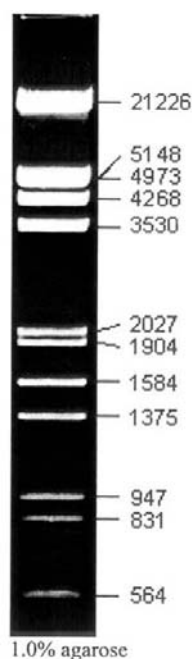


Fig. 3.1. Size standard for agarose gel electrophoresis. λ phage DNA digested with *EcoRI* and *HindIII*, sizes of bands in bp.

3.2.5 Isolation of DNA fragments from agarose gels

To purify specific DNA fragments, peculiar bands were cut from the gel after electrophoretic separation and the DNA extracted from the gel with the QIAquick Gel Extraction Kit (Qiagen, UK) according to the manufacturer's instructions.

3.2.6 Ligation

For the sub-cloning of a specific DNA fragment into a new vector, matching restriction sites are required at both ends of the DNA insert and in the vector. To ensure a directed insertion of the DNA fragment into the vector, two different restriction enzymes were used for 5' and 3' ends of vector and insert, which also prevented the re-ligation of the linearised vector during the following ligation.

For a ligation, the following reagents were added to a chilled reaction tube:

- 100ng cut vector DNA
- 300-400ng insert DNA
- ligase buffer to a final concentration of 1x
- 0.3 μ l T4 DNA ligase

ddH₂O was added up to 10-15 μ l of total volume, the reaction mixed by gently pipetting and incubated over night at 4°C. Subsequently, the reaction could be used for the transformation of competent cells or alternatively stored at -20°C.

3.2.7 Creation of lamin A cDNA constructs by site-directed mutagenesis

To create lamin A/C cDNAs with disease specific mutations, a site-directed mutagenesis PCR was performed which introduced the appropriate mutations. As this work was done by Drs. J.A. Ellis and C.A. Brown, respectively, only a brief description of the method is given.

A full length human pre-lamin A cDNA in pET-1 (kind gift from Helen Kent, Laboratory of Molecular Biology, MRC, Cambridge, UK) was sub-cloned into pcDNA3.1 (Invitrogen, UK) with *BamHI* at the 5' and *XbaI* at the 3' end and used as a starting template to synthesise

twelve mutant cDNA pre-lamin A constructs. All the constructs chosen were known to occur in AD-EDMD patients, and some additionally cause other diseases associated with the *LMNA* gene (Table 1.3). The positions of the mutations within the *LMNA* gene are shown in Fig. 1.8. Site-directed mutagenesis was performed on the wild type pre-lamin A cDNA clone by PCR, incorporating restriction sites *Bam*H1 at the 5' end and *Xba*1 at the 3' end, to generate the following mutations T150P, E358K, R527P, L530P, E358K+C<T1698 and the polymorphism C<T1698. The PCR reaction conditions were as follows: 95°C for 3 minutes (1 cycle), 94°C for 1 minute, $T_m-10^\circ\text{C}$ for 1 minute, 74°C for 1.5 minutes (5 cycles), then 94°C for 1 minute, $T_m-5^\circ\text{C}$ for 1 minute, 74°C for 1.5 minutes (25 cycles), then a final extension at 74°C for 7 minutes. *Pfx* DNA polymerase (Gibco-BRL, UK) was used to ensure maximum fidelity and at the manufacturer's recommended conditions. The PCR fragments generated were cloned 5' *Bam*H1- 3' *Xba*1 into pEGFP-C1 (Clontech, UK) which adds the Enhanced Green Fluorescent protein in frame with the N-terminus of the pre-lamin A cDNA. All of the constructs were sequenced in their entirety by Cytomyx DNA sequencing service, Cambridge, UK. The lamin A constructs were then sub-cloned into pcDNA3.1(+) 5' *Bam*H1 - 3' *Xba*1 which placed a T7 promoter at the 5' end of the pre-lamin cDNAs, for the *in vitro* transcription/ translation reactions.

The pre-lamin A cDNA constructs encoding for the mutants R50S, R133P, delQ355, E361K, R541S, G602S were made in Dr. C.A. Brown's laboratory in a similar manner but cloned with *Sal*1 at the 5' end and *Bam*H1 at the 3' end into pEGFP-C3. These were then sub-cloned into pcDNA3.1(+) with an *Eco*R1 site at the 5' end and *Xba*1 site at the 3' end, for the *in vitro* transcription/translation reactions.

3.2.8 Creation of lamin C cDNA constructs by site-directed mutagenesis

A full-length human lamin C cDNA was a kind gift from Georg Krohne (Division of Electron Microscopy, University of Würzburg, Germany) supplied in pBluescript KS⁺ cloned with *Bam*H1 at the 5' end and *Eco*R1 at the 3' end, but which also contained the lamin C 5'UTR. To create both wild type (lacking 5'UTR) and the T150P lamin C mutant, the lamin A-specific 3' tail was replaced with the lamin C-specific 3' tail by using a unique *Mfe*1 restriction enzyme site around residue 466 in lamin A/C. Both wild type lamin A (in pEGFP-C1) and C (in pKS⁺) cDNAs were cut 5' *Bam*H1 - 3' *Mfe*1. The 5' end of lamin A (residues 1-466) was isolated and ligated into the 3' end (from residue 466) of the lamin C cDNA in pKS⁺. The constructs were then confirmed by sequencing. To create the lamin C mutants

R527P and L530P, site-directed mutagenesis was performed on wild type lamin C in pKS⁺, as described for the equivalent lamin A mutants, but incorporating the restriction sites *Bam*H1 at the 5' end and *Eco*R1 at the 3' end. These were then cloned into pKS⁺ for DNA sequencing. The wild type and all the lamin C mutants were then subcloned 5' *Bam*H1- 3' *Eco*R1 into pcDNA3.1(+), and from there 5' *Bam*H1- 3' *Xba*1 into pEGFP-C1 and pDsRed2-C1 (Clontech, UK). The lamin C cDNA constructs were also FLAG-tagged at their amino-terminus by sub-cloning 5' *Bam*H1 - 3' *Eco*R1 into pCMV-Tag2A (Stratagene, UK).

3.2.9 Emerin cDNA construct

A full length human emerin cDNA cloned 5' *Bam*H1- 3' *Sal*1 in pBluescript KS⁻ [Ellis *et al.* 1998] was sub-cloned 5' *Bam*H1- 3' *Xho*1 into pcDNA3.1(+) for the *in vitro* transcription/translation reactions.

3.2.10 *In vitro* transcription/translation of lamins A/C and emerin

For binding assays and subsequent immunoprecipitation of the bound proteins, wild type emerin, lamin A and C as well as mutant lamin A and C cDNA constructs in pcDNA3.1(+) were synthesised *in vitro* using the coupled transcription/translation TNT T7 Reticulocyte Lysate System (L4610, Promega, UK). This was used according to the manufacturer's instructions and as described in Ellis *et al.* 1998.

In brief, the reaction components were added to a chilled reaction tube in the following order:

TNT rabbit reticulocyte lysate	12.5 µl
Nuclease-free water	6.5 µl
TNT reaction buffer (25x)	1 µl
Amino acid mixture minus methionine 1mM	0.5 µl
RNasin Ribonuclease Inhibitor (40u/µl)	1 µl
TNT T7 RNA polymerase	0.5 µl
[³⁵ S]methionine (>1000Ci/mmol at 10mCi/ml)	1 µl
DNA template (~1 µg)	2 µl

Thereafter, the reaction was incubated for 90 minutes at 30°C. For expressing the pCMV-Tag2A-lamin C constructs (adds a FLAG tag to 5' end of lamin C), T3 RNA polymerase (80U/µl, Promega) substituted the T7 RNA polymerase supplied in the kit. Synthesised

proteins were labelled with L-[³⁵S]methionine (AG1094, Amersham Biosciences, UK) in a final volume of 25 µl. Reaction efficiency of the *in vitro* synthesised proteins was monitored with control reactions of wild type lamins, no DNA template at all and a luciferase control supplied with the kit. Protein products were separated on 10% SDS-PAGE gels (see 3.3.4) and radiolabelled proteins visualised by autoradiography with Kodak BIOMAX-MR film.

3.3 Protein biochemistry

3.3.1 Cell culture

Cells were routinely maintained in Dulbeccos modified Eagle's medium (DMEM, Sigma, UK) supplemented with 10% fetal bovine serum (FBS, Gibco, UK), 2 mM glutamine and 1% (v/v) penicillin/streptomycin and were grown at 37 °C in 5% CO₂. Culture media and sera were from Sigma and Gibco, UK. Passaging was performed 2-3 times per week: the cell monolayer was briefly rinsed with sterile PBS (see 3.3.3), trypsinized (5 minutes at 37°C) to detach the cells from the surface of the culture vessel and the trypsinisation process stopped with 5 volumes of culture medium. After a short centrifugation (5 minutes at 1000rpm), cells were resuspended in culture medium and ¼ to 1/10 of the suspension seeded into a new culture vessel or into the old culture vessel which had been thoroughly rinsed with PBS

3.3.2 Transfection of adherent cells

For the expression of exogenous A-type lamins in culture cells, two different transfection reagents were used which enclose the added plasmid DNA and transport it via endocytosis into the cell. Since cell density is crucially important for reproducible results, COS7 fibroblasts or C2C12 myoblasts were trypsinized (5 minutes at 37°C) to detach them from the surface of the culture vessel and counted in a Neubauer cell counting chamber (see Fig. 3.2). Subsequently, cells were seeded at a concentration of 2.0×10^5 cells per well of a six well plate and incubated over night at 37°C, 5% CO₂ which left them sub-confluent (60-70%) and ready for transfection.

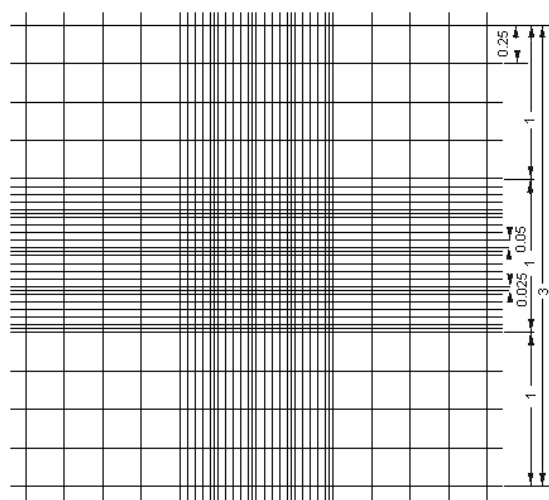


Fig. 3.2. Neubauer counting chamber. Spaces in mm; all cells in the four 1mm² squares (each subdivided into 16 smaller squares) were counted and the cell concentration calculated with the following equation : (cell count / 4) x 10⁴ = cells per ml

For microscopic analysis of the transfected cells, they were plated on coverslips (either 22mm square or 12mm Ø round ones) in the six well plates. Transfection quality DNA was prepared from *E. coli* DH5α cells and

purified on Qiagen columns according to the QIAprep Spin Miniprep kit protocol (see 3.2.1). For localisation studies of the EGFP and DsRed2 cDNA constructs under the fluorescence microscope, COS7 and C2C12 cells were transfected by following the SuperFect™ Transfection Protocol from Qiagen (UK) using a SuperFect:DNA ratio of 1:6 with 1-2µg of DNA per well. For double transfections, equal amounts of DNA of both the EGFP and DsRed2 cDNA constructs (up to 1-2 µg DNA per well) were used. Cells were transfected for 4 hours and a time course for optimal expression levels without their being more that 5% of cells over-expressing, was performed at 37°C, 5%CO₂. The optimum expression time was found to be 16-18 hours.

To analyse the localisation of the EGFP-lamin A constructs on the electron microscopic level and for the FRAP experiments at the confocal laser scanning microscope, COS7 fibroblasts were transfected with the Effectene reagent using an Effectene:DNA ratio of 1:25 (0.4µg DNA per well) according to the manufacturer's instructions. The transfection efficiency proved to be slightly higher (~20-25% of cells) than with SuperFect reagent and the cells expressed the fusion proteins faster; therefore, they could be used for FRAP studies as soon as 6 hours after transfection.

3.3.3 Cell harvest for SDS-PAGE

PBS (phosphate buffered saline)	140 mM NaCl
	2.6 mM KCl
	6.4 mM Na ₂ HPO ₄
	1.4 mM KH ₂ PO ₄ in ddH ₂ O, pH 7.4

SDS-PAGE sample buffer 1	60 mM Tris-HCl, pH 6.8 10% glycerol 2% (w/v) SDS 5% β -mercapto-ethanol
SDS-PAGE sample buffer 2	200 mM Tris-HCl, pH 8.8 5 mM Na ₂ EDTA 1 M sucrose 4 % (w/v) SDS 0.1 % (w/v) bromophenol blue 1.5 mg/ml DTT (diluted 1:100 from stock solution)
DTT reducing agent (stock solution)	150 mg/ml DTT in 10 mM Na acetate, pH 5.2 store in aliquots at -20°C

To harvest adherent cells from the well of a six well plate, the culture medium was aspirated off and the cell layer washed with 2 ml of sterile PBS. The six well plate was then placed on ice, to prevent protein degradation in the subsequent steps of sample preparation.

The cells were scraped from the bottom of the well with a cell scraper, suspended in 0.75 ml of ice-cold PBS and transferred into a 1.5ml reaction tube. This procedure was repeated with another 0.75 ml of PBS to obtain as many cells as possible; in some cases, a proteinase inhibitor cocktail (1 μ l/ml PBS, Sigma, UK) was added to the PBS prior to cell resuspension. The cells were collected by centrifuging for 2 minutes at 11000 rpm, 4 $^{\circ}$ C in a table-top centrifuge, the supernatant was discarded and the cell pellet re-suspended in 50 μ l ice-cold PBS. If the size of the pellet differed noticeably from the normal pellet size of one well of a six well plate, the added PBS volume was adjusted accordingly. To homogenize the cell mixture, the cells were sonicated on ice for a maximum of 10 seconds per sample; however, this sonication treatment was not essential. Thereafter, sample buffer was added to the cell suspension (same volume as cell suspension), mixed well and boiled for 5 minutes at 95 $^{\circ}$ C, prior to being used in SDS-PAGE (see 3.3.4) or to being stored at -20°C .

Both types of SDS-PAGE sample buffer gave the same results; for practical reasons, sample buffer 1 was used for the electrophoresis of EGFP and DsRed2 fusion proteins, whereas sample buffer 2 was used for *in vitro* synthesised proteins and binding studies.

3.3.4 SDS polyacrylamide gel electrophoresis

Protein mixtures were separated according to their molecular weight in a discontinuous polyacrylamide gel system using SDS (sodium dodecyl sulphate) to create dissociating

conditions. The gel and buffer system was first described by Thomas and Kornberg (1975), the chosen acrylamide concentration in normal gels varied between 10-12% depending on the size of the desired proteins. For gradient gels the polyacrylamide concentration gradient ranged from 8-20%.

Resolving gel (acrylamide concentration between 8-20%)	30% acrylamide / bisacrylamide mix (37.5:1) up to the end concentration of PA in the gel 0.75 M Tris-HCl, pH 8.8 0.1% SDS 0.1% APS (freshly prepared !) 0.03% TEMED up to 10 ml with ddH ₂ O for 2 mini gels
Stacking gel (acrylamide concentration 3.9%)	30% acrylamide / bisacrylamide mix (37.5:1) up to the end concentration of PA in the gel 188 mM Tris-HCl, pH 6.8 0.1% SDS 0.3% APS 0.1% TEMED up to 5 ml with dH ₂ O for 2 mini gels
Running buffer	50 mM Tris-HCl, pH 8.3-8.8 384 mM glycine 0.1% SDS
Gel stain solution	20-25% methanol or propan-2-ol 7.5-10% glacial acetic acid (GAA) 0.025-0.1% Coomassie Blue (Serva Blau R250)
Gel destain solution	20% methanol or propan-2-ol 7.5-10% GAA
Sucrose solution	20% (w/v) sucrose 0.01% (w/v) bromophenol blue

Glass plates, spacers and combs were cleaned with ethanol, assembled and the sides as well as the bottom of the spacer-glass plates complex sealed with liquid agarose (0.5-2%). The resolving gel solution was prepared, thoroughly mixed and poured between the glass plates up to ~ 2-2.5cm below the top edge of the glass plates to leave room for the stacking gel. To ensure an even polymerisation at the top, ddH₂O or ddH₂O-saturated butanol was pipetted gently on top of the gel. After its solidification (45-60 minutes), the water or butanol was discarded and the polyacrylamide mixture for the stacking gel poured on top. The comb was immediately inserted air bubble-free into the stacking gel and removed only after complete

polymerisation (>30 minutes), preferably in the presence of running buffer to avoid tearing of the wells.

Since gradient gels allow a better separation of proteins with a big size difference, gels with a polyacrylamide gradient between 8-20% were used in some cases. Several gradient gels were poured simultaneously in a gradient former apparatus in which they were filled from the bottom by a small pump. Connected to the pump was a polyacrylamide reservoir containing a 8% solution which was slowly mixed with a 20% solution to form the concentration gradient in the resolving gel. To clear the reservoirs, plastic tubing and pump from liquid polyacrylamide, a 20% sucrose solution was pumped through after the polyacrylamide. Polymerisation time and pouring of the stacking gels followed the procedure for normal gels. For the subsequent gel electrophoresis, a gel was placed in the electrophoresis chamber filled with running buffer, the protein samples in sample buffer re-heated to 95°C for 3-5 minutes, centrifuged for 1 minute at 11000rpm and loaded into the wells of the gel (maximum well volume ~15µl).

To determine the molecular weight of the proteins in the samples, marker proteins were loaded into separate wells, usually at either end of the gel, at a dilution of 1:10 in sample buffer (see Fig. 3.3). Empty wells were filled with sample buffer dyed blue by bromophenol blue to enable the running front to be seen.

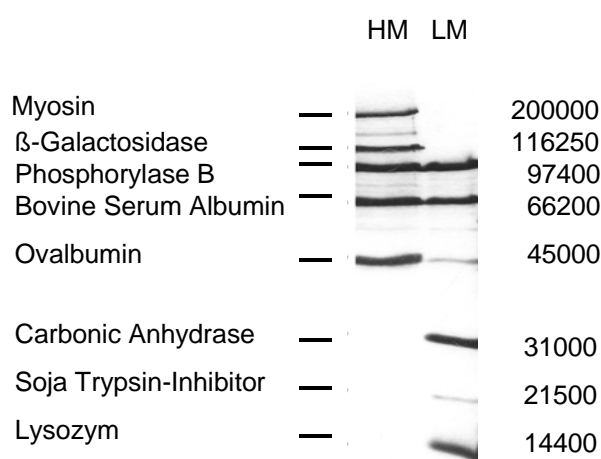


Fig. 3.3. Marker proteins for SDS-PAGE (18% acrylamide concentration). Left proteins, right molecular weight in Dalton (High marker, HM and Low Marker, LM, from BIO-RAD, UK).

The electrophoresis chamber was connected to a power supply and electrophoresis performed at 20-40mA for 1.5-2.5 hours. Afterwards, the glass plates were disassembled and the stacking gel removed, so that the resolving gel could be used further for immunoblotting.

In the case of running radiolabelled proteins on the gel, the gel was stained for 45 minutes to detect the marker proteins and de-stained for 20 minutes prior to being dried on a vacuum gel drier.

3.3.5 Immunoblot

For the identification of specific proteins in a mixture of proteins, an immunoblot was performed. The term ‘blotting’ refers to the transfer of separated proteins from a gel matrix to a nitrocellulose membrane. Specific antibodies can then easily recognize and bind to the immobilised proteins and are detected themselves by enzyme-conjugated secondary antibodies.

The electrophoretic transfer was performed in a ‘semi-dry’ procedure by Kyhse-Anderson (1984), based on a method by Towbin *et al.* (1979). Two different buffer systems were used.

TBST (Tris buffered saline with Tween-20)	140 mM NaCl 10 mM Tris-HCl, pH 7.4 0,5% (v/v) Tween-20
Buffer 1	25 mM Tris-HCl, pH 10.4 20% methanol
Buffer 2	300 mM Tris-HCl, pH 10.4 20% methanol
Buffer 3	25 mM Tris-HCl, pH 9.4 40 mM DL-norleucine 20% methanol
Buffer 4	4.2 mM Tris-HCl, pH 8.3 32 mM glycine 10% methanol, prepare freshly !
Stripping buffer	62.5 mM Tris-HCl, pH 6.7 100 mM β -mercaptoethanol 2% SDS

The proteins were electrophoretically separated (see 3.3.4) and the resolving gel equilibrated in buffer 3 (or buffer 4, if this buffer was used) for 15 minutes. A gel-sized piece of nitrocellulose and several pieces of Whatman filter paper were soaked in the appropriate buffers and stacked together with the gel in the blotting apparatus according to Fig. 3.4. Air-bubbles that prevent transfer of proteins were removed by rolling a glass tube across the stack.

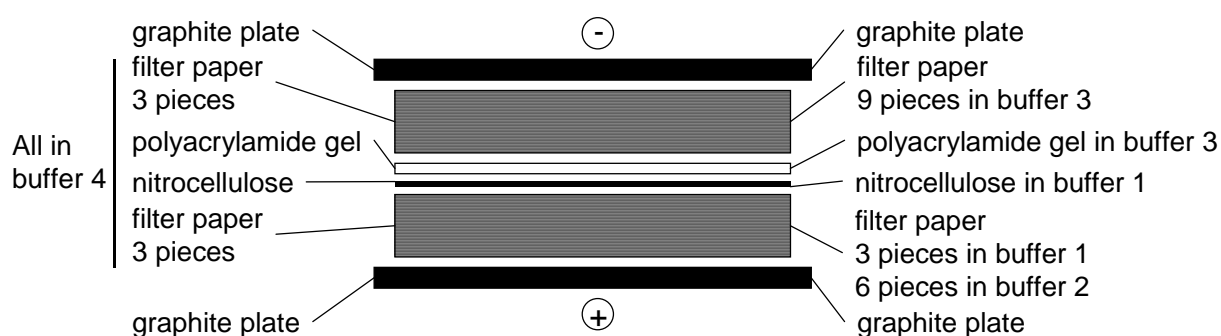


Fig. 3.4. Stacking scheme for an immunoblot (Western blot). Two different buffer systems could be used: stacking with buffer 4 shown on the left, stacking with buffers 1-3 on the right.

The electrophoretic protein transfer was performed at a constant current intensity of 0.8 mA/cm² for 1-1.5 hours. The proteins, negatively charged by SDS, migrate from the gel towards the nitrocellulose. After the transfer, the nitrocellulose was stained with Ponceau S for 5 minutes to visualize the transferred proteins, the molecular weight standard proteins were marked with a pencil and the Ponceau S dye washed off in big volumes of TBST.

The polyacrylamide gels were either disposed off directly or stained with Coomasse Blue (in staining solution) over night at RT, de-stained for several hours and stored dried.

To block unspecific protein binding sites on the nitrocellulose, the membrane was incubated 1-2 hours at RT or over night at 4°C in 5-10% (w/v) dried milk powder in TBST. Thereafter, the incubation with the primary antibody in 5-10% (w/v) dried milk powder in TBST followed according to Table 3.2. Subsequent washings with TBST (3x10 minutes or 4x15 minutes at RT) removed unbound antibody. The specific primary antibodies were detected by peroxidase-conjugated secondary ones (anti-mouse or anti-rabbit, respectively, diluted 1:5000 in 5-10% (w/v) dried milk powder in TBST) with an incubation time of 1-2 hours at RT. After a further washing step (as above), the bound secondary antibodies were visualized by enhanced chemical luminescence (ECL, Amersham, UK).

Table 3.2. Dilution of primary antibodies for immunoblot.

Antibody	Dilution	Incubation time / temperature
α-emerin AP8	1:1000	2h at RT or over night at 4°C
α-lamin A/C R27	1:1000	1-2h at RT or overnight at 4°C
α-GFP	1:500	1h at RT
α-FLAG M2	1:250	2h at RT or overnight at 4°C
α-actin 2G2	1:1000	1h at RT

Since the nitrocellulose with cell lysates was used for the subsequent incubations with different antibodies, the previous ones, primary as well as secondary antibodies, had to be stripped off the membrane first. The nitrocellulose was washed with TBST and incubated for 30 minutes at 50°C in stripping buffer while rocking. After several washes in big volumes of TBST and a new blocking in 10% (w/v) dried milk powder in TBST for 1h at RT, the membrane was ready for further use with another primary antibody.

3.3.6 Immunoprecipitation of *in vitro* synthesised proteins

Solubilisation buffer	50 mM Tris-HCl, pH 7.4
	50 mM NaCl
	2 mM MgCl ₂
	1% (v/v) Triton X-100

For the *in vitro* binding assays half a TNT reaction mix of wild type emerin was mixed with either a full lamin A or lamin C reaction mix and incubated overnight at 4°C. Chilled solubilisation buffer was added to a final volume of 0.5ml to each sample mix and left on ice for 20 minutes, mixing intermittently. A pre-immune clearance was performed by adding 10µl of protein A-sepharose in PBS (50 mg/ml) to each sample mix and rotating them for 1 hour at 4°C. The sepharose beads were collected by centrifugation in a microfuge at 11,600xg, 4°C for 1 minute, and the supernatant transferred to a fresh reaction tube. At this point, a 15µl aliquot of the supernatant was mixed with SDS-PAGE sample buffer to obtain a ‘Total’ fraction of the lamin C immunoprecipitation (IP). To perform the co-immunoprecipitations, anti-emerin antibody AP8 was added to the supernatants to a final concentration of 1:100. The samples were incubated for 2 hours at 4°C, rotating. The bound antibody/protein complexes were captured with 100µl of protein A-sepharose per sample mix. Tubes were again rotated for 1 hour at 4°C and the beads collected by centrifugation as described above. The supernatant containing the unbound proteins was decanted off and kept. The beads were washed 3 x 5 minutes at 4°C in solubilisation buffer and 2 x 5 minutes at 4°C in 50 mM Tris-HCl, pH 7.4. Both the supernatants containing unbound proteins and the sepharose beads were resuspended in SDS-PAGE sample buffer and heated to 95°C for 2 minutes. Proteins were then separated on 10% normal or 8-20% gradient SDS-PAGE gels and radiolabelled proteins visualised by autoradiography (see 3.3.4).

To confirm that the immunoprecipitated proteins were lamin C or emerin, and not contaminating proteins from the reticulolysate system, the SDS-PAGE gels were immunoblotted instead with anti-FLAG M2 and AP8 antibodies respectively.

Quantitative analysis of the autoradiographs was performed using the Gene Genius Bioimaging system Gene Tools 3.00 22 programme (Syngene, Cambridge, U.K.). A box was drawn around equivalent gel band areas and the number of pixels counted. Background correction was accounted for and wild type lamin A assigned the arbitrary value of 100.

3.4 Light and electron microscopy

3.4.1 Immunofluorescence microscopy

For microscopic visualisation, transfected cells (see 3.3.2) were washed once with phosphate buffered saline (PBS), prior to being fixed in methanol for 10 minutes at -20°C , followed by acetone for another 5 minutes at -20°C . After air-drying, the cells were blocked with PBS/0.2% (w/v) fish gelatin (blocking buffer) 3 x 10 minutes and transferred to a humidified chamber for primary antibody incubation. The cells transfected with the EGFP-lamin A constructs were incubated either with the anti-emerin AP8 antibody or the anti-lamin C AB3702 antibody. As controls, COS7 cells transfected with some of the EGFP-lamin A mutations were also incubated with either anti-lamin B2 (X223) or anti-lamin A/C (R27) antibodies. The cells that were transfected with lamin C constructs only were incubated with the anti-emerin antibody. Incubation time for the primary antibody was 1 hour at RT, for details of dilution, dilutants and washing buffer see Table 3.3. After washing for 3 x 5 minutes, the cells were incubated for 45 minutes with anti-rabbit IgG conjugated-rhodamine (Chemicon, UK) at a final concentration of 1:100 in blocking buffer or anti-mouse IgG conjugated-Texas Red (Dianova, Germany) at the same concentration in PBS. Thereafter the coverslips were washed 3 x 5 minutes and then the cell nuclei stained with DAPI (4',6-Diamidino-2-phenylindole) or with Hoechst dye (Hoechst 33258) at $1\mu\text{g/ml}$ in PBS. The cells were washed twice in PBS, dehydrated for 1 minute in ethanol and air-dried prior to mounting the coverslips in AF1 mounting medium (Cityfluor Ltd, London, UK) or in Mowiol 4-88 (Hoechst, Germany). Cells which were double-transfected with EGFP-lamin A and pDsRed2-lamin C were only fixed and stained with DAPI or Hoechst dye as above. Endogenous emerin staining in the double transfection experiments was not possible due to the microscope not being fitted with an appropriate filter for a third colour.

Table 3.3. Dilution of primary antibodies for immunofluorescence microscopy.

Antibody	Dilution	Dilutant / washing buffer
α -emerin AP8	1:25-1:50	PBS/0.2% (w/v) fish gelatin
α -lamin C	1:25	PBS/0.2% (w/v) fish gelatin
α -lamin A/C R27	1:100	PBS
α -lamin B2 X223	1 :100	PBS

Immunofluorescence microscopy was performed using a Leica DMR fluorescence microscope, fitted with a Leica HCX Plan-Fluotar 100x/1.3 oil lens and Chroma Technology filter set 61002 (DAPI/FITC/Texas red; S360/40X, S492/18X, S572/23X). Images were captured on a Photometrics Coolsnap HQ camera, which calculated an automatic exposure time, using MetaMorph 5.0r6 software (Universal Imaging Corp., USA). For deconvolution microscopy, a series of images acquired at 1 μ m focal intervals were digitally processed first using the MetaMorph 5.0r6 software, then with AutoDeblur 9.1.2/AutoVisualize9.0 (AutoQuant, USA; www.aqi.com) to yield stacks of confocal slices. Most figures used in this thesis show the maximum projections of picture stacks obtained from a deconvolution of 20 iterations and are composed using Adobe Photoshop 6.0.

For the endogenous lamin C staining, a Zeiss Axioplan 2 (Zeiss, Germany) with a Zeiss Plan-Neofluar 40x lens having a numerical aperture of 0.75 and the appropriate rhodamine and GFP emission filters was used. Pictures were taken with a Hamamatsu Orca-ER camera and digitally processed with Openlab 3.0.9 (Improvision, UK) and Adobe Photoshop 6.1.1 software. Part of the co-transfection experiments were photographed with a Axiophot Stereo HB050 (Zeiss, Germany), the lenses and filters used were as above.

For taking pictures of the endogenous lamin B2 staining, a confocal laser scanning microscope (CLSM, Leica TCS-SP, Germany) with a Leica Neofluar 40x lens having a numerical aperture of 1.25 was used. EGFP and Texas-Red were excited with an Ar/Kr laser at a wavelength of 488nm and 568nm, respectively. Fluorescence signals as well as the corresponding phase contrast image were captured simultaneously by a photomultiplier.

3.4.2 FRAP analysis of living cells

COS7 cells were grown on coverslips and transfected with different EGFP-lamin A mutants 6-16 hours prior to being used for analysis (see 3.3.2). Then the coverslips were placed face down in a drop of culture medium on a microscope slide and the edges sealed with Fixogum rubber cement which kept the cells alive and healthy for up to 60 minutes at RT.

For FRAP (fluorescent recovery after photobleaching) analysis of transfected cells, a suitable area with cells not over-expressing the EGFP-fusion protein was scanned once at the confocal laser scanning microscope (prebleach, see also 3.4.1), followed by a bleach pulse of 1 second of a spot with 1 μ m in diameter. Thereafter, a time series of fluorescent pictures was taken with 4% laser power (intensity for bleach point = 100%). Time intervals were as follows: 20 x 2 seconds, 10 x 5 seconds, 20 x 10 seconds, 10 x 20 seconds and 5 x 60 seconds. Since the scanning took ~2 seconds per image, total FRAP time of one experiment was approx. 20 minutes.

The mean of at least 10 experiments per lamin A mutation was used to calculate FRAP recovery curves from background corrected values as described by Phair and Misteli (2000):

$$I_{rel} = T_0 I_t / T_t I_0$$

With

I_{rel} = relative fluorescent intensity, T_0 = total cellular intensity during prebleach, T_t = total cellular intensity at timepoint t, I_0 = average intensity in the region of interest during prebleach, I_t = average intensity in the region of interest at time point t.

To account for value fluctuations, statistical analysis was performed using an unpaired student's t-test (www.graphpad.com/quickcalcs/ttest1.cfm), calculating with the means, the standard deviation SD and the sample number n.

3.4.3 Electron microscopy

Since the fluorescence microscopy of cells transfected with EGFP-lamin A mutants resulted in such a variety of different phenotypes, transfected cells were subjected to electron microscopy to examine the localisation of the fusion protein in greater detail.

Cacodylate buffer	50 mM cacodylic acid Na-salt trihydrate
2.5% glutaraldehyde with ions	5 ml 25% glutaraldehyde
	2.5 ml 1 M KCl
	1.25 ml 0.1 M MgCl ₂
	41.25 ml 50 mM cacodylate buffer, pH 7.2
Osmium tetroxide	2% OsO ₄ (w/v) in 50 mM cacodylate buffer
Uranyl acetate	0.5% UAc (w/v) in ddH ₂ O
Epon solution A	(1 ml \cong 1.077g)
	50 ml DDSA

	31 ml Epon 812 (Serva, Heidelberg)
Epon solution B	(1 ml \cong 1.212g)
	44.5 ml MNA
	50 ml Epon 812
Epon mix	(4:3 w/w)
	24.6g solution A
	20.8g solution B
	0.8 ml DMP-30
Lead citrate by Reynolds (1963)	1.33g lead nitrate
	1.76g sodium citrate
	8 ml 1 N NaOH
	up to 50 ml with boiled ddH ₂ O

For electron microscopic inspection, COS7 cells were grown on CELLocate coverslips (Eppendorf, Germany) and transfected with the EGFP-lamin A constructs as described in 3.3.2. 16-18 hours after transfection, cells were screened under a fluorescence microscope (Zeiss Axiophot Stereo HB 050 with Neofluar lenses and an appropriate filter for EGFP emission) for cells expressing the fusion proteins and fixed for 45 minutes with 2.5% (w/v) glutaraldehyde in PBS. After a wash in cacodylate buffer, cells were subsequently fixed for 1 hour with 2% OsO₄ in 50 mM cacodylate (pH 7.2), prior to incubation overnight in 0.5% uranyl acetate (in ddH₂O) at 4°C. The cells on the coverslips were then washed in ddH₂O, dehydrated in an ethanol series (5 minutes each in 50, 70, 90, 96% and 2 x 100%) and in propylene oxide (2 x 5 minutes) and embedded in Epon812 (first in an 1:1 propylene oxide/Epon mix for 2-4 hours at RT, then overnight at 60°C in Epon812).

After the Epon was hardened, the coverslips were removed, the samples ultrathin sectioned (slice thickness ~60-80nm) and the sections transferred onto copper EM grids which were coated with Pioloform F (Wacker-Chemie GmbH, Germany). For optimising the contrast, the sections were incubated again in uranyl acetate for 20 minutes, washed with ddH₂O, incubated in lead citrate for 8 minutes, washed again and air-dried.

Thereafter, sections could be analysed with a Zeiss EM10 (Zeiss/LEO, Germany) at a cathode voltage of 80kV. At least two coverslips were processed for each mutation, with 2-3 transfected cells per coverslip.

4 Results

4.1 Exogenous expression of lamin A and C constructs in COS7 cells analysed by immunofluorescence microscopy

4.1.1 Do mutations in the lamins A and C affect their intracellular localisation ?

It is essential for the function of a protein to be correctly localised. For example, enzymes need the right micro climate (pH, ionic strength) to work and bind to their specific partners, transmembrane proteins need to be anchored in a lipid bilayer and DNA-binding proteins like histones need to reach the nucleus to associate with the DNA.

A-type lamins form the nuclear lamina, an intermediate filament network underlining the inner nuclear membrane, where they play a crucial role in maintaining the structural integrity of the nucleus, anchoring of the heterochromatin, gene regulation etc. Therefore, it is of great interest to elucidate whether A-type lamins with mutations typical for AD-EDMD can still localise correctly to the nuclear envelope, and whether they disturb the localisation of some of their endogenous binding partners, i.e. emerin. Another interesting question arises when we think of the interaction of lamin A with lamin C: what happens if one or even both binding partners are mutated ? Would these mutations affect cell division ? And even more importantly: would there be any differences between lamin A and C with the same mutation ? The easiest way to answer these questions is by immunofluorescence microscopy. For this reason, nine missense mutations (R50S, R133P, T150P, E358K, E361K, R527P, L530P, R541S and G602S), one deletion mutation (delQ355), one polymorphism (C<T1698) and a 'double-mutant' (E358K+C<T1698) were created in the pre-lamin A cDNA sequence by site-directed mutagenesis and tagged with EGFP (enhanced green fluorescent protein) at the amino terminus. After transient transfection into an appropriate cell line, their localisation was examined using a fluorescence microscope. For lamin C, only three mutations were available (T150P, R527P and L530P) and these were fused to the DsRed2 protein to allow differentiation between lamin A and lamin C constructs in double transfection experiments. All transfections were performed in C2C12 mouse myoblast cells and COS7 green monkey fibroblast cells and gave the same results in both cell lines. Since the antibody staining for endogenous proteins worked slightly better in the COS7 fibroblasts, only those pictures will be shown.

4.1.2 The lamin A and C constructs expressed by COS7 cells are of the expected sizes

To prove that the proteins expressed by the transfected cells were in fact lamins of the correct size, cell lysates of cells transfected with the different mutations were run on a 10% SDS-polyacrylamide gel and immunoblotted for lamin A/C (Fig. 4.1) and GFP or DsRed2, respectively (data not shown). Protein loading was normalised by immunoblotting for actin (data not shown).

The immunoblot shows the expected sizes for the fusion proteins, approximately 110-113 kDa for EGFP-lamin A wild type and mutations and ~97 kDa for the DsRed2-lamin C constructs. The apparent size difference of mutations R50S, R133P, delQ355, E361K, R541S and G602S in comparison to the rest of the mutations is due to a different cloning protocol which added several amino acids from an extra DNA sequence in frame with the lamin A sequence and therefore led to a bigger end product. Expression levels appeared to be similar, except for the lamin A polymorphism C<T1698 which was expressed at lower levels. No effect of the exogenous proteins on the endogenous lamins could be observed. However, a possible effect could be masked by the low transfection efficiency: 85% of cells in the immunoblotted total cell lysates were not transfected and thus endogenous lamin levels would appear normal.

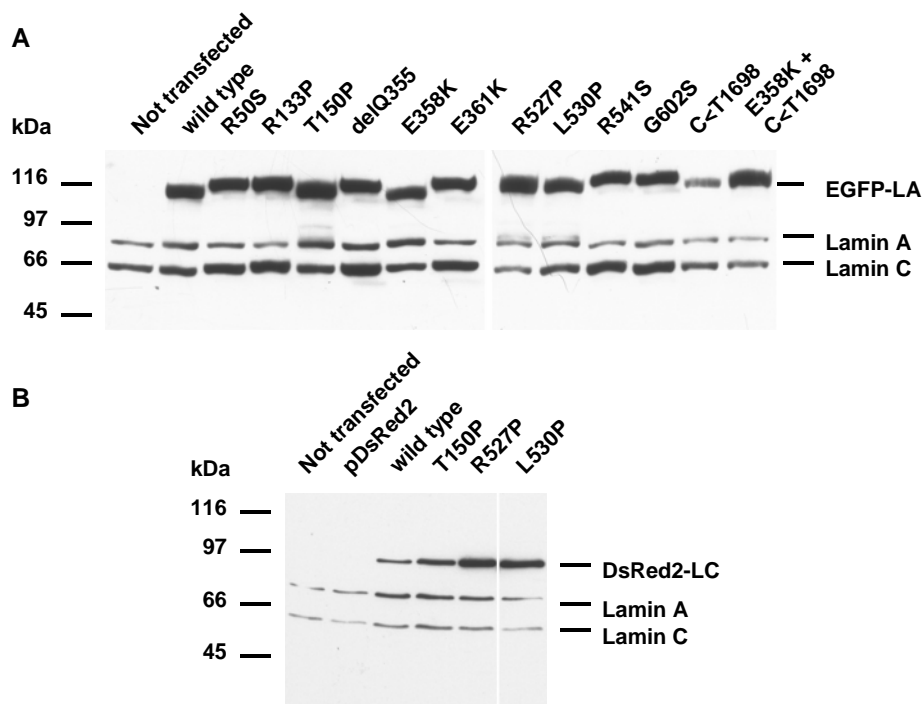


Fig. 4.1. Immunoblot showing the expression levels of EGFP-lamin A (A) and pDsRed2-lamin C (B) transfected into COS7 cells alongside endogenous lamin A/C levels. Cell lysates from a transfection experiment were blotted with anti-lamin A/C antibody R27. LA, lamin A; LC, lamin C. The molecular weight markers in kDa are indicated on the left.

4.1.3 Exogenously expressed lamin A with the mutation T150P does not disrupt the distribution of endogenous A-type lamins

Exogenous protein expression is likely to affect the corresponding endogenous protein pool in the transfected cells. To determine the effect of exogenous lamin A on the endogenous A-type lamins, COS7 cells were transfected with selected EGFP-lamin A mutations and counterstained with R27 antibody which recognises both exogenous EGFP-lamin A and endogenous lamins A and C. However, analysis under the fluorescence microscope proved difficult, since the strong expression levels of exogenous EGFP-lamin A and the resulting bright fluorescence of the EGFP itself as well as the intense antibody staining masked the antibody staining of the endogenous A-type lamins nearly completely (Fig. 4.2, see wild type and mutation R133P).

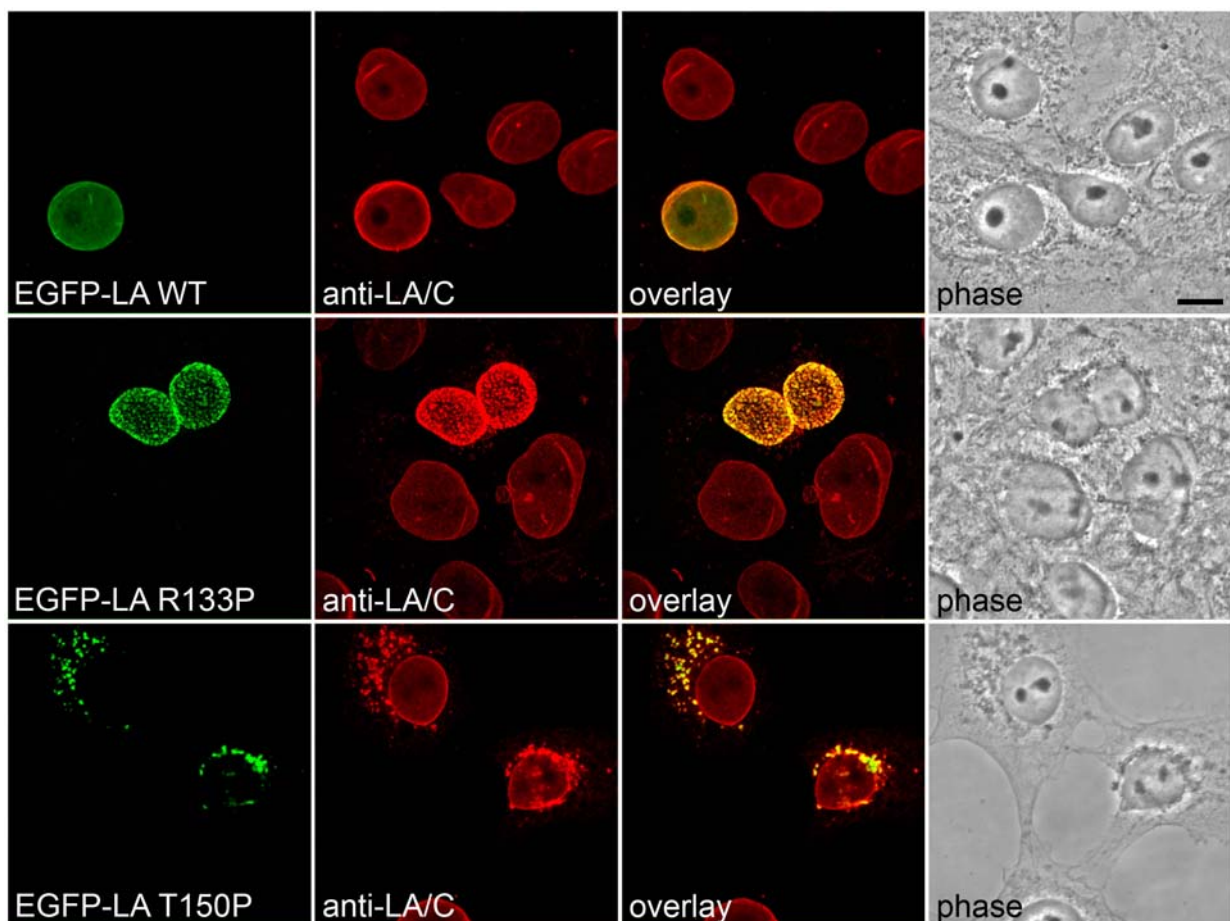


Fig. 4.2. Immunofluorescence analysis of the influence of exogenous EGFP-lamin A expressed by transiently transfected COS7 cells on the endogenous lamin A/C. The EGFP-lamin A localisation is monitored by EGFP fluorescence (green), endogenous lamin A/C with Texas-Red (red). Co-localisation between EGFP-lamin A and endogenous lamin A/C is shown in the overlay panels, total cell morphology can be examined in the phase contrast images. Pictures were taken with a confocal laser scanning microscope. Bar 10 μ m.

The only mutation for which a statement about the endogenous lamins A and C could be made was T150P; this EGFP-lamin A mutation localised exclusively to the cytoplasm, therefore leaving the nucleus free of the masking influence of the EGFP-lamin A. The distribution of the endogenous lamins A and C appeared to be unaffected by the exogenous proteins and looked like the wild type phenotype.

4.1.4 Exogenously expressed lamin A proteins do not form heterodimers with endogenous lamin B2

A-type lamins are not the only lamins found in mammalian cells, essential for cell survival are in fact the B-type lamins B1 and B2. It has been shown that A and B-type lamins can form heterodimers *in vitro* [Georgatos *et al.* 1988, Ye and Worman 1995], so an effect of the mutated exogenous lamin A on the endogenous lamin B could be considered likely. Nevertheless, transient transfections of COS7 fibroblasts with selected EGFP-lamin A mutations and counter-staining for endogenous lamin B2 with antibody X223 did not give evidence to support this theory: while the endogenous lamin B2 seemed to co-localise with the lamin A constructs that show a wild type phenotype (Fig. 4.3, see WT and R527P), the typical wild type localisation of endogenous lamin B2 remained constant even when the simultaneously expressed lamin A mutations exhibited a fine granular pattern along the nuclear rim (Fig. 4.3, see R133P and delQ355). If the two lamin types form heterodimers, we would expect to see a change in the distribution of endogenous lamin B2, with its localisation approaching the localisation pattern of the mutated lamin A constructs. Since this is not the case, these results support the conclusion that lamins A and B2 do not dimerise *in vivo* and form distinct networks at the nuclear envelope, as was suggested previously [Izumi *et al.* 2000, Moir *et al.* 2000, Haraguchi *et al.* 2001].

This theory is further supported by the distribution pattern of the lamin A polymorphism C<T1698 which produced globular aggregates along the inner nuclear membrane (Fig. 4.3, see C<T1698). Lamin B2 was completely excluded from these aggregates, indicating that it could not penetrate the dense aggregates of this lamin A polymorphism. Apart from the displacement from the nuclear rim caused by the aggregation of the exogenous lamin A, the localisation of endogenous lamin B2 appeared normal.

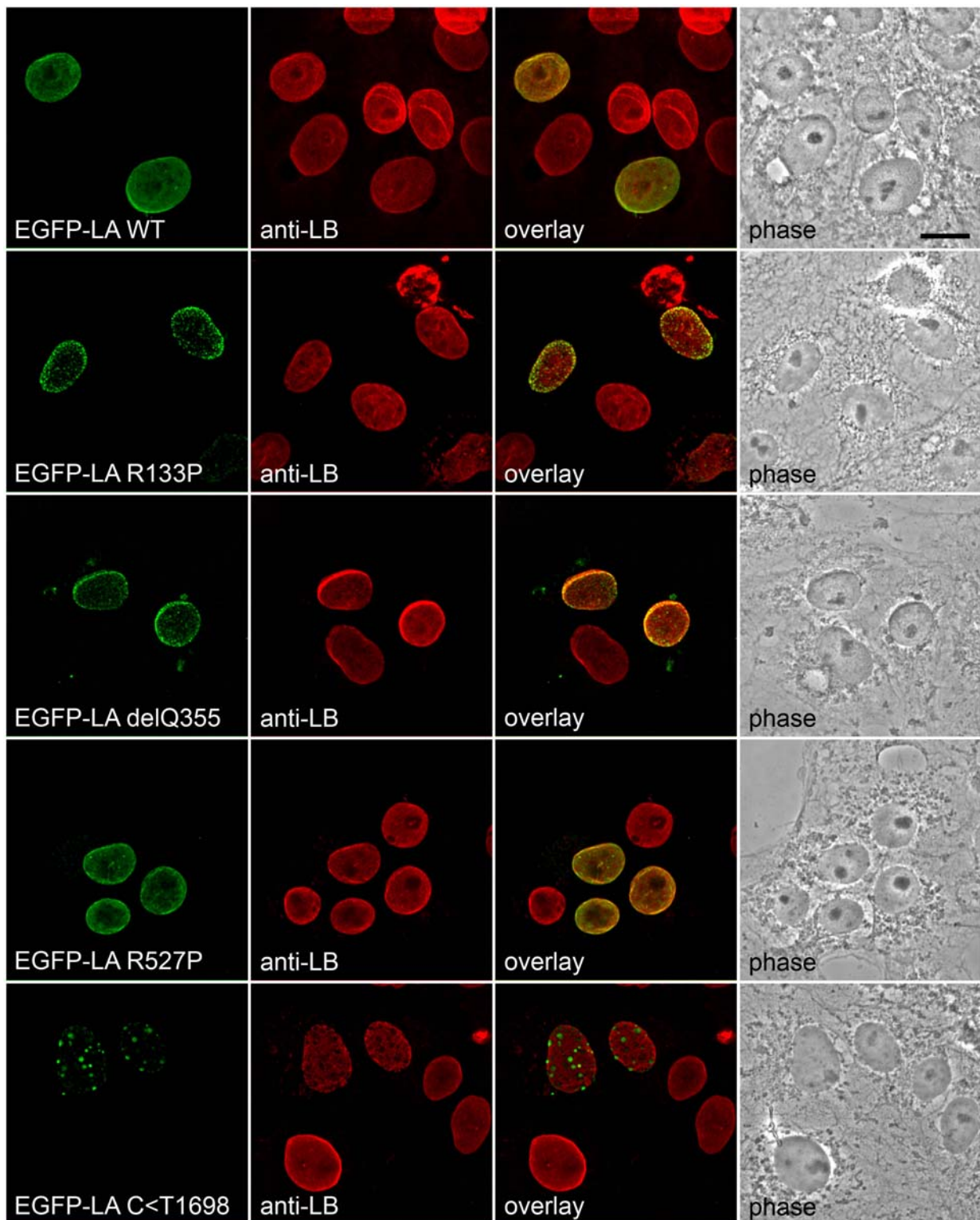


Fig. 4.3. Immunofluorescence analysis of the influence of exogenous EGFP-lamin A expressed by transiently transfected COS7 cells on the endogenous lamin B2. The EGFP-lamin A localisation is monitored by EGFP fluorescence (green), endogenous lamin B2 with Texas-Red (red). Co-localisation between EGFP-lamin A and endogenous lamin B2 is shown in the overlay panels, total cell morphology can be examined in the phase contrast images. Pictures were taken with a confocal laser scanning microscope. Bar 10 μ m.

4.1.5 Exogenous expression of lamin A constructs reveals 3 categories of localisation phenotypes

Immunofluorescence analysis of transiently transfected COS7 and C2C12 cells expressing the different EGFP-lamin A mutations led to the observation of a wide spectrum of nuclear localisation phenotypes as well as a variation in the number of cells showing each type of defect. Table 4.1 summarises these findings together with the localisation phenotypes of the endogenous proteins emerin and lamin C.

The optimum expression time for the exogenous lamin A constructs was determined to lie between 16-18 hours post-transfection; at that time, wild type EGFP-lamin A was correctly localised to the nuclear lamina and less than 10% of cells showed signs of protein over-expression by exhibiting large aggregates (over 0.4 μ m in diameter) in the nucleus and the cytoplasm. The number and size of these aggregates increased considerably (over 0.7 μ m in diameter) over time post-transfection and prevented immunofluorescence analysis of the nuclear envelope.

4.1.5.1 Category 1: wild type phenotype of exogenous lamin A mutations

Wild type EGFP-lamin A exhibited the typical lamin localisation: a continuous circle along the nuclear envelope in at least 90% of the transfected cells (see Fig. 4.4). The remaining 10% showed a mis-localisation of exogenous lamin A in a range of nuclear staining patterns and internal foci. However, these structures, which included variations in size, shape, number of intranuclear foci and nucleoplasmic staining intensity, reflect the movements of lamins throughout the cell cycle [Barbie *et al.* 2004]. Endogenous emerin was localised correctly at the nuclear envelope, therefore providing a perfect co-localisation staining with exogenous wild type lamin A.

During nuclear envelope disassembly/reassembly in mitosis, endogenous emerin assumed a continuous staining pattern across the mid-body, in places intermittently enriched (see Fig. 4.4, arrow in panel E358K). The mid-body connects the two daughter cells and contains the remains of the mitotic spindle. This normal distribution of emerin just prior to the completion of cytokinesis [Dabauvalle *et al.* 1999] was the one followed by the endogenous emerin in the case of COS7 cells transfected with wild type EGFP-lamin A; the exogenous lamin A itself also took up the normal distribution pattern during mitosis (data not shown).

Results

Table 4.1. Transfection efficiencies and percentage of cells exhibiting abnormalities when exogenously expressing EGFP-lamin A in COS7 cells.

Mutation	Percentage of cells transfected	% of transfected cells exhibiting normal lamin A localisation Emerin localisation	% of transfected cells with small nuclear aggregates Emerin localisation	% of transfected cells with large, nuclear aggregates and/or cytoplasmic aggregates Emerin localisation	Endogenous lamin C nuclear staining
Wild type	15%	>90% emerin normal	<10% emerin normal	0%	Normal
R50S	15%	90% emerin normal	0% emerin normal	10% emerin reduced at NE, some cytoplasmic	ND
R133P	15%	60% emerin normal	40% emerin reduced at NE	0%	ND
T150P	15%	0%	0%	100%; aggregates in the cytoplasm 50-70% emerin relocated to cytoplasm.	Nuclear foci Reduced in 10% of cells
DelQ355	15%	10% emerin normal	80% emerin reduced at NE	10%; aggregates in nucleus & cytoplasm emerin in cytoplasm	ND
E358K	15%	90% emerin normal	5% emerin normal	5% emerin slightly reduced at NE	Reduced in all cells 80% slightly, 20% strongly
E361K	15%	80% emerin normal	20% emerin slightly reduced at NE	0%	ND
R527P	15%	80% emerin reduced at NE	20% emerin reduced at NE; cytoplasmic	0%	Reduced in all cells
L530P	15%	>90% emerin normal	<10% emerin reduced at NE; cytoplasmic	0%	Reduced in 20% of cells
R541S	5%	>90% emerin normal	<10% emerin slightly reduced at NE and in cytoplasm	0%	ND
G602S	15%	>90%, emerin normal or reduced (~50% of cells)	<10% emerin reduced at NE	0%	ND
C<T1698	15%	0%	20% emerin reduced at NE; in aggregates	80% emerin co-localised in aggregates	Reduced in 20% of cells
E358K + C<T1698	15%	10% emerin normal	70% emerin reduced at NE; in aggregates	20% Emerin co-localised in aggregates	Reduced in 50% of cells

NE nuclear envelope, ND not done.

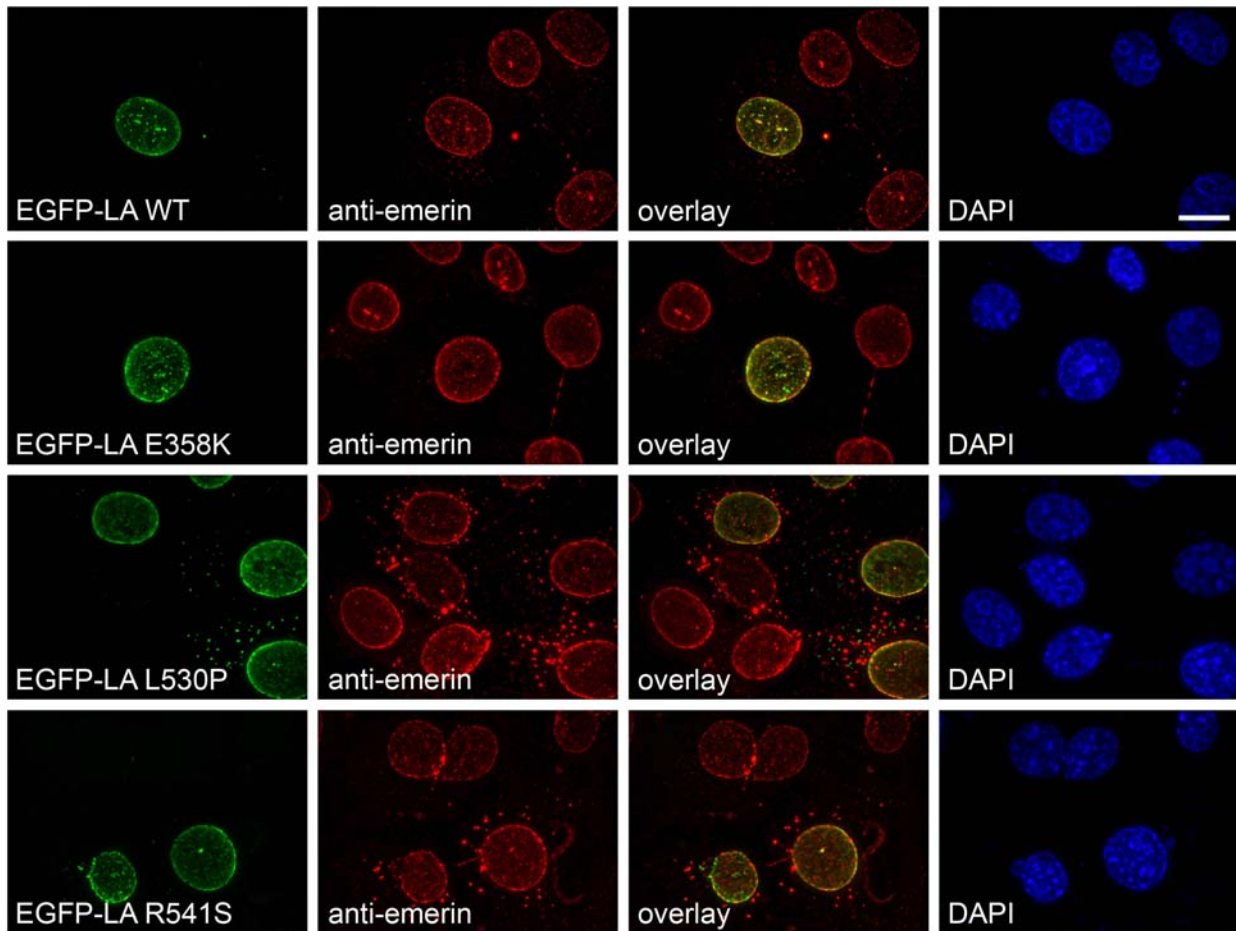


Fig. 4.4. Intracellular localisation of wild type and lamin A mutants as EGFP fusion proteins transiently expressed by COS7 cells: category 1 (wild type-like appearance). The EGFP-lamin A localisation is monitored by EGFP fluorescence (green), endogenous emerlin with rhodamine (red). Co-localisation between EGFP-lamin A and endogenous emerlin is shown in the overlay panels, DNA staining is with DAPI (blue). Pictures were taken with a fluorescence microscope, shown are the deconvoluted maximum projections of a series of pictures. Bar 10 μ m.

In the three lamin A mutations belonging to category 1, E358K, L530P and R541S, normal nuclear lamina localisation was observed in more than 90% of the transfected cells, with no gross changes in nuclear structure as seen by chromatin staining with DAPI (Fig. 4.4). As in the wild type, the remaining 10% of transfected cells displayed a range of mis-localisation phenotypes for the exogenous lamin A, concurrent with a slight reduction in endogenous emerlin at the nuclear envelope.

All three mutations behaved like the wild type during mitosis, along with endogenous emerlin which appeared normal as well (data not shown).

4.1.5.2 Category 2: a range of phenotypes of exogenous lamin A mutations

The second category of mutants contained the mutations R50S, R133P, E361K, R527P, G602S and the mutation E358K together with the polymorphism C<T1698 (Figs. 4.5.1 and 4.5.2). In this category, a bigger variety of phenotypes was observed for each mutation, with a more severe phenotype in the small number of transfected cells which showed an abnormal phenotype.

Similar to category 1, the majority of the cells expressing these lamin A mutants exhibited the normal phenotype (between 60-90% for R50S, R133P, E361K, R527P and G602S, see Table 4.1), with E358K+C<T1698 being the only exception with approximately 70% of transfected cells showing fine granules of EGFP-lamin A along the nuclear rim. Abnormalities in the remaining transfected cells in all mutants of this category included both fine and large (but still smaller than 0.4 μm) nuclear aggregates of lamin A, as well as displacement to cytoplasmic aggregates after cell division in the case of R50S (Fig. 4.5.1, b1).

Endogenous emerin appeared to be distributed normally in transfected cells which were in interphase (Fig. 4.5.1, rows a, c, e and Fig. 4.5.2, rows a and e) apart from mutation G602S where it was reduced at the nuclear envelope in about 50% of transfected cells (Fig. 4.5.2, compare c2 to d2). Interestingly, this normal localisation pattern of emerin was disturbed when cells expressing a category 2 mutation (with the exception of G602S) had just undergone cell division (Fig. 4.5.1, rows b, d, f and Fig. 4.5.2, rows b and f). Here, a range of phenotypes could be observed: in the R133P mutant, exogenous lamin A and endogenous emerin followed a wild type distribution pattern during nuclear envelope disassembly / reassembly in mitosis and emerin located correctly to the mid-body (Fig. 4.5.1, row d). In the mutations R50S, E361K and E358K+C<T1698, endogenous emerin levels were reduced at the nuclear envelope and / or mis-localised in aggregates in either nucleus or cytoplasm (Fig. 4.5.1, rows b, f, Fig. 4.5.2, row f). The lamin A mutant R527P exhibited the most severe phenotype, taking up a very punctuate EGFP-lamin A staining within the nucleoplasm and re-distributing emerin to the perinuclear regions as aggregates (Fig. 4.5.2, row b) in cells which had recently divided.

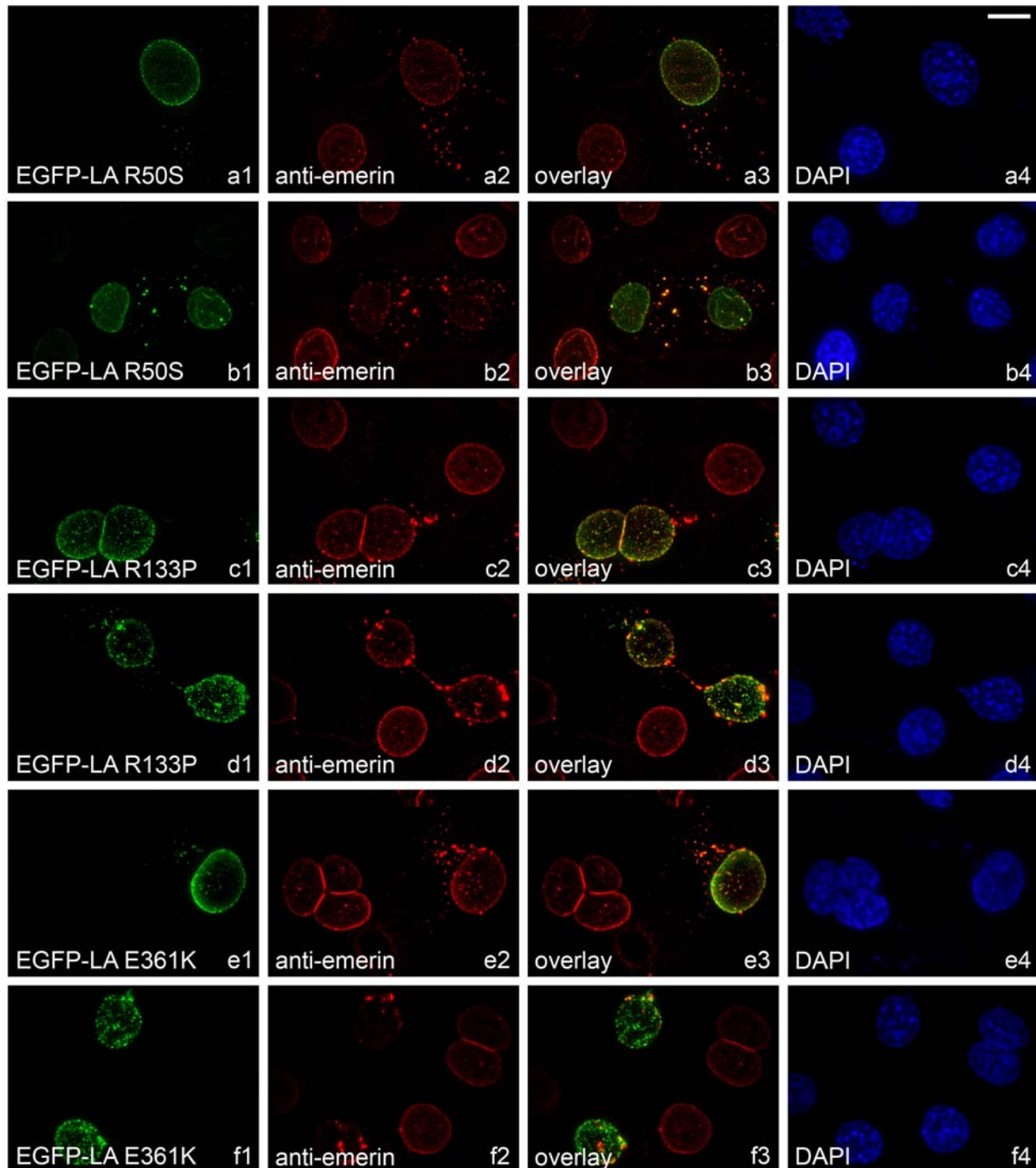


Fig. 4.5.1. Intracellular localisation of lamin A mutants as EGFP fusion proteins transiently expressed by COS7 cells: category 2 (range of phenotypes), part 1. The EGFP-lamin A localisation is monitored by EGFP fluorescence (green), endogenous emerin with rhodamine (red). Co-localisation between EGFP-lamin A and endogenous emerin is shown in the overlay panels, DNA staining is with DAPI (blue). Rows a, c and e show cells in interphase, rows b, d and f show cells just after mitosis. Pictures were taken with a fluorescence microscope, shown are the deconvoluted maximum projections of a series of pictures. Bar 10 μ m.

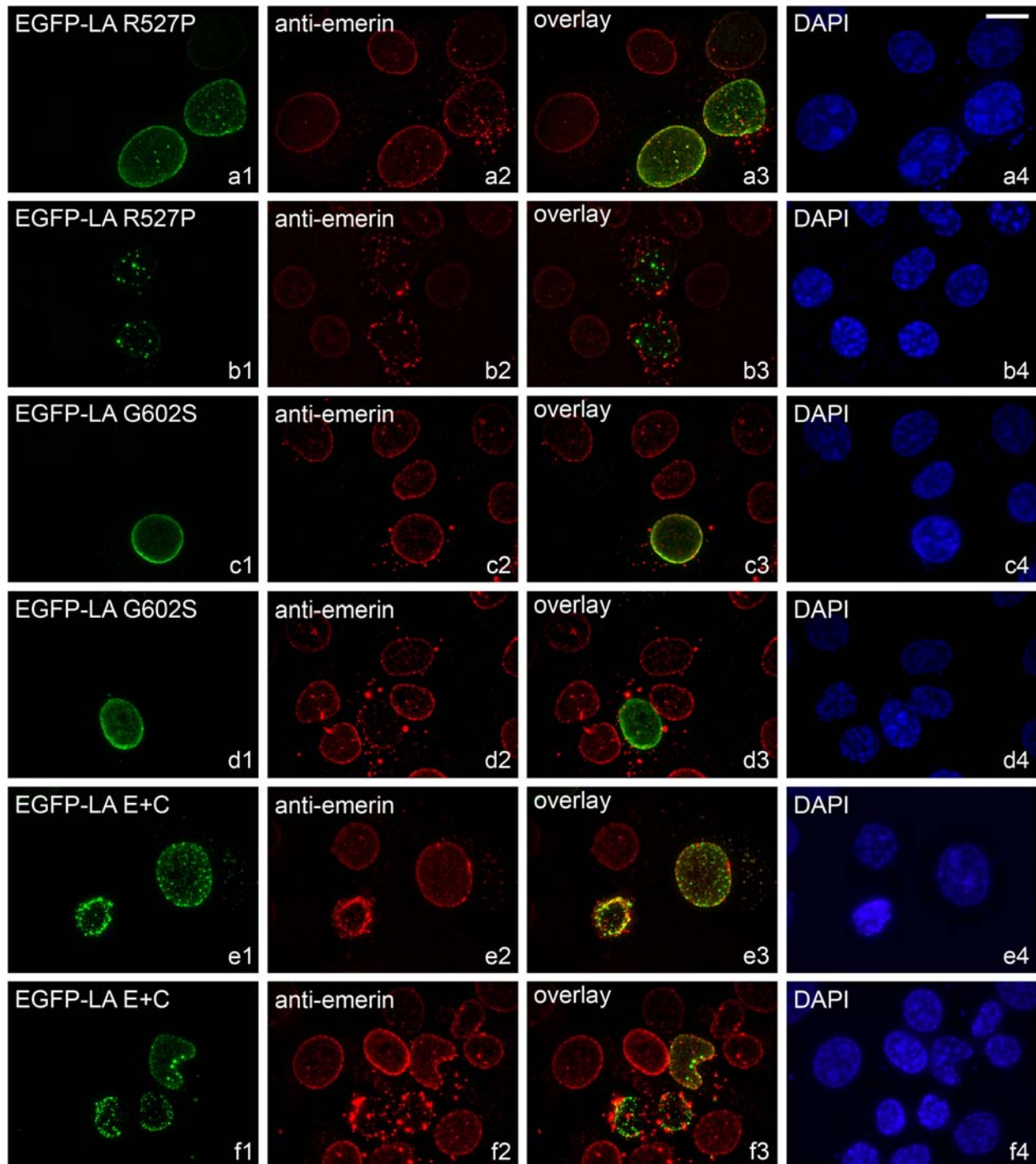


Fig. 4.5.2. Intracellular localisation of lamin A mutants as EGFP fusion proteins transiently expressed by COS7 cells: category 2 (range of phenotypes), part 2. The EGFP-lamin A localisation is monitored by EGFP fluorescence (green), endogenous emerlin with rhodamine (red). Co-localisation between EGFP-lamin A and endogenous emerlin is shown in the overlay panels, DNA staining is with DAPI (blue). Rows a, c, d and e show cells in interphase, rows b and f show cells just after mitosis. Pictures were taken with a fluorescence microscope, shown are the deconvoluted maximum projections of a series of pictures. E+C E358K+C<T1698, bar 10 μ m.

4.1.5.3 Category 3: mis-localisation of exogenous lamin A mutations

The EGFP-lamin A mutants of the third category, namely T150P, delQ355 and the polymorphism C<T1698, demonstrated the most abnormal phenotype of all mutants examined, with a frequency of 90-100% in the cells expressing these mutations.

In all transfected cells, lamin A T150P was grossly mis-localised in interphase cells (Fig. 4.6, row a) as well as in mitotic cells (Fig. 4.6, row b), suggesting a nuclear assembly defect. The aggregates of exogenous lamin A assumed a rod-like shape, occasionally aggregating into larger structures (especially when the level of protein expression was higher), which were found both in the perinuclear region and the cytoplasm (Fig. 4.6, rows a and b). Little or no nuclear lamina or nucleoplasmic staining could be observed. Endogenous emerin levels appeared strongly reduced at the nuclear envelope in 50-70% of transfected cells because of its re-location to the cytoplasm. However, cells transfected with T150P did not exhibit any form of co-localisation between endogenous emerin and exogenous lamin A at any stage of the cell cycle, indicative of an altered binding ability of the lamin A mutant T150P to emerin. The mis-localisation of endogenous emerin increased in cells which had recently undergone cell division (Fig. 4.6, b2): while the mid-body remnant between the two daughter cells gave a wild type pattern for emerin staining, the targeting of endogenous emerin to the newly assembled nuclear envelopes of the two cells seemed delayed.

The observation of a more severe phenotype in daughter cells after mitosis was also true for cells expressing the lamin A mutation delQ355. In interphase, the cells exhibited a fine punctuate nuclear lamina and normal nucleoplasmic staining for exogenous lamin A as well as normal endogenous emerin staining (Fig. 4.5, row c), whereas after cell division, exogenous lamin A presented a more punctuated distribution at the nuclear envelope, the nucleoplasm, the perinuclear region and the mid-body (Fig. 4.6, d1). Endogenous emerin was mis-targeted and seemed to be completely excluded from the nucleus (Fig. 4.6, d2). However in contrast to mutant T150P, endogenous emerin co-localised perfectly with the exogenous lamin A of mutant delQ355 at the perinuclear region and the mid-body (Fig. 4.6, d3) which suggests that the binding of emerin to the mutant lamin A is the cause for its mis-localisation. In cells expressing the polymorphism C<T1698, the exogenous lamin A formed small aggregates at the nuclear lamina and in the nucleoplasm in interphase (Fig. 4.6, e1), not unlike the strong punctuate staining pattern of delQ355 after mitosis. This mis-localisation of exogenous lamin A became much more distinctive in cells which had recently divided and the aggregate size also increased (Fig. 4.6, f1).

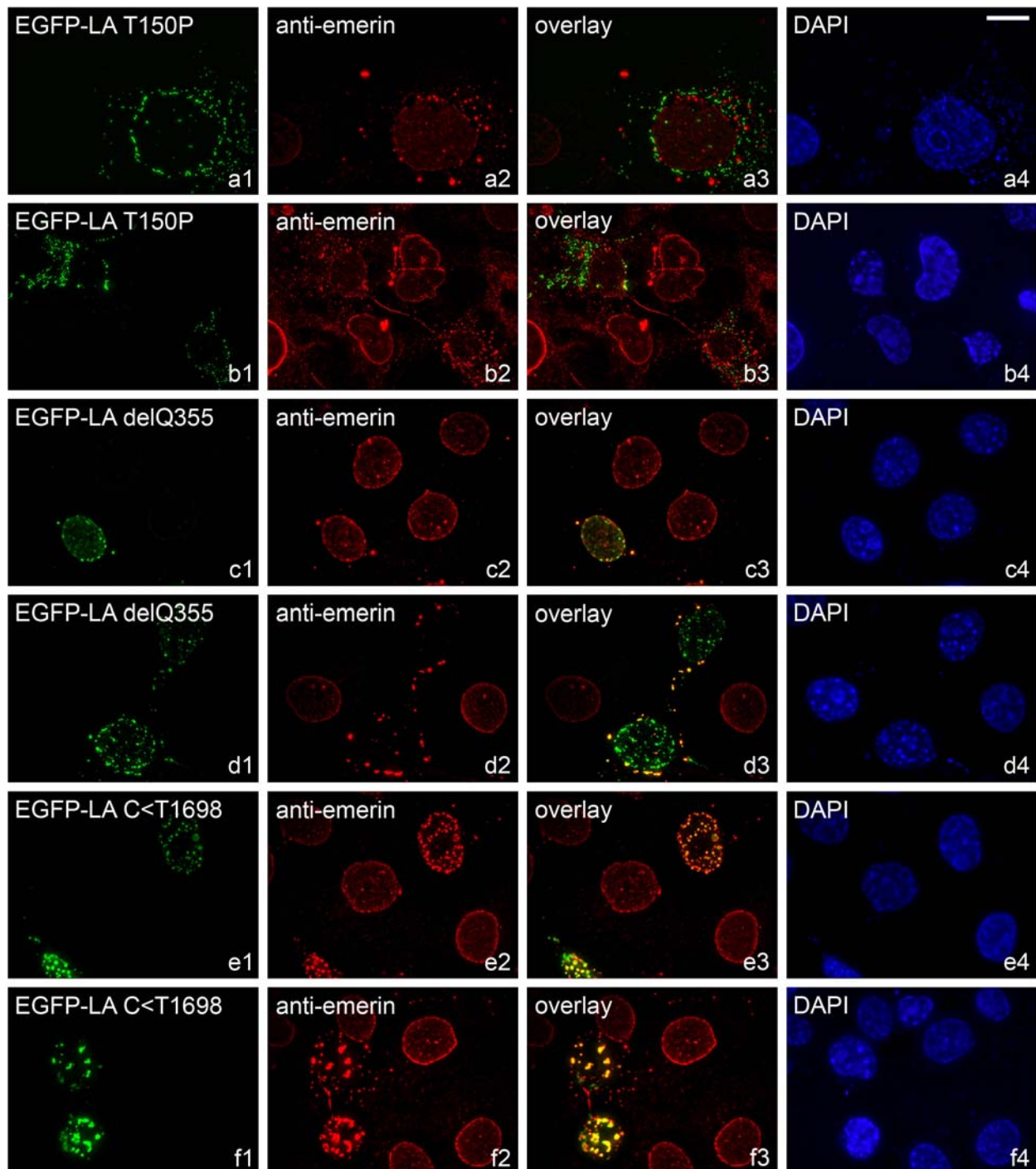


Fig. 4.6. Intracellular localisation of lamin A mutants as EGFP fusion proteins transiently expressed by COS7 cells: category 3 (severe mis-localisation). The EGFP-lamin A localisation is monitored by EGFP fluorescence (green), endogenous emerlin with rhodamine (red). Co-localisation between EGFP-lamin A and endogenous emerlin is shown in the overlay panels, DNA staining is with DAPI (blue). Rows a, c and e show cells in interphase, rows b, d and f show cells just after mitosis. Pictures were taken with a fluorescence microscope, shown are the deconvoluted maximum projections of a series of pictures. Bar 10 μ m.

Endogenous emerin distribution was severely affected and mirrored the staining pattern of the exogenous lamin A, therefore co-localising exactly with the mutant lamin A (Fig. 4.6, e2, e3 and f2, f3). The aberrant nuclear phenotype of this polymorphism came as a surprise, since the nucleic acid alteration does not change the amino acid sequence of the protein and also does not lead to a truncated protein (see Fig. 4.1, immunoblot of transfected cells).

4.1.5.4 Endogenous lamin C is affected by some of the lamin A mutations

Lamins A and C form heterodimers and it has been demonstrated that lamin C needs binding to lamin A for incorporation into the nuclear lamina [Vaughan *et al.* 2001]. Most mutations causing EDMD lie within the sequence part common to both lamin A and C and therefore affect both proteins. However, since the autosomal form of EDMD is inherited as a dominant trait and most patients are heterozygous for the mutation, both normal and mutant proteins exist in the patient's cells. To determine the effect of mutated proteins on the normal protein pool, we examined the endogenous lamin C levels in COS7 cell expressing EGFP-lamin A mutants. Unfortunately, due to the extreme brightness of the EGFP and the poor quality of the available anti-lamin C antibody, the immunofluorescence signals of endogenous lamin C were often too low for detection, so data could only be collected for some of the mutations (see Table 4.1).

As expected, in cells transfected with exogenous wild type lamin A the distribution of endogenous lamin C appeared completely normal, with the endogenous lamin C co-localising perfectly with exogenous lamin A (Fig. 4.7). A similar phenotype was observed in cells expressing EGFP-lamin A L530P, though in about 20% of transfected cells endogenous lamin C levels seemed to be reduced. Interestingly, expression of the lamin A mutant E358K, which typically exhibited a wild type distribution pattern and was therefore classed in category 1, revealed a much more pronounced effect on endogenous lamin C: it was reduced in all transfected cells to at least some degree.

The mutations R527P and E358K+C<T1698 also showed a reduced nuclear lamina and nucleoplasmic staining of endogenous lamin C. Most interesting, however, was the influence that the lamin A mutation and the polymorphism from category 3, T150P and C<T1698, exerted on the expression of endogenous lamin C. T150P interfered with the distribution of lamin C in about 5% of transfected cells. The expression of EGFP-lamin A C<T1698 affected endogenous lamin C in a much less severe way than it affected emerin distribution, only 20% of transfected cells exhibited a reduction in lamin C levels.

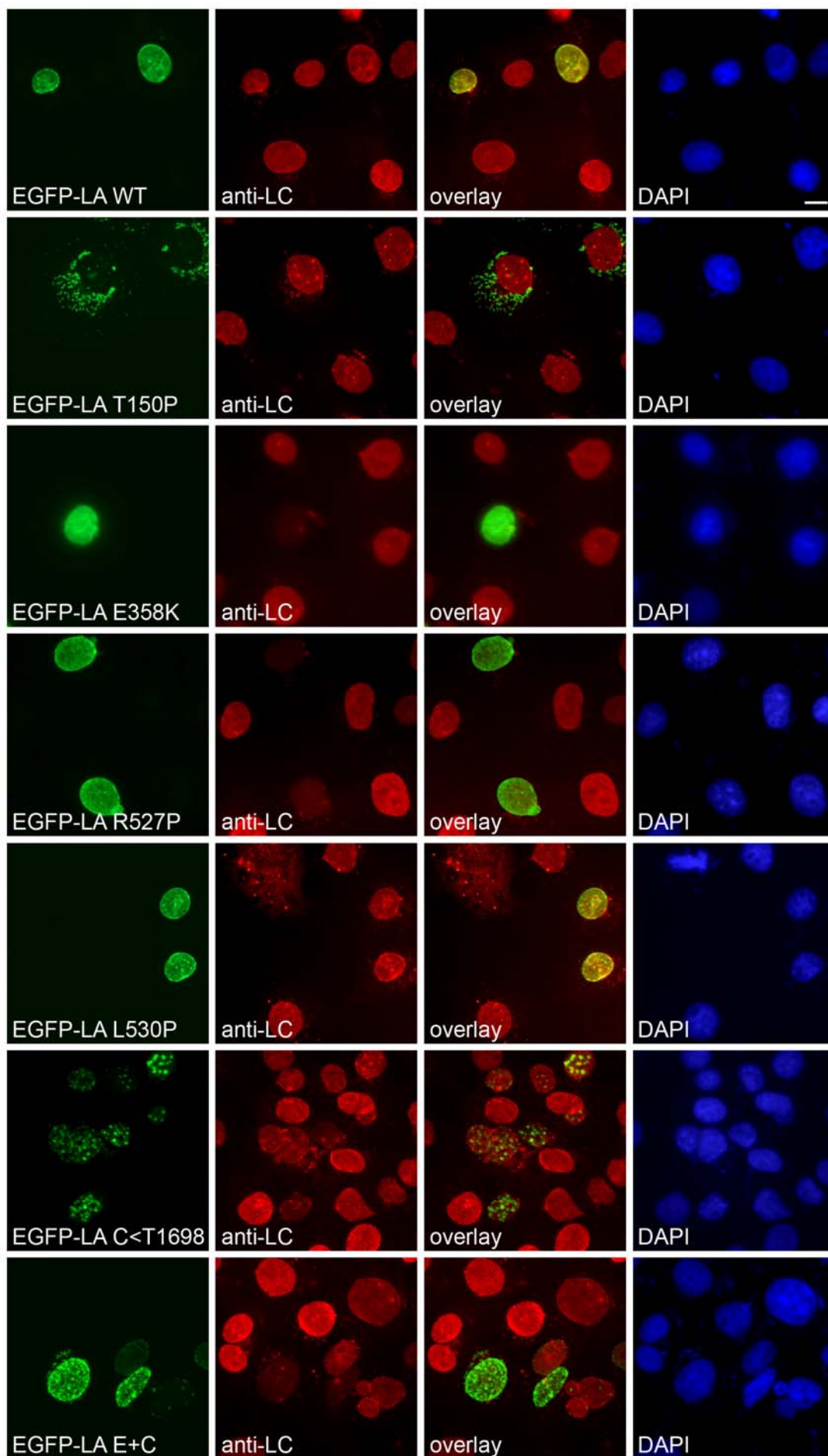


Fig. 4.7 (previous page). Immunofluorescence analysis of the influence of exogenous EGFP-lamin A expressed by transiently transfected COS7 cells on the endogenous lamin C. The EGFP-lamin A localisation is monitored by EGFP fluorescence (green), endogenous lamin C with rhodamine (red). Co-localisation between EGFP-lamin A and endogenous lamin C is shown in the overlay panels, DNA staining is with DAPI (blue). Pictures were taken with a Zeiss Axiophot fluorescence microscope. Bar 10µm.

4.1.6 Exogenously expressed lamin C constructs form aggregates in the nucleus

To determine the nuclear localisation of mutant lamin C, three LMNA mutations (T150P, R527P, L530P) were selected which covered the range of aberrant nuclear phenotypes observed in the lamin A transfection experiments. Their lamin C equivalents were cloned into the vector pDsRed2-C1 and the resulting constructs transfected into COS7 cells.

Immunofluorescence analysis revealed a very unexpected outcome: instead of resembling the localisation pattern of their equivalent lamin A construct, exogenously expressed lamin C appeared as large, regular shaped aggregates in the nucleoplasm. No difference was observed between wild type and the mutants (Fig. 4.8). Only 5% of the transfected cells showed a small amount of exogenous lamin C correctly localised to the nuclear lamina. The same results were obtained with shorter expression times for the proteins, with the earliest observation being performed at 6 hours post-transfection (data not shown). Additionally, these results indicated that simple over-expression could not be the cause for the protein aggregation. Unfortunately, the fluorescence intensity of the lamin C aggregates led to a bleed through into the other channels of the microscope, thus preventing the examination of the antibody staining of endogenous proteins such as emerin and lamin A.

Even though the DsRed2-protein by itself was distributed evenly in the cytoplasm of transfected cells (Fig. 4.8), the possibility of a transfection artefact remained (e.g. DsRed1 proteins aggregate with each other when expressed as fusion proteins, although the DsRed2 protein is advertised as avoiding this problem). This possibility was ruled out by re-cloning the lamin C constructs into the pEGFP vector used for the lamin A experiments. However, the cells transfected with the EGFP-lamin C fusion proteins exhibited exactly the same aberrant phenotype (Fig. 4.8, only the wild type EGFP-lamin C is shown).

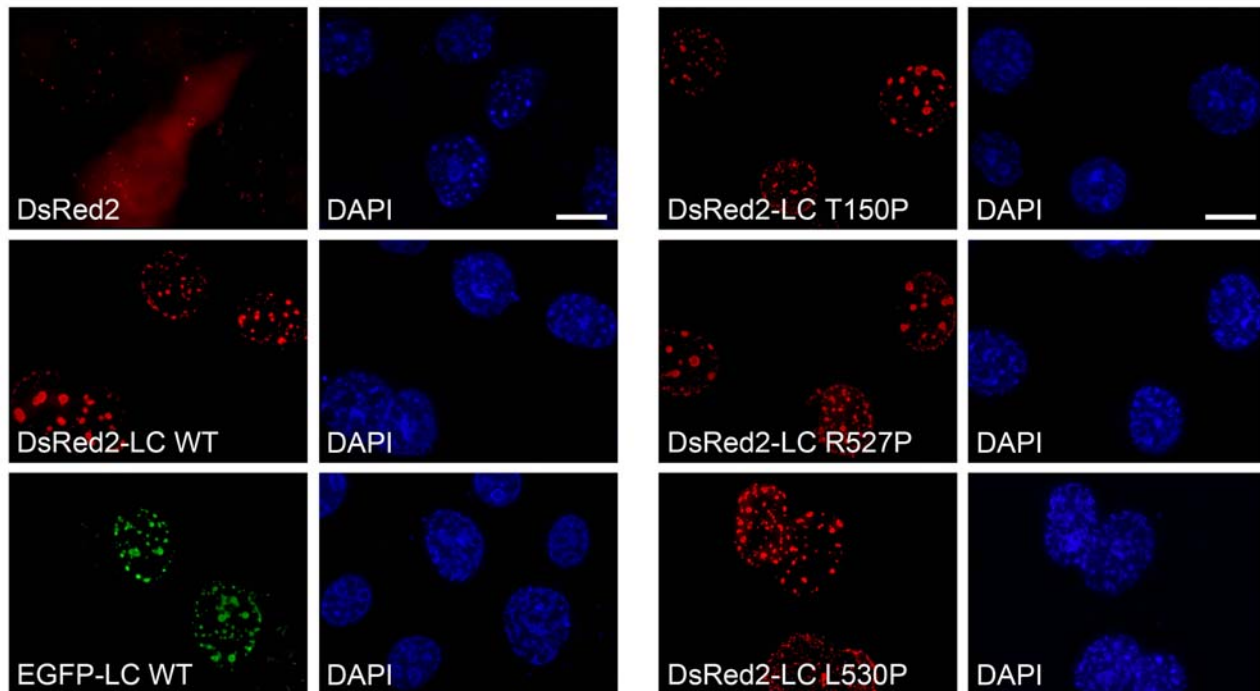


Fig. 4.8. Intracellular localisation of transiently expressed lamin C DsRed2 or EGFP fusion proteins and DsRed2 alone in COS7 cells. The DsRed2 and DsRed2-lamin C localisation is monitored by DsRed2 fluorescence (red), EGFP-lamin C wild type by EGFP fluorescence (green). DNA staining is with DAPI (blue). Pictures were taken with a fluorescence microscope, shown are the deconvoluted maximum projections of a series of pictures. Bar 10 μ m.

4.1.7 Lamin C requires co-expression with lamin A to be targeted to the nuclear lamina

The exogenously expressed lamin C was able to reach the nucleoplasm before aggregating, therefore we assume that it was folded correctly and transported into the nucleus, but was then unable to assemble into the nuclear lamina. Supporting this theory, Horton *et al.* reported that incorporation of lamin C into the lamina of P19 EC cells failed in the absence of lamin A [Horton *et al.* 1992]. Similarly, a nuclear aggregate phenotype was observed in transfected MEFs from the *Lmna* knock-out mouse (*Lmna*^{-/-}) which were expressing a wild type lamin C construct (in pcDNA3.1 with a HA tag) [Raharjo *et al.* 2001]. Co-expression with wild-type lamin A restored the normal lamin C localisation at the nuclear lamina. We therefore tested the lamin A and C mutants available for comparable behaviour in COS7 fibroblasts.

In cells expressing wild type DsRed2-lamin C and wild type EGFP-lamin A for 18 hours, both exogenous wild type lamin A and C were correctly localised at the nuclear lamina (Fig. 4.9), confirming that lamin C requires lamin A for nuclear lamina incorporation. Therefore, the mis-localisation of DsRed2-lamin C alone is also not due to aggregation of the DsRed2.

Subsequently, cells were co-transfected with each lamin A mutant and its equivalent lamin C mutant (mutations T150P, R527P, L530P). In all cases, the cells expressing both exogenous proteins exhibited a similar nuclear localisation pattern to that of the EGFP-lamin A mutant transfected on its own, i.e. wild type distribution for R527P and L530P and cytoplasmic aggregation of T150P. While in cells expressing the mutations R527P and L530P, a significant reduction of the nuclear lamin C aggregates was observed with the lamin C being re-directed to the nuclear rim by the exogenous lamin A (Fig. 4.9), this was not true for cells transfected with the mutation T150P. Here, the exogenous lamin A seemed unable to re-locate its lamin C counterpart which remained nucleoplasmic, although the nuclear aggregates were finer than when it was expressed alone. However, this might be due to the lower DNA concentration used for each A-type lamin in the double transfections.

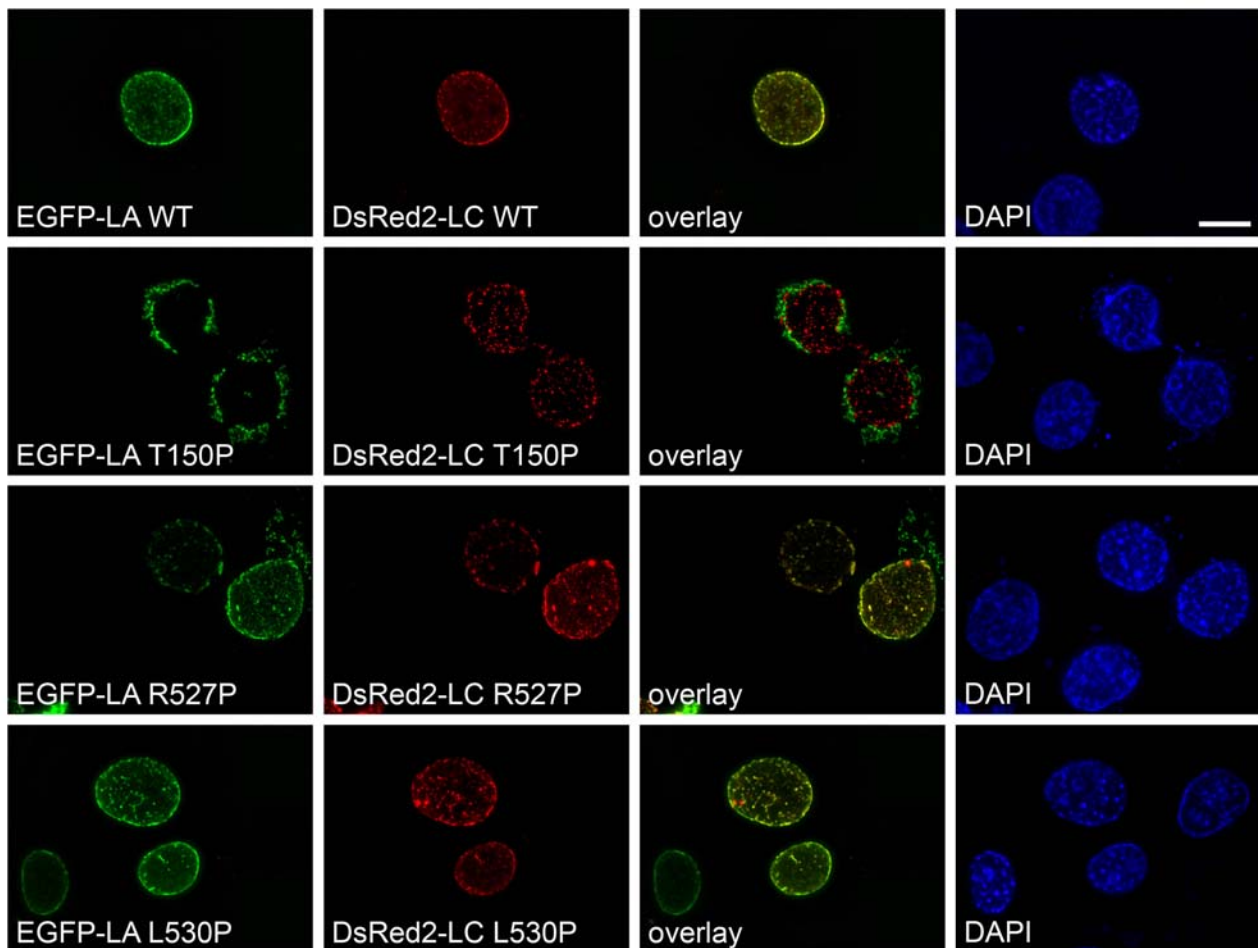


Fig. 4.9. Intracellular localisation of EGFP-lamin A and DsRed2-lamin C fusion proteins transiently expressed together in COS7 cells: expression of lamin A mutants with the equivalent lamin C mutants. The EGFP-lamin A localisation is monitored by EGFP fluorescence (green), that of DsRed2-lamin C by DsRed2 fluorescence (red). Co-localisation between EGFP-lamin A and DsRed2-lamin C is shown in the overlay panels (yellow), DNA staining is with DAPI (blue). Pictures were taken with a fluorescence microscope, shown are the deconvoluted maximum projections of a series of pictures. Bar 10 μ m.

4.1.8 Exogenous wild type lamin A can correct the localisation of all lamin C mutants, but not vice versa

Wild type as well as mutant lamin A could re-direct its equivalent lamin C to its correct nuclear lamina localisation and thus seemed to be the dominant partner of the heterodimer in the process of lamina assembly. To ascertain the degree of this dominance, each wild type A-type lamin was expressed together with the opposing mutant A-type lamin.

Exogenous wild type lamin A localised correctly at the nuclear lamina in the presence of any of the three exogenous lamin C mutants tried and it prevented the formation of lamin C nuclear aggregates by incorporating it into the lamina (Fig. 4.10, compare the cell single-transfected with lamin C L530P to the one double-transfected with both wild type lamin A and mutant lamin C L530P). When wild type lamin C was co-expressed with either of the lamin A mutants R527P or L530P, it localised at the nuclear envelope, mimicking the nuclear lamina distribution of the exogenous lamin A (Fig. 4.10). However, a different phenotype was obtained by co-expression of wild type lamin C with the lamin A mutation T150P: each exhibited a localisation pattern which was identical to that observed when they were expressed individually. Exogenous lamin A T150P remained aggregated in the perinuclear region of the cytoplasm, whereas exogenous wild type lamin C reached the nucleus and formed aggregates there.

These results confirm earlier findings that lamin C requires lamin A for the correct targeting to the nuclear envelope. Obviously, even mutant forms of lamin A can direct lamin C to the nuclear lamina, provided they are able to assemble into the lamina themselves.

4.1.9 Most lamin A mutants form heterodimers with wild type lamin C

Co-transfection experiments do not only give evidence for the exogenous lamin A mutants' ability to re-direct exogenous lamin C to the nuclear lamina, but also for their ability to dimerise with a wild type lamin. In the cells of most AD-EDMD patients, both the wild type and mutant alleles of the *LMNA* gene are expressed and may or may not interact with each other. In order to determine the effect of mutant lamin A on its ability to dimerise, COS7 cells were co-transfected with the wild-type DsRed2-lamin C construct and the different EGFP-lamin A mutations (Fig. 4.11).

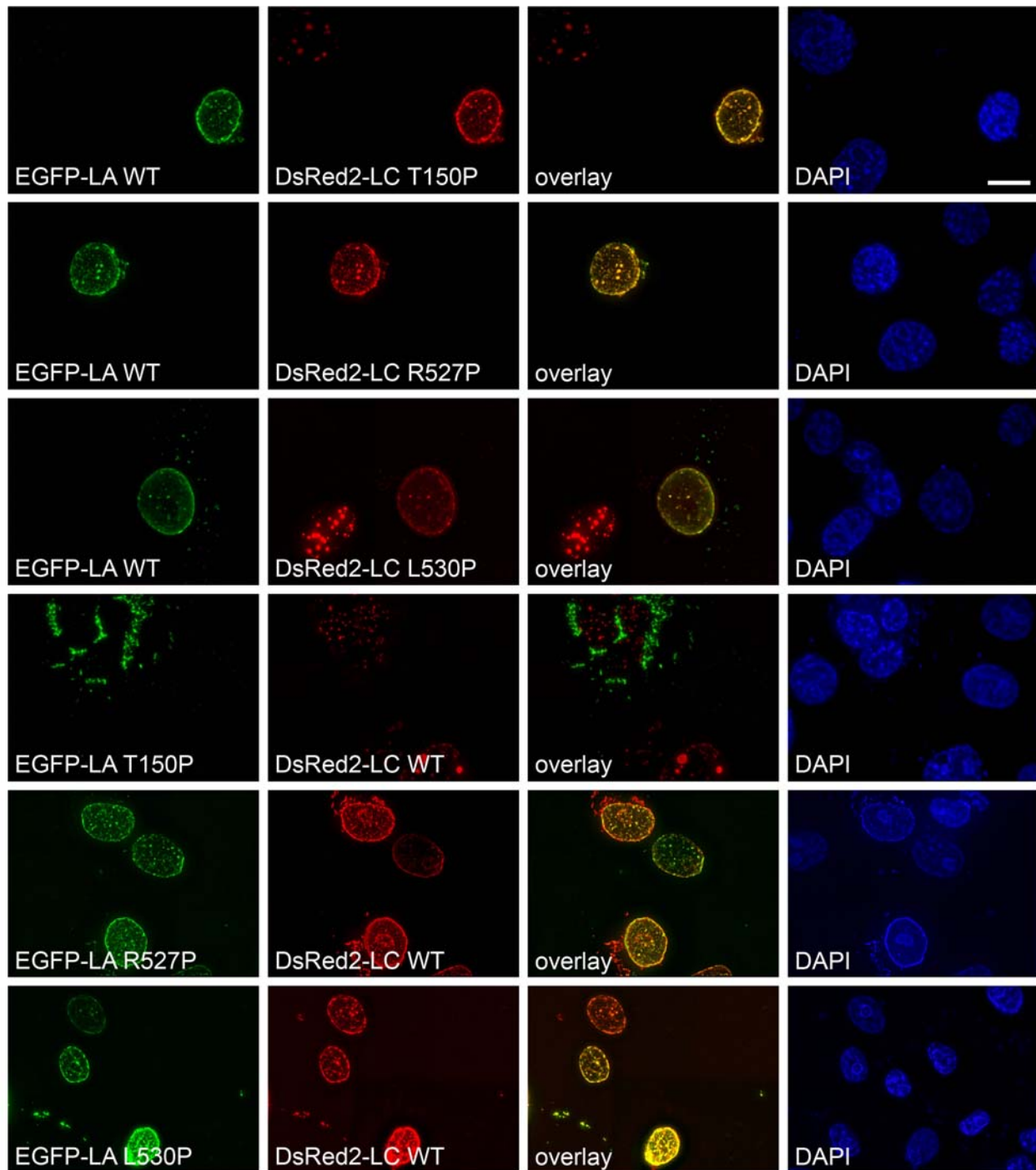


Fig. 4.10. Intracellular localisation of EGFP-lamin A and DsRed2-lamin C fusion proteins transiently expressed together in COS7 cells: expression of one wild type A-type lamin with the opposing mutant A-type lamin. The EGFP-lamin A localisation is monitored by EGFP fluorescence (green), that of DsRed2-lamin C by DsRed2 fluorescence (red). Co-localisation between EGFP-lamin A and DsRed2-lamin C is shown in the overlay panels (yellow), DNA staining is with DAPI (blue). Pictures were taken with a fluorescence microscope, shown are the deconvoluted maximum projections of a series of pictures. Bar 10 μ m.

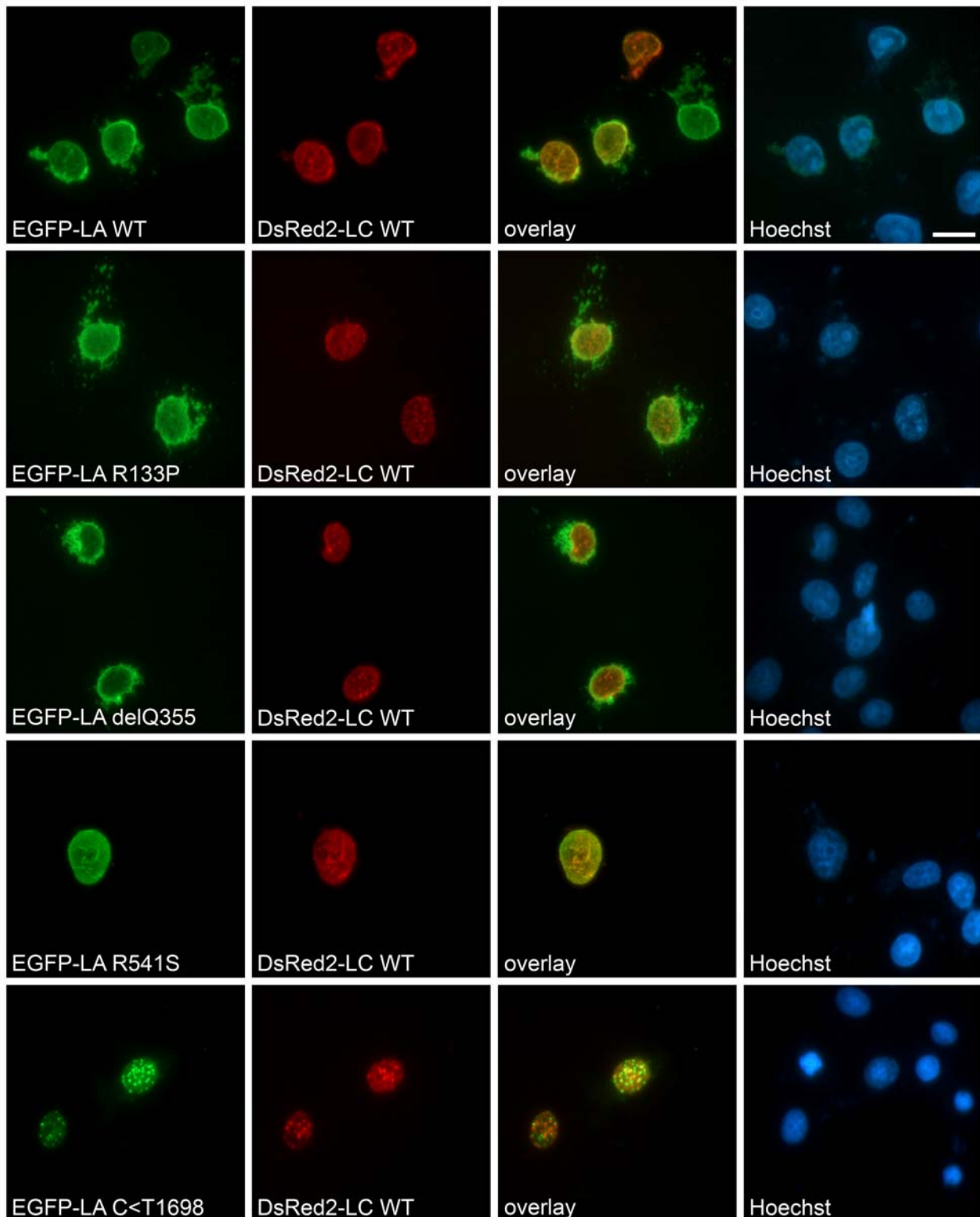


Fig. 4.11. Intracellular localisation of EGFP-lamin A and DsRed2-lamin C fusion proteins transiently expressed together in COS7 cells: expression of wild type lamin C with different lamin A mutants. The EGFP-lamin A localisation is monitored by EGFP fluorescence (green), that of DsRed2-lamin C by DsRed2 fluorescence (red). Co-localisation between EGFP-lamin A and DsRed2-lamin C is shown in the overlay panels (yellow), DNA staining is with Hoechst (blue). Pictures were taken with a Zeiss Axiophot fluorescence microscope. Bar 10 μ m.

Most of the lamin A mutations studied (R50S, E358K, E358K+C<T1698, E361K, R541S, G602S) seemed able to form heterodimers like wild type lamin A and target the exogenous lamin C correctly to the nuclear envelope (Fig. 4.11, only R541S is shown as an example for this group). In the cases of the lamin A mutants R133P and delQ355, transfected cells exhibited a slightly less pronounced relocation of the exogenous lamin C towards the nuclear rim, indicating that these lamin A mutants are still able to interact with a different A-type lamin, although to a lesser extent (Fig. 4.11). The mutations appeared to impair lamin dimerisation, but did not disrupt it completely. The exact opposite happens with the polymorphism C<T1698: both EGFP-lamin A and DsRed2-lamin C fusion proteins form distinct nuclear aggregates, independent from each other (Fig. 4.11). Co-localisation between the two could not be observed (see especially left cell in C<T1698 panel of Fig. 4.11), suggesting that the exogenous lamin A can only form homodimers. This result is consistent with the one obtained from exogenous expression of this lamin A polymorphism and simultaneous staining for endogenous lamin B2, where the B-type lamin was excluded from the EGFP-lamin A aggregates. Interestingly, the double mutant E358K+C<T1698 showed a wild type phenotype. Thus the phenotype of the point mutation E358K seemed to dominate over the phenotype of the polymorphism in respect to an ability to dimerise.

Taken together, the EDMD causing mutations of lamin A that we have analysed did not sufficiently alter their rod domain to disturb the formation of heterodimers, the only exceptions being T150P and C<T1698 which both lead to extreme mis-localisation of the exogenous proteins.

4.1.10 Altered nuclear localisation of mutated lamins A/C may cause EDMD

Exogenous expression of mutant forms of lamin A and C in COS7 fibroblasts resulted in the confirmation of published data as well as new and unexpected findings. Lamin A mutations could be divided into three categories according to their intracellular distribution, the frequency of changes of their localisation and their effect on endogenous proteins such as emerin and lamin C.

Cells expressing category 1 mutations (E358K, L530P, R541S) exhibited a localisation pattern similar to that of exogenous wild type lamin A, with no alterations in emerin distribution and only a slight reduction in lamin C levels in cells expressing the E358K mutant. For cells expressing the mutations L530P and E358K, the same results have been described [Holt *et al.* 2003], although Raharjo *et al.* reported a loss of emerin nuclear

envelope localisation for L530P [Raharjo *et al.* 2001] and Östlund *et al.* the formation of intranuclear foci for EGFP-lamin A E358K [Östlund *et al.* 2001].

Lamin A mutations of category 2 (R50S, R133P, E361K, R527P, G602S, E358K+C<T1698) presented a variety of nuclear localisation patterns and emerin distribution, usually dependent on the cell cycle. While these results are well-known for the mutation R527P [Holt *et al.* 2001, Östlund *et al.* 2001, Bechert *et al.* 2003], the other mutations of this category have not been examined before.

The most severe phenotype was produced by cells expressing the mutations and polymorphism of category 3: T150P, delQ355 and C<T1698, where a strong mis-localisation of the exogenous proteins occurred. In addition, they seemed to disturb normal nuclear envelope assembly after mitosis, probably by mis-localising emerin or by delaying its re-distribution to the newly formed nuclear envelope.

Figure 4.12 shows the positions of the lamin A mutations of the three categories; it is clear that there is no hot spot or protein domain in the lamin A sequence to create the phenotypes observed. In fact, defects caused by two mutations (or polymorphisms) seem to influence each other: the mutation E358K alone presents a wild type phenotype, while the polymorphism C<T1698 exhibits a severe mis-localisation of exogenous lamin A. Combined into one construct, however, they show an intermediate phenotype, which means that the mutation can partly correct the mis-localisation of the polymorphism.

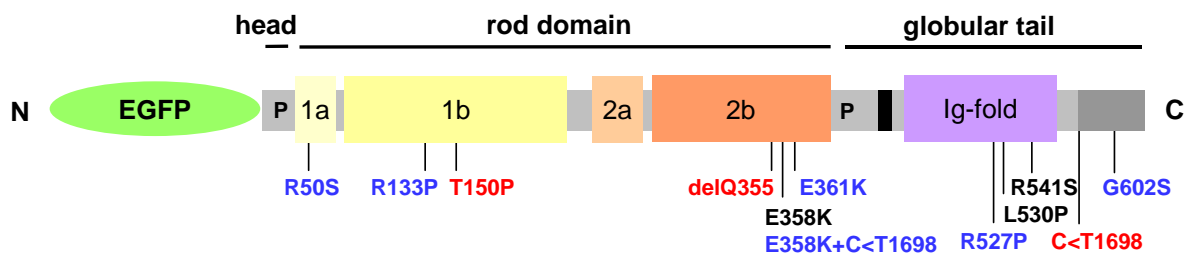


Fig. 4.12. Schematic diagram of the EGFP-lamin A sequence indicating the positions of EDMD causing mutations of category 1 (black), 2 (blue) and 3 (red). N amino-terminus, C carboxyl-terminus.

Interestingly, expression of exogenous lamin C constructs produced a very different localisation pattern: the wild type construct and all mutations (T150P, R527P, L530P) formed big, spherical aggregates in the nucleoplasm. However, co-transfection of the culture cells with a wild type-like or at least a near wild type-like exogenous lamin A (WT and all mutants

except T150P and C<T1698) restored the nuclear lamina localisation of exogenous lamin C, be it wild type lamin C or one of the mutants used.

These results confirm the essential role of lamin A for the correct localisation of lamin C at the nuclear lamina and additionally imply that lamin C-specific mutations may produce a milder laminopathy on account of the normal lamin A being able to incorporate the mutant lamin C into the nuclear lamina. This theory is supported by the one known lamin C-specific mutation, R571S, described by Fatkin *et al.* (1999): affected individuals presented with a milder DCM phenotype than patients with mutations in both lamin A and C. This also provides an explanation as to how lamin A-specific mutations can cause a laminopathy with similar severity as mutations affecting both A-type lamins.

Our conclusion is therefore that laminopathies caused by lamin A-specific mutations can be due to either mis-localisation of the protein or failed protein-protein interactions, whereas lamin C-specific laminopathies are caused exclusively by the altered interaction of lamin C with its binding partners.

4.2 Exogenous expression of lamin A constructs in COS7 cells analysed by electron microscopy

4.2.1 Are there ultrastructural changes of the nuclear envelope in cells expressing lamin A mutations ?

In X-linked EDMD, distinct nuclear abnormalities like nuclear membrane fragility, partial breakdown and nucleoplasm extrusion were found in some muscles of patients [Fidziańska *et al.* 1998]. Nuclei of skeletal muscle from AD-EDMD patients can also show an altered morphology: cells derived from patients with the *LMNA* mutation R453W exhibited loss of chromatin and deep invaginations of the nuclear envelope, forming pseudoinclusions still connected with the cytoplasm [Fidziańska and Hausmanowa-Petrusewicz, 2003]. In another case with the mutation R377H, lymphoblastoid nuclei of the patient displayed a rather striking phenotype with blebbing of the nuclear envelope and detachment of the peripheral heterochromatin from the nuclear rim, whereas in fibroblast, myoblast and sectioned muscle nuclei only membrane invaginations occurred [Reichart *et al.* 2004].

To date, neither cell lines nor muscle sections derived from AD-EDMD patients with mutations used in this study have been examined on an ultrastructural level. The only exceptions were the lamin A mutations R527P, for which about 10% of muscle nuclei showed a rearrangement and reduction of peripheral heterochromatin [Sabatelli *et al.* 2001], and E358K, where the nuclei appeared normal [Sewry *et al.* 2001]. Since cell lines or biopsy material from patients with these mutations were not available, the question arose of what defects possibly caused by the mutations could be observed in transfected culture cells.

In order to perform electron microscopy on cells expressing different lamin A mutations, COS7 fibroblasts were grown on Cellocate coverslips to enable their definite identification after transfection, transfected with the various EGFP-lamin A mutation constructs, then embedded in Epon and ultra-thin sectioned. Electron microscopic inspection of the samples revealed a close connection to the results obtained by immunofluorescence microscopy, i.e. their classification into three categories, but also some unexpected findings not seen by previous light microscopy.

4.2.2 Exogenous expression of wild type lamin A thickens the nuclear lamina

A transfection rate of around 15-20% of all COS7 fibroblasts meant that the majority of the cells did not express the mutant lamin A, thus it was vitally important to clearly identify the transfected cells. While in light microscopy the transfected cells indicated themselves via their EGFP fluorescence, this was not the case for electron microscopy. One possibility to locate the transfected cells in the sample would be their staining with antibodies conjugated to colloidal gold particles; however, this technique can drastically alter cell morphology and had therefore to be avoided.

For this reason, the COS7 cells were grown on Cellocate coverslips on which a numbered identification grid was engraved. Prior to the fixation of the cells for the EM embedding protocol, the cells on the coverslips were screened for EGFP expression under the fluorescence microscope. Only such cells were chosen which produced the same phenotype as the majority of cells in interphase for any one mutation seen by previous fluorescence microscopy (see chapter 4.1). Pictures were taken from individual cells and their approximate location on the coverslip was marked on a paper grid identical to the one on the coverslip. Figure 4.13 shows an example of this procedure for cells transfected with wild type EGFP-lamin A, with an arrow indicating the same cell in EGFP fluorescence (a1), phase contrast (a2) and electron microscopy (a3). The cells can easily be identified by the shape of their nucleus as well as by the number, size and shapes of their nucleoli, which are clearly visible in both phase contrast pictures and electron micrographs.

In untransfected control fibroblasts, the nucleus assumed a near ovoid shape enclosed by the continuous band of the nuclear envelope (Fig. 4.13, b1). Upon higher magnification, the inner and outer nuclear membranes could be seen, connected at the nuclear pore complexes, and underlined on the nucleoplasmic side by an approximately 10 nm thick layer of intermediate electron density, the nuclear lamina (Fig. 4.13, b2). COS7 cells expressing exogenous wild type lamin A closely resembled untransfected control cells, thus confirming that the expression of the exogenous protein did not alter the morphology of the nuclear envelope (Fig. 4.13, a3, a4). As the only difference to untransfected controls, cells expressing the exogenous lamin A appeared to have a thicker lamina (~15-20 nm thick), which can be explained by the correct insertion of the exogenous protein into the nuclear lamina in addition to the endogenous protein.

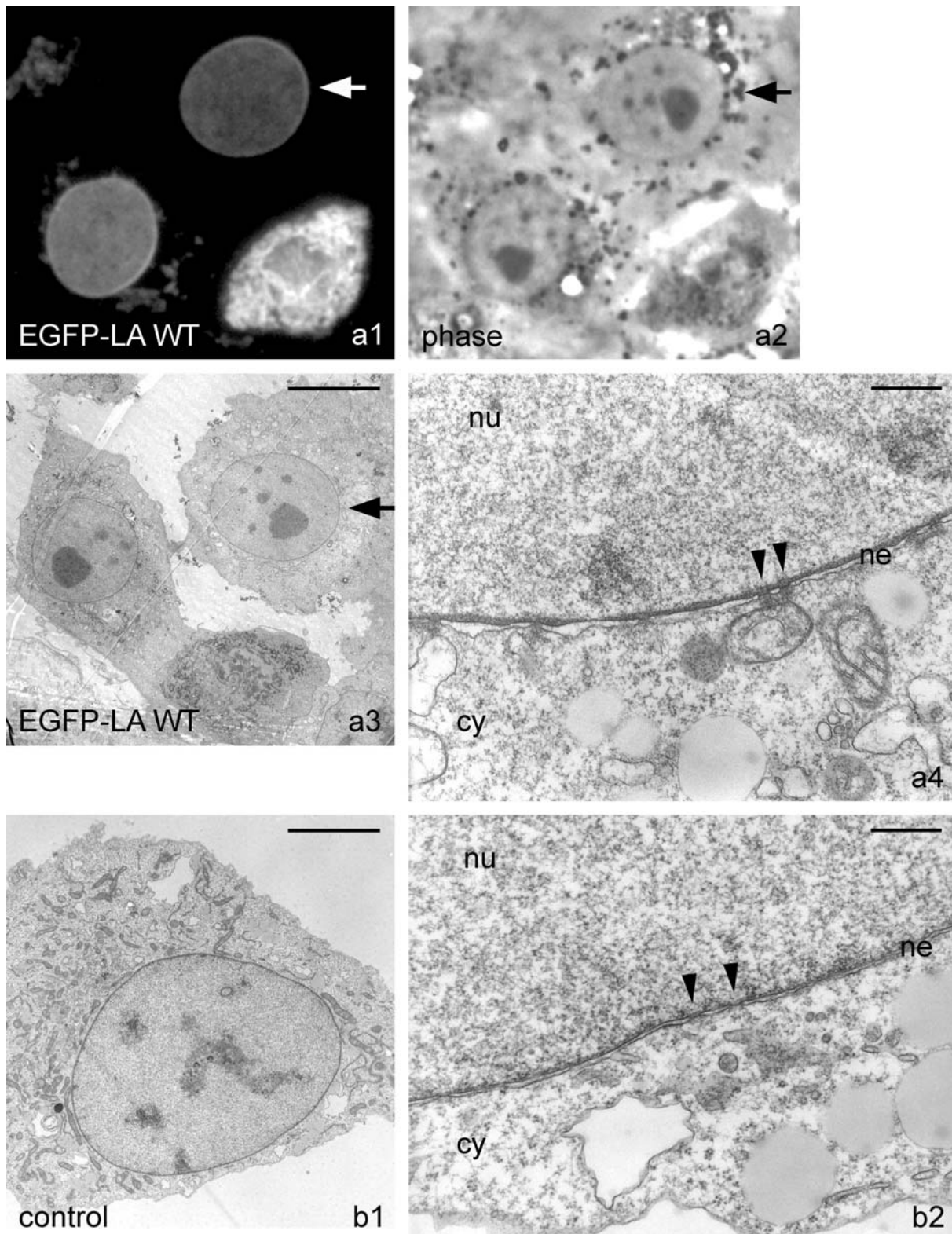


Fig. 4.13. Electron micrographs from ultra-thin sections of COS7 fibroblasts exogenously expressing wild type EGFP-lamin A and untransfected control cells. Picture a1 shows the EGFP fluorescence and a2 the phase contrast image of the cells in the electron micrograph a3, with an arrow marking the corresponding cell, shown at higher magnification in a4. Row b shows electron micrographs of an untransfected control fibroblast. Arrowheads indicate nuclear pore complexes in a4 and b2. Ne nuclear envelope, nu nucleoplasm, cy cytoplasm. Bars in a3 (also valid for a1, a2) 10 μm , in b1 5 μm , in a4 and b2 100 nm.

4.2.3 Lamin A mutations of category 1 show a wild type phenotype

COS7 cells expressing exogenous lamin A mutations of category 1 (E358K, L530P, R541S) exhibited a wild type-like phenotype, with the thick, continuous band of the nuclear lamina along the inner nuclear membrane. The lamina of the mutants E358K and L530P appeared to be even thicker than in the wild type (Fig. 4.14, a and b, respectively), whereas in mutation R541S, it did not quite reach the thickness of the wild type lamina (Fig. 4.14, c). However, these size differences are probably caused by the different expression rates of the lamin A mutants: the more exogenous lamin A is synthesised and inserted into the nuclear lamina, the thicker it becomes.

Although the lamin A mutations of category 1 presented a wild type phenotype with no gross changes in nuclear and chromatin architecture, some minor alterations could be observed. In cells expressing the mutation E358K, aggregates of the same appearance and electron density as the nuclear lamina were seen in the perinuclear region, often next to nuclear pore complexes (Fig. 4.14, arrows in a2). This phenomenon was not detected in any of the previous immunofluorescence examinations, excluding the possibility of simple over-expression of the EGFP fusion protein. This led to the suggestion that the aggregates consisted of lamins which accumulated outside the nuclear pore complexes because of an impaired transport into the nucleus, possibly caused by the dense network of the exogenous protein. Due to technical problems with the immunogold-localisation and the resulting insufficient antibody-labelling, however, it was not possible to determine whether these aggregates were indeed formed by lamins and by which type of them; thus, the true nature of the aggregates remains unclear.

Cells expressing the lamin A mutant L530P exhibited a normal nuclear shape and the thickened nuclear lamina typical for transfected cells. In some places, membrane invaginations occurred on the nucleoplasmic side of the nuclear lamina, reminiscent of a second nuclear envelope (Fig. 4.14, asterisks in b2).

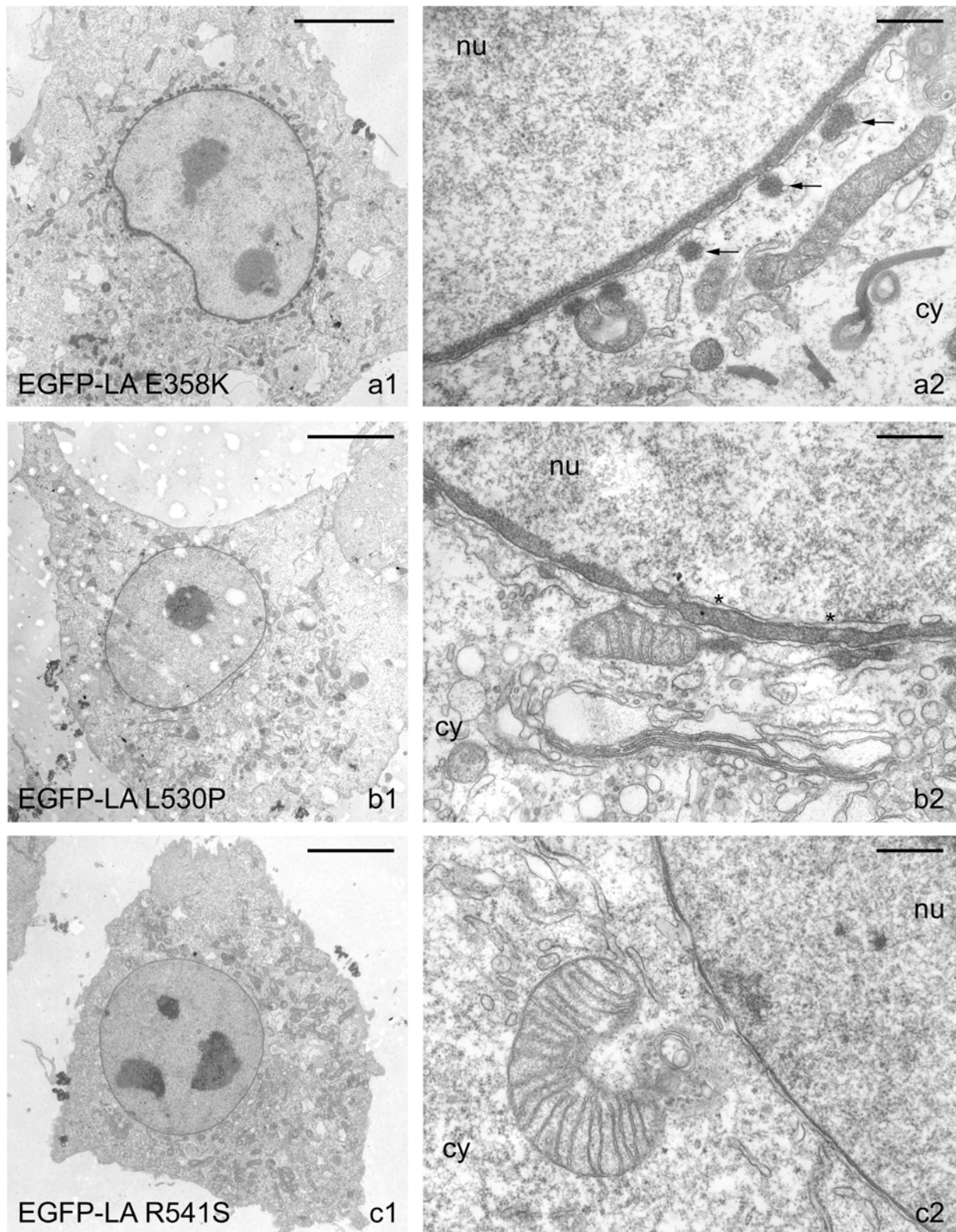


Fig. 4.14. Electron micrographs from ultra-thin sections of COS7 fibroblasts exogenously expressing EGFP-lamin A mutations of category 1. Arrows in a2 indicate cytoplasmic electron-dense aggregates next to nuclear pore complexes in the lamin A mutant E368K, asterisks in b2 mark membrane invaginations on the nucleoplasmic side of the nuclear lamina appearing occasionally in lamin A mutant L530P. Nu nucleoplasm, cy cytoplasm. Bars in a1, b1, c1 5 μ m, in a2, b2 and c2 100 nm.

4.2.4 Lamin A mutations of category 2 present a variety of phenotypes

By fluorescence microscopy examination, a wide variety of phenotypes could be observed in fibroblasts transfected with lamin A mutations of category 2, ranging from a wild type-like localisation pattern of the exogenous protein to its mis-localisation, especially during different stages of the cell cycle. The results obtained by electron microscopy confirmed these findings, but revealed also some new features in nuclear envelope and lamina architecture.

In COS7 cells expressing the lamin A mutant R50S the overall ovoid shape of the nucleus remained, but instead of the nuclear envelope forming a smooth, straight band around the nucleoplasm, it appeared as a slightly jagged band (Fig. 4.15.1, a1). Higher magnification showed no disruptions of the nuclear membranes; the thick layer of the nuclear lamina underlined the nuclear envelope, but appeared thinner in places with a bend (Fig. 4.15.1, a2). Taken together, these observations made the nuclei with a lamina partly consisting of lamin A mutant R50S look distinctly more fragile than those of cells expressing other lamin A mutations.

Only such interphase cells were selected for electron microscopic inspection, which resembled most closely the phenotype of the majority of transfected cells as seen by fluorescence microscopy. Unexpectedly, cells expressing EGFP-lamin A R133P clearly showed a granular pattern along the nuclear rim. The electron dense layer of the nuclear lamina containing the exogenous protein was enriched in patches adjacent to the nuclear membranes, with these aggregates slightly protruding from the nucleus (Fig. 4.15.1, row b and arrows in b2). Obviously, the lamin A mutation R133P was still able to attach itself to the inner nuclear membrane, but subsequently accumulated in aggregates, possibly because of a binding defect to another interaction partner. It is also likely that this granular pattern represents the normal distribution for this mutation, since the difference in localisation observed by fluorescence microscopy can be explained by different expression levels in transfected cells: if the expression is low, the protein granules along the nuclear rim remain small and thus the resolution of a light microscope cannot distinguish them from the wild type phenotype.

For the mutant E361K, the transfected cells exhibited a wild type-like morphology (Fig. 4.15.1, row c). The nuclear envelope showed a certain similarity to cells expressing mutation R50S, with some minor bends of the nuclear membranes and a sometimes discontinuous nuclear lamina (Fig. 4.15.1, c2), but the overviews of the entire nuclei confirmed their wild type shape (Fig. 4.15.1, c1), without the alterations of mutant R50S.

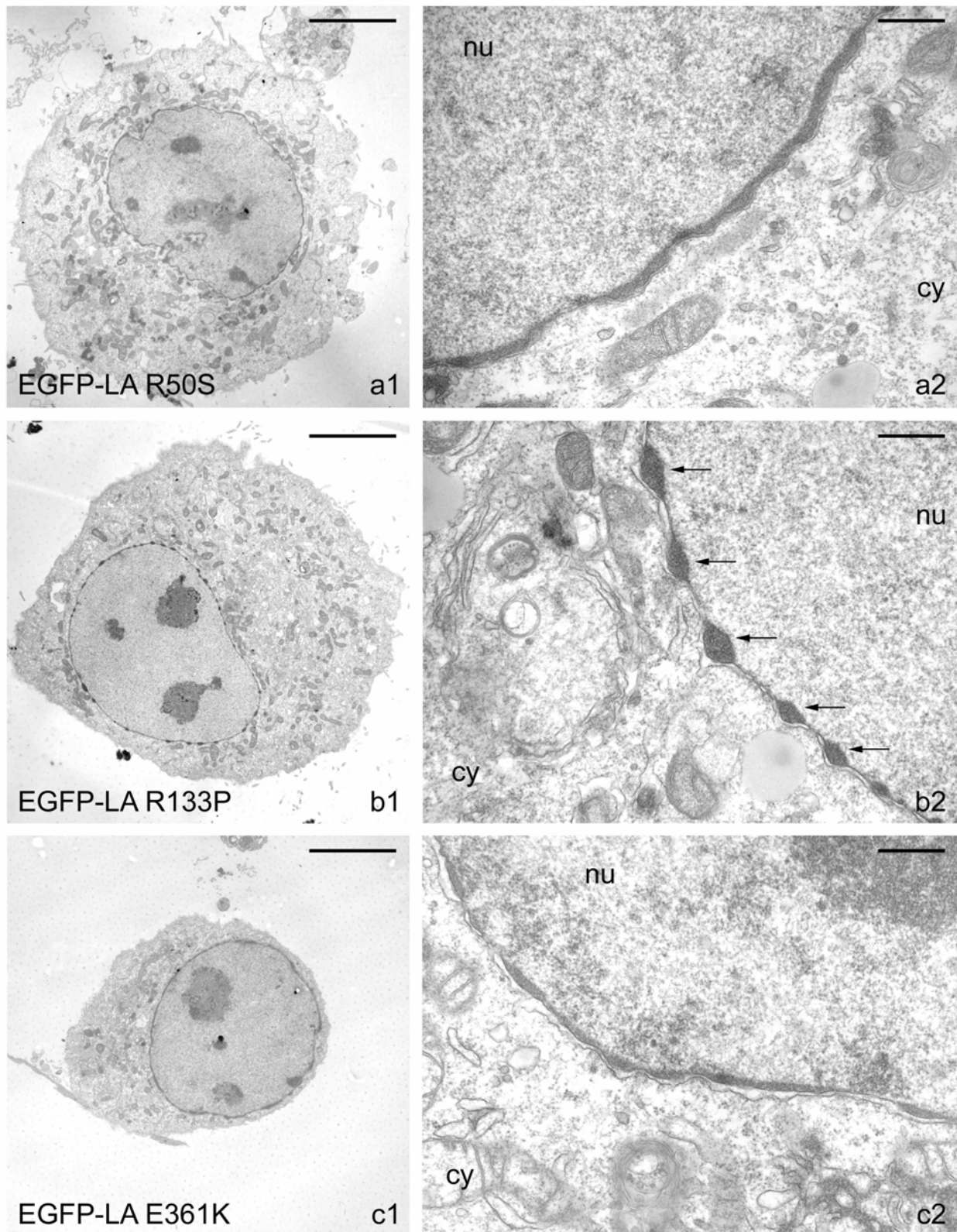


Fig. 4.15.1. Electron micrographs from ultra-thin sections of COS7 fibroblasts exogenously expressing EGFP-lamin A mutations of category 2, part 1. Arrows in b2 indicate the fine aggregates along the nuclear envelope formed by lamin A mutation R133P. Nu nucleoplasm, cy cytoplasm. Bars in a1, b1, c1 5 μ m, in a2, b2 and c2 100 nm.

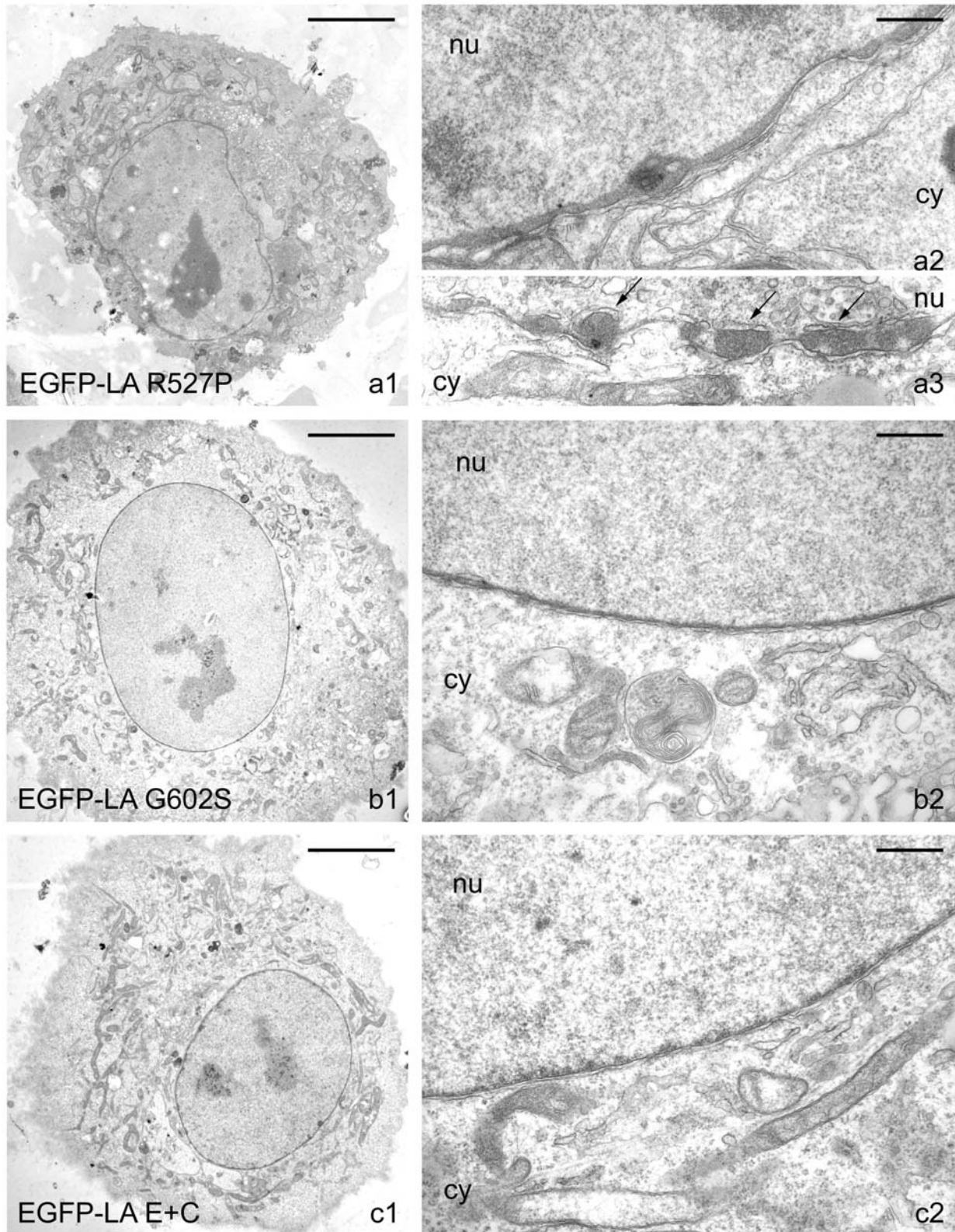


Fig. 4.15.2. Electron micrographs from ultra-thin sections of COS7 fibroblasts exogenously expressing EGFP-lamin A mutations of category 2, part 2. Arrows in a3 indicate additional membranes on the nucleoplasmic side of the nuclear lamina seen occasionally in lamin A mutation R527P. Nu nucleoplasm, cy cytoplasm. Bars in a1, b1, c1 5 μ m, in a2 (also valid for a3), b2 and c2 100 nm.

Fibroblasts expressing the lamin A mutation R527P gave a rather wild type-like impression, with undisturbed inner and outer nuclear membranes and a thick band of lamins underlining them (Fig. 4.15.2, a1 and a2). However, the nuclei appeared slightly deformed and the nuclear envelope did not stretch smoothly around the nucleoplasm, but was bent in places, which may indicate a decrease in nuclear stability. In cells over-expressing the exogenous protein, these nuclear alterations became even more marked and the previously continuous nuclear lamina dispersed to form proteinaceous aggregates at the nuclear rim, often surrounded by a second set of membranes on the nucleoplasmic side (Fig. 4.15.2, arrows in a3).

The transfection of COS7 cells with the lamin A mutation G602S resulted in a nuclear shape and a nuclear envelope morphology identical to that of cells transfected with the wild type protein (Fig. 4.15.2, b1); the thick band of the nuclear lamina proved that the exogenous lamin A was correctly incorporated into it (Fig. 4.15.2, b2). This finding matched exactly the one obtained by fluorescence microscopy, where the exogenous protein localised like the wild type lamin A and only the distribution of endogenous emerin seemed disturbed in some cases. In cells expressing exogenous lamin A with both the mutation E358K and the polymorphism C<T1698, a near wild type-like phenotype was observed (Fig. 4.15.2, c1). Only closer inspection of the nuclear envelope revealed that the electron dense band of the nuclear lamina did not quite mimic the smoothness and continuing thickness of the lamina formed by the exogenous wild type protein, but appeared somewhat jagged (Fig. 4.15.2, c2). Nevertheless, these results resembled surprisingly the wild type, compared to the much more pronounced mis-localisation of the exogenous lamin A seen by fluorescence microscopy.

4.2.5 Lamin A mutations of category 3 are strongly mis-localised

Electron microscopic examination of COS7 fibroblasts transfected with lamin A mutations of category 3 confirmed their strong mis-localisation observed by light microscopy. The mutant lamin A T150P localised exclusively to big aggregates in the cytoplasm (Fig. 4.16, arrows in a1 and a2 indicate protein aggregates) and the nuclear lamina lacked the increase in thickness typical for exogenous lamin A insertion. In these protein clusters, no higher order structures like paracrystals could be observed, suggesting that no protein organisation beyond dimerisation or maybe tetramerisation occurred (for higher magnification of such an aggregate, see also inset a3 in Fig. 4.16). Since the NLS was intact in the mutant protein, yet it did not reach the nucleus, the T<P mutation in the rod domain of the protein sufficiently disrupted its tertiary structure to cause it to aggregate in transit to the nucleus.

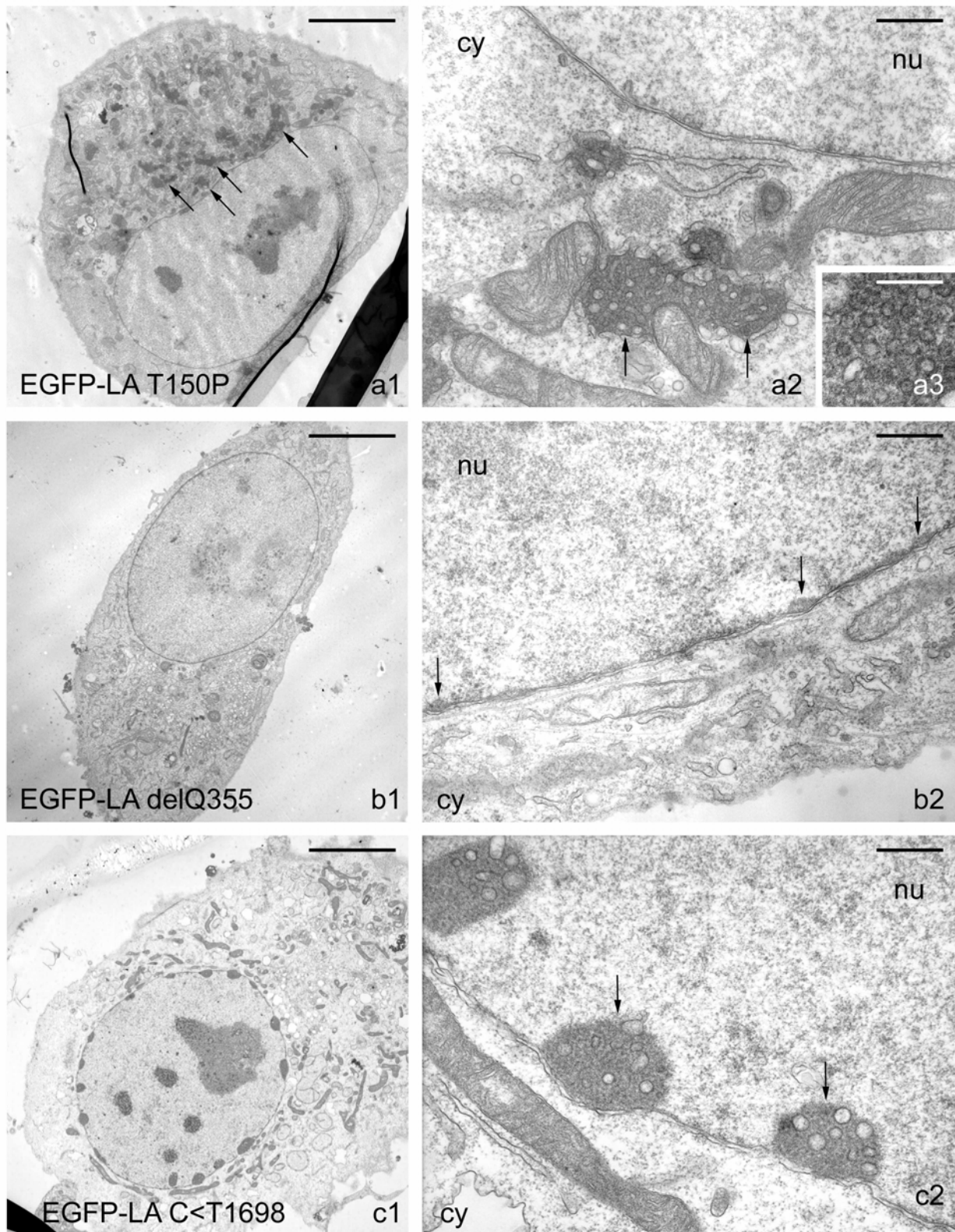


Fig. 4.16. Electron micrographs from ultra-thin sections of COS7 fibroblasts exogenously expressing EGFP-lamin A mutations of category 3. Arrows in a1 and a2 indicate cytoplasmic aggregates of lamin A mutant T150P, arrows in b2 and c2 mark aggregates at nuclear lamina of lamin A mutation delQ355 and polymorphism C<T1698, respectively. Nu nucleoplasm, cy cytoplasm. Bars in a1, b1, c1 5 μ m, in a2, b2 and c2 100 nm, in a3 50 nm (higher magnification of cytoplasmic aggregate).

On first sight, the expression of lamin A deletion mutant Q355 led to a wild type-like appearance of the cells (Fig. 4.16, b1). Closer examination of the nuclear envelope revealed, however, the forming of lamin aggregates along the nuclear rim, similar to those of the mutant R133P (Fig. 4.16, arrows in b2). This result indicated that the mutant protein was still able to insert itself into the nuclear lamina, but then accumulated in patches instead of distributing itself evenly in the network of the lamina. Although the size of the aggregates was less prominent than in R133P, the phenomenon occurred much more frequently in mutation delQ355 (in all cells examined), thus confirming the results obtained by fluorescence microscopy.

Electron micrographs of COS7 fibroblasts transfected with the polymorphism C<T1698 firmly established the phenotype first seen by light microscopy: The mutant protein accumulated in big, spherical aggregates at the nuclear envelope (Fig. 4.16, row c). An organised structure within these aggregates could not be observed; in fact, they resembled strongly the aggregates formed by the mutation T150P (Fig. 4.16, compare aggregates marked by arrows in a2 to those in c2). The ability of the exogenous protein to integrate into the nuclear lamina seemed impaired, leading to only few attachment sites at the nuclear envelope and, due to the high expression levels of the mutated lamin A, its uncoordinated aggregation at these sites.

4.2.6 Ultrastructural changes in nuclear lamina architecture caused by lamin A mutations may contribute to EDMD

Electron microscopic examination of COS7 fibroblasts transfected with different lamin A mutants established their allocation into 3 categories (see Fig. 4.17 for categorisation). The variety of phenotypes and the accompanying nuclear abnormalities observed especially in group 2 were evident on an ultrastructural level. This range in defects from none to severe nuclear alterations in one mutation corresponds to that reported in AD-EDMD patients, where only 10% of the preserved myofibres are affected [Sabatelli *et al.* 2001].

In mutations of category 1, the wild type-like appearance of the nuclear envelope and overall nuclear shape in transfected cells seen by fluorescence microscopy was confirmed by electron microscopy. The exogenous lamin A was correctly incorporated into the nuclear lamina, the thickness of which increased because of the additional protein. Surprisingly, cells expressing the mutation E358K exhibited proteinaceous aggregates of the same electron density as the nuclear lamina in their perinuclear region, a feature not reported from muscle nuclei from

AD-EDMD patients [Sewry *et al.* 2001]. The true nature of these aggregates remains to be determined, however, to distinguish between a preparation or transfection artefact and a real pathological change.

Three mutations of category 2 produced unexpected nuclear alterations: nuclei with mutant protein R50S looked more fragile due to a slightly jagged nuclear envelope, while cells expressing the mutation R133P exhibited a discontinuous nuclear lamina forming patches along the nuclear rim. Similar aggregates of the exogenous protein surrounded by intranuclear membranes were displayed in cells over-expressing mutant R527P. This specific feature was not observed in muscle nuclei from patients with this mutation, where changes in the heterochromatin distribution prevailed [Sabatelli *et al.* 2001]. However, these on first sight contradictory observations could be due to different mechanical stress as well as altered gene expression which affects the two cell types in a different manner.

Electron micrographs from fibroblasts transiently expressing one of the mutations from category 3 supported the results obtained by light microscopy. The mutant lamin A T150P did not reach the nucleus (at least not at detectable levels), but aggregated in the cytoplasm. Both mutants delQ355 and C1698T formed proteinaceous aggregates of varying size at the nuclear envelope.

Any of these nuclear abnormalities observed in transfected culture cells may occur in muscle tissue of AD-EDMD patients, although to a lesser extent as in these cells which synthesise the exogenous protein above endogenous levels. Thus, muscle degeneration could well be explained by nuclear instability due to an insufficient lamin network at the nuclear envelope, as was suggested by Manilal *et al.* (1999) and Tsuchiya *et al.* (1999) according to their structural weakness hypothesis.

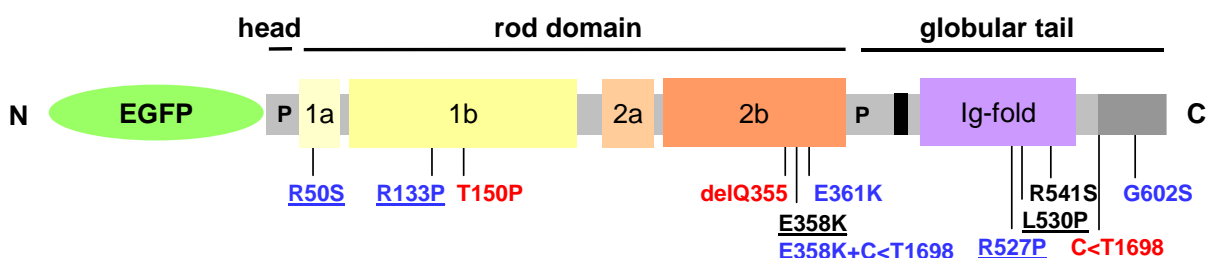


Fig. 4.17. Schematic diagram of the EGFP-lamin A sequence indicating the positions of EDMD causing mutations of localisation category 1 (black), 2 (blue) and 3 (red). Mutations showing additional ultrastructural abnormalities are underlined. N amino-terminus, C carboxyl-terminus.

Cells from laminopathy patients frequently exhibit more severe changes in nuclear architecture than transfected cell systems [Sabatelli *et al.* 2001, Vigouroux *et al.* 2001, Sewry *et al.* 2003], indicating that additional factors contribute to the disease phenotypes, which are unable to be reproduced in the laboratory. While electron microscopic inspection of transfected culture cells cannot replace the examination of biopsy material from patients for the detection of tissue-specific defects, it is still a powerful tool to study the distribution of mutated proteins within single cells.

4.3 Altered mobility of exogenously expressed lamin A mutants analysed by fluorescence recovery after photobleaching (FRAP)

4.3.1 Do mutations in lamin A alter its mobility within the nuclear lamina ?

The nuclear lamina is a filamentous network composed of lamin proteins that underlies the inner nuclear membrane. Via integral membrane proteins of the nuclear envelope and other protein interaction partners within the nucleus, the lamina is thought to connect the cytoskeleton with the nucleoplasmic scaffold. Therefore, the nuclear lamin network may play a fundamental role in maintaining both anchoring and structural integrity of the cell nucleus [for review, see Gruenbaum *et al.* 2005].

A-type lamins are firmly integrated into this protein network by forming paracrystalline arrays, showing very low mobility within the lamina [Gilchrist *et al.* 2004, Broers *et al.* 1999], and thus ensure the network's stability. Due to the forces created during muscle movement, the nuclei of muscle cells have to be able to withstand strong mechanical stresses to remain functional. If mutations in the *LMNA* gene weaken this stabilising system, however, the death of the more fragile nuclei would explain the EDMD-specific tissue damages [Manilal *et al.* 1999, Tsuchiya *et al.* 1999]. Alternatively, the regeneration process in a muscle fibre could be delayed, since more fragile nuclei would reduce the proliferation capability of the satellite cells responsible for muscle regeneration [Fairley *et al.* 1999].

Mutated lamin A proteins presumably are not as closely associated with the nuclear lamina as wild type lamin A, indicated by their strong mis-localisation (see chapters 4.1 and 4.2) or by an increased mobility of these proteins at the nuclear periphery.

For a better understanding of the effects of EDMD-associated mutations on lamin A function, fluorescence recovery after photobleaching (FRAP) was used to investigate the protein dynamics of GFP-tagged wild-type and mutant lamin A in transfected COS7 cells. A defined area of a living cell is bleached irreversibly by a single, high-powered spot laser pulse, then the recovery of the fluorescence signal in the bleached area as the consequence of movement of the GFP-fusion protein is recorded by sequential imaging scans. The kinetics of recovery are a measure for the mobility of the labelled protein [White and Stelzer, 1999]. Only lamin A mutations which mainly exhibited a near wild type phenotype in transiently transfected cells were studied, i.e. R50S, R133P, delQ355, E358K, E361K, R527P, L530P, R541S and G602S, since mutations that caused a gross mis-localisation or aggregation of the fusion protein were considered incapable of normal nuclear lamina incorporation.

4.3.2 The E361K mutation in the rod domain of lamin A increases its mobility

For FRAP analysis of lamin A mutations, COS7 fibroblasts were transiently transfected with either wild type or mutant EGFP-lamin A cDNA constructs. As a different transfection reagent was used than for normal fluorescence microscopy, a protein expression time of six hours often proved to be sufficient for FRAP experiments.

The transfected cells were screened at the confocal laser scanning microscope for a cell exhibiting the right amount of EGFP-lamin A expression (strong fluorescence, but no over-expression) and a spot (\varnothing 1 μ m) was bleached at the nuclear lamina. The fluorescence of this region of interest (ROI) was then followed at defined time intervals (between 2 seconds and 1 minute) over a period of up to 20 minutes. Longer examination was not possible due to cell movement which caused the ROI to leave the level of focus. FRAP recovery curves were generated from background subtracted images. To calculate the loss of fluorescence attributed to the imaging process alone, the total cellular fluorescence at each time point was compared to the initial total fluorescence and the measured pixel intensities used to normalise the fluorescence intensity for each ROI [Phair and Misteli, 2000]. The mean relative fluorescence intensity for each time point was then calculated for 10 to 14 cells of each of the EGFP-lamin A proteins, wild type as well as mutants.

For wild type EGFP-lamin A, fluorescence at the nuclear lamina was visibly bleached after the bleach pulse (Fig. 4.18.1A, top panel), and only about 15% of the signal recovered over the time course of the experiments (Fig. 4.18.1A, recovery curve). The recovery curve also showed that the exogenous wild type lamin A moved back into the bleached area only very slowly, indicating that a large proportion of approximately 85% of this protein was immobile at the nuclear periphery within the time-frame used. This immobility of wild type EGFP-lamin A is consistent with findings by Gilchrist and co-workers [Gilchrist *et al.* 2004] and gives evidence for its incorporation into a stable polymer with only a very slow subunit exchange.

FRAP analysis of the mutations in the coiled-coil domain of lamin A presented different mobility phenotypes for the exogenous proteins. The recovery kinetics for the mutants R133P and delQ355 were indistinguishable from the wild-type (Fig. 4.18.2), with a signal recovery of well below 20% for both. The mutations R50S and E358K (Fig. 4.18.1B and 4.18.3A, respectively) appeared to recover slightly faster from the bleach pulse and reached a higher fluorescence signal plateau at about 25% of the original value during the time-course analysed, suggesting that less of these lamin A mutants were in an immobile fraction.

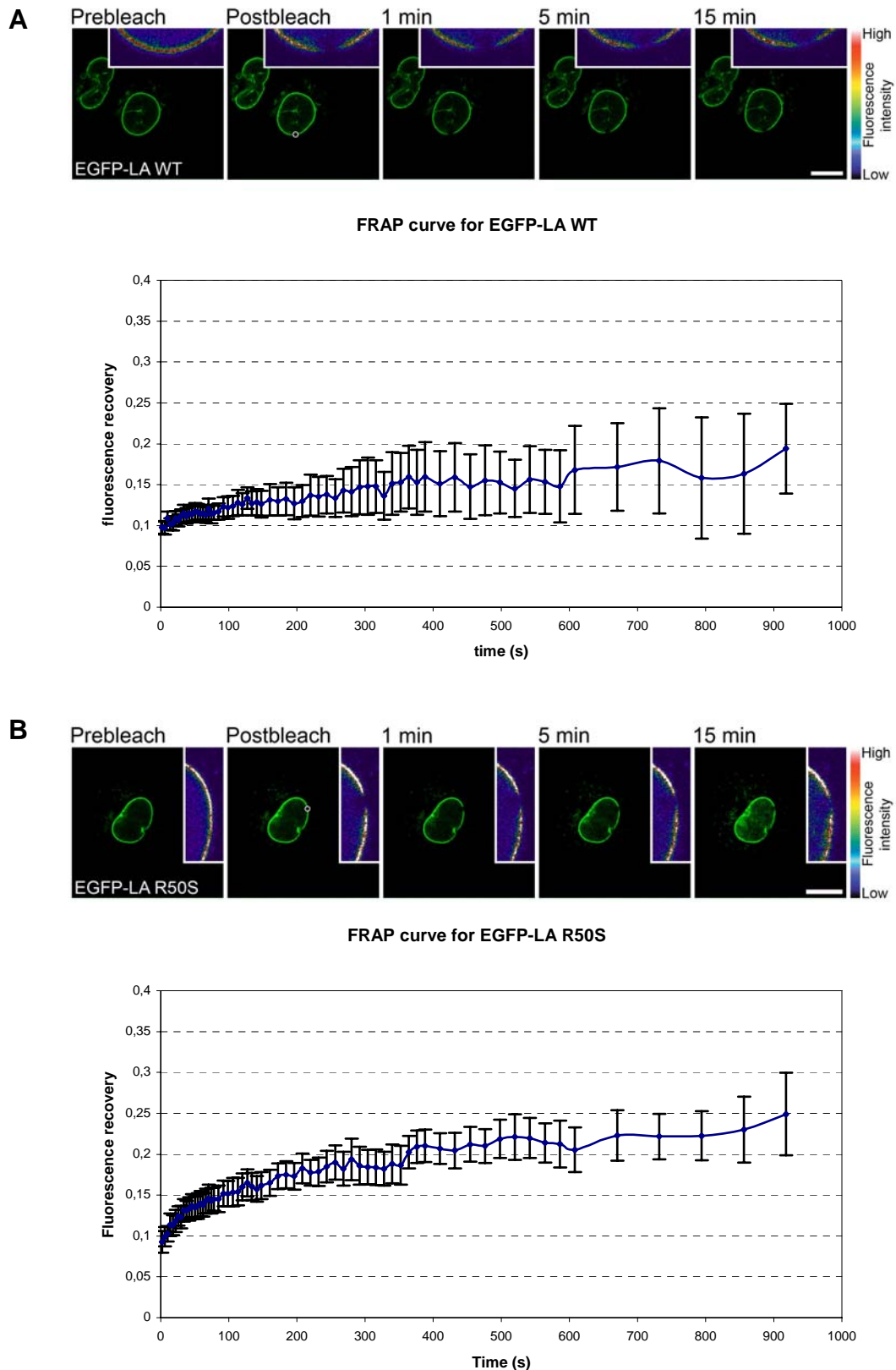


Fig. 4.18.1. FRAP analysis of wild type EGFP-lamin A and its mutations in the rod domain, part 1. (A) WT and (B) R50S lamin A in transiently transfected COS7 cells. Images of the top panel were captured before and after bleach pulse (white circle marks the bleach spot), with inset showing the enlarged area of the bleach spot in pseudocolours for better visibility. Graphs below show mean (\pm SEM) relative fluorescence in the bleach area during FRAP, averaged over 10-14 cells each.

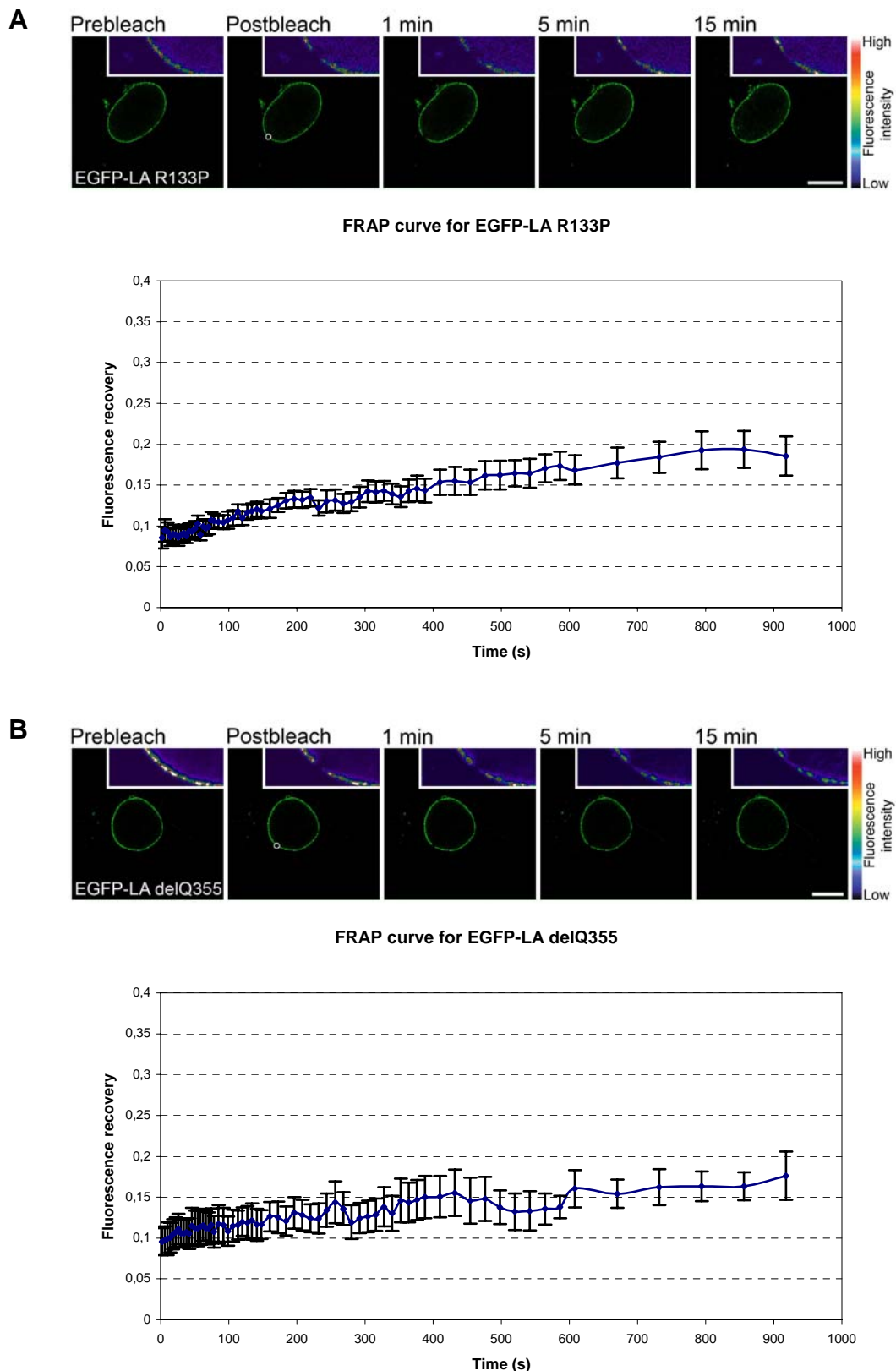


Fig. 4.18.2. FRAP analysis of EGFP-lamin A mutations in the rod domain, part 2. (A) R133P and (B) delQ355 lamin A in transiently transfected COS7 cells. Images of the top panel were captured before and after bleach pulse (white circle marks the bleach spot), with inset showing the enlarged area of the bleach spot in pseudocolours for better visibility. Graphs below show mean (\pm SEM) relative fluorescence in the bleach area during FRAP, averaged over 10-14 cells each.

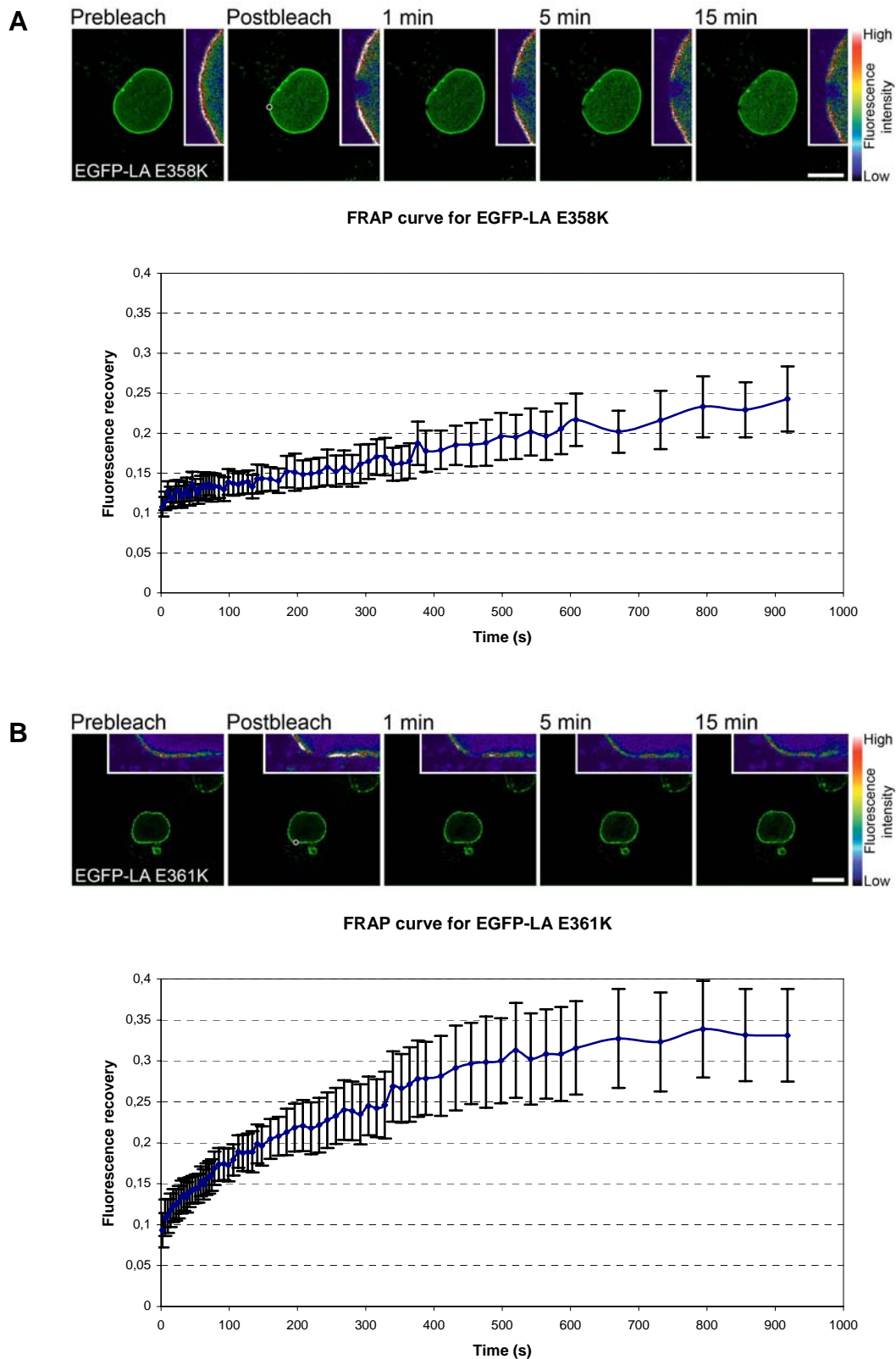


Fig. 4.18.3. FRAP analysis of EGFP-lamin A mutations in the rod domain, part 3. (A) E358K and (B) E361K lamin A in transiently transfected COS7 cells. Images of the top panel were captured before and after bleach pulse (white circle marks the bleach spot), with inset showing the enlarged area of the bleach spot in pseudocolours for better visibility. Graphs below show mean (\pm SEM) relative fluorescence in the bleach area during FRAP, averaged over 10-14 cells each.

However, comparison to the wild type in an unpaired student's t-test revealed that none of these four lamin A mutations exhibited a statistically significant difference to the wild type protein and therefore these cannot reliably be declared to be more mobile.

Although most mutations of the lamin A rod domain showed recovery kinetics similar to the wild type, a dramatic difference in dynamics was seen for the mutation E361K (Fig. 4.18.3B). Its recovery curve increased much more rapidly and also a higher proportion of the fluorescence of this mutation recovered (up to 33% as the mean, but up to 100% in some single cell experiments). Indeed, statistical analysis confirmed it to be significantly more mobile than wild type lamin A ($p < 0.05$ at $t = 500$ s), indicating that the E361K lamin A mutation leads to a less stable integration of the protein into the nuclear lamina than the wild type or any of the other mutations.

4.3.3 Mutations in the lamin A globular domain have no effect on protein mobility

Mutations in the C-terminal globular domain of lamin A were not expected to affect its dimerisation and nuclear lamina incorporation, leaving the exogenous proteins in the immobile state of the wild type form. This assumption was confirmed by the protein dynamics observed during the course of the FRAP studies. Fluorescence signal recovery of the lamin A mutants R541S and G602S was nearly identical to that of the wild type (Fig. 4.19.2), with the recovery reaching a plateau at only 15% of the initial signal over the time course of the experiment. Like in the wild type, the majority (>85%) of the exogenous protein seemed immobile at the nuclear periphery.

For the lamin A mutations R527P and L530P, a slightly increased recovery rate of about 25% was observed (Fig. 4.19.1), although this appeared to be within normal statistical value fluctuation. In fact, statistical analysis proved all four mutations of the globular domain studied by FRAP experiments not to be significantly different from wild type lamin A with regard to its protein dynamics. Therefore, mutations in the globular domain of lamin A seem unlikely to cause EDMD by a mechanism that disturbs nuclear stability through altered protein mobility.

A recent report showed a higher mobility of lamin A mutant L530P during FRAP analysis within a longer observation period of 65 minutes [Gilchrist *et al.* 2004]. It recovered more rapidly and compared to the wild type, a higher proportion of the fluorescence (~40%) was recovered, suggesting that less of L530P lamin A is in an immobile fraction. There are several explanations as to why these results seem to contradict our findings.

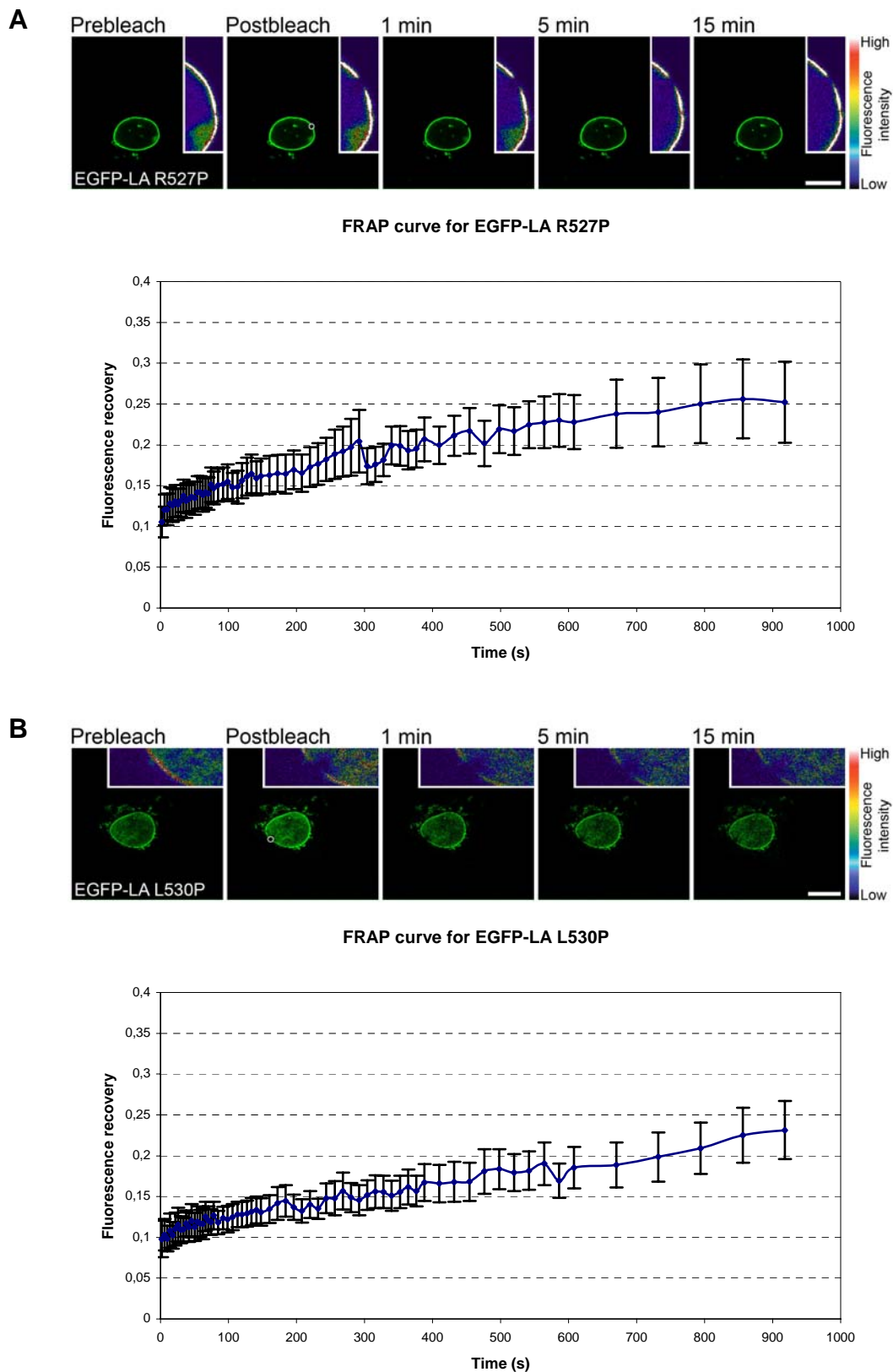


Fig. 4.19.1. FRAP analysis of EGFP-lamin A mutations in the globular domain, part 1. (A) R527P and (B) L530P lamin A in transiently transfected COS7 cells. Images of the top panel were captured before and after bleach pulse (white circle marks the bleach spot), with inset showing the enlarged area of the bleach spot in pseudocolours for better visibility. Graphs below show mean (\pm SEM) relative fluorescence in the bleach area during FRAP, averaged over 10-14 cells each.

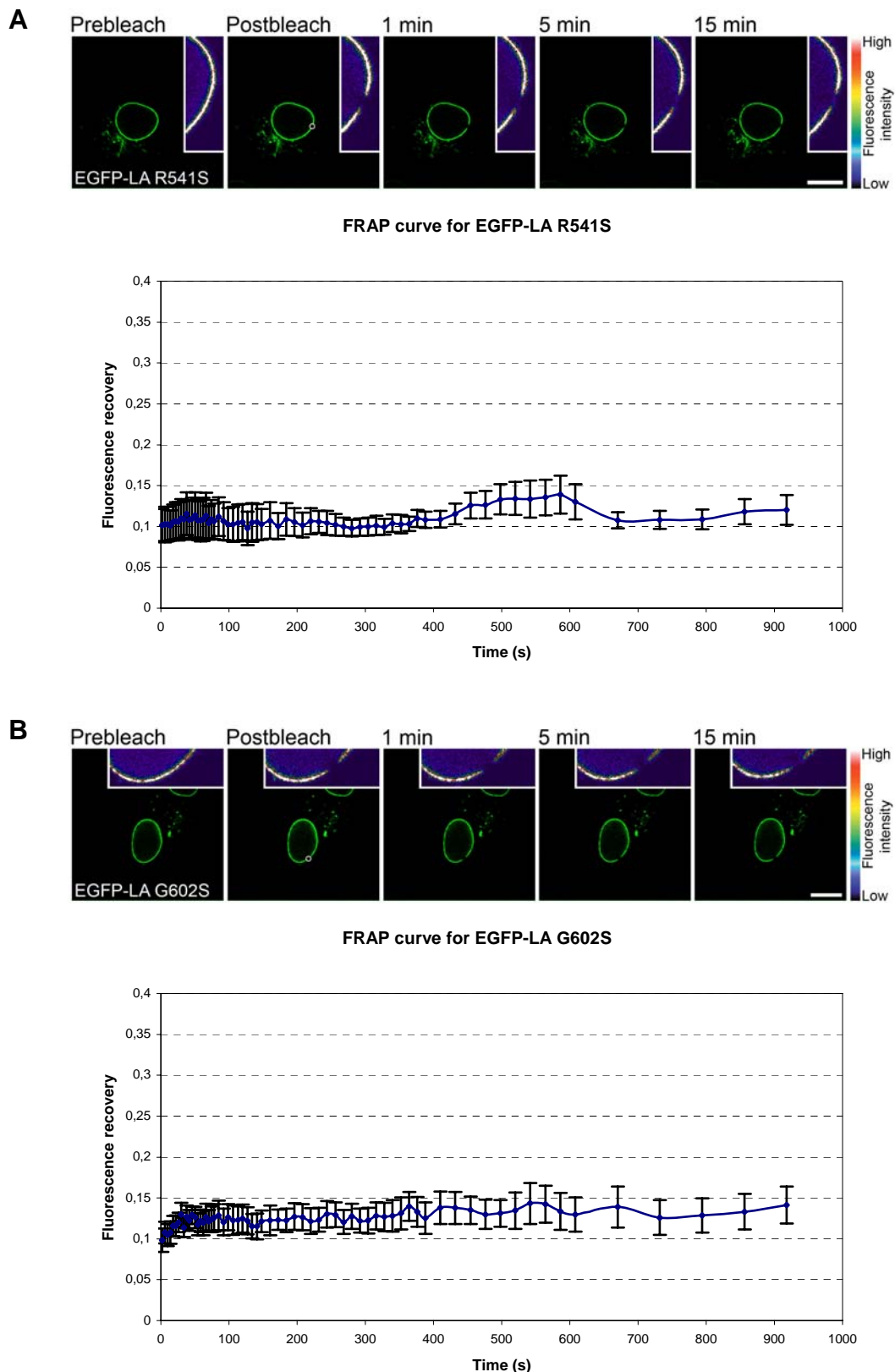


Fig. 4.19.2. FRAP analysis of EGFP-lamin A mutations in the globular domain, part 2. (A) R541S and (B) G602S lamin A in transiently transfected COS7 cells. Images of the top panel were captured before and after bleach pulse (white circle marks the bleach spot), with inset showing the enlarged area of the bleach spot in pseudocolours for better visibility. Graphs below show mean (\pm SEM) relative fluorescence in the bleach area during FRAP, averaged over 10-14 cells each.

An important point are the different lengths of the experiments, since Gilchrist *et al.* could follow protein dynamics in transfected cells in a time scale three times longer than was possible with our FRAP microscope settings. In our studies, the L530P recovery indicated a higher mobility, though without statistical significance; a longer FRAP time-frame for this mutation may confirm the findings of Gilchrist and co-workers. On the other hand, these authors did not perform a statistical analysis for their results, so no statement about their statistical significance can be made. Finally, human HT1080 fibrosarcoma cells were used in their paper which might not be comparable to the simian COS7 fibroblast cells used in this study. However, differences in protein dynamics of one lamin A mutation in different cell types and the resulting change in nuclear integrity thereof may emphasize tissue-specific effects of a mutation, and therefore shed further light on the molecular causes of the laminopathies.

4.3.4 Altered protein mobility may explain some lamin A mutants causing EDMD

Nuclear stability is provided by the filamentous lamin network at the nuclear lamina. During lamina assembly, two lamin molecules dimerise along their central α -helical rod domains, then the dimers associate in a head-to-tail manner to form lamin filaments [for review, see Krohne, 1998]. Once incorporated into the nuclear lamina, mobility of the A-type lamin proteins is greatly limited, as has been shown by fluorescence recovery after photobleaching (FRAP) of fluorescent lamins that were micro-injected into culture cells [Schmidt and Krohne 1995] and of exogenously expressed GFP-tagged lamins [Gilchrist *et al.* 2004, Broers *et al.* 1999].

A strong and intact nuclear lamina may be vital for muscle cells to resist the mechanical stresses occurring in the muscle tissue, therefore mutations in A-type lamins that disturb this stabilising system may explain the defects typical for muscular dystrophies. If lamin A mutants are not as tightly anchored at the nuclear periphery as the wild type, FRAP analysis can determine their enhanced protein mobility. While wild type EGFP-lamin A proved to be as immobile as expected at the nuclear periphery, some of the point mutations exhibited a faster fluorescence recovery indicating altered protein dynamics (for overview of FRAP results, see Fig. 4.20). Four lamin A mutations (R133P, delQ355, R541S and G602S) were indistinguishable in their FRAP recovery kinetics from the wild type protein and a further four (R50S, E358K, R527P and L530P) exhibited only a slight increase in protein mobility, without differing statistically significantly from the wild type.

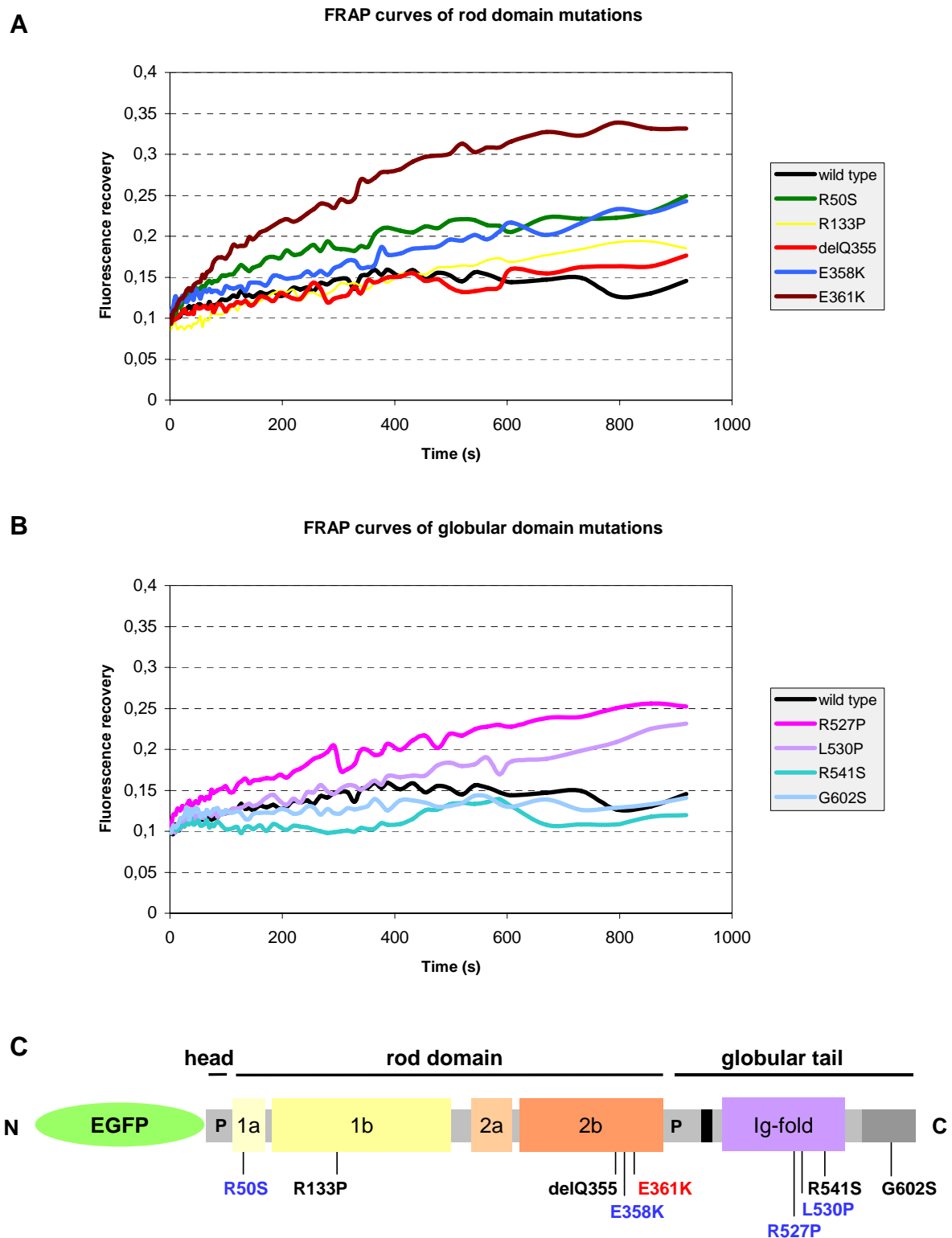


Fig. 4.20. Overview of results obtained by FRAP analysis from exogenously expressed EGFP-lamin A mutants. (A) Protein dynamics of lamin A mutations of the rod domain shown by superimposed FRAP recovery curves. The mutation E361K exhibits the highest mobility. (B) Protein dynamics of lamin A mutants of the globular domain shown by superimposed FRAP curves. (C) Schematic diagram of the EGFP-lamin A sequence indicating the positions of EDMD causing mutations with normal (black), slightly (blue) or strongly increased (red) protein mobility. N amino-terminus, C carboxyl-terminus.

The most pronounced alteration in dynamics was seen for the mutation E361K which appeared to be the most mobile of all mutants tested. In a recent report, a patch of negative electrostatic potential at the C-terminal end of the lamin A rod domain (DEYQELLD, residues 357 to 364, net charge -4) has been identified to play an important role in the head-to-tail assembly of the nuclear lamins [Strelkov *et al.* 2004]. E361 lies within this amino acid sequence and carries a negative charge, so a change to lysine (positively charged) would represent a major alteration by disrupting the overall acidic character of this part of the helix. Weakened interactions between this acidic patch of one lamin dimer and the corresponding positive patch on another may impede correct assembly into longitudinal lamin polymers, leading to increased mobility of the mutated dimers. In the end, a possibly more fragile nucleus is less capable of withstanding mechanical stress. The E358 residue may follow a similar way of functioning, since it carries another one of the negative charges of the acidic patch and is also mutated to a lysine [Strelkov *et al.* 2004]. It remains to be elucidated, however, why this mutation does not alter lamin A protein dynamics as strongly as the E361K mutation, at least during the observation time used. A longer time-course for the FRAP experiments may solve this problem. Alternatively, the differences in protein kinetics observed between these two mutations may reflect their different positions in the patch's heptad sequence which may contribute differentially to the binding of other lamin dimers. Finally, FRAP analysis led us to the conclusion that indeed some lamin A mutations, namely E361K, may lead to EDMD because its structural role at the inner nuclear membrane is altered. However, there seem to be other mechanisms by which mutations in nuclear lamins can cause such a variety of diseases.

4.4 Lamin A/C-emerin interactions *in vitro*

4.4.1 Do mutations in lamin A and C impair their binding to emerin ?

Protein-protein interactions are often the key to protein function and one important binding partner for lamin A/C is the transmembrane protein emerin. The binding domain for emerin lies within the region common to both A-type lamins, from residues 364 to 566 [Sakaki *et al.* 2001]. To date, only one of the lamin A mutations (L530P) examined in this thesis has been tested for its binding ability to emerin in a co-immunoprecipitation assay and completely failed to bind [Raharjo *et al.* 2001]. Despite a report that gave evidence that the preferred binding partner of emerin is lamin C [Vaughan *et al.* 2001], no studies have specifically addressed the lamin C-emerin interaction.

So can mutations in A-type lamins affect their binding to emerin, even though several of them occur outside the mapped emerin-lamin A/C binding domain ? Furthermore, do the lamin C mutations exhibit the same binding behaviour as their lamin A counterparts ?

In order to investigate the effect of *LMNA* mutations on the ability of lamin A and C to interact separately with emerin, all three proteins were expressed using a reticulocyte lysate system and co-precipitated with the anti-emerin antibody AP8 [Ellis *et al.* 1998]. Co-immunoprecipitation with proteins synthesised by this *in vitro* transcription/translation system should avoid possible variations in solubility from the nuclear lamina that could be caused by the different lamin mutations.

4.4.2 *In vitro* synthesis of lamin A/C mutants and emerin

It is vitally important to maintain the correct sequences for the different lamin mutations, therefore the lamin A and C constructs from the DNA sequenced pEGFP and pDsRed2 vectors were sub-cloned into pcDNA3.1(+). This vector provided the T7 promoter necessary for the transcription/translation reaction. After synthesis in the reticulocyte lysate mixture, the ³⁵S-methionine labelled lamin A and C and full-length emerin constructs were analysed for expression levels by SDS-PAGE and subsequent autoradiography (Fig. 4.21).

The *in vitro* transcription/translation reaction yielded high amounts of protein of the expected sizes (Fig. 4.21, compare the lanes for emerin and lamin A/C in A to that of the standard control luciferase). All lamin A constructs were synthesised with a similar efficiency to wild type lamin A, except T150P, which expressed at slightly lower levels.

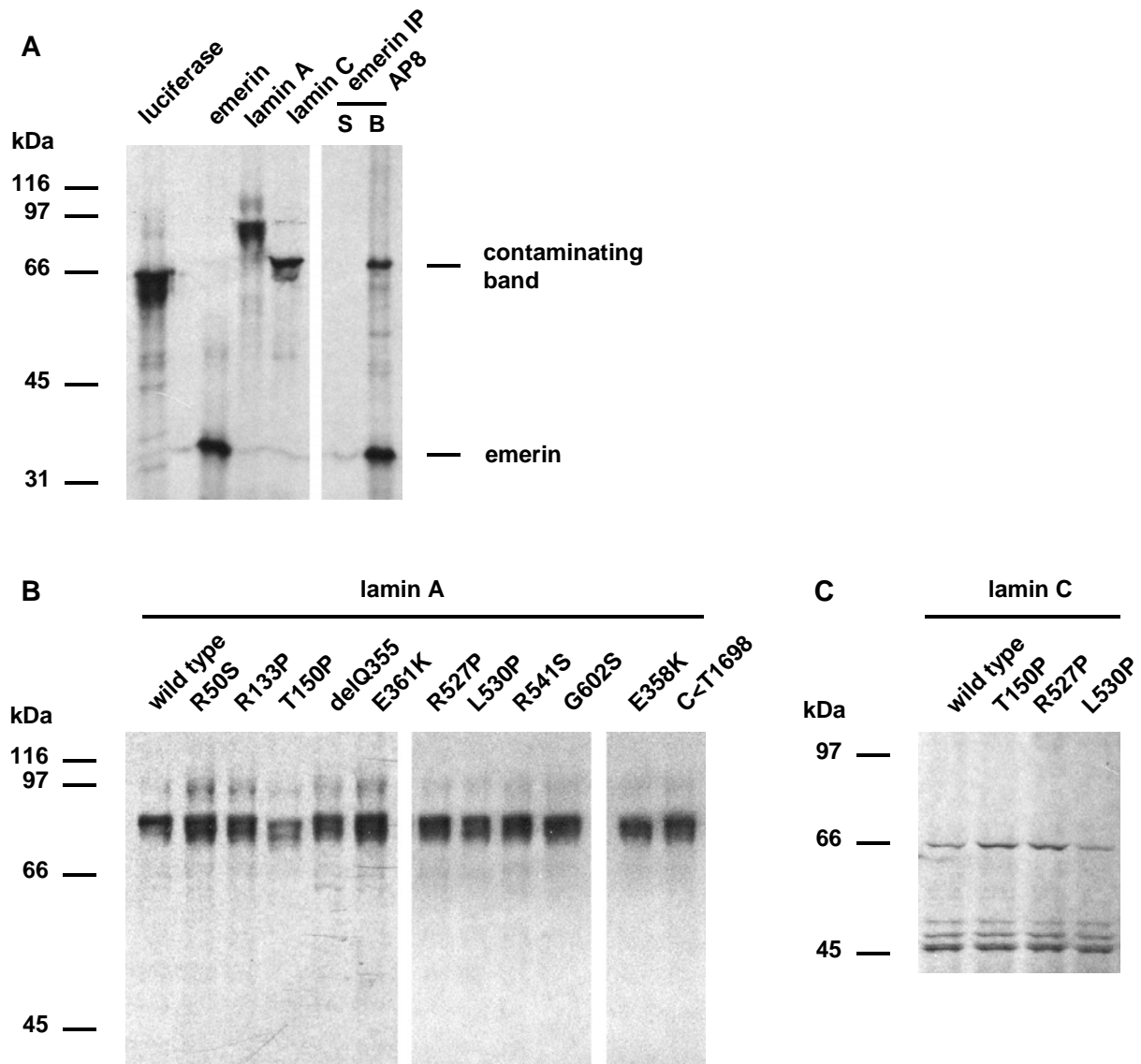


Fig. 4.21. Autoradiographs of *in vitro* transcription/translation reactions of lamin A/C constructs. (A) TNT reaction controls luciferase, emerin, lamin A and lamin C in pcDNA3.1(+) are shown, 1/25th of the total reaction volume was loaded per lane on a 10% SDS gel. On the right, a control immunoprecipitation (IP) of emerin with the AP8 antibody revealed a contaminating band of ~70kDa in the bound protein (B) fraction, but not in the supernatant (S). (B) An aliquot of the TNT reaction of each of the different lamin A mutations in pcDNA3.1 was analysed by 10% SDS-PAGE (1/25th of total reaction volume per lane). (C) The efficiency of the TNT reaction of lamin C constructs in pCMV-Tag2A (FLAG) was tested on a 8-20% gradient SDS gel (2/25th of total reaction volume per lane).

Since pre-lamin A cDNA sequences were used, the double band on the autoradiography demonstrated the presence of both the pre-lamin and mature lamin A isoforms (Fig. 4.21B), suggesting lamin A processing was not affected by any of the mutations. However, a problem with the size of the lamin C constructs arose when the efficiency of the anti-emerin AP8

antibody to immunoprecipitate *in vitro* synthesised emerin from the lysate was tested (Fig. 4.21, IP lanes in A). While the antibody captured about 90% of the total amount of emerin synthesised per transcription/translation reaction and was therefore shown to be suitable for immunoprecipitation (IP) experiments (Fig. 4.21A, compare supernatant lane to bound protein lane), it also cross-reacted with a contaminating band. This band migrated on 10% SDS-PAGE with a similar mobility to the pcDNA3.1(+)-lamin C construct and was not seen in a control IP with pre-immune serum which precipitated no proteins (data not shown).

In order to bypass the obscuring influence of this contaminating band on the results of the emerin-lamin C IPs, the lamin C cDNA constructs were sub-cloned into the pCMV-Tag2A vector. This vector encoded for a FLAG tag at the N-terminus of the protein which allowed independent confirmation of lamin C in the co-immunoprecipitations by immunoblotting with the anti-FLAG antibody M2. To further simplify the identification of the lamin C signal by increasing its separation from the contaminating band, the pCMV-Tag2A-lamin C-emerin binding assays were analysed on 8-20% gradient SDS-PAGE.

All four lamin C constructs available were expressed at similar levels in TNT reactions, except possibly L530P (Fig. 4.21C), although the reaction efficiency was lower than for the lamin A constructs. This difference in yields might be explained by the use of a T3 RNA polymerase required for transcription of the pCMV vector in a reaction system optimised for T7 polymerase (for the pcDNA3.1(+) constructs). Lower molecular weight bands were also observed which were attributed to lamin C degradation products.

No data could be collected for the lamin A double mutant E358K+C<T1698, as the transcription/translation reactions yielded no protein at all. It is not clear whether this failure in protein expression is due to an intrinsic problem with this double mutation or to a cloning error, although the latter seems unlikely as the cloning procedure was repeated several times.

4.4.3 Mutant lamin A proteins show different emerin-binding capabilities

During the co-immunoprecipitation assays, approximately 75% of wild type lamin A present in the mixed lysates was captured together with 90% of the emerin (data not shown). The majority of the mutant lamin A constructs demonstrated a similar strength of interaction to emerin as the wild type protein, with the mutation R133P binding with a higher affinity (Fig. 4.22). However, for the three mutations T150P, R527P and L530P, a significant decrease in binding to emerin was observed (Fig. 4.22A).

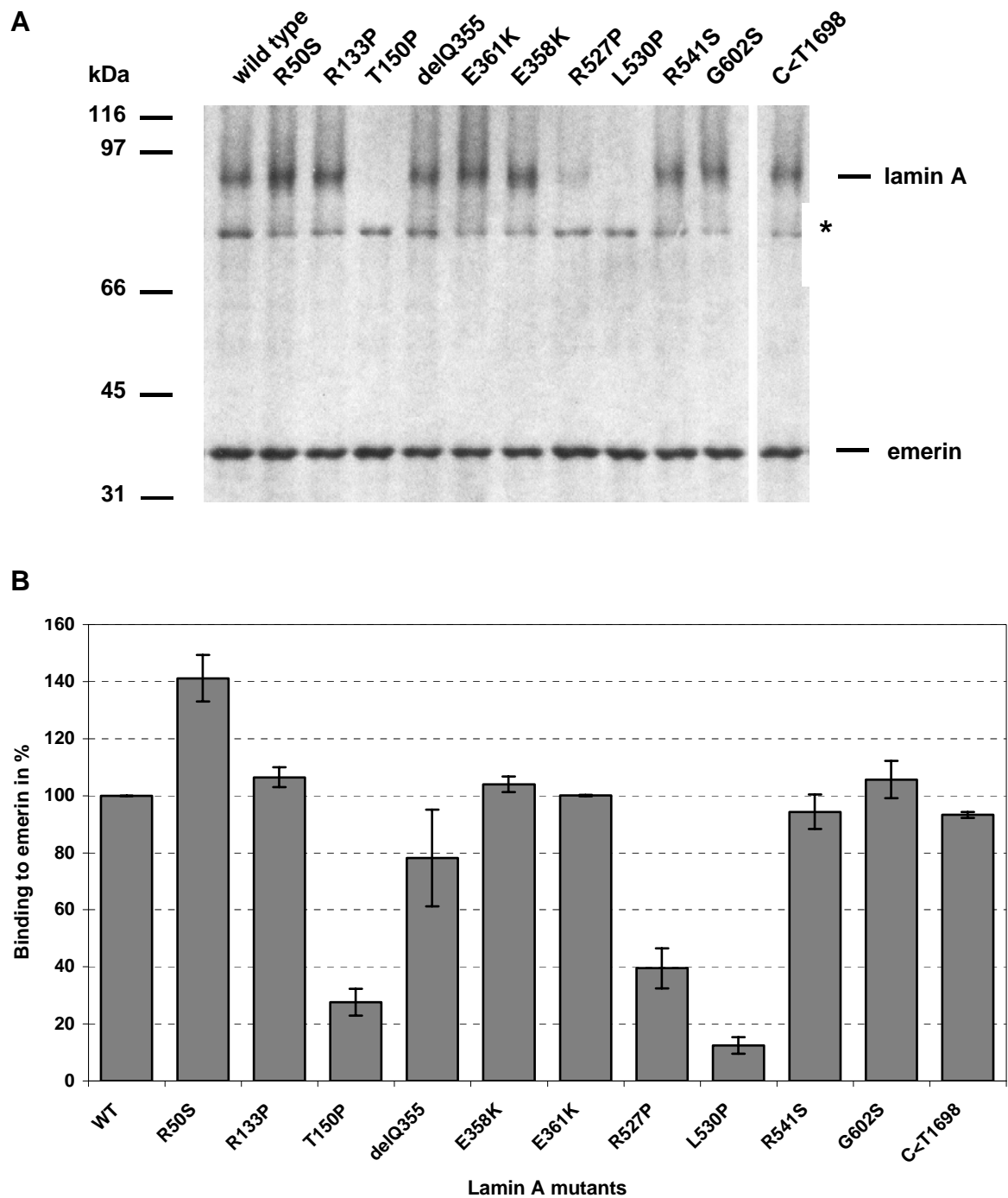


Fig. 4.22. Co-immunoprecipitation of wild type and mutant lamin A constructs with emerin. (A) Autoradiograph of an exemplary SDS gel loaded with precipitates from co-IPs of lamin A mutations and emerin. Mutants T150P, R527P and L530P exhibited strongly reduced binding to emerin. (B) Graphic demonstration of quantitative analysis (for exact values, see table 4.2), with the small bars indicating the standard error of the means (SEM).

* contaminating band.

In order to verify these differences in interaction strength, quantitative analysis with the Gene Tools programme of the Gene Genius Bioimaging system was performed (Table 4.2, see also Fig. 4.22B for visualisation), with the number of experiments per mutation ranging from two to four. Wild type lamin A was assigned an emerin binding capacity of 100% and served as the standard for comparison with the mutant proteins.

The biggest group of mutations, including R133P, E358K, E361K, R541S, G602S and the polymorphism C<T1698, presented a wild type phenotype, with an emerin interaction strength from 93 to 106%. Two mutations showed a slightly stronger variation: R50S bound the strongest to emerin (141% compared to the wild type), while deletion mutant Q355 produced a weaker interaction with emerin at only 78% binding capacity. However, the decrease in affinity to emerin was most prominent in the three mutations T150P, R527P and L530P, with 28%, 39% and 12% mean emerin binding, respectively. Especially noteworthy here is that the mutation T150P which lies outside the mapped emerin binding domain of lamin A leads to such a reduction in binding capacity. This data suggests that the mutation T150P has a considerable influence on protein conformation and might block the access to the interaction site for emerin.

Table 4.2. Quantitative analysis of mutant lamin A-emerin co-immunoprecipitation assays.

Mutation	Mean emerin binding in %	SEM	n
WT	100	± 0	5
R50S	141.17	± 8.12	2
R133P	106.44	± 3.51	2
T150P	27.55	± 4.66	4
delQ355	78.08	± 16.97	2
E358K	103.95	± 2.76	2
E361K	100.04	± 0.29	2
R527P	39.49	± 7.08	3
L530P	12.42	± 2.86	4
R541S	94.36	± 6.02	3
G602S	105.67	± 6.47	2
C<T1698	93.25	± 1.05	2

SEM standard error of the means, n number of experiments

4.4.4 Lamin C mutants T150P, R527P and L530P maintain a wild type-like emerin interaction

With lamin A mutants T150P, R527P and L530P exhibiting a reduced ability to interact with emerin, co-immunoprecipitations of their lamin C counterparts and emerin were performed to investigate whether these A-type lamins react in a similar manner. Since the mutations are in a region common to lamin A and C, we expected that any one mutation would have a similar effect on lamin C as it has on lamin A with respect to emerin binding. In all cases, approximately 90% of the lamin C synthesised in the reticulocyte lysate was co-immunoprecipitated with 90% of the emerin (data not shown). More surprisingly, all three mutations showed the same strong binding to emerin as the wild type, a reduced affinity like in their lamin A counterparts could not be observed (Fig. 4.23).

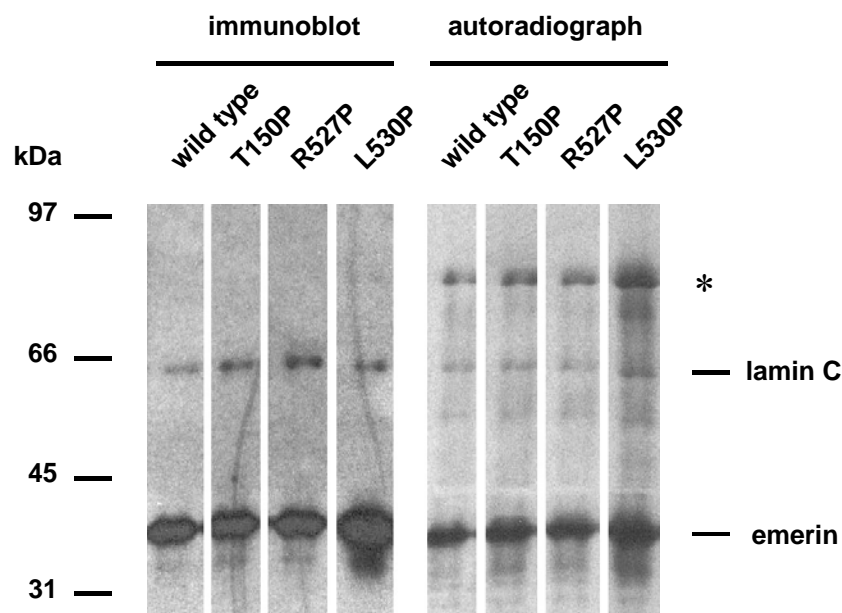


Fig. 4.23. Co-immunoprecipitation of wild type and mutant lamin C constructs with emerin. Precipitates from a co-IP of lamin C and emerin were separated on a 8-20% gradient SDS gel and immunoblotted for FLAG-tagged lamin C with an anti-FLAG antibody and for emerin with the AP8 antibody (left). Thereafter, autoradiography was performed on the dried nitrocellulose (right). All lamin C constructs bind to emerin, similar to the wild type protein. * contaminating band.

For a clear identification of the lamin C bands, the precipitated proteins of the co-immunoprecipitations were immunoblotted with an anti-FLAG antibody prior to direct autoradiography on the dried nitrocellulose. Both methods showed emerin binding for wild type lamin C as well as for the three mutated proteins (see Fig. 4.23).

4.4.5 Weakened emerin interaction of some lamin A mutations may lead to EDMD

Mutations in the *LMNA* gene are predicted to disrupt interactions between A-type lamins and their binding partners. Although the emerin binding domain has been mapped to the region common to both lamin A and C, the individual amino acids directly involved in this interaction have not been identified. Different binding residues for the A-type lamins would create a certain functional specificity for each, and also allow them to bind simultaneously. Biomolecular interaction analysis using a BIAcore has demonstrated a direct interaction between emerin and lamin A with a molar ratio of between 2:1 and 3:1 [Clements *et al.* 2000], indicating multiple emerin-binding sites exist on lamin A. The same could be true for lamin C. Additionally, competition experiments suggested that lamin C represents emerin's preferred interaction partner from the group of both A- and B-type lamins [Vaughan *et al.* 2001]. We could show that the lamin C mutants T150P, R527P or L530P still bind to emerin, whereas the complementary lamin A mutants fail to do so, supporting this theory of interaction preference.

All three mutations introduce a proline (and thus a kink) into the amino acid sequence which is likely to alter the 3D protein structure sufficiently to impede emerin binding to lamin A. Residue T150 lies within coil 1b of the central rod domain which is required for lamin homo/heterodimer formation. Altering it to a proline, a known α -helix breaker, most likely disrupts both local coiled-coil and higher ordered filament formation. Considering the observed inability to bind to emerin and the strong mislocalisation of the EGFP-fusion protein (see chapters 4.1 and 4.2), the T150P mutation seems to produce a severely mis-folded protein which is unable to fulfil its functions in filament assembly and emerin interaction.

Both R527 and L530 are evolutionary conserved residues and lie within the common emerin binding domain. The 3D structure of this C-terminal globular domain in the human A-type lamins has recently been determined to resemble a typical Ig-fold [Krimm *et al.* 2002, for residues 430-545, Dhe-Paganon *et al.* 2002, for residues 436-552]. The L530P mutation concerns a hydrophobic residue buried in the central core of a β sheet [Krimm *et al.* 2002], leaving it unavailable for direct interaction with emerin. Presumably, the change to a proline in the core perturbs the domain conformation sufficiently to disrupt emerin binding. R527 is located in the centre of a β sheet within a surface exposed positive patch area and could thus interact with emerin directly. Its amide proton is involved in a backbone-backbone hydrogen bond which is disrupted by the proline substitution, thus leading to a destabilisation of the 3D structure of the domain [Krimm *et al.* 2002].

Therefore, the R527P mutation could inhibit emerin binding by two molecular mechanisms, either via direct protein-protein interaction through altered surface charges or via destabilisation of the 3D structure of the Ig-like domain. Fig. 4.24 shows the location of the three mutations T150P, R527P and L530P which demonstrate a decreased emerin binding affinity within the lamin A amino acid sequence.

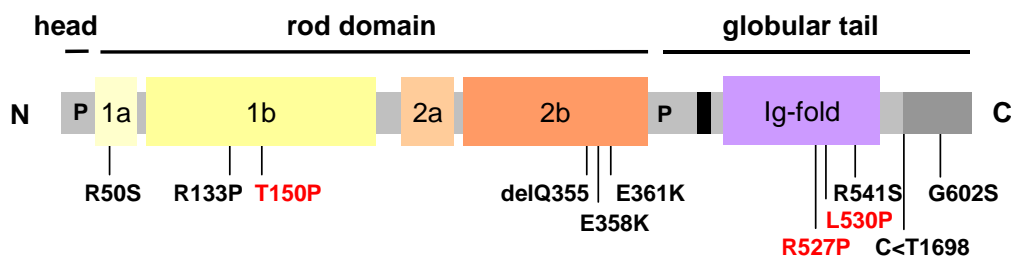


Fig. 4.24. Schematic diagram of the lamin A sequence indicating the positions of EDMD causing mutations with normal (black) or strongly reduced (red) emerin binding. N amino-terminus, C carboxyl-terminus.

The interesting question is, however, why these three mutations in lamin C do not mimic the emerin binding behaviour of their lamin A counterparts. Our *in vitro* results are supported by an *in vivo* study on cells from an FPLD patient with a R482L *LMNA* mutation. Co-immunoprecipitation of emerin with A-type lamins from cells derived from this laminopathy patient precipitated only lamin C, but not lamin A, further confirming emerin's preference for the former [Capanni *et al.* 2003].

The two A-type lamins differ only by their C-terminal tails, the lamin C-specific one being six residues (VSGSRR) long. Its shortness makes it unlikely to affect the structure of the adjacent globular domain, but the presence of two arginines with their positive charges implies its potential as a protein interaction site. The existence of a second, higher-affinity binding site for emerin in the lamin C-specific carboxyl tail would explain how all the examined lamin C mutants retain their emerin binding ability, while the respective lamin A mutants lose it. Further experimental evidence will be necessary to establish this possible second emerin binding domain in lamin C; it would be interesting to determine whether the only lamin C-specific mutation known, R571S which weakens the positive charges of the tail region [Fatkin *et al.* 1999], is still able to interact with emerin.

4.4.6 Summary of results

To summarise all results obtained during the analysis of the lamin A/C mutations, table 4.3 gives a simplified overview.

Results

Table 4.3. Summary of results obtained by analysis of *LMNA* mutations.

Mutation	Localisation in interphase	after mitosis	of endogenous lamin B2	of endogenous emerin	Localisation ability for exogenous lamin C	Ultra-structural cell morphology	Protein mobility	<i>In vitro</i> binding to emerin
LA wild type	Nuclear rim staining of ex. LA and end. LA/C	Normal at nuclear rim	Nuclear rim staining	Normal at nuclear rim	Re-directs all ex. LC constructs to nuclear rim	Nuclear lamina thickened by ex. LA	Very low	+
LA R50S	WT-like for ex. LA	Near normal, effects on emerin	ND	Normal in interphase, reduced after mitosis	Re-directs ex. LC WT to nuclear rim	NL thickened, but less continuous	Low	++
LA R133P	Fine aggregates of ex. LA at nuclear rim	Stronger aggregation, effects on emerin	Nuclear rim staining	Normal in interphase, aggregated at NE after mitosis	Re-directs ex. LC WT to nuclear rim	Fine aggregates at NL	Very low	+
LA T150P	Cytoplasmic aggregates of ex. LA, end. LA/C normal	Ex. LA mis-loc., effects on emerin	ND	Normal in interphase, reduced + aggregated after mitosis	Distinct localisation, LA WT re-directs LC mut, not v.v.	Aggregates in cytoplasm, NE + NL normal	ND	--
LA delQ355	Very fine aggregates of ex. LA at nuclear rim	Punctuate stain. more pronounced, effects on emerin	Nuclear rim staining	Normal in interphase, cytoplasm. aggregates after mitosis	Re-directs ex. LC WT to nuclear rim	Very fine aggregates at NL	Very low	±
LA E358K	WT-like for ex. LA, end. LC strongly reduced	Normal at nuclear rim	ND	Normal at nuclear rim	Re-directs ex. LC WT to nuclear rim	NL thickened, aggregates outside NPCs	Low	+
LA E361K	WT-like for ex. LA	Slightly disturbed nuclear rim stain.	ND	Normal in interphase, aggreg. after mitosis	Re-directs ex. LC WT to nuclear rim	NL thickened, but less continuous than WT	Increased	+
LA R527P	WT-like for ex. LA, end. LC reduced	Punctuate staining after mitosis	Nuclear rim staining	Normal in interphase, delayed localisation after mitosis	Re-directs all ex. LC constructs to nuclear rim	NL thickened, with membrane invaginations	Low	-
LA L530P	WT-like for ex. LA and end. LC	Normal at nuclear rim	ND	As WT	Re-directs all ex. LC constructs to nuclear rim	NL thickened, some membrane invaginations	Low	--
LA R541S	WT-like for ex. LA	Normal at nuclear rim	ND	As WT	Re-directs ex. LC WT to nuclear rim	NL thickened	Very low	+
LA G602S	WT-like for ex. LA	Normal at nuclear rim	ND	Normal at nuclear rim, reduced in 50% of cells	Re-directs ex. LC WT to nuclear rim	NL thickened	Very low	+
LA C<T1698	Aggregates of ex. LA at nuclear rim, end. LC partially reduced	Aggregates at nuclear rim, effects on emerin	NE staining, exclusions at ex. LA aggregates	Co-localisation with ex. LA aggregates	Distinct aggregates of ex. LA and LC	Massive aggregates along at NL, no paracrystal formation	ND	+
LA E358K +C<T1698	Very fine aggregates of ex. LA at nuclear rim, end. LC reduced	As in interphase	ND	Normal in interphase, aggregated after mitosis	Re-directs ex. LC WT to nuclear rim	NL less thick and continuous as in WT	ND	ND
LC wild type	Intranuclear aggregates	Increased nuclear rim staining	ND	ND	NA	ND	ND	+
LC T150P	As WT		ND	ND	NA	ND	ND	+
LC R527P	As WT		ND	ND	NA	ND	ND	+
LC L530P	As WT		ND	ND	NA	ND	ND	+

Ex. exogenous, end. endogenous, LA lamin A, LC lamin C, LB2 lamin B2, NA not applicable, ND not determined, NE nuclear envelope, NL nuclear lamina, NPC nuclear pore complex, v.v. vice versa, WT wild type

5 Discussion

5.1 How to study disease-causing mutations in human genes

The laminopathies comprise a wide range of human diseases with different tissue-specific defects: from disorders weakening skeletal and cardiac muscle and bones over those impairing fat distribution and glucose metabolism, to those affecting neuronal function. Although mutations in the *LMNA* gene cause such a wide diversity in defects, the disorders themselves are very rare, with only a few affected individuals per million people. Due to the scarcity of laminopathy patients, it proved difficult therefore to obtain enough biological samples (biopsy material or cultured cells from human patients) for further research.

So which other methods are available for detailed investigations of the molecular causes? A *Lmna*^{-/-} mouse model has been created [Sullivan *et al.* 1999]; the homozygous mice, without detectable levels of A-type lamins, develop muscular dystrophy and heart pathology as well as axonal degeneration and white fat re-distribution [Sullivan *et al.* 1999]. *Lmna*^{+/-} mice, unlike the heterozygous human patients, do not show any clinical symptoms, thus indicating that this knock-out animal system can only be used to study the general functions of A-type lamins, but not the specific effects of disease-causing mutations. While the *LMNA* mutation L530P is in fact well documented to cause AD-EDMD [Bonne *et al.* 1999], *Lmna*^{L530P/L530P} knock-in mice exhibit a more severe phenotype markedly reminiscent of symptoms observed in progeria patients [Mounkes *et al.* 2003a]. In addition, polymorphic variation may be involved in the progression of the disorders (the most obvious example being the SNP C<T1698) which may not be present in the mouse. So although the mouse model is the preferred object for investigations of the mammalian organism and the interactions between its different tissues, it seems sub-optimal for mutational analysis.

As an alternative, cultured cell lines derived from specific cell populations like myoblasts and fibroblasts have several advantages. Mammalian cell lines are widely available, easy to handle and to examine with microscopic and biochemical methods, allowing a quick analysis of numerous *LMNA* mutations. Additionally, transfected cells expressing exogenous mutant A-type lamins also produce their own endogenous wild type lamins A/C, thus mimicking the situation in the cells of a human patient. Due to their heterozygosity, they synthesise both wild type and mutant A-type lamin proteins, therefore the interaction between the two forms of lamin A/C must be considered an important part in the pathogenesis of the disorder.

Of course, we must not make the mistake of transferring the results obtained in the cell culture model one to one into the human body, since we cannot reproduce many of the tissue-specific factors involved in determining the disease phenotype. Cell culture data needs to be viewed alongside the data from both patient's tissue and the animal model. On the cellular level, however, our studies provide valuable clues as to why simple point mutations in the lamin A/C gene lead to such a variety of cell type-specific defects.

5.2 Possible molecular mechanisms of lamin A mutations leading to Emery-Dreifuss muscular dystrophy

Twelve *LMNA* mutations and polymorphisms were analysed in respect of their intracellular localisation, their influence on cell and nuclear morphology, their stability within the nuclear lamina and their emerin interaction. A wide variety of cellular phenotypes was observed leading to the conclusion that several different mechanisms may be responsible for EDMD.

5.2.1 Mutations in the rod domain of lamin A mainly impair lamin filament assembly

5.2.1.1 R50S

The lamin A mutation R50S presented a phenotype similar to wild type in transfected cells, only filament formation within the nuclear lamina appeared disturbed by electron microscopic inspection. FRAP analysis revealed slightly increased protein mobility, indicating that mutant lamin A dimers were not as stably integrated into the nuclear lamina as the wild type protein. Residue R50 lies within an evolutionary conserved area in coil 1A of the rod domain involved in head-to-tail filament assembly [Strelkov *et al.* 2002] which could be impaired by the replacement of an arginine with its positive charge with an uncharged serine. The importance of this residue is further emphasised by the existence of other mutations, i.e. to proline, also causing AD-EDMD [Novelli, D'Apice, 2003]. We therefore propose that the lamin A mutation R50S weakens the nuclear lamina by its insufficient interaction with other lamins in head-to-tail filament formation, leading to nuclear damage and, in the long run, to the tissue-specific defects of a muscular dystrophy according to the mechanical stress hypothesis.

Alternatively, the mutation may impair binding to other, yet unknown proteins or to proteins of which the binding domain in lamin A has not been mapped, such as LAP1, BAF, MAN1 or

the nesprins [Zastrow *et al.* 2004]. Further investigations are necessary to elucidate possible protein interaction deficits of this *LMNA* mutant.

5.2.1.2 R133P

EGFP-lamin A with the mutation R133P formed small, but stable aggregates along the inner nuclear membrane, with a slight delay in nuclear lamina assembly of the exogenous protein after mitosis and subsequent effects on emerin. Otherwise, this mutant behaved like the wild type. The amino acid affected locates to a series of four heptad repeats in coil 1B which is unique to nuclear lamins [Herrmann and Aebi, 2004], and the mutation replaces a positively charged arginine with a hydrophobic proline. The positive charge at this position may play an important role for lamin function, since its loss due to mutation to the also hydrophobic leucine residue leads to a generalised lipodystrophy (LIRLLC) as well as to atypical Werner's syndrome [Novelli and D'Apice, 2003, Chen *et al.* 2003].

The change to proline also introduces a kink into the α -helix with the potential to disturb the 3D structure of the rod structure and thus dimerisation. Indeed, while exogenous lamin A could still interact with exogenous lamin C, an effect of the mutant lamin A on the distribution of the endogenous lamin B2, indicative of heterodimer formation, could not be observed. Scientists disagree about whether A- and B-type lamins form heterodimers or assemble into distinct networks [for review, see Zastrow *et al.* 2004], but the lamin B filament network seems to provide a scaffolding for A-type lamin filament assembly [Gruenbaum *et al.* 2003]. It is therefore likely to assume that mutant lamin A, with a slightly changed protein and possibly also dimer conformation and lacking a positive charge in a sensitive area is unable to use B-type lamins for proper nuclear lamina incorporation. The irregularity of such a lamina, despite the stability of the mutated lamin A protein filaments, might not withstand the increased mechanical stresses in muscle tissue thus leading to muscular dystrophy.

In light of the disorders caused by other mutations at this amino acid position, however, an altered protein binding ability of the lamin A mutation R133P may also be responsible for the disease, similar to the mutation R50S.

5.2.1.3 T150P

The most drastic phenotype of all lamin A mutations displayed was mutant T150P: the exogenous protein formed huge cytoplasmic aggregates and did not bind to emerin. The amino acid alteration to a proline and its characteristic as a α -helix breaker obviously led to a severe mis-folding of the protein directly after synthesis, rendering both nuclear localisation signal and emerin-binding domain unable to fulfil their functions. Further support for an altered secondary structure of the rod domain comes from the fact that none of the lamin aggregates, upon closer electron microscopic inspection, exhibited areas of a paracrystalline morphology, which would be indicative of regular polymer formation. In contrast, intact *Xenopus* lamin A expressed in Sf9 cells readily assembles into cytoplasmic paracrystals [Krohne *et al.* 1998].

If the same mis-folding process occurs in human patients, we can assume that the mutated protein would not reach the nucleus, being degraded soon after translation in the cytoplasm. The EDMD phenotype could therefore be explained by haploinsufficiency of the A-type lamins of the one remaining wild type allele, either leading to structural weakness of the nucleus or to a lack in scaffolding sites for other interaction partners. Unfortunately, the clinical report of AD-EDMD patients carrying the T150P mutation does not contain immunohistochemistry or protein biochemistry analysis to corroborate our findings [Felice *et al.* 2000].

There is, however, a second theory to be considered: since a threonine as a potential phosphorylation site is affected by the mutation, an altered protein phosphorylation might contribute to the disease phenotype. Higher ordered lamin filament formation is regulated by phosphorylation on specific lamin residues, which also controls the efficiency of nuclear localisation [Haas and Jost, 1993]. Although mitotic phosphorylation mainly uses two conserved serines flanking the lamin rod domain [Leukel and Jost, 1995], residues phosphorylated *in vitro* by PKC have been identified within the coiled-coil domain in murine A-type lamins, i.e. a threonine at position 199 [Eggert *et al.* 1993]. Indeed, a recent report demonstrated the hyperphosphorylation of lamin A/C during myoblast differentiation or proliferation and in mature muscle, which was strikingly reduced in laminopathic myoblasts and muscle fibres [Cenni *et al.* 2005]. Therefore, the loss of a potential phosphorylation site resulting in a decreased phosphorylation ability of lamin A and a subsequently disturbed interaction with a muscle-specific partner might well be involved in the pathogenic mechanism of Emery-Dreifuss muscular dystrophy.

5.2.1.4 DelQ355

The lamin A deletion mutant Q355 is another one of the mutations presenting a phenotype differing from that of the wild type protein, though only in a cell cycle-dependent manner. While transfected cells in interphase exhibited a very fine punctuate staining of the exogenous protein along the nuclear envelope, with normal protein mobility and emerin distribution, this picture changed after mitosis. Directly after cell division, the exogenous lamin A formed cytoplasmic aggregates together with endogenous emerin and nuclear envelope re-localisation was delayed for both proteins. Both A-type lamins and emerin have been proposed to play roles in nuclear reassembly after mitosis [Lopez-Soler *et al.* 2001, Bengtsson and Wilson, 2004]; a delay in nuclear envelope reassembly due to the mutant lamin A and its potential dominant negative effect on the wild type lamin A as well as on emerin would presumably slow down proliferation and differentiation of satellite cells in human muscle fibres. Since satellite cells are a requirement of muscle regeneration, their failure to replace damaged muscle fibres would lead to the typical symptoms of muscular dystrophies, as has been suggested previously [Fairley *et al.* 1999].

However, mainly skeletal and cardiac muscle is affected in AD-EDMD, other rapidly dividing cell types like that of blood or skin show less abnormalities. Therefore, other mechanisms are probably involved in the pathogenesis of this mutation, i.e. altered protein interaction. Several proteins bind to the area around residue Q355, like LAP2 α , MOK2 and E1B 19K [Zastrow *et al.* 2004], the most likely candidate being the retinoblastoma protein (Rb) [Broers *et al.* 2004]. This transcriptional repressor, with important functions in cell cycle control and differentiation of mesenchymal cells, binds to residues 247 to 355 in the lamin A rod domain [Ozaki *et al.* 1994, Novitch *et al.* 1999, Hansen *et al.* 2004]. In a mouse myoblast cell line, nuclear lamin speckles were reorganised early during differentiation into myotubes in cyclin D3-expressing cells, and Rb has been shown to be essential for this process [Mariappan and Parnaik, 2005]. Together with an inhibited expression of the muscle regulatory factor myogenin in myoblasts with disrupted lamin structures, both A-type lamins and Rb seem to play a crucial role in the muscle differentiation program [Mariappan and Parnaik, 2005].

The deletion of Q355 in the lamin A rod domain removes the last of a row of three glutamines at the very end of the Rb binding domain which might be important for Rb recognition. Since residue 355 locates to a sensitive, hydrophobic spot at position d of its heptad repeat, it is also plausible to think that the loss of this amino acid sufficiently disrupts the heptad formation to impede Rb interaction. In any case, a changed interaction of Rb with lamin A mutant delQ355

would explain both the cell cycle specific effects observed in our cell culture model as well as the muscle loss due to failed regeneration in human muscular dystrophy patients. However, no direct experimental evidence is available to support our theory of a weakened mutant lamin A-Rb binding, therefore further research is required to unveil possible protein interaction defects of this *LMNA* mutation.

5.2.1.5 E358K

Cells transfected with the lamin A mutation E358K were nearly indistinguishable from the wild type displaying normal nuclear rim staining for both the exogenous protein and endogenous emerin. Only endogenous lamin C appeared reduced at the nuclear envelope. These results stand partially in contrast to the work of other groups who reported the formation of intranuclear foci of this mutation, but who also observed normal emerin distribution [Östlund *et al.* 2001, Holt *et al.* 2003]. An explanation for this apparent difference in protein localisation might be the use of different cell lines and especially different expression times for the exogenous protein. In fact, even wild type-lamin A, if exogenously expressed in HeLa cells for a longer time course up to 72h post-transfection, was synthesised in a 20-fold increase compared to endogenous lamin A and aggregated in the nucleus [Bechert *et al.* 2003], implying that this is mainly due to over-expression of the exogenous protein. Since endogenous levels of mutant protein in heterozygous patient's cells are unlikely ever to reach such a high plateau, we consider our shorter expression times of 16-18h a better model for mutational analysis.

The exchange of a glutamic acid with a lysine in this mutation changes the negative charge into a positive one, with potential consequences including both altered protein interaction abilities and impaired lamin filament assembly. The mutation affects protein binding sites for several proteins, their functions ranging from structure (LAP2 α) over gene regulation (MOK2) to signalling pathways (E1B 19K). It may also comprise those interaction partners with so far unmapped binding sites in lamin A, such as LAP1, BAF, MAN1 and the nesprins [Zastrow *et al.* 2004]. However, without experimental data the possibility of an interrupted protein interaction of lamin A mutant E358K still remains to be elucidated.

Residue E358 is a highly conserved amino acid at the end of coil 2B of A-type lamins from *Drosophila* to man [Herrmann and Aebi, 2004], which has been shown to play a crucial role in the head-to-tail assembly of lamin polymers [Strelkov *et al.* 2002, 2004]. A slight increase in mobility was observed in our FRAP studies for the exogenous mutant protein in the lamina

of transfected cells, indicating that the mutant lamin A was not as tightly attached to the nuclear filament network as the wild type protein. A loss of associations between different lamin filaments, however, as well as their insufficient integration into the lamina would severely compromise nuclear integrity and stability. In human muscle tissue, such a weakened nuclear lamina would be more susceptible to damage by mechanical stress, the obvious consequences being the typical symptoms of EDMD.

5.2.1.6 E361K

The lamin A mutation E361K resembled the mutation E358K in many aspects: it leads to the same amino acid substitution within an evolutionary conserved motif involved in lamin filament assembly. Also, the exogenous protein exhibited a wild type-like distribution in transfected cells and emerin localisation remained normal except slight disturbances after mitosis. Thus, altered protein-protein interactions seemed a likely explanation for the tissue-specific defects of EDMD, the mutation probably affecting the same interaction partners and their binding sites in lamin A than the mutation E358K.

In this case, however, there is strong support for the structural weakness hypothesis, since FRAP analysis revealed a significantly increased mobility of the exogenously expressed protein in the nuclear lamina. Co-transfection assays with DsRed2-lamin C and its subsequent re-direction to the nuclear envelope proved the heterodimer formation of two A-type lamins, thus ruling out a destabilisation of the elementary dimer structure by the lamin A mutation. The alteration of the surface electrostatic potential caused by the mutation, however, may have an effect on a particular dimer-dimer interaction mode, ultimately leading to a disrupted higher order filament and nuclear lamina formation. The resulting, more fragile nucleus then would not be able to withstand the mechanical forces created in muscle tissues and a muscular dystrophy phenotype develops.

5.2.2 Mutations in the globular tail domain of lamin A are likely to disturb protein-protein interactions

5.2.2.1 R527P

Unlike the mutations in the coiled-coil domain of lamin A/C, mutations in their globular tail domains are not expected to markedly disturb dimerisation and higher order filament formation. It was therefore not surprising to find that cells expressing the lamin A mutant R527P displayed a wild type localisation pattern of the exogenous protein as well as a normal emerin and lamin B2 distribution, only the levels of endogenous lamin C seemed slightly reduced. Our observations of a wild type distribution of mutant lamin A, emerin and lamin B2 are consistent with previous reports from several other groups [Östlund *et al.* 2001, Holt *et al.* 2003, Bechert *et al.* 2003], thus establishing this phenotype in transiently transfected cells.

In vitro binding assays revealed a weaker protein interaction between the lamin A mutant R527P and emerin. *In vivo* evidence supports our findings: in *Lmna*^{-/-} mouse embryonic fibroblasts, exogenously expressed mutant lamin A failed to re-direct emerin from the ER to the nuclear envelope [Holt *et al.* 2003], indicating a disturbed lamin A-emerin interaction.

Residue R527 locates to the centre of β sheet 8 within the Ig-fold of the lamin A/C tail domain and is exposed to the surface [Krimm *et al.* 2002]. Its amide proton is involved in a backbone-backbone hydrogen bond which consistently protects it against solvent exchange [Krimm *et al.* 2002]. Mutation to proline not only disrupts the β sheet hydrogen bond network, but also introduces a kink into the secondary structure, thus destabilising the entire 3D structure of the β sheet and, consequently, the Ig-fold. This conformational change of the lamin A globular tail is unlikely to affect dimerisation and lamin filament formation, but certainly impairs the interaction with emerin and weakens lamin A-emerin complexes at the nuclear envelope. Therefore, the muscle-specific defects of EDMD may be explained by a decreased nuclear stability with subsequent muscle damage, since the lamin A-emerin complexes not only confer mechanical strength to the nucleus by themselves, but also provide scaffolding sites for other structural proteins like nuclear actin, the nesprins, LAPs and MAN1 [for reviews, see Zastrow *et al.* 2004, Bengtsson and Wilson, 2004].

Although electron microscopic examination of transfected cells with their slightly irregular nuclear envelopes supports the structural weakness hypothesis for mutation R527P, the rearrangement of peripheral heterochromatin in patient's muscle cells [Sabatelli *et al.* 2001] indicates that other mechanisms might play a role in the pathophysiology of EDMD as well.

Nuclear lamins represent attachment sites for heterochromatin at the nuclear periphery, either through direct DNA interaction via their globular tail or via connecting proteins, i.e. BAF, and exert a silencing influence on transcription [for review, see Mattout-Drubezki and Gruenbaum, 2003]. If their anchoring function is disrupted by a mutation of amino acid 527 in lamin A, altered gene expression may therefore occur. The importance of this residue and its possible involvement in gene regulation is further emphasised by the emergence of several other laminopathies caused by mutations at R527, such as FPLD and MAD (both R527H) and HGPS (R527C) [Novelli and D'Apice, 2003, Novelli *et al.* 2002].

5.2.2.2 L530P

The lamin A mutation L530P has frequently been chosen as an object for examination, and our results confirm the previous reports about its wild type-like appearance in transfected cells [Östlund *et al.* 2001, Raharjo *et al.* 2001]. Accordingly, its inability to bind to emerin has been shown *in vitro*, in a transcription/translation binding assay similar to our experimental procedure, as well as *in vivo*, when the mutant lamin A failed to retain emerin at the nuclear envelope in transfected *Lmna*^{-/-} mouse embryonic fibroblasts [Raharjo *et al.* 2001].

The hydrophobic leucine at residue 530 lies near the end of β strand 8 of the Ig-fold, but is buried in the core of the β sheet [Dhe-Paganon *et al.* 2002, Krimm *et al.* 2002], at a position conserved in different classes of the Ig domain family [Halaby *et al.* 1999]. A substitution to proline, although maintaining the hydrophobic character of this residue, is predicted to perturb stable folding of the domain and potentially diminish protein stability [Dhe-Paganon *et al.* 2002]. It certainly disrupts the 3D structure sufficiently to almost completely abolish emerin binding *in vitro* and *in vivo*.

The increase in mobility of the mutant protein within the nuclear lamina during FRAP experiments [Gilchrist *et al.* 2004], albeit only slight in our own studies, indicates an improper integration of lamin A L530P into the filament network of the lamina. Whether this is due to an impaired head-to-tail assembly because of a conformational change in the lamin A C-terminus or due to the lack of emerin-binding as anchorage at the inner membrane of the nuclear envelope remains unclear. However, the direct consequence of a less stable nuclear lamina is a more fragile nucleus which would invariably cause damage to the nuclei of muscle fibres subjected to strong mechanical forces. This would lead to the progressive loss of muscle tissue as seen in AD-EDMD.

In addition, the *LMNA* mutation L530P with its disrupted 3D structure of the globular tail domain might not only impede its binding capability to emerin, but to other interaction partners as well. Likely candidates range from structural proteins, such as actin and LAP2 α , to chromatin and gene regulatory proteins, such as the DNA itself and SREBP1, and end with proteins mediating signalling processes, like PKC α and 12(S)-LOX [Zastrow *et al.* 2004]. This notion is lent further credence by the fact that *Lmna*^{L530P/L530P} knock-in mice not only develop symptoms of a muscular dystrophy, but also show signs of progeroid syndromes [Mounkes *et al.* 2003a]. So other tissues than muscle are affected as well, which can therefore hardly be explained by the mechanical stress hypothesis alone. Further investigations are required to identify other altered protein interactions and to elucidate to which extent structural weakness and gene regulation contribute to the EDMD phenotype of lamin A mutation L530P.

5.2.2.3 R541S

The mechanisms by which the lamin A mutation R541S causes muscular dystrophy remains somewhat of a mystery, as in all aspects studied – protein localisation, dimerisation, mobility and emerin interaction – the mutant turned out to be indistinguishable from the wild type phenotype.

R541 is one of the last residues of the lamin Ig-fold and locates to the centre of β strand 9. Its buried side chain participates in the stabilisation of the β sandwich through hydrophobic contacts with the core of the domain [Krimm *et al.* 2002]. A mutation to serine shortens the side chain considerably and this, in addition to the loss of a positive charge, might lead to a conformational change, presumably disturbing protein interaction sites. The importance of this residue for domain stabilisation is further stressed by the existence of mutations to histidine and cysteine, which cause EDMD and DCM, respectively [Bonne *et al.* 2001].

The globular tail domain of lamin A represents a binding site for a variety of proteins; for residue 541, those concerned are in fact the same as for residue 530 [see above and Zastrow *et al.* 2004]. Since we observed no morphological abnormalities in transfected cells, we assume that a potentially disturbed protein interaction affects mainly gene regulatory or signal transduction partners, i.e. PKC α , SREBP1 or 12(S)-LOX. While SREBP1 is involved in lipogenesis and adipocyte differentiation [Horton, 2002], both PKC α and 12(S)-LOX are general mediators of signal transduction pathways [Ron and Kazanietz, 1999, Liu *et al.* 1994], able to interact with each other. They might therefore play a role in muscle-specific signalling

events, for example in activating the expression of genes required for muscle regeneration, the failure of which would lead to muscular dystrophy symptoms. Although, without direct experimental evidence, we can only speculate about the true mechanism by which *LMNA* mutation R541S causes disease.

5.2.2.4 G602S

The *LMNA* mutation G602S is the only one studied which is unique to one of the A-type lamins due to its location in the specific C-terminal tail of lamin A. This is, however, its most spectacular feature, since cells transfected with this mutant lamin A closely resembled cells expressing the wild type protein, apart from a slight reduction in endogenous emerin staining in about half of the transfected cells. *In vitro* binding to emerin was detected at normal levels. The mutation changes a glycine into a serine, thus adding another polar amino acid to this already serine-rich region of lamin A. The most plausible explanation for this mutation to cause disease is altered protein interaction ability; similar to the mutation R541S. Likely interaction partners are the gene regulatory and signal transduction proteins binding to the C-terminal tail of lamin A (PKC α , SREBP1, 12(S)-LOX).

Interestingly, the mutation G602S has recently been found in a woman with type A insulin resistance without signs of lipodystrophy [Young *et al.* 2005]. Cultured fibroblasts of the patient exhibited in their majority a wild type phenotype, with normal lamin and emerin distribution consistent with our results in transfected cells; a small minority (~6%) of the cells had dysmorphic nuclei with herniations lacking endogenous lamins [Young *et al.* 2005]. The authors suggest a possible dysregulation of the serine/threonine kinase PKC α during pathogenesis, because increased phosphorylation of proteins involved in the insulin signalling pathway has been linked to the disorder and PKC α inhibits insulin signalling [Zick, 2003, Young *et al.* 2005]. Since EDMD patients may develop wasting of adipose as well as of muscle tissue [Mercuri *et al.* 2004], it is well conceivable that a mutation predominantly associated with adipocyte malfunctioning like G602S may extend its effects on muscle fibres and myoblast differentiation. Presumably, the exact nature of the disorder is then controlled by the genetic background of the affected individual.

5.2.2.5 C<T1698 and E358K+C<T1698

Microscopic examination of cells expressing the lamin A polymorphism C<T1698 revealed the most surprising phenotype of all lamin A constructs tested in this study. The exogenous lamin A accumulated in huge spherical aggregates at the inner nuclear membrane, excluding both endogenous lamin B2 and exogenous lamin C from these aggregates. Endogenous emerin co-localised with the exogenous lamin A and, as therefore expected, bound to the mutant protein *in vitro*.

So how can a single nucleotide polymorphism (SNP) with no obvious alteration in the amino acid sequence of the protein cause such an unusual distribution pattern? The SNP changes the last position of codon 566; this amino acid is the last one shared by lamin A and lamin C [Fisher *et al.* 1986], implying that a splicing error might occur during mRNA processing. We could not detect any changes in protein size due to altered mRNA splicing or to a possible disequilibrium in the expression of lamin A and lamin C, as we used a lamin A cDNA construct without intron sequences in our experiments. Accordingly, both the *in vitro* synthesised protein and the *in vivo* expressed EGFP-fusion protein were of wild type size. However, major alterations in protein size or in relative expression levels of A-type lamins would certainly cause disease and have therefore to be considered unlikely, especially in the light of an 1698T allele frequency of approximately 0.5 in Inuit [Hegele *et al.* 2001]. A minor alteration, though, involving the loss or addition of only a few amino acids due to defective splicing, would maintain the essential functions of the wild type protein, only its interaction capability to specific partners may be impaired. It would also account for the association of this polymorphism with obesity-related traits and metabolic syndrome in several aboriginal populations [Steinle *et al.* 2004, Hegele *et al.* 2001, 2000]. Alternatively, the 1698T allele may give rise to a less stable mRNA, with a subsequently decreased translation efficiency and therefore slightly lower protein levels.

Speculatively, the protein arising from the 1698T allele interacts preferentially with itself and not with A-type lamins of the 1698C allele or B-type lamins, thus leading to the accumulation of the 'mutant' protein in patches along the nuclear envelope and its improper incorporation into the lamina. The extreme phenotype observed in our transfection studies, although, is most likely the result of over-expression of the exogenous lamin A and therefore an experimental artefact. Nevertheless, such an artificial exaggeration of a phenotype provides us with the first indication of what could go wrong in human cells.

Heterozygous individuals (1698C/T) possess equivalent amounts of the two putative lamin A isoforms, so presumably dimerisation and head-to-tail assembly of lamin A and its integration into the pre-existing lamina is undisturbed. In people homozygous for this polymorphism (1698T/T), the expression at normal endogenous levels still gives an inconspicuous appearance; otherwise, they would develop clinical laminopathic symptoms which is not the case in this frequent SNP. However, we assume that the lamin A isoform originating from the 1698T allele is integrated less perfectly into the nuclear lamina than its 1698C allele counterpart, thus leading to a slightly weaker nucleus (but below disease causing levels).

A reduced translation from a less stable mRNA would similarly weaken the nuclear lamina due to the slightly lower levels of synthesised A-type lamins. From this point of view, it would be interesting to determine the 1698C/T allele frequencies of the *LMNA* gene in top athletes; their muscle tissue has to withstand much greater mechanical forces and this to a more frequent extent, so we would expect to find the 1698C allele as the prevailing genotype. In patients with a true amino acid mutation, such as E358K, the additional weakening effect of the 1698C<T polymorphism may lead to a more severe clinical phenotype of EDMD, which is in fact the case [C.A. Brown, personal communication]. In our transfection studies, we observed an intermediate phenotype, ranging between the phenotypes created by the mutation and the SNP alone. Thus we propose that the grave course of EDMD in patients with both the mutation E358K and the SNP C<T1698 is due to the combination and accumulation of the molecular effects of both alterations, namely the decrease in nuclear stability and its consequences according to the structural weakness and mechanical stress hypothesis.

5.2.3 Classification of lamin A mutations

Taking into account all our results as well as those of other groups, we can now classify the *LMNA* mutations analysed in this study. As a general observation, the mutations can be divided into two groups: those mutations locating to the lamin A rod domain always exhibit features typical for structural defects, such as an irregular nuclear lamina or an increased protein mobility within, whereas mutations of the globular tail domain seem to involve gene regulatory processes. Fig. 5.1 presents an overview of the proposed functional defects of the analysed lamin A mutations.

Since the lamin rod domain mediates dimerisation and higher order filament formation, mutations in this part of the protein mainly impede integration into the filament network. Three mutations (R50S, E358K, E361K) directly affect evolutionary conserved sequences

responsible for head-to-tail assembly of lamin dimers; our results suggest that their less stable incorporation into the nuclear lamina may make the nuclei of muscle fibres more susceptible to mechanical stress and may therefore lead to dystrophic symptoms. The severe phenotype of the mutations R133P, T150P and delQ355 in transfected cells also indicate a weakened nuclear lamina. Additionally, altered protein phosphorylation may play a role during the pathogenesis of lamin A mutant T150P and an impaired interaction with gene regulation and cell cycle control factors such as Rb in the case of delQ355.

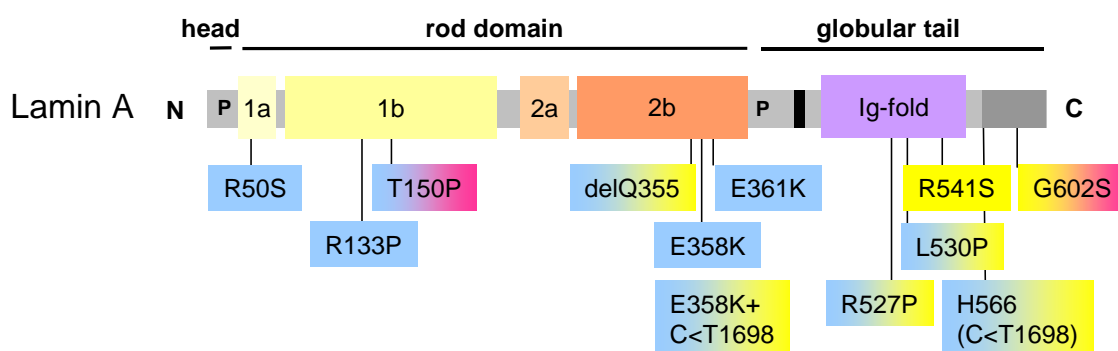


Fig. 5.1. Proposed functional defects of lamin A mutations causing Emery-Dreifuss muscular dystrophy. Based on current incomplete knowledge, defects were loosely colour-coded as blue (architectural), yellow (gene regulation) and pink (signal transduction). Note that this model is highly speculative for some functional defects, i.e. signalling in G602S. N amino-, C carboxyl-terminus.

Of the lamin A mutations within the globular tail domain, only mutants R527P and L530P show clear indications of a decreased nuclear integrity, although this might mainly be due to their inability to bind to emerin. The loss of lamin A-emerin complexes at the inner nuclear membrane may subsequently interfere with stabilisation of the nucleus via other structural proteins or interaction with gene regulatory proteins for which the complexes provide scaffolding sites. The mutations R541S and G602S do not obviously affect nuclear lamina structure; the most likely explanation for their mechanism to cause disease is an alteration in gene regulation, the exact nature of which is still unknown. The mutation G602S may additionally be involved in disrupted cell signalling pathways via PKC α . The single nucleotide polymorphism C<T1698, however, remains somewhat of a mystery. Although the mechanical stress hypothesis appears the most plausible to explain the tissue-specific defects of a combined mutation such as E358K and the polymorphism, altered gene expression may also play a role in EDMD pathophysiology.

5.3 Lamin A and lamin C are differentially dysfunctional in Emery-Dreifuss muscular dystrophy

In the present study and the accompanying paper [Motsch *et al.* 2005], we have analysed ten *LMNA* mutations associated with causing AD-EDMD and one polymorphism of the lamin A/C gene, to ascertain whether lamin A and C contribute differentially to the observed cellular phenotype. Although mutant lamin A and C are both dysfunctional in our experiments, they appear differentially effected, but depend on one another for normal function. The emerin-lamin A and emerin-lamin C containing protein complexes at the nuclear envelope may therefore each be involved in specific functions.

So far, most studies of other groups expressed mutant lamin A and C individually in tissue culture cells, regardless of the fact that in the cells of human patients, both mutated A-type lamins exist. We therefore examined the cell phenotype created by co-expression of both mutant lamin A and lamin C with the same *LMNA* mutation in COS7 cells.

Incorporation of lamin C into the nuclear lamina has been shown to require lamin A in Swiss 3T3 cells [Pugh *et al.* 1997] and P19 EC (embryonal carcinoma) cells [Horton *et al.* 1992]. Compared to recombinant GST-lamin A, recombinant GST-lamin C injected into Swiss 3T3 cells (which express both A-type lamins) integrated more slowly into the nuclear lamina and formed intranuclear foci prior to its nuclear lamina incorporation. These intranuclear foci quickly disappeared upon co-injection of recombinant lamin A [Pugh *et al.* 1997].

SW13 cells (human adrenal cortex carcinoma cells) express very low levels of endogenous lamin A and mis-localise endogenous lamin C as well as exogenously expressed GFP-lamin C to the nucleoplasm. After the introduction of exogenous GFP-lamin A, both lamin C protein pools gained their correct localisation within the nuclear lamina [Vaughan *et al.* 2001]. The inability of lamin C to target to the nuclear lamina in the absence of lamin A is also seen in the mouse model. *Lmna*^{-/-} mouse embryonic fibroblasts (MEFs) lack both A-type lamins and exogenous expression of either wild type or mutant lamin C fusion proteins led to the formation of nuclear aggregates. Co-transfection with wild type lamin A restored the ability of the lamin C constructs to associate with the nuclear envelope [Raharjo *et al.* 2001].

MEFs from mice homozygous for the L530P *Lmna* mutation exhibit nuclear abnormalities typical for *LMNA* mutations. While lamin A levels were reduced at the nuclear lamina, lamin C was completely relocated to the cytoplasm, with an overall decrease in stability for both A-type lamins [Mounkes *et al.* 2003a]. Similarly, cells derived from a patient with the *LMNA*

mutation R377H (gives rise to AD-EDMD) lacked both A-type lamins from the nucleus, with a reduced half-life of lamin A [Reichart *et al.* 2004].

Using the EGFP/DsRed2 expression system, we confirm the important role of lamin A in lamin C nuclear lamina localisation. The endogenous lamin A levels were insufficient to target exogenous wild type lamin C to the nuclear lamina of COS7 cells, but co-transfection with wild type lamin A restored the correct nuclear lamina incorporation of exogenous lamin C. Our findings also lend further credence to the notion that the targeting of lamin C to the nuclear lamina is due to its heterodimer formation with lamin A, implying a mandatory threshold level of lamin A for lamin C nuclear lamina incorporation. Accordingly, the amount of exogenous lamin C directed to the nuclear lamina was directly proportional to the amount of exogenous lamin A integrated into the lamina. In addition, the majority of lamin A mutations was able to perform this function, provided the lamin A mutants themselves achieved a nuclear lamina localisation.

All of the cited studies as well as our own results support the theory that lamin A and C are not equivalent in their nuclear lamina assembly characteristics. The specific *LMNA* mutations, but also the cell type being used, appear to affect lamin A and lamin C differentially, thus indicating that they possess distinct nuclear functions. Collectively these experiments suggest that lamin C requires additional protein-protein interactions compared to lamin A for a stable nuclear lamina incorporation.

Previous reports did not discern the effects of the same mutation in the *LMNA* gene on both the emerin-lamin A and emerin-lamin C protein interactions. We demonstrate that for three (T150P, R527P and L530P) of our ten *LMNA* mutations studied only the lamin A-emerin interaction was disrupted. *In vivo* evidence supports our findings: Co-immunoprecipitation of emerin with the A-type lamins from cells derived from an FPLD patient with the *LMNA* mutation R482L brought down only lamin C [Capanni *et al.* 2003] implicating that the lamin A-emerin interaction alone was dysfunctional. The intriguing question remains though: why is the lamin C-emerin interaction retained for this subset of *LMNA* mutations? Although the emerin binding site lies within the region common to both A-type lamins (residues 364-566)[Sakaki *et al.* 2001], specific, yet unidentified residues may play a role in the direct interaction between each A-type lamin and emerin. Their existence would create functional specificity for each interaction, and also permit the two lamins to bind simultaneously. In fact, biomolecular interaction analysis showed that emerin and lamin A interact with a molar ratio

of between 2:1 and 3:1; this finding suggests multiple emerin-binding sites on lamin A and implies that they could also exist on lamin C [Clements *et al.* 2000].

The *LMNA* mutations R527P and L530P both lie within the known emerin binding domain of A-type lamins, in the centre of the Ig-fold. Their introduction of a proline into the amino acid sequence is thought to disrupt the 3D structure of the domain sufficiently to impede protein-protein interaction [Krimm *et al.* 2002, Dhe-Paganon *et al.* 2002], which we have shown to be the case for emerin. To explain the retention of the lamin C-emerin interaction of these two mutations we propose that additional protein binding sites exist in the lamin-specific tail regions. Due to its shortness of 6 residues (VSGSRR), the lamin C-specific tail is unlikely to affect or be affected by the structure of the adjacent globular domain. However, the presence of arginines with their positive charges implies its potential as a protein binding site. Therefore we consider it very probable that lamin C R527P and L530P retain their interaction with emerin through a second, higher-affinity interaction site, which is most likely located to the specific tail region. Emerin's preference for lamin C has also been shown in competition assays which determined the specificity of the emerin-lamin complexes and the relative strengths of emerin interactions with specific lamin subtypes [Vaughan *et al.* 2001], thus supporting this theory of a second emerin-binding site.

Residue T150 lies within the interior of coil 1b of the rod domain and is therefore not directly involved in emerin binding. The coiled-coil domain of lamin A exhibits a slight bend in its wild type form [Strelkov *et al.* 2004]; this bend may be drastically increased by mutation to a proline at position 150. It is conceivable to think that, during protein translation and folding, this potential kink in the rod domain allows the formation of intramolecular interactions, i.e. salt bridges, between the 98 amino acids long lamin A-specific tail and the N-terminus of the protein. Consequently, severe mis-folding of the protein would occur, rendering both the NLS and the emerin-binding region inaccessible for other proteins and therefore functionally inactive. This model would explain why we see aggregates of this mutant lamin A in the cytoplasm and why emerin is unable to interact with this lamin A in our binding assay. The much shorter C-terminal specific tail of lamin C, on the other hand, is unlikely to reach another part of the protein, even with a bent rod; thus the mutant lamin C retains its functionality for both its transport into the nucleus and its interaction with emerin.

In conclusion our data provides evidence that lamin A and C can contribute differentially to the molecular phenotype which arises from *LMNA* mutations causing AD-EDMD. The emerin-lamin A and emerin-lamin C protein interactions are involved in different nuclear functions and therefore contribute separately to the laminopathy phenotype. A hierarchical relationship between emerin, lamin A and lamin C has been previously proposed [Vaughan *et al.* 2001, Hutchison *et al.* 2001] which is supported by our findings: in this model, lamin A is responsible for the nuclear lamina incorporation of lamin C which in turn recruits emerin to the inner nuclear membrane. If a mutant lamin A is unable to assemble within the nuclear lamina, lamin C shares the same fate and remains nucleoplasmic, causing emerin to mislocalise from the nuclear envelope [Raharjo *et al.* 2001]. In a reversed mechanism, lamin C remains nucleoplasmic in emerin-deficient fibroblasts derived from X-EDMD patients, as its interaction with lamin A alone is not sufficient for stable nuclear lamina integration [Markiewicz *et al.* 2002].

These studies and our experimental data emphasize the importance of the lamin C-emerin interaction in maintaining nuclear envelope integrity. Mutations in the *LMNA* gene affect both A-type lamins differently, since lamin A is the dominant partner concerning the targeting and incorporation of the heterodimer into the nuclear lamina, whereas lamin C is the preferred A-type interaction partner for emerin. Further research may elucidate the functional differences between the emerin-lamin A and the emerin-lamin C interactions in different tissues of laminopathy patients. This would shed light on the strange case of the lamin A/C gene, mutations of which can cause such a diversity of clinical phenotypes.

6 Summary

Emery-Dreifuss muscular dystrophy (EDMD) is a rare genetic disorder characterised by early contractures of the elbows, Achilles tendons and spine, slowly progressive muscle wasting and cardiomyopathy associated with cardiac conduction defect. The autosomal dominant form is caused by mutations in the *LMNA* gene which gives rise to lamin A and lamin C proteins by alternative splicing. These A-type lamins, together with B-type lamins, form the nuclear lamina, a network of intermediate filament proteins underlining the nuclear envelope.

In order to ascertain the role lamin A and C separately contribute to the molecular phenotype, we analysed ten *LMNA* mutations and one single nucleotide polymorphism (SNP) in transfection studies in COS7 fibroblasts and, partially, in C2C12 myoblasts. The EGFP or DsRed2 tagged lamins were exogenously expressed either individually or both A-types together and examined by light and electron microscopy. The protein mobility of lamin A mutants was determined by FRAP analysis. Additionally, a co-immunoprecipitation binding assay of *in vitro* synthesised A-type lamins and emerin was performed. Eight of the *LMNA* mutations (R50S, R133P, E358K, E358K+C<T1698, E361K, R527P, L530P, R541S and G602S) and the SNP C<T1698, when expressed in lamin A, exhibited a range of nuclear mis-localisation patterns from a wild type phenotype to the formation of nuclear aggregates. Two mutations (T150P and delQ355) led to the severe mis-localisation of the exogenous protein and additionally affected nuclear envelope reassembly and mid-body protein composition after mitosis. Exogenously expressed DsRed2 tagged wild type and mutant lamin C was only inserted into the nuclear lamina if co-expressed with the equivalent EGFP tagged lamin A construct, except for the T150P mutation which prevented either lamin from reaching the nuclear lamina. The T150P, R527P and L530P mutations reduced the ability of lamin A, but not lamin C from binding to emerin.

These data indicate that mutations in the rod domain of lamin A mainly impair its function as a structural protein, whereas mutations of the globular tail domain appear to disrupt protein-protein interactions important for gene regulation and signal transduction processes. In addition, our results suggest specific functional roles for the emerin-lamin A and emerin-lamin C containing protein complexes; this is the first report to propose that the A-type lamin mutations may be differentially dysfunctional for the same *LMNA* mutation.

7 Zusammenfassung

Die Emery-Dreifuss Muskeldystrophie, eine seltene genetische Erkrankung, ist gekennzeichnet durch frühzeitige Sehnenverkürzung im Ellenbogen, an der Achillessehne und am Rückgrat, einen langsam fortschreitenden Muskelschwund sowie einer Kardiomyopathie mit Herzreizleitungsstörungen. Die autosomal-dominante Form wird von Mutationen im *LMNA*-Gen verursacht, welches durch alternatives Spleißen die Laminproteine A und C hervorbringt. Diese sogenannten A-Typ Lamine bilden zusammen mit den B-Typ Laminen die Kernlamina, ein Netzwerk aus Intermediärfilamentproteinen, welches innen an der Kernhülle anliegt.

Um festzustellen, inwiefern Lamin A und Lamin C jeweils einzeln zum molekularen Phänotyp beitragen, wurden zehn *LMNA*-Mutationen und ein Einzelnukleotid-Polymorphismus (SNP) in Transfektionsstudien mit COS7-Fibroblasten, und teilweise auch C2C12-Myoblasten, analysiert. Die EGFP- oder DsRed2-markierten Lamine wurden entweder einzeln oder beide A-Typ Lamine zusammen exogen exprimiert und sowohl licht- als auch elektronenmikroskopisch untersucht. Die Beweglichkeit von Lamin A-Mutanten in der Kernlamina wurde durch FRAP-Analyse ermittelt und zusätzlich Ko-Immünpräzipitationsbindungsstudien mit *in vitro* hergestellten A-Typ Laminproteinen und Emerin durchgeführt.

Exprimiert in Lamin A wiesen acht Mutationen (R50S, R133P, E358K, E358K+ C<T1698, E361K, R527P, L530P, R541S und G602S) sowie der SNP C<T1698 eine große Bandbreite an Fehlverteilungsmustern im Kern auf, welche von der wildtypischen Verteilung bis zur Bildung von Proteinaggregaten im Kern reichte. Zwei Mutationen (T150P und delQ355) führten zu extremer Mislokalisierung des exogenen Proteins und beeinflussten außerdem den Wiederaufbau der Kernhülle nach der Mitose sowie die Proteinzusammensetzung des Mid-bodies. Sowohl der Wildtyp als auch alle Mutanten von DsRed2-markiertem Lamin C wurde nur in die Kernlamina eingebaut, wenn gleichzeitig auch dessen Lamin A-Gegenstück (EGFP-markiert) exogen exprimiert wurde. Als Ausnahme verhinderte die Mutation T150P den Einbau beider A-Typ Lamine in die Lamina. Die *LMNA*-Mutationen T150P, R527P und L530P verringerten die Bindung von Emerin an Lamin A, aber nicht die an Lamin C.

Diese Daten deuten darauf hin, dass Mutationen in der stäbchenförmigen Domäne von Lamin A hauptsächlich dessen Funktion als Strukturprotein beeinträchtigen, wohingegen Mutationen in der globulären Schwanzdomäne Protein-Protein-Interaktionen zu behindern scheinen, die bei der Genregulation und Signaltransduktion von Bedeutung sind. Zusätzlich schlagen diese Ergebnisse spezifische funktionelle Rollen für die Emerin-Lamin A und Emerin-Lamin C-Proteinkomplexe vor, was darauf schließen lässt, dass die beiden A-Typ Lamine durch dieselbe *LMNA*-Mutation unterschiedlich in ihrer Funktion gestört werden.

8 Abbreviations

A	Ampere
AD	autosomal dominant
APS	ammonium persulphate
Bis	N, N'- methylene bisacrylamide
bp	base pairs
BSA	bovine serum albumin
CLSM	confocal laser scanning microscope
dH ₂ O	de-ionised water
DMSO	di-methyl sulfoxide
DNA	desoxyribonucleic acid
ECL	enhanced chemical luminescence
EDTA	ethylene di-amine tetra-acetic acid
EtOH	ethanol
FCS	fetal calf serum
Fig.	figure
FRAP	fluorescence recovery after photobleaching
x g	times g forces
GAA	glacial acetic acid
h	hour
Ig	immunoglobulin
kDa	kiloDalton
l	liter
M	Mol
m	meter or milli (10 ⁻³)
M _r	relative molecular mass
M _w	molecular weight [g / Mol]
mab	monoclonal antibody
MetOH	methanol
min	minute
μ	mikro (10 ⁻⁶)
n	nano (10 ⁻⁹)
NLS	nuclear localisation signal

OD	optical density
ov	overnight
p	pico (10^{-12})
PAGE	polyacrylamide gel electrophoresis
PEG	polyethylene glycol
PFA	paraformaldehyde
PBS	phosphate buffered saline
PMSF	phenylmethylsulfonylfluoride
RNA	ribonucleic acid
RNase	ribonuclease
rpm	rounds per minute
RT	room temperature
SDS	sodium dodecyl sulphate
SNP	single nucleotide polymorphism
Tab.	table
TBST	Tris buffered saline with Tween-20
TEM	transmission electron microscope
TEMED	N, N, N', N' – tetramethylethylenediamine
Tris	Tris-(hydroxymethyl)-aminomethane
Tween-20	polyoxyethylene-sorbitan monolaurate
U	unit
V	Volt
w/v	weight per volume
w/w	weight per weight

9 References

- Aebi, U., Cohn, J., Buhle, L. and Gerace, L.** (1986). The nuclear lamina is a meshwork of intermediate-type filaments. *Nature* **323**, 560-564
- Agarwal, A.K., Fryns, J.P., Auchus, R.J. and Garg, A.** (2003). Zinc metalloproteinase, ZMPSTE24, is mutated in mandibuloacral dysplasia. *Hum. Mol. Genet.* **12**, 1995-2001
- Alsheimer, M., von Glasenapp, E., Schnolzer, M., Heid, H. and Benavente, R.** (2000). Meiotic lamin C2: The unique amino-terminal hexapeptide GNAEGR is essential for nuclear envelope association. *Proc. Natl. Acad. Sci. USA* **97**, 13120-13125
- Apel, E.D., Lewis, R.M., Grady, R.M. and Sanesi, J.R.** (2000). Syne-1, a dystrophin-and Klarsicht-related protein associated with synaptic nuclei at the neuromuscular junction. *J. Biol. Chem.* **275**, 31986-31995
- Barbie, D. A., Kudlow, B. A., Frock, R., Zhao, J., Johnson, B. R., Dyson, N., Harlow, E and Kennedy, B. K.** (2004). Nuclear reorganisation of mammalian DNA synthesis prior to cell cycle exit. *Mol. Cell Biol.* **24**, 595-607
- Barton, R.M. and Worman, H.J.** (1999). Prenylated prelamin A interacts with Narf, a novel nuclear protein. *J. Biol. Chem.* **274**, 30008-30018
- Bechert, K., Lagos-Quintana, M., Harborth, J., Weber, K. and Osborn, M.** (2003). Effects of expressing lamin A mutant protein causing Emery-Dreifuss muscular dystrophy and familial partial lipodystrophy in HeLa cells. *Exp. Cell. Res.* **286**, 75-86
- Bengtsson, L. and Wilson, K.L.** (2004). Multiple and surprising functions for emerin, a nuclear membrane protein. *Curr. Opin. Cell Biol.* **16**, 73-79
- Berger, R., Theodor, L., Shoham, J., Gokkel, E., Brok-Simoni, F., Avraham, K.B., Copeland, M.G., Jenkins, N.A., Rechavi, G. and Simon, A.J.** (1996). The characterization and localization of the mouse thymopoietin/lamina-associated polypeptide 2 gene and its alternatively spliced products. *Genome Res.* **6**, 361-370
- Bione, S., Maestrini, E., Rivella, S., Mancini, M., Regis, S., Romeo, G. and Toniolo, D.** (1994). Identification of a novel X-linked gene responsible for Emery-Dreifuss muscular dystrophy. *Nature Genet.* **8**, 323-327
- Birnboim, H.C. and Doly, J.** (1979). A rapid alkaline extraction procedure for screening recombinant plasmid DNA. *Nucl. Acids Res.* **7**, 1513-1522
- Bonne, G., di Barletta, M.R., Varnous, S., Bécane, H.M., Hammouda, E.H., Merlini, L., Muntoni, F., Greenberg, C.R., Gary, F., Urtizberea, J.A., Duboc, D., Fardeau, M., Toniolo, D. and Schwartz, K.** (1999). Mutations in the gene encoding lamin A/C cause autosomal dominant Emery-Dreifuss muscular dystrophy. *Nature Genetics* **21**, 285-288
- Bonne, G., Mercure, E., Muchir, A., Urtizberea, A., Bécane, H.M., Recan, D., Merlini, L., Wehnert, M., Boor, R., Reuner, U., Vorgerd, M., Wicklein, E.M., Eymard, B.,**

- Duboc, D., Penisson-Besnier, I., Cuisset, J.M., Ferrer, X., Desguerre, I., Lacombe, D., Bushby, K., Pollitt, C., Toniolo, D., Fardeau, M., Schwartz, K. and Muntoni, F. (2000). Clinical and molecular spectrum of autosomal dominant Emery-Dreifuss muscular dystrophy due to mutations of the lamin A/C gene. *Ann. Neurol.* **48**, 170-180
- Bonne, G., Muchir, A., Helbling-Leclerc, A., Massart, C. and Schwartz, K. (2002). Clinical and genetical heterogeneity of laminopathies. *Acta Myologica* **20**, 138-144
- Bossie, C.A. and Sanders, M.M. (1993). A cDNA from *Drosophila melanogaster* encodes a lamin C-like intermediate filament protein. *J. Cell Sci.* **104**, 1263-1272
- Broers, J.L.V., Hutchison, C.J. and Ramaekers, F.C.S. (2004). Laminopathies. *J. Pathol.* **204**, 478-488
- Broers, J.L.V., Machiels, B.M., van Eys, G.J.J.M., Kujipers, H.J.H., Manders, E.M.M., van Driel, R. and Ramaekers, F.C.S. (1999). Dynamics of the nuclear lamina as monitored by GFP-tagged A-type lamins. *J. Cell Sci.* **112**, 3463-3475
- Broers, J.V.L., Peeters, E.A.G., Kujipers, H.J.H., Endert, J., Bouten, C.V., Oomens, C.W., Baaijens, F.P. and Ramaekers, F.C. (2004a). Decreased mechanical stiffness in LMNA^{-/-} cells is caused by defective nucleo-cytoskeletal integrity. Implications for the development of laminopathies. *Hum. Mol. Genet.* **13**, 2567-2580
- Brown, C.A., Lanning, R.W., McKinney, K.Q., Salvino, A.R., Cherniske, E., Crowe, C.A., Darras, B.T., Gominak, S., Greenberg, C.R., Grossmann, C., Heydemann, P., Mendell, J.R., Pober, B.R., Sasaki, T., Shapiro, F., Simpson, D.A., Suchowersky, O. and Spence, J.E. (2001). Novel and recurrent mutations in lamin A/C in patients with Emery-Dreifuss muscular dystrophy. *Am. J. Med. Genet.* **102**, 359-367
- Cai, M., Huang, Y., Zheng, R., Wei, S.Q., Ghirlando, R., Lee, M.S., Craigie, R., Gronenborn, A.M. and Clore, G.M. (1998). Solution structure of the cellular factor BAF responsible for protecting retroviral DNA from autointegration. *Nat. Struct. Biol.* **5**, 903-909
- Cao, H. and Hegele, R.A. (2000). Nuclear lamin A/C R428Q mutation in Canadian kindreds with Dunnigan-type familial partial lipodystrophy. *Hum. Mol. Genet.* **9**, 109-112
- Cao, H. and Hegele, R.A. (2003). LMNA is mutated in Hutchinson-Gilford progeria but not in Wiedemann-Rautenstrauch progeroid syndrome. *J. Hum. Genet.* **48**, 271-274
- Capanni, C., Cenni, V., Mattioli, E., Sabatelli, P., Ognibene, A., Columbaro, M., Parnail, V. K., Wehnert, M., Maraldi, N. M. *et al.* (2003). Failure of lamin A/C to functionally assemble in R482L mutated FPLD fibroblasts: altered intermolecular interaction with emerin and implications for gene transcription. *Exp. Cell. Res.* **291**, 122-134
- Capanni, C., Mattioli, E., Columbaro, M., Lucarelli, E., Parnaik, V.K., Novelli, G., Wehnert, M., Cenni, V., Maraldi, N.M., Squarzoni, S. and Lattanzi, G. (2005). Altered pre-lamin A processing is a common mechanism leading to lipodystrophy. *Hum. Mol. Genet.* **14**, 1489-1502

- Cartegni, L., di Barletta, R.M., Barresi, R., Squarzone, S., Sabatelli, P., Maraldi, N.M., Mora, M., Di Blasi, C., Cornelio, F., Merlini, L., Villa, A., Cobiachi, F. and Toniolo, D.** (1997). Heart specific localization of emerin : new insights into Emery-Dreifuss muscular dystrophy. *Hum. Mol. Genet.* **6**, 2257-2264
- Caux, F., Dubosclard, E., Lascols O., Buendia, B., Chazouilleres, O., Cohen, A., Courvalin, J.C., Laroche, L., Capeau, J., Vigouroux, C. and Christin-Maitre, S.** (2003). A new clinical condition linked to a novel mutation in lamins A and C with generalized lipodystrophy, insulin-resistant diabetes, disseminated leukomelanodermic papules, liver steatosis, and cardiomyopathy. *J. Clin. Endocrinol. Metab.* **88**, 1006-1013
- Cenni, V., Sabatelli, P., Mattioli, E., Marmioli, S., Capanni, C., Ognibene, A., Squarzone, S., Maraldi, N.M., Bonne, G., Columbaro, M., Merlini, L. and Lattanzi, G.** (2005). Lamin A N-terminal phosphorylation is associated with myoblast activation: impairment in Emery-Dreifuss muscular dystrophy. *J. Med. Genet.* **42**, 214-220
- Cestan, R. and Lejonne, P.** (1902). Une myopathie avec rétractions familiales. *Nouvelle Iconographie de la Salpêtrière* **15**, 38-52
- Chau, B.N. and Wang, J.Y.J.** (2003). Coordinated regulation of life and death by Rb. *Nat. Rev. Cancer* **3**, 130-138
- Chen, L., Lee, L., Kudlow, B.A., Dos Santos, H.G., Sletvold, O., Shafeghati, Y., Botha, E.G., Garg, A., Hanson, N.B., Martin, G.M., Mian, I.S., Kennedy, B.K. and Oshima, J.** (2003). LMNA mutations in atypical Werner's syndrome. *Lancet* **362**, 440-445
- Chung, C.T., Niemela, S.L. and Miller, R.H.** (1989). One-step preparation of competent *E. coli*: Transformation and storage of bacterial cells in the same solution. *Proc. Natl. Acad. Sci. USA* **86**, 2172-2175
- Clements, L., Manilal, S., Love, D.R., and Morris, G.E.** (2000). Direct interaction between emerin and lamin A. *Biochem. Biophys. Res. Commun.* **267**, 709-714
- Cohen, M., Lee, K.K., Wilson, K.L. and Gruenbaum, Y.** (2001). Transcriptional repression, apoptosis, human disease and the functional evolution of the nuclear lamina. *Trends Biochem. Sci.* **26**, 41-47
- Collas, P. and Courvalin, J.-C.** (2000). Sorting nuclear membrane proteins at mitosis. *Trends in Cell Biology* **10**, 5-8
- Columbaro, M., Mattioli, E., Lattanzi, G., Rutigliano, C., Ognibene, A., Maraldi, N.M. and Squarzone, S.** (2001). Staurosporine treatment and serum starvation promote the cleavage of emerin in cultured mouse myoblasts : involvement of a caspase-dependent mechanism. *FEBS Lett.* **509**, 423-429
- Cuconati, A. and White, E.** (2002). Viral homologs of BCL-2: role of apoptosis in the regulation of virus infection. *Genes Dev.* **16**, 2465-2478

- Dabauvalle, M.-C. and Franke, W.** (1982). Karyophilic proteins: polypeptides synthesised *in vitro* accumulate in the nucleus on microinjection into the cytoplasm of amphibian oocytes. *Proc. Natl. Acad. Sci. USA*. **79**, 5302-5306
- Dabauvalle, M.-C., Müller, E., Ewald, A., Kress, W., Krohne, G. and Müller, C.R.** (1999). Distribution of emerin during the cell cycle. *Eur. J. Cell Biol.* **78**, 749-756
- Dechat, T., Gotzmann, J., Stockinger, A., Harris, C.A., Talle, M.A., Siekierka, J.J. and Foisner, R.** (1998). Detergent-salt resistance of LAP2 α in interphase nuclei and phosphorylation-dependent association with chromosomes early in nuclear assembly implies functions in nuclear structure dynamics. *EMBO J.* **17**, 4887-4902
- Dechat, T., Korbei, B., Vaughan, O.A., Vlcek, S., Hutchison, C.J. and Foisner, R.** (2000). Lamina-associated polypeptide 2 α binds intranuclear A-type lamins. *J. Cell Sci.* **113**, 3473-3484
- De la Luna, S., Allen, K.E., Mason, S.L. and La Thangue, N.B.** (1999). Integration of a growth-suppressing BTB/POZ domain protein with the DP component of the E2F-transcription factor. *EMBO J.* **18**, 212-228
- De Sandre-Giovannoli, A., Bernard, R., Cau, P., Navarro, C., Amiel, J., Boccaccio, I., Lyonnet, S., Stewart, C.L. Munnich, A., Le Merrer, M. and Levy, N.** (2003). Lamin A truncation in Hutchison-Gilford progeria. *Science* **300**, 2055
- De Sandre-Giovannoli, A., Chaouch, M., Kozlov, S., Vallat, J.M., Tazir, M., Kassouri, N., Szepietowski, P., Hammadouche, T., Vandenberghe, A., Stewart, C.L., Grid, D. and Levy, N.** (2002). Homozygous defects in LMNA, encoding lamin A/C nuclear-envelope proteins, cause autosomal recessive axonal neuropathy in human (Charcot-Marie-Tooth disorder type 2) and mouse. *Am. J. Hum. Genet.* **70**, 726-736
- Dhe-Paganon, S., Werner, E.D., Chi, Y-I. and Shoelson, S.E.** (2002). Structure of the globular tail of nuclear lamin. *J. Biol. Chem.* **277**, 17381-17384
- Di Barletta, R.M., Ricci, E., Galuzzi, G., Tonali, P., Mora, M., Morandi, L., Romorini, A., Voit, T., Orstavik, K.H., Merlini, L., Trevisan, C., Biancalana, V., Hausmanova-Petrusewicz, I., Bione, S., Ricotti, R., Schwartz, K., Bonne, G. and Toniolo, D.** (2000). Different mutations in the LMNA gene cause autosomal dominant and autosomal recessive Emery-Dreifuss muscular dystrophy. *Am. J. Hum. Genet.* **66**, 1407-1412
- Dreger, M., Bengtsson, L., Schoneberg, T., Otto, H. and Hucho, F.** (2001). Nuclear envelope proteomics: Novel integral membrane proteins of the inner nuclear membrane. *Proc. Natl. Acad. Sci. USA* **98**, 11943-11948
- Dreuillet, C., Tillit, J., Kress, M. and Ernoult-Lange, M.** (2002). *In vivo* and *in vitro* interaction between human transcription factor MOK2 and nuclear lamin A/C. *Nucleic Acid Res.* **30**, 4634-4642
- Duband-Goulet, I. and Courvalin, J.C.** (2000). Inner nuclear membrane protein LBR preferentially interacts with DNA secondary structures and nucleosomal linker. *Biochemistry* **39**, 6483-6488

- Earnshaw, W.C.** (1995). Nuclear changes in apoptosis. *Curr. Opin. Cell Biol.* **7**, 337-343
- Eggert, M., Radomsky, N., Linder, D., Tripier, D., Traub, P. and Jost, E.** (1993). Identifikation of novel phosphorylation sites in murine A-type lamins. *Eur. J. Biochem.* **213**, 659-671
- Ellis, J.A., Craxton, M., Yates, J.R.W. and Kendrick-Jones, J.** (1998). Aberrant intracellular targeting and cell cycle-dependent phosphorylation of emerin contribute to the Emery-Dreifuss muscular dystrophy phenotype. *J. Cell Sci.* **111**, 781-792
- Emery, A.E.H.** (1989). Emery-Dreifuss syndrome. *J. Med. Genet.* **26**, 637-641
- Emery, A.E.H.** (2000). Emery-Dreifuss muscular dystrophy – a 40 year retrospective – Review article. *Neuromusc. Disord.* **10**, 228-232
- Emery, A.E.H. and Dreifuss, F.E.** (1966). Unusual type of benign X-linked muscular dystrophy. *J. Neurol. Neurosurg. Psychiatry* **29**, 338-342
- Eriksson, M., Brown, W.T., Gordon, L.B., Glynn, M.W., Singer, J., Scott, L., Erdos, M.R., Robbins, C.M., Moses, T.Y., Berglund, P., Dutra, A., Pak, E., Durkin, S., Csoka, A.B., Boehnke, M., Glover, T.W. and Collins, F.S.** (2003). Recurrent de novo point mutations in lamin A cause Hutchinson-Gilford progeria syndrome. *Nature* **423**, 293-298
- Fairley, E.A.L., Kendrick-Jones, J. and Ellis, J.A.** (1999). The Emery-Dreifuss muscular dystrophy phenotype arises from aberrant targeting and binding of emerin at the inner nuclear membrane. *J. Cell Sci.* **112**, 2571-2582
- Fairley, E.A.L., Riddell, A., Ellis, J.A. and Kendrick-Jones, J.** (2002). The cell cycle dependent mislocalisation of emerin may contribute to the Emery-Dreifuss muscular dystrophy phenotype. *J. Cell Sci.* **115**, 341-354
- Fatkin, D., MacRae, C., Sasaki, T., Wolff, M.R., Porcu, M., Frenneaux, M., Atherton, J., Vidaillet Jr., H.J., Spudich, S., De Girolami, U., Seidman, J.G. and Seidman, C.E.** (1999). Missense mutations in the rod domain of the lamin A/C gene as causes of dilated cardiomyopathy and conduction-system disease. *N. Engl. J. Med.* **341**, 1715-1724
- Favreau, C., Higuete, D., Courvalin, J.C., Buendia, B.** (2004). Expression of a mutant lamin A that causes Emery-Dreifuss muscular dystrophy inhibits *in vitro* differentiation of C2C12 myoblasts. *Mol. Cell. Biol.* **24**, 1481-1492
- Felice, K.J., Schwartz, R.C., Brown, C.A., Leier, C.R. and Grunnet, M.L.** (2000). Autosomal dominant Emery-Dreifuss dystrophy due to mutations in rod domain of the lamin A/C gene. *Neurology* **55**, 275-280
- Fidziańska, A. and Hausmanowa-Petrusewicz, I.** (2003). Architectural abnormalities in muscle nuclei. Ultrastructural differences between X-linked and autosomal dominant forms of EDMD. *J. Neurol. Sci.* **210**, 47-51

- Fidziańska, A., Toniolo, D. and Hausmanowa-Petrusewicz, I.** (1998). Ultrastructural abnormality of sarcolemmal nuclei in Emery-Dreifuss muscular dystrophy. *J. Neurol. Sci.* **159**, 88-93
- Fisher, D.Z., Chaudhary, N. and Blobel, G.** (1986). cDNA sequencing of nuclear lamins A and C reveals primary and secondary structure homology to intermediate filament proteins. *Proc. Natl. Acad. Sci. USA* **83**, 6450-6454
- Foisner, R.** (2003). Cell cycle dynamics of the nuclear envelope. *Scientific World J.* **3**, 1-20
- Foisner, R. and Gerace, L.** (1993). Integral membrane proteins of the nuclear envelope interact with lamins and chromosomes, and binding is modulated by mitotic phosphorylation. *Cell* **73**, 1267-1279
- Fridkin, A., Mills, E., Margalit, A., Neufeld, E., Lee, K.K., Feinstein, N., Cohen, M., Wilson, K.L. and Gruenbaum, Y.** (2004). Matefin, a *C.elegans* germ-line specific SUN-domain nuclear membrane protein, is essential for early embryonic and germ cell development. *Proc. Natl. Acad. Sci. USA* **101**, 6987-6992
- Furukawa, K.** (1999). LAP2 binding protein 1 (L2BP1/BAF) is a candidate mediator of LAP2-chromatin interaction. *J. Cell Sci.* **112**, 2485-2492
- Furukawa, K. and Hotta, Y.** (1993). cDNA cloning of a germ cell specific lamin B3 from mouse spermatocytes and analysis of its function by ectopic expression in somatic cells. *EMBO J.* **12**, 97-106
- Furukawa, K., Inagaki, H. and Hotta, Y.** (1994). Identification and cloning of an mRNA coding for a germ cell-specific A-type lamin in mice. *Exp. Cell Res.* **212**, 426-430
- Furukawa, K., Sugiyama, S., Osouda, S., Goto, H., Inagaki, M., Horigome, T., Omata, S., McConnell, M., Fisher, P.A. and Nishida, Y.** (2003). Barrier-to-autointegration factor plays crucial roles in cell cycle progression and nuclear organization in *Drosophila*. *J. Cell Sci.* **116**, 3811-3823
- Gareiss, M., Eberhardt, K., Krüger, E., Kandert, S., Bohm, C., Zentgraf, H., Müller, C.R. and Dabauvalle, M.C.** (2005). Emerin expression in early development of *Xenopus laevis*. *Eur. J. Cell Biol.* **84**, 295-309
- Georgatos, S.D., Meier, J. and Simos, G.** (1994). Lamins and lamin-associated proteins. *Cur. Opin. Cell Biol.* **6**, 347-353
- Georgatos, S.D., Stournaras, C. and Blobel, G.** (1988). Heterotypic and homotypic associations between the nuclear lamins: site-specificity and control by phosphorylation. *Proc. Natl. Acad. Sci. USA* **85**, 4325-4329
- Gerace, L., Blum, A. and Blobel, G.** (1978). Immunocytochemical localization of the major polypeptides of the nuclear pore complex-lamina fraction. *J. Cell Biol.* **79**, 546-566
- Gerace, L. und Burke, B.** (1988). Functional organization of the nuclear envelope. *Annu. Rev. Cell Biol.* **4**, 335-374

- Gilchrist, S., Gilbert, N., Perry, P., Östlund, C., Worman, H.J. and Bickmore, W.A.** (2004). Altered protein dynamics of disease-associated lamin A mutants. *BMC Cell Biol.* **5**, 46
- Görlich, D. and Mattaj, I.W.** (1996). Nucleocytoplasmic transport. *Science* **271**, 1513-1518
- Goldman, R.D., Gruenbaum, Y., Moir, R.D., Shumaker, D.K. and Spann, T.P.** (2002). Nuclear lamins: building blocks of nuclear architecture. *Genes Dev.* **16**, 533-547
- Gotzmann, J., Vlcek, S. and Foisner, R.** (2000). Caspase-mediated cleavage of the chromosome-binding domain of lamina-associated polypeptide 2 α . *J. Cell Sci.* **113**, 3769-3780
- Gough, L.L., Fan, J., Chu, S., Winnick, S. and Beck, K.A.** (2003). Golgi localization of syne-1. *Mol. Biol. Cell* **14**, 2410-2424
- Gruenbaum, Y., Goldman, R.D., Meyuhas, R., Mills, E., Margalit, A., Fridkin, A., Dayani, Y., Prokocimer, M. and Enosh, A.** (2003). The nuclear lamina and its functions in the nucleus. *Int. Rev. Cytol.* **226**, 1-62
- Gruenbaum, Y., Landesman, Y., Drees, B., Bare, J.W., Saumweber, H., Paddy, M.R., Sedat, J.W., Smith, D.E., Benton, B.M. and Fisher, P.A.** (1988). *Drosophila* nuclear lamin precursor Dm₀ is translated from either of two developmentally regulated mRNA species apparently encoded by a single gene. *J. Cell Biol.* **106**, 585-596
- Gruenbaum, Y., Lee, K.K., Liu, J., Cohen, M. and Wilson, K.L.** (2002). The expression, lamin-dependent localization and RNAi depletion phenotype for emerin in *C.elegans*. *J. Cell Sci.* **115**, 923-929
- Gruenbaum, Y., Margalit, A., Goldman, R.D., Shumaker, D.K. and Wilson, K.L.** (2005). The nuclear lamina comes of age. *Nat. Rev. Mol. Cell Biol.* **6**, 21-31
- Guillemin, K., Williams, T. and Krasnow, M.A.** (2001). A nuclear lamin is required for cytoplasmic organization and egg polarity in *Drosophila*. *Nature Cell Biol.* **3**, 848-851
- Haas, M. and Jost, E.** (1993). Functional analysis of phosphorylation sites in human lamin A controlling lamin disassembly, nuclear transport and assembly. *Eur. J. Cell Biol.* **62**, 237-247
- Halaby, D.M., Poupon, A. and Mornon, J.** (1999). The immunoglobulin fold family: sequence analysis and 3D structure comparisons. *Protein Eng.* **12**, 563-571
- Hansen, J.B., Jorgensen, C., Petersen, R.K., Hallenborg, P., De Matteis, R., Boye, H.A., Petrovic, N., Enerback, C.V., Nedergaard, J., Cinti, S., te Riele, H. and Kristiansen, K.** (2004). Retinoblastoma protein functions as a molecular switch determining white versus brown adipocyte differentiation. *Proc. Natl. Acad. Sci. USA* **101**, 4112-4117
- Haraguchi, T., Holaska, J.M., Yamane, M., Koujin, T., Hashiguchi, N., Mori, C., Wilson, K.L. and Hiraoka, Y.** (2004). Emerin binding to Btf, a death-promoting transcriptional repressor, is disrupted by a missense mutation that causes Emery-Dreifuss muscular dystrophy. *Eur. J. Biochem.* **271**, 1035-1045

- Haraguchi, T., Koujin, T., Hayakawa, T., Kaneda, T., Tsutsumi, Ch., Omamoto, N., Akazawa, Ch., Sukegawa, J., Yoneda, Y. and Hiraoka, Y.** (2000). Live fluorescence imaging reveals early recruitment of emerin, LBR, RanBP2, and Nup153 to reforming functional nuclear envelopes. *J. Cell Sci.* **113**, 779-794
- Haraguchi, T., Koujin, T., Segura-Totten, M., Lee, K.K., Matsuoka, Y., Yoneda, Y., Wilson, K.L. and Hiraoka, Y.** (2001). BAF is required for emerin assembly into the reforming nuclear envelope. *J. Cell Sci.* **114**, 4575-4585
- Harborth, J., Elbashir, S.M., Bechert, K., Tuschl, T. and Weber, K.** (2001). Identification of essential genes in cultured mammalian cells using small interfering RNAs. *J. Cell Sci.* **114**, 4557-4565
- Harris, C.A., Andryuk, P.J., Cline, S.C., Natarajan, A., Siekierka, J.J. and Goldstein, G.** (1994). Three distinct human thymopoietins are derived from alternatively spliced mRNAs. *Proc. Natl. Acad. Sci. USA* **91**, 6283-6287
- Hauptmann, A. and Tannhäuser, S.J.** (1941). Muscular shortening and dystrophy – a heredofamilial disease. *Arch. Neurol. Psychiatr* **46**, 654-664
- Heald, R. and McKeon, F.** (1990). Mutations of phosphorylation sites in lamin A that prevent nuclear lamina disassembly in mitosis. *Cell* **61**, 579-589
- Hedgecock, E.M. and Thomson, J.N.** (1982). A gene required for nuclear and mitochondrial attachment in the nematode *Caenorhabditis elegans*. *Cell* **30**, 321-330
- Hegele, R.A., Cao, H., Harris, S.B., Zinman, B., Hanley, A.J. and Anderson, C.M.** (2000). Genetic variation in *LMNA* modulates plasma leptin and indices of obesity in aboriginal Canadians. *Physiol Genomics.* **3**, 39-44
- Hegele, R.A., Huff, M.W. and Young, K.T.** (2001). Common genomic variation of *LMNA* modulates indexes of obesity in Inuit. *J. Clin. Endocrinol. Metab.* **86**, 2747-2751
- Heitlinger, E., Peter, M., Häner, M., Lustig, A., Aebi, U. and Nigg, E.A.** (1991). Expression of chicken lamin B2 in *Escherichia coli*: Characterization of its structure, assembly and molecular interactions. *J. Cell Biol.* **113**, 485-495
- Hellemans, J., Preobrazhenska, O., Willaert, A., Debeer, P., Verdonk, P.C., Costa, T., Janssens, K., Menten, B., Van Roy, N., Vermeulen, S. J., Savarirayan, R., Van Hul, W., Vanhoenacker, F., Huylebroeck, D., De Paepe, A., Naeyaert, J. M., Vandesompele, J., Speleman, F., Verschueren, K., Coucke, P. J. and Mortier, G. R.** (2004). Loss-of-function mutations in *LEMD3* result in osteopoikilosis, Buschke-Ollendorff syndrome and melorheostosis. *Nat. Genet.* **36**, 1213-1218
- Hennekes, H. and Nigg, E.** (1994). The role of isoprenylation in membrane attachment of nuclear lamins. *J. Cell Sci.* **107**, 1019-1029
- Herrmann, H. and Aebi, U.** (2004). Intermediate filaments: Molecular structure, assembly mechanism, and integration into functionally distinct intracellular scaffolds. *Annu. Rev. Biochem.* **73**, 749-789

- Higuchi, Y., Hongou, M., Ozawa, K., Kokawa, H. and Masaki, M.** (2005). A family of Emery-Dreifuss muscular dystrophy with extreme difference in severity. *Pediatr. Neurol.* **32**, 358-360
- Höger, T.H., Grund, Ch., Franke, W.W. and Krohne, G.** (1991). Immunolocalization of lamins in the thick nuclear lamina of human synovial cells. *Eur. J. Cell Biol.* **54**, 150-156
- Höger, T.H., Krohne, G. and Franke, W.W.** (1988). Amino acid sequence and molecular characterization of murine lamin B as deduced from cDNA clones. *Eur. J. Cell Biol.* **47**, 283-290
- Höger, T.H., Zatloukal, K., Waizenegger, I. and Krohne, G.** (1990). Characterization of a second highly conserved B-type lamin present in cells previously thought to contain only a single B-type lamin. *Chromosoma* **99**, 379-390
- Hoffmann, K., Dreger, C.K., Olins, A.L., Olins, D.E., Shultz, L.D., Lucke, B., Karl, H., Kaps, R., Muller, D., Vaya, A., Aznar, J., Ware, R.E., Sotelo Cruz, N., Lindner, T.H., Herrmann, H., Reis, A. and Sperling, K.** (2002). Mutations in the gene encoding the lamin B receptor produce an altered nuclear morphology in granulocytes (Pelger-Huët anomaly). *Nature Genet.* **31**, 410-414
- Holaska, J.M., Kowalski, A.K. and Wilson, K.L.** (2004). Emerin caps the pointed end of actin filaments: Evidence for an actin cortical network at the nuclear inner membrane. *PLOS Biol.* **2**, e231
- Holaska, J.M., Lee, K.K., Kowalski, A.K. and Wilson, K.L.** (2003). Transcriptional repressor germ cell-less (GCL) and barrier-to-autointegration factor (BAF) compete for binding to emerin *in vitro*. *J. Biol. Chem.* **278**, 6969-6975
- Holt, I., Östlund, C., Stewart, C.L., thi Man, N., Worman, H.J. and Morris, G. E.** (2003) Effect of pathogenic missense mutations in lamin A on its interaction with emerin *in vivo*. *J. Cell Sci.* **116**, 3027-3035
- Horton, H., McMorro, I. and Burke, B.** (1992). Independent expression and assembly properties of heterologous lamins A and C in embryonal carcinomas *Eur. J. Cell Biol.* **57**, 172-183
- Horton, J.D.** (2002). Sterol regulatory element-binding proteins: transcriptional activators of lipid synthesis. *Biochem. Soc. Trans.* **30**, 1091-1095
- Hutchison, C.J.** (2002). Lamins: building blocks or regulators of gene expression? *Nat. Rev. Mol. Cell Biol.* **3**, 848-858
- Hutchison, C.J., Alvarez-Reyes, M. and Vaughan, O.A.** (2001). Lamins in disease: why do ubiquitously expressed nuclear envelope proteins give rise to tissue-specific disease phenotypes? *J. Cell Sci.* **114**, 9-19
- Izumi, M., Vaughan, O.A., Hutchison, C.J. and Gilbert, D.M.** (2000). Head and/or CaaX domain deletions of lamin proteins disrupt preformed lamin A and C but not lamin B structure in mammalian cells. *Mol. Biol. Cell* **11**, 4323-4337

- Johnson, B.R., Nitta, R.T., Frock, R.L., Mounkes, L., Barbie, D.A., Stewart, C.L., Harlow, E. and Kennedy, B.K.** (2004). A-type lamins regulate retinoblastoma protein function by promoting subnuclear localization and preventing proteosomal degradation. *Proc. Natl. Acad. Sci. USA* **101**, 9677-9682
- Jongens, T.A., Hay, B., Jan, L.Y. and Jan, Y.N.** (1992). The germ cell-less gene product: A posteriorly localized component necessary for germ cell development in *Drosophila*. *Cell* **70**, 569-584
- Kasof, G.M., Goyal, L. and White, E.** (1999). Btf, a novel death-promoting transcriptional repressor that interacts with Bcl-2-related proteins. *Mol. Cell. Biol.* **19**, 4390-4404
- Kitten, G. and Nigg, E.** (1991). The CaaX motif is required for isoprenylation, carboxyl methylation and nuclear membrane association of lamin B₂. *J. Cell Biol.* **113**, 13-23
- Klapper, M., Exner, K., Kempf, A., Gehrig, C., Stuurmann, N., Fisher, P.A. and Krohne, G.** (1997). Assembly of A- and B-type lamins studied *in vivo* with the baculovirus system. *J. Cell Sci.* **110**, 2519-2532
- Krimm, I., Östlund, C., Gilquin, B., Couprie, J., Hossenlopp, P., Mornon, J-P., Bonne, G., Courvalin, J-C., Worman, H. J. and Zinn-Justin, S.** (2002). The Ig-like structure of the C-terminal domain of lamin A/C, mutated in muscular dystrophies, cardiomyopathy and partial lipodystrophy. *Structure* **10**, 811-823.
- Krohne, G.** (1998). Lamin assembly *in vivo*. *Subcellul. Biochem.* **31**, 563-586
- Krohne, G., Wolin, S., McKeon, F., Franke, W. and Kirschner, M.** (1987). Nuclear lamin LI of *Xenopus laevis*: cDNA cloning, amino acid sequence and binding specificity of a member of the lamin B subfamily. *EMBO J.* **6**, 3801-3808
- Kyhse-Anderson, J.** (1984). Electroblothing of multiple gels: a simple apparatus without buffertank for rapid transfer of proteins from polyacrylamide to nitrocellulose. *J. Biochem. Biophys.* **10**, 203-209
- Lachner, M., O'Carroll, D., Rea, S., Mechtler, K. and Jenuwein, T.** (2001). Methylation of histone H3 lysine 9 creates a binding site for HP1 proteins. *Nature* **410**;116-120
- Lammerding, J., Schulze, P.C., Takahashi, T., Kozlov, S., Sullivan, T., Kamm, R.D., Stewart, C.L. and Lee, R.T.** (2004). Lamin A/C deficiency causes defective nuclear mechanics and mechanotransduction. *J. Clin. Invest.* **113**, 370-378
- Lattanzi, G., Cenni, V., Marmioli, S., Capanni, C., Mattioli, E., Merlini, L., Squarzone, S. and Maraldi, N.M.** (2003). Association of emerin with nuclear and cytoplasmic actin is regulated in differentiating myoblasts. *Biochem. Biophys. Res. Commun.* **303**, 764-770
- Lee, H., Habas, R. and Abate-Shen, C.** (2004). Msx1 cooperates with histone H1B for inhibition of transcription and myogenesis. *Science* **304**, 1675-1678
- Lee, K.K., Gruenbaum, Y., Spann, P., Liu, J., and Wilson, K.L.** (2000). *C. elegans* nuclear envelope proteins emerin, MAN1, lamin, and nucleoporins reveal unique timing of nuclear envelope breakdown during mitosis. *Mol. Biol. Cell* **11**, 3089-3099

- Lee, K.K., Haraguchi, T., Lee, R.S., Koujin, T., Hiraoka, Y. and Wilson, K.L. (2001). Distinct functional domains in emerin bind lamin A and DNA-bridging protein BAF. *J. Cell Sci.* **114**, 4567-4573
- Lee, K.K., Star, D., Liu, J., Cohen, M., Han, M., Wilson, K.L. and Gruenbaum, Y. (2002). Lamin-dependent localization of Unc-84, a protein required for nuclear migration in *C.elegans*. *Mol. Biol. Cell* **13**, 892-901
- Lee, M.S. and Craigie, R. (1998). A previously unidentified host protein protects retroviral DNA from autointegration. *Proc. Natl. Acad. Sci. USA* **95**, 1528-1533
- Leukel, M. and Jost, E. (1995). Two conserved serines in the nuclear localisation signal flanking region are involved in the nuclear targeting of human lamin A. *Eur. J. Cell. Biol.* **68**, 133-142
- Lewis, J.A., Elmer, J.S., Skimming, J., McLafferty, S., Fleming, J. and McGee, T. (1987). Cholinergic receptor mutants of the nematode *Caenorhabditis elegans*. *J. Neurosci.* **7**, 3059-3071
- Libotte, T., Zaim, H., Abraham, S., Padmakumar, V.C., Schneider, M., Lu, W., Munck, M., Hutchison, C., Wehnert, M., Fahrenkrog, B., Sauder, U., Aebi, U., Noegel, A.A. and Karakesisoglou, I. (2005). Lamin A/C dependent localization of nesprin-2, a giant scaffold at the nuclear envelope. *Mol. Biol. Cell* **16**, 3411-3424
- Lin, F., Blake, D.L., Callebaut, I., Skerjanc, I.S., Holmer, L., McBurney, M.W., Paulin-Levasseur, M. and Worman, H.J. (2000). MAN1, an inner nuclear membrane protein that shares the LEM domain with lamina-associated polypeptide 2 and emerin. *J. Biol. Chem.* **275**, 4840-4847
- Liu, B., Maher, R.J., Hannun, Y.A., Porter, A.T. and Honn, K.V. (1994). 12(S)-HETE enhancement of prostate tumor cell invasion: selective role of PKC alpha. *J. Natl. Cancer Inst.* **86**, 1145-1151
- Liu, J., Lee, K.K., Segura-Totten, M., Neufeld, E., Wilson, K.L. and Gruenbaum, Y. (2003). MAN1 and emerin have overlapping function(s) essential for chromosome segregation and cell division in *Caenorhabditis elegans*. *Proc. Natl. Acad. Sci. USA* **100**, 4598-4603
- Liu, J., Rolef-Ben Shahar, T., Riemer, D., Spann, P., Treinin, M., Weber, K., Fire, A. and Gruenbaum, Y. (2000). Essential roles for *Caenorhabditis elegans* lamin gene in nuclear organization, cell cycle progression, and spatial organization of nuclear pore complexes. *Mol. Biol. Cell.* **11**, 3937-3947
- Liu, J., Song, K. and Wolfner, M.F. (1995). Mutational analyses of fs(1)YA, an essential, developmentally regulated, nuclear envelope protein in *Drosophila*. *Genetics* **141**, 1473-1481
- Lloyd, D.J., Trembath, R.C. and Shackleton, S. (2002). A novel interaction between lamin A and SREBP1: implications for partial lipodystrophy and other laminopathies. *Hum. Mol. Genet.* **11**, 769-777

- Loewinger, L. and McKeon, F.** (1988). Mutations in the nuclear lamin proteins resulting in their aberrant assembly in the cytoplasm. *EMBO J.* **7**, 2301-2309
- Lopez-Soler, R.I., Moir, R.D., Spann, T.P., Stick, R. and Goldman, R.D.** (2001). A role for nuclear lamins in nuclear envelope assembly. *J. Cell Biol.* **154**, 61-70
- Luderus, M.E., den Blaauwen, J.L., de Smit, O.J., Compton, D.A. and van Driel, R.** (1994). Binding of matrix attachment regions to lamin polymers involves single-stranded regions and the minor groove. *Mol. Cell Biol.* **14**, 6297-6305
- Macara, I.G.** (2001). Transport into and out of the nucleus. *Microbiol. Mol. Biol. Rev.* **65**, 570-594
- Machiels, B.M., Zorenc, A.H., Endert, J.M., Kuijpers, H.J., van, E.G., Ramaekers, F.C. and Broers, J.L.** (1996). An alternative splicing product of the lamin A/C gene lacks exon 10. *J. Biol. Chem.* **271**, 9249-9253
- Maison, C., Pyrpasopoulou, A., Theodoropoulos, P.A. and Georgatos, S.D.** (1997). The inner nuclear membrane protein LAP1 forms a native complex with B-type lamins and partitions with spindle-associated mitotic vesicles. *EMBO J.* **16**, 4839-4850
- Malone, C.J., Fixsen, W.D., Horvitz, H.R. and Han, M.** (1999). UNC-84 localizes to the nuclear envelope and is required for nuclear migration and anchoring during *C.elegans* development. *Development* **126**, 3171-3181
- Malone, C.J., Misner, L., Le Bot, N., Tsai, M.C., Campbell, J.M., Ahringer, J. and White, J.G.** (2003). The *C.elegans* Hook protein, ZYG-12, mediates the essential attachment between the centrosome and nucleus. *Cell* **115**, 825-836
- Manilal, S., Sewry, C.A., Pereboev, A., thi Man, N., Gobbi, P., Hawkes, S., Love, D.R. and Morris, G.E.** (1999). Distribution of emerin and lamins in the heart and implications for Emery-Dreifuss muscular dystrophy. *Hum. Mol. Genet.* **8**, 353-359
- Manilal, S., thi Man, N. and Morris, G.E.** (1998). Colocalization of emerin and lamins in interphase nuclei and changes during mitosis. *Biochem. Biophys. Res. Commun.* **249**, 643-647
- Manilal, S., thi Man, N., Sewry, C.A., and Morris, G.E.** (1996). The Emery-Dreifuss muscular dystrophy protein, emerin, is a nuclear membrane protein. *Hum. Mol. Genet.* **5**, 801-808
- Mansharamani, M., Hewetson, A. and Chilton, B.S.** (2001). An atypical nuclear P-type ATPase is a RING-finger binding protein. *J. Biol. Chem.* **276**, 3641-3649
- Mansharamani, M. and Wilson, K.L.** (2005). Nuclear membrane protein MAN1: direct binding to emerin *in vitro* and two modes of binding to BAF. *J. Biol. Chem.* **280**, 13863-13870
- Maraldi, N.M., Squarzone, S., Sabatelli, P., Capanni, C., Mattiolo, E., Ognibene, A. and Lattanzi, G.** (2005). Laminopathies: Involvement of structural nuclear proteins in the pathogenesis of an increasing number of human diseases. *J. Cell. Physiol.* **203**, 319-327

- Mariappan, I. and Parnaik, V.K.** (2005). Sequestration of pRb by cyclin D3 causes intranuclear reorganization of lamin A/C during muscle cell differentiation. *Mol. Biol. Cell* **16**, 1948-1960
- Markiewicz, E., Ledran, M. and Hutchison, C.J.** (2005). Remodelling of the nuclear lamina and nucleoskeleton is required for skeletal muscle differentiation *in vitro*. *J. Cell Sci.* **118**, 409-420
- Markiewicz, E., Venables, R., Alvarez-Reyes, M., Quinlan, R., Dorobek, M., Hausmanowa-Petruciewicz, I. and Hutchison, C.J.** (2002). Increased solubility of lamins and redistribution of lamin C in X-linked Emery–Dreifuss muscular dystrophy fibroblasts. *J. Struct. Biol.* **140**, 241-253
- Martelli, A.M., Bortul, R., Tabellini, G., Faenza, I., Cappellini, A., Bareggi, R., Manzoli, L. and Cocco, L.** (2002). Molecular characterization of protein kinase C-alpha binding to lamin A. *J. Cell Biochem.* **86**, 320-330
- Martin, L., Crimando, C. and Gerace, L.** (1995). cDNA cloning and characterization of lamina-associated polypeptide 1C (LAP1C), an integral protein of the inner nuclear membrane. *J. Biol. Chem.* **270**, 8822-8828
- Martins, S.B., Eide, T., Steen, R.L., Jahnsen, T., Skalhegg, B.S. and Collas, P.** (2000). HA95 is a protein of the chromatin and nuclear matrix regulating nuclear envelope dynamics. *J. Cell Sci.* **113**, 3703-3711
- Martins, S.B., Eikvar, S., Furukawa, K. and Collas, P.** (2003). HA95 and LAP2 β mediate a novel chromatin-nuclear envelope interaction implicated in initiation of DNA replication. *J. Cell. Biol.* **160**, 177-188
- Mattout-Drubezki, A. and Gruenbaum, Y.** (2003). Dynamic interactions of nuclear lamina proteins with chromatin and transcriptional machinery. *Cell. Mol. Life Sci.* **60**, 2053-2063
- McKeon, F., Kirschner, M.W. and Caput, D.** (1986). Homologies both in primary and secondary structure between nuclear envelope and intermediate filament proteins. *Nature* **318**, 463-468
- Mercuri, E., Poppe, M., Quinlivan, R., Messina, S., Kinali, M., Demay, L., Bourke, J., Richard, P., Sewry, C., Pike, M., Bonne, G., Muntoni, F. and Bushby, K.** (2004). Extreme variability of phenotype in patients with an identical missense mutation in the lamin A/C gene: from congenital onset with severe phenotype to milder classic Emery-Dreifuss variant. *Arch. Neurol.* **61**, 690-694
- Mislow, J.M., Kim, M.S., Davis, D.B. and McNally, E.M.** (2002a). Myne-1, a spectrin repeat transmembrane protein of the myocyte inner nuclear membrane, interacts with lamin A/C. *J. Cell Sci.* **115**, 61-70
- Mislow, J.M., Holaska, J.M., Kim, M.S., Lee, K.K., Segura-Totten, M., Wilson, K.L. and McNally, E.M.** (2002b). Nesprin-1alpha self-associates and binds directly to emerin and lamin A in vitro. *FEBS Lett.* **525**, 135-140

- Moir, R.D., Yoon, M., Khuon, S. and Goldman, R.D.** (2000). Nuclear lamins A and B1: different pathways of assembly during nuclear envelope formation in living cells. *J. Cell Biol.* **151**, 1155-1168
- Morris, G.E.** (2000). Nuclear proteins and cell death in inherited neuromuscular disease – Invited Review. *Neuromusc. Disord.* **10**, 217-227
- Morris, G.E. and Manilal, S.** (1999). Heart to heart : from nuclear proteins to Emery-Dreifuss muscular dystrophy. *Hum. Mol. Genet.* **8**, 1847-1851
- Motsch, I., Kaluarachchi, M., Emerson, L.J., Brown, C.A., Brown, S.C., Dabauvalle, M.-C. and Ellis, J.A.** (2005). Lamin A and lamin C are differentially dysfunctional in autosomal dominant Emery-Dreifuss muscular dystrophy. *Eur. J. Cell Biol.* (in press)
- Mounkes, L.C., Burke, B. and Stewart, C.L.** (2001). The A-type lamins: Nuclear structural proteins as a focus for muscular dystrophy and cardiovascular disease. *Trends Cardiovasc. Med.* **11**, 280-285
- Mounkes, L.C., Kozlov, S., Burke, B. and Stewart, C.L.** (2003). The laminopathies: nuclear structure meets disease. *Curr. Opin. Genet. Dev.* **13**, 223-230
- Mounkes, L.C., Kozlov, S., Hernandez, L., Sullivan, T. and Stewart, C.L.** (2003a). A progeroid syndrome in mice is caused by defects in A-type lamins. *Nature* **423**, 298-301
- Muchir, A., Bonne, G., van der Kooij, A.J., van Meegen, M., Baas, F., Bolhuis, P.A., de Visser, M. and Schwartz, K.** (2000). Identification of mutations in the gene encoding lamins A/C in autosomal dominant limb girdle muscular dystrophy with atrioventricular conduction disturbances (LGMD1B). *Hum. Mol. Genet.* **9**, 1453-1459
- Nagano, A., Koga, R., Ogawa, M., Kurano, Y., Kawada, J., Okada, R., Hayashi, Y.K., Tsukahara, T. and Arahata, K.** (1996). Emerin deficiency at the nuclear membrane in patients with Emery-Dreifuss muscular dystrophy. *Nature Genetics* **12**, 254-259
- Nakayama, T., Ciu, Y. and Christian, J.L.** (2000). Regulation of BMP/Dpp signalling during embryonic development. *Cell. Mol. Life Sci.* **57**, 934-956
- Navarro, C., De Sandre-Giovannoli, A., Bernard, R., Boccaccia, I., Boyer, A., Genevieve, D., Hadj-Rabia, S., Gaudy-Marqueste, C., Smitt, H.S., Vabres, P., Fivre, L., Verlos, A., Van Essen, T., Flori, E., Hennekam, R., Beemer, F.A., Laurent, N., Le Merrer, M., Cau, P. and Levy, N.** (2004). Lamin A and ZMPSTE24 (FACE-1) defects cause nuclear disorganisation and identify restrictive dermopathy as a lethal neonatal laminopathy. *Hum. Mol. Genet.* **13**, 2493-2503
- Nedivi, E., Fieldust, S., Theill, L.E. and Hevron, D.** (1996). A set of genes expressed in response to light in the adult cerebral cortex and regulated during development. *Proc. Natl. Acad. Sci. USA* **93**, 2048-2053
- Nigg, E.A.** (1992). Assembly and cell cycle dynamics of the nuclear lamina. *Semin. Cell Biol.* **3**, 245-253

- Nikolova, V., Leimena, C., McMahon, A.C., Tan, J.C., Chandar, S., Jogia, D., Kesteven, S.H., Michalicek, J., Otway, R., Verheyen, F., Rainer, S., Stewart, C.L., Martin, D., Feneley, M.P. and Fatkin, D.** (2004). Defects in nuclear structure and function promote dilated cardiomyopathy in lamin A/C-deficient mice. *J. Clin. Invest.* **113**, 357-369
- Nili, E., Cojocaru, G.S., Kalma, Y., Ginsberg, D., Copeland, N.G., Gilbert, D.J., Jenkins, N.A., Berger, R., Shaklai, S., Amariglio, N., Brok-Simoni, F., Simon, A.J. and Rechavi, G.** (2001). Nuclear membrane protein LAP2beta mediates transcriptional repression alone and together with its binding partner GCL (germ-cell-less). *J. Cell Sci.* **114**, 3297-3307
- Novelli, G. and D'Apice, M.R.** (2003). The strange case of the 'lumper' lamin A/C gene and human premature aging. *Trends Mol. Med.* **9**, 370-375
- Novelli, G., Muchir, A., Sangiuolo, F., Helbling-Leclerq, A., D'Apice, M.R., Massart, C., Capon, F., Sbraccia, P., Federici, M., Lauro, R., Tudisco, C., Palotta, R., Scarano, G., Dallapiccola, B., Merlini, L. and Bonne, G.** (2002). Mandibuloacral dysplasia is caused by a mutation in LMNA-encoding lamin A/C. *Am. J. Hum. Genet.* **71**, 426-431
- Novitch, B.G., Spicer, D.B., Kim, P.S., Cheung, W.L. and Lassar, A.B.** (1999). pRb is required for MEF2-dependent gene expression as well as cell cycle arrest during skeletal muscle differentiation. *Curr. Biol.* **9**, 449-459
- Östlund, C., Bonne, G., Schwartz, K. and Worman, H. J.** (2001). Properties of lamin A mutants found in Emery-Dreifuss muscular dystrophy, cardiomyopathy and Dunnigan-type partial lipodystrophy. *J. Cell Sci.* **114**, 4435-4445
- Östlund, C., Ellenberg, J., Hallberg, E., Lippincott-Schwartz, J. and Worman, H.J.** (1999). Intracellular trafficking of emerin, the Emery-Dreifuss muscular dystrophy protein. *J. Cell Sci.* **112**, 1709-1719
- Ognibene, A., Sabatelli, P., Petrini, S., Squarzone, S., Riccio, M., Santi, S., Villanova, M., Palmeri, S., Merlini, L. and Maraldi, N.M.** (1999). Nuclear changes in a case of X-linked Emery-Dreifuss muscular dystrophy. *Muscle Nerve* **22**, 864-869
- Olioudaki, H., Kourmouli, N., Drosou, V., Bakou, A., Theodoropoulos, P.A., Singh, P.B., T., G. and Georgatos, S.D.** (2001). Histones H3/H4 form a tight complex with the inner nuclear membrane protein LBR and heterochromatin protein 1. *EMBO Rep.* **2**, 920-935
- Osada, S., Ohmori, S.Y. and Taira, M.** (2003). XMAN1, an inner nuclear membrane protein, antagonizes BMP signalling by interacting with Smad1 in *Xenopus* embryos. *Development* **130**, 1783-1794
- Ozaki, T., Saijo, M., Murakami, K., Enomoto, H., Taya, Y. and Sakiyama, S.** (1994). Complex formation between lamin A and the retinoblastoma gene product: identification of the domain on lamin A required for its interaction. *Oncogene* **9**, 2649-2653

- Padan, R., Nainudel-Epszteyn, S., Goitein, R., Fainsod, A. and Gruenbaum, Y.** (1990). Isolation and characterisation of the *Drosophila* nuclear envelope otefin cDNA. *J. Biol. Chem.* **265**, 7808-7813
- Padmakumar, V.C., Abraham, S., Braune, S., Noegel, A.A., Tunggal, B., Karakesisoglou, I., Korenbaum, E.** (2004). Enaptin, a giant actin-binding protein, is an element of the nuclear membrane and the actin cytoskeleton. *Exp. Cell Res.* **295**, 330-339
- Pederson, T. and Aebi, U.** (2002). Actin in the nucleus: what form and what for ? *J. Struct. Biol.* **140**, 3-9
- Pendas, A.M., Zhou, Z., Cadinanos, J., Freije, J.M., Wang, J., Hultenby, K., Astudillo, A., Wernerson, A., Rodriguez, F., Tryggvason, K. and Lopez-Otin, C.** (2002). Defective pre-lamin A processing and muscular and adipocyte alterations in Zmpste24 metalloproteinase-deficient mice. *Nat. Genet.* **31**, 94-99
- Pestic-Dragovich, L., Stojiljkovic, L., Philimonenko, A.A., Nowak, G., Ke, Y., Settlege, R.E., Shabanowitz, J., Hunt, D.F., Hozak, P. and de Lanerolle, P.** (2000). A myosin I isoform in the nucleus. *Science* **290**, 337-341
- Peter, M., Heitlinger, E., Haner, M., Aebi, U. and Nigg, E.A.** (1991). Disassembly of *in vitro* formed lamin head-to-tail polymers by CDC2 kinase. *EMBO J.* **10**, 1535-1544
- Peter, M., Nakagawa, J., Doree, M., Labbe, J.C. and Nigg, E.A.** (1990). *In vitro* disassembly of the nuclear lamina and M phase-specific phosphorylation by cdc2 kinase. *Cell* **61**, 591-602
- Phair, R.D. and Misteli, T.** (2000). High mobility of proteins in the mammalian cell nucleus. *Nature* **404**, 604-609
- Pugh, G.E., Coates, P.J., Lane, E.B., Raymond, Y. and Quinlan, R.A.** (1997). Distinct nuclear assembly pathways for lamins A and C lead to their increase during quiescence in Swiss 3T3 cells. *J. Cell Sci.* **110**, 2483-2493
- Raharjo, W.H., Enarson, P., Sullivan, T., Stewart, C.L. and Burke, B.** (2001). Nuclear envelope defects associated with LMNA mutations cause dilated cardiomyopathy and Emery-Dreifuss muscular dystrophy. *J. Cell Sci.* **114**, 4447-4457
- Rao, L., Modha, D. and White, E.** (1997). The E1B 19K protein associates with lamins *in vivo* and its proper localization is required for inhibition of apoptosis. *Oncogene* **15**, 1587-1597
- Reichart, B., Klafke, R., Dreger, C., Krüger, E., Motsch, I., Ewald, A., Schäfer, J., Reichmann, H., Müller, C.R. and Dabauvalle, M.-C.** (2004). Expression and localization of nuclear proteins in autosomal-dominant Emery-Dreifuss muscular dystrophy with LMNA R377H mutation. *BCM Cell Biol.* **5**, 12
- Rolls, M.M., Stein, P.A., Taylor, S.S., Ha, E., McKeon, F. and Rapoport, T.A.** (1999). A visual screen of a GFP-fusion library identifies a new type of nuclear envelope membrane protein. *J. Cell Biol.* **146**, 29-44

- Ron, D. and Kazanietz, M.G.** (1999). New insights into the regulation of protein kinase C and novel phorbol ester receptors. *FASEB J.* **13**, 1658-1676
- Rosenberg-Hasson, Y., Renert-Pasca, M. and Volk, T.** (1996). A *Drosophila* dystrophin-related protein, MSP-300, is required for embryonic muscle morphogenesis. *Mech. Dev.* **60**, 83-94
- Rowland, L.P., Fetell, M., Olarte, M., Hays, A., Singh, N. and Wanat, F.E.** (1979). Emery-Dreifuss muscular dystrophy. *Ann. Neurol.* **5**, 111-117
- Sabatelli, P., Lattanzi, G., Ognibene, A., Columbaro, M., Capanni, C., Merlini, L., Maraldi, N.M. and Squarzone, S.** (2001). Nuclear alterations in autosomal-dominant Emery-Dreifuss muscular dystrophy. *Muscle Nerv* **24**, 826-829
- Sakaki, M., Koike, H., Takahashi, T., Sasagawa, N., Tomioka, A., Arahata, K. and Ishiura, S.** (2001). Interaction between emerin and nuclear lamins. *J. Biochem.* **129**, 321-327
- Sasseville, A.M. and Langelier, Y.** (1998). *In vitro* interaction of the carboxy-terminal domain of lamin A with actin. *FEBS Lett.* **425**, 485-489
- Schenk, P. and Mathias, E.** (1920). Zur Kasuistik der Dystrophia musculorum progressiva retrahens. *Klin. Wochenschr.* **57**, 557-558
- Schirmer, E.C., Guan, T. and Gerace, L.** (2001). Involvement of the lamin rod domain in heterotopic lamin interactions important for nuclear organization. *J. Cell Biol.* **153**, 479-490
- Schmidt, M. and Krohne, G.** (1995). *In vivo* assembly kinetics of fluorescently labelled *Xenopus* lamin A mutants. *Eur. J. Cell Biol.* **68**, 345-354
- Schmidt-Zachmann, M.S., Dargemont, C., Kühn, L.C. and Nigg, E.A.** (1993). Nuclear export of proteins: The role of nuclear retention. *Cell* **74**, 493-504
- Segura-Totten, M., Kowalski, A.K., Craigie, R. and Wilson, K.L.** (2002). Barrier-to-autointegration factor: major roles in chromatin decondensation and nuclear assembly. *J. Cell Biol.* **158**, 475-485
- Senior, A. and Gerace, L.** (1988). Integral membrane proteins specific to the inner nuclear membrane and associated with the nuclear lamina. *J. Cell Biol.* **107**, 2029-2036
- Sewry, C.A., Brown, S.C., Mercuri, E., Bonne, G., Feng, L., Camici, G., Morris, G. E. and Muntoni, F.** (2001). Skeletal muscle pathology in autosomal dominant Emery-Dreifuss muscular dystrophy with lamin A/C mutations. *Neuropath. Appl. Neurobiol.* **27**, 281-290
- Shackleton, S., Lloyd, D.J., Jackson, S.N., Evans, R., Niermeijer, M.F., Singh, B.M., Schmidt, H., Brabant, G., Kumar, S., Durrington, P.N., Gregory, S., O'Rahilly, S. and Trembath, R.C.** (2000). *LMNA* encoding lamin A/C is mutated in partial lipodystrophy. *Nature Genet.* **24**, 153-156

- Shimi, T., Koujin, T., Segura-Totten, M., Wilson, K.L., Hiraoka, Y. and Haraguchi, T.** (2004). Dynamic interaction between BAF and emerin revealed by FRAP, FLIP and FRET analyses in living HeLa cells. *J. Struct. Biol.* **147**, 31-41
- Shumaker, D.K., Lee, K.K., Tanhehco, Y.C., Craigie, R. and Wilson, K.L.** (2001). LAP2 binds to BAF-DNA complexes: Requirements for the LEM domain and modulation by variable regions. *EMBO J.* **20**, 1754-1764
- Silve, S., Dupuy, P.H., Ferrara, P. Loison, G.** (1998). Human lamin B receptor exhibits sterol C14-reductase activity in *Saccharomyces cerevisiae*. *Biochim. Biophys. Acta.* **1392**, 233-244
- Simos, G., Maison, C., and Georgatos, S.D.** (1996). Characterization of p18, a component of the lamin B receptor complex and a new integral membrane protein of the avian erythrocyte nuclear envelope. *J. Biol. Chem.* **271**, 12617-12625
- Southern, E.** (1979). Gel electrophoresis of restriction fragments. *Meth. Enzymol.* **68**, 152-176
- Spann, T.P., Goldman, A.E., Wang, C., Huang, S. and Goldman, R.D.** (2002). Alteration of nuclear lamin organization inhibits RNA polymerase II-dependent transcription. *J. Cell Biol.* **156**, 603-608
- Spann, T.P., Moir, R.D., Goldman, A.E., Stick, R. and Goldman, R.D.** (1997). Disruption of nuclear lamin organization alters the distribution of replication factors and inhibits DNA synthesis. *J. Cell Biol.* **136**, 1201-1212
- Squarzoni, S., Sabatelli, P., Ognibene, A., Toniolo, D., Cartegni, L., Cobianchi, F., Petrini, S., Merlini, L. and Maraldi, N.M.** (1998). Immunocytochemical detection of emerin within the nuclear matrix. *Neuromusc. Disord.* **8**, 338-344
- Starr, D.A. and Han, M.** (2002). Role of ANC-1 in tethering nuclei to the actin cytoskeleton. *Science* **11**, 406-409
- Starr, D.A., Hermann, G.J., Malone, C.J., Fixsen, W.D., Priess, J.R., Horvitz, H.R. and Han, M.** (2001). Unc-83 encodes a novel component of the nuclear envelope and is essential for proper nuclear migration. *Development* **128**, 5039-5050
- Steen, R.L., Martins, S.B., Tasken, K. and Collas, P.** (2000). Recruitment of protein phosphatase 1 to the nuclear envelope by A-kinase anchoring protein AKAP149 is a prerequisite for nuclear lamina assembly. *J. Cell Biol.* **150**, 1251-1262
- Steinle, N.I., Kazlauskaitė, R., Imumorin, I.G., Hsueh, W.C., Pollin, T.I., O'Connell, J.R., Mitchell, B.D. and Shuldiner, A.R.** (2004). Variation in the lamin A/C gene: associations with metabolic syndrome. *Arterioscler. Thromb. Vasc. Biol.* **9**, 1708-1713
- Stierle, V., Couprie, J., Östlund, C., Krimm, I., Zinn-Justin, S., Hossenlopp, P., Worman, H.J., Courvalin, J.C. and Duband-Goulet, I.** (2003). The carboxyl-terminal region common to lamins A and C contains a DNA binding domain. *Biochemistry* **42**, 4819-4828

- Strelkov, S.V., Herrmann, H., Geisler, N., Wedig, T., Zimbelmann, R., Aebi, U. and Burkhard, B.** (2002). Conserved segments 1A and 2B of the intermediate filament dimer: Their atomic structures and role in filament assembly. *EMBO J.* **21**, 1255-1266
- Strelkov, S.V., Schumacher, J., Burkhard, P., Aebi, U. and Herrmann, H.** (2004). Crystal structure of the human lamin A coil 2B dimer: Implications for the head-to-tail association of nuclear lamins. *J. Mol. Biol.* **343**, 1067-1080
- Stuurman, N., Heins, S. and Aebi, U.** (1998). Nuclear lamins: their structure, assembly and interactions. *J. Struct. Biol.* **122**, 42-66
- Sullivan, T., Escalante-Alcalde, D., Bhatt, H., Anver, M., Bhat, N., Nagashima, K., Steward, C.L. and Burke, B.** (1999). Loss of A-type lamin expression compromises nuclear envelope integrity leading to muscular dystrophy. *J. Cell Biol.* **147**, 913-919
- Tang, K., Finley, R.L., Nie, D. and Honn, K.V.** (2000). Identification of 12-lipoxygenase interaction with cellular proteins by yeast two-hybrid screening. *Biochemistry* **39**, 3185-3191
- Taniura, H., Glass, C. and Gerace, L.** (1995). A chromatin binding site in the tail domain of nuclear lamins that interacts with core histones. *J. Cell Biol.* **131**, 33-44
- ten Dijke, P. and Hill, C.S.** (2004). New insights into TGF β -Smad signalling. *Trends Biochem. Sci.* **29**, 265-273
- Thomas, J.O. and Kornberg, R.D.** (1975). An octamer of histones in chromatin and free in solution. *Proc. Natl. Acad. Sci. USA* **72**, 2626-2630
- Thorne, H.V.** (1967). Electrophoretic characterization and fractionation of polyoma virus DNA. *J. Mol. Biol.* **24**, 203
- Towbin, H., Staehlin, T. and Gordon, J.** (1979). Electrophoretic transfer of proteins from polyacrylamid gels to nitrocellulose sheets : procedure and some applications. *Proc. Natl. Acad. Sci. USA* **76**, 4350-4354
- Tsuchiya, Y., Hase, A., Ogawa, M., Yorifuji, H. and Arahata, K.** (1999). Distinct regions specify the nuclear membrane targeting of emerin, the responsible protein for Emery-Dreifuss muscular dystrophy. *Eur. J. Biochem.* **259**, 859-865
- Tsukahara, T., Tsujino, S. and Arahata, K.** (2002). CDNA microarray analysis of gene expression in fibroblasts of patients with X-linked Emery-Dreifuss muscular dystrophy. *Muscle Nerve* **25**, 898-901
- Tzur, Y.B., Hersh, B.M., Horvitz, H.R. and Gruenbaum, Y.** (2002). Fate of the nuclear lamina during *Caenorhabditis elegans* apoptosis. *J. Struct. Biol.* **137**, 146-153
- Vaughan, A., Alvarez-Reyes, M., Bridger, J.M., Broers, J.L., Ramaekers, F.C., Wehnert, M., Morris, G.E., Whitfield, W.G.F. and Hutchison, C.J.** (2001). Both emerin and lamin C depend on lamin A for localization at the nuclear envelope. *J. Cell Sci.* **114**, 2577-2590

- Vigouroux, C., Auclair, M., Dubosclard, E., Pouchelet, M., Capeau, J., Courvalin, J.-C. and Buendia, B.** (2001). Nuclear envelope disorganisation in fibroblasts from lipodystrophic patients with heterozygous R482Q/W mutations in the lamin A/C gene. *J. Cell Sci.* **114**, 4459-4468
- Vlcek, S., Dechat, T. and Foisner, R.** (2001). Nuclear envelope and nuclear matrix interactions and dynamics. *Cell. Mol. Life Sci.* **58**, 1758-1765
- Vlcek, S., Just, H., Dechat, T. and Foisner, R.** (1999). Functional diversity of LAP2 α and LAP2 β in postmitotic chromosome association is caused by an α -specific nuclear targeting. *EMBO J.* **18**, 6370-6384
- Vlcek, S., Korbei, B. and Foisner, R.** (2002). Distinct functions of the unique C-terminus of LAP2 α in cell proliferation and nuclear assembly. *J. Biol. Chem.* **277**, 18898-18907
- Voit, T., Krogmann, O., Lenard, H.G. et al.** (1988). Emery-Dreifuss muscular dystrophy : disease spectrum and differential diagnosis. *Neuropediatrics* **19**, 62-71
- Wagner, N., Schmitt, J. and Krohne, G.** (2004). Two novel LEM-domain proteins are splice products of the annotated *Drosophila melanogaster* gene CG9424 (*Bocksbeutel*). *Euro. J. Cell Biol.* **82**, 605-616
- Wang, X., Xu, S., Rivolta, C., Li, L.Y., Peng, G.H., Swain, P.K., Sung, C.H., Swaroop, A., Berson, E.L., Dryja, T.P. and Chen, S.** (2002). Barrier to autointegration factor interacts with the cone-rod homeobox and represses its transactivation function. *J. Biol. Chem.* **277**, 43288-43300
- Waterham, H.R., Koster, J., Mooyer, P., Noort Gv, G., Kelley, R.I., Wilcox, W.R., Wanders, R.J., Hennekam, R.C. and Oosterwijk, J.C.** (2003). Autosomal recessive HEM/Greenberg skeletal dysplasia is caused by 3 beta-hydroxysterol delta 14-reductase deficiency due to mutations in the lamin B receptor gene. *Am. J. Hum. Genet.* **72**, 1013-1017
- White, J. and Stelzer, E.** (1999). Photobleaching GFP reveals protein dynamics inside live cells. *Trends Cell Biol.* **9**, 61-65
- Wilkinson, F.L., Holaska, J.M., Zhang, Z., Sharma, A., Manilal, S., Holt, I., Stamm, S., Wilson, K.L. and Morris, G.E.** (2003). Emerin interacts *in vitro* with the splicing-associated factor, YT521-B. *Eur. J. Biochem.* **270**, 2459-2466
- Wilson, K.L.** (2000). The nuclear envelope, muscular dystrophy and gene expression. *Trends Cell Biol.* **10**, 125-129
- Wolff, N., Gilquin, B., Courchay, K., Callebaut, I., Worman, H.J. and Zinn-Justin, S.** (2001). Structural analysis of emerin, an inner nuclear membrane protein mutated in X-linked Emery-Dreifuss muscular dystrophy. *FEBS Lett.* **501**, 171-176
- Worman, H.J. and Courvalin, J.C.** (2004). How do mutations in lamins A and C cause disease ? *J. Clin. Invest.* **113**, 349-351

- Worman, H.J., Evans, C.D. and Blobel, G.** (1990). The lamin B receptor of the nuclear envelope inner membrane: a polytopic protein with eight potential transmembrane domains. *J. Cell Biol.* **117**, 245-258
- Yates, J.R.W. and Wehnert, M.** (1999). The Emery-Dreifuss muscular dystrophy database. *Neuromusc. Disord.* **9**, 199 (<http://www.path.cam.ac.uk/emd>)
- Ye, Q. and Worman, H.J.** (1995). Protein-protein interactions between human nuclear lamins expressed in yeast. *Exp. Cell Res.* **219**, 292-298
- Ye, Q. and Worman, H.J.** (1996). Interaction between an integral protein of the nuclear envelope inner membrane and human chromodomain proteins homologous to *Drosophila* HP1. *J. Biol. Chem.* **271**, 14653-14656
- Young, J., Morbois-Trabut, L., Couzinet, B., Lascols, O., Dion, E., Béréziat, V., Fève, B., Richard, I., Capeau, J., Chanson, P. and Vigouroux, C.** (2005). Type A Insulin resistance syndrome revealing a novel lamin A mutation. *Diabetes* **54**, 1873-1878
- Zastrow, M.S., Vlcek, S. and Wilson, K.L.** (2004). Proteins that bind A-type lamins: integrating isolated clues. *J. Cell Sci.* **117**, 979-987
- Zhang, Q., Ragnauth, C.D., Greener, J.M., Shanahan, C.M. and Roberts, R.G.** (2002). The nesprins are giant actin-binding proteins, orthologous to *Drosophila* muscle protein MSP-300. *Genomics* **80**, 473-481
- Zhang, Q., Ragnauth, C.D., Skepper, J.N., Worth, N.F., Warren, D.T., Roberts, R.G., Weissberg, P.L., Ellis, J.A. and Shanahan, C.M.** (2005). Nesprin-2 is a multi-isoformic protein that binds lamin and emerin at the nuclear envelope and forms a subcellular network in skeletal muscle. *J. Cell. Sci.* **118**, 673-687
- Zhang, Q., Skepper, J.N., Yang, F., Davies, J.D., Hegyi, L., Roberts, R.G., Weissberg, P.L., Ellis, J.A. and Shanahan, C.M.** (2001). Nesprins: A novel family of spectrin-repeat-containing proteins that localize to the nuclear membrane in multiple tissues. *J. Cell Sci.* **114**, 4485-4498
- Zhen, Y.Y., Libotte, T., Munck, M., Noegel, A.A. and Korenbaum, E.** (2002). NUANCE, a giant protein connecting the nucleus and actin cytoskeleton. *J. Cell. Sci.* **115**, 3207-3222
- Zheng, R., Ghirlando, R., Lee, M.S., Mizuuchi, K., Krause, M. and Craigie, R.** (2000). Barrier-to-autointegration factor (BAF) bridges DNA in a discrete, higher-order nucleoprotein complex. *Proc. Natl. Acad. Sci. USA* **97**, 8997-9002
- Zick, Y.** (2003). Role of Ser/Thr kinases in the uncoupling of insulin signaling. *Int. J. Obes. Relat. Metab. Disord.* **27** (Suppl. 3):S56 –S60

10 Curriculum vitae

Personal details

Isabell Motsch
Diplom-Biologin
born 24th February 1976 in Bad Kissingen, Germany
single, no children

Address

Scheffelstraße 7
97688 Bad Kissingen
Tel: 0049 (0)971 2686
Email: isabell.motsch@gmx.de

Present status

since 05/2001 PhD student of Prof. Dr. M.-C. Dabauvalle at the department of
cell and developmental biology at the bavarian
Julius-Maximilians-University Würzburg, Germany

University education

05/2001-11/2003 Guest scientist (during the course of PhD studies) in the laboratory of
Dr. J.A. Ellis, Randall Centre, King's College, London, UK
Funded by DAAD sholarships

10/1995-02/2001 Master of Science (M.Sc. \cong Diplom) in biology at the bavarian Julius-
Maximilians-University Würzburg
Subjects: Cell and developmental biology, genetics, biotechnology
Title of the Diploma work: Emerin- und Lamin A/C-Expression
in EDMD-Patientenzellen

School education

09/1986-06/1995 A-levels (Abitur) at the Gymnasium Bad Kissingen
09/1982-07/1986 elementary school in Bad Kissingen

Computer skills

Microsoft Word, PowerPoint and Excel, Adobe Photoshop, Improvision
Openlab and Universal Imaging MetaMorph
Experience with Apple MacIntosh

Language skills

German – native language
English – fluent in spoken and written form
French – working knowledge
Latin – basic knowledge

Publications

Motsch, I., Kaluarachchi, M., Emerson, L.J., Brown, C.A., Brown, S.C., Dabauvalle, M.-C. and Ellis, J.A. (2005). Lamin A and lamin C are differentially dysfunctional in autosomal dominant Emery-Dreifuss muscular dystrophy. *Eur. J. Cell Biol.* (in press)

Reichart, B., Klafke, R., Dreger, C., Krüger, E., Motsch, I., Ewald, A., Schäfer, J., Reichmann, H., Müller, C.R. and Dabauvalle, M.-C. (2004). Expression and localization of nuclear proteins in autosomal dominant Emery-Dreifuss muscular dystrophy with *LMNA* R377H mutation. *BMC Cell Biol.* 2004 Mar 30;5(1):12.

Motsch, I., Kaluarachchi, M., Dabauvalle, M.-C. and Ellis, J.A. (2003). Localisation of lamin A and lamin C proteins containing mutations leading to Emery-Dreifuss muscular dystrophy and their binding properties to emerin. Poster presentation at the SEB symposium 'Communication and gene regulation at the nuclear envelope' from 16-19th July 2003 at the University of Durham, Durham, UK.

Interests

Science fiction and fantasy literature, classical music, aquaristics (tropical freshwater fish), meeting with friends

Bad Kissingen

Ehrenwörtliche Erklärung

(gemäß § 4, Abs. 3, S. 3, 5 und 8 der Promotionsordnung für Biologie
an der Universität Würzburg)

Hiermit erkläre ich ehrenwörtlich, dass die vorliegende Arbeit von mir selbständig und nur unter Verwendung der angegebenen Quellen und Hilfsmittel angefertigt wurde.

Weiterhin habe ich noch keinen Promotionsversuch unternommen oder diese Dissertation in gleicher oder ähnlicher Form in einem anderen Prüfungsverfahren vorgelegt.

Bad Kissingen, den

.....
Isabell Motsch